Pretreatment of hemp fibers for utilization in strong biocomposite materials

Liu, Ming; Meyer, Anne S.; Thygesen, Anders

Publication date:
2016

Document Version
Publisher's PDF, also known as Version of record

Pretreatment of hemp fibers for utilization in strong biocomposite materials

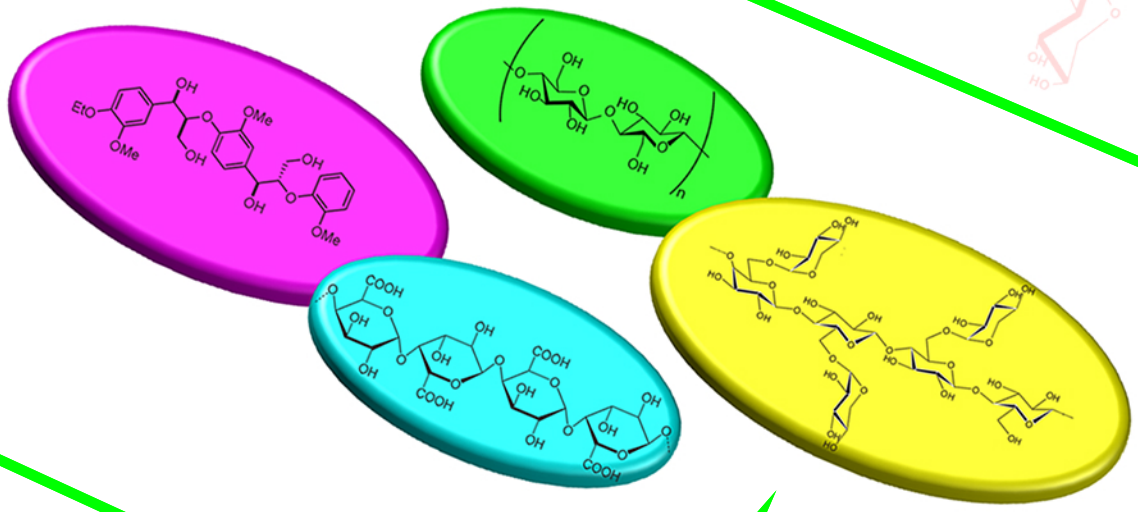

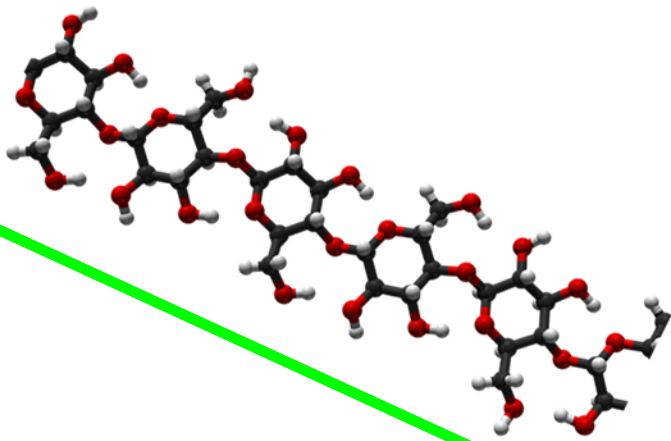

Ming Liu (刘明)

Ph.D. Thesis

Sep. 2016

DTU Chemical Engineering
Department of Chemical and Biochemical Engineering

Pretreatment of hemp fibers for utilization in strong biocomposite materials

This thesis was prepared by

Ming Liu (刘明)

Supervised by

Professor Anne S. Meyer (main supervisor)

Project leader Anders Thygesen (co-supervisor)

September 2016

Center for Bioprocess Engineering

Department of Chemical and Biochemical Engineering

Technical University of Denmark

PREFACE

This thesis is submitted in fulfillment of requirements for the Doctorate (PhD) degree at the Technical University of Denmark (DTU). The work presented in this thesis was conducted during my PhD study at the Department of Chemical and Biochemical Engineering, DTU from 15th September 2013 until 14th September 2016. The PhD study was supervised by:

Main supervisor; Professor, PhD, Anne S. Meyer (BioEng, DTU)

Co-supervisor; Project leader, PhD, Anders Thygesen (BioEng, DTU)

The PhD study was part of the CelFiMat project (No. 0602-02409B: ″High quality cellulosic fibers for strong biocomposite materials") financed by the Danish Council for Independent Research. The PhD study was also financially supported by scholarship from the China Scholarship Council (CSC, no. 201304910245).

Hemp fiber treatments and chemical composition analysis of hemp fibers were performed at the Center for Bioprocess Engineering (BioEng), DTU. Composite manufacturing and tensile testing for hemp fibers and composites were performed at the Section of Composites and Materials Mechanics, Department of Wind Energy, DTU. Microscopic observation of hemp bast fibers and composites was performed at the Department of Forest Products/Wood Science, Swedish University of Agricultural Sciences (SLU). Analytical work on lignin moieties by Py-GC/MS was done at the University of Hamburg. Hemp fiber surface and thermal properties characterization by FTIR and TGA, respectively were carried out at the Danish Polymer Center (DPC), DTU.

Ming Liu

DTU, 14th of September, 2016

ACKNOWLEDGEMENTS

I sincerely thank my supervisor Anne S. Meyer and my co-supervisor Anders Thygesen for accepting me as a PhD student at BioEng. I am very grateful to Anne S. Meyer for the thorough supervision, continuous encouragement and support, and valuable comments throughout this study. I also thank to Anders Thygesen for co-supervision, for assisting with communication between different project partners. And I am grateful to Bo Madsen (DTU) and Geffrey Daniel and Dinesh Fernando (SLU) for sharing knowledge, access to facilities, valuable comments and inspiring discussions. Jürgen Odermatt and Jens Berger (University of Hamburg) and Liyun Yu (DTU) are acknowledged for access to their analytical facilities, assistance with the analytical work and valuable comments on the results.

I would like to thank Fauziah Binti Marpani, Mohd Shafiq Mohd Sueb, Stavros Kalafatakis and Kristian Barrett, with whom I shared an office, for their valuable help and sharing of laughs and thoughts.

Special thanks go to my colleagues Marcel Tutor Ale, Andreas Baum, Birgitte Zeuner, Jesper Holck and for assistance with the use of HPAEC-PAD, RP-HPLC and NIR, valuable discussions concerning the results from the analytical work, and contributions to my publications. Mateusz Jakub Łężyk is thanked for teaching me how to use the ÄKTA protein purification systems, and Annette Eva Jensen is thanked for assistance with use the HPAEC-PAD.

Jonas Heininge Kreutzfeldt in the fiber laboratory at DTU Wind Energy is acknowledged for help with fiber specimen preparation and composites manufacturing. Jan Sjølin in the test laboratory at DTU Wind Energy is acknowledged for assistance with fiber and composites tensile testing.

Finally, I wish to thank my parents for their support and my wife Xiujuan Li for her never ending love and continuous understanding and support.

ABSTRACT

Hemp is the common name for *Cannabis sativa* cultivated for industrial use. Compared to synthetic fibers (e.g. glass fiber), hemp fibers have many advantages such as low cost, low density (1.5 g/cm^3) and high specific strength and stiffness. As a result of increasing environmental awareness, interest in hemp fiber reinforced composites is increasing because of a high potential of manufacturing hemp fiber reinforced polymer composites with acceptable mechanical properties at low cost. In order to expedite the application of natural fibers in polymer composites, hemp fibers need to be treated before being incorporated in matrix polymers to optimize the properties of fibers and fiber reinforced composites. The overall objective of this study was therefore to focus on understanding the correlation between chemical composition and morphology of hemp fibers and mechanical properties of hemp fibers, and furthermore to establish the relationship between the mechanical properties of hemp fiber reinforced composites and the chemical composition and morphology of hemp fibers after different fiber treatments.

The first part of this study investigated the effect of harvest time and stem sections on mechanical properties of hemp fibers in order to correlate the mechanical properties of hemp fibers to their chemical composition and morphology. Harvest time (or growth stage) and stem sections were found to have an effect on the mechanical properties of hemp fibers. The variations in mechanical properties of hemp fibers can be explained by the differences in chemical composition and morphology. Untreated hemp bast fibers with high cellulose content had high stiffness and tensile strength. In addition, the presence of secondary fibers was found to reduce the favorable mechanical properties of hemp fibers.

It was our intention to find the key factors that damage fiber properties during traditional field retting. In order to compare and demonstrate the significant effect of the targeted factors, controlled fungal retting was performed using *P. radiata* Cel 26 and *C. subvermispora*. Controlled fungal retting with *P. radiata* Cel 26 and *C. subvermispora* removed pectin more efficiently than traditional field retting. Fibers with the highest mechanical properties were obtained by controlled fungal retting with *P. radiata* Cel 26. As a result, composites with *P. radiata* Cel 26 retted fibers had higher mechanical properties regarding stiffness and tensile strength compared with composites with field retted fibers. The differences in mechanical properties of fibers and fiber reinforced composites were presumably due to the effect of cellulase enzymes activity, which can degrade the cellulose and damage fibers.

Further work was conducted to examine the presence of different enzymes activity during field retting and controlled fungal retting with white rot fungi *P. radiata* Cel 26. Cellulase, polygalacturonase, galactanase and xyloglucan (XG)-specific endoglucanase activity was determined in the crude extracts from hemp bast fibers after field retting and controlled fungal retting using *P. radiata* Cel 26 at varied durations (i.e. 7, 14 and 20 days). Cellulase activity was shown to be the crucial factor that caused reduction in mechanical properties of hemp fibers and hemp fiber reinforced composites. The extracts from field retted hemp bast fibers exhibited much higher cellulase enzyme activity compared to extracts from *P. radiata* Cel 26 retted hemp fibers. The extracts from *P. radiata* Cel 26 retted hemp fibers had much high polygalacturonase activity compared to that from field retted fibers.

It is certain that cellulase has a negative impact on fiber properties. Mono-component pectinase enzymes were thereby tested on hemp bast fibers combined with hydrothermal pre-treatment. Enhanced removal of pectin from hemp fibers was found to produce a positive impact on hemp fiber reinforced composites. Further work was performed to understand the role of different cell wall components (i.e. pectin, hemicellulose and lignin) in contributing to tensile properties of fiber reinforced composites. Pectin removal was found to increase both composite stiffness and UTS. Hemicellulose removal increased composite stiffness, but decreased composite UTS due to the removal of xyloglucans. The changes in mechanical properties of fiber reinforced composites correlated with chemical composition of differently treated hemp fibers via composite porosity. This may provide a way to reshape and optimize the natural cellulose fibers for composite use.

Oxidation of lignin using laccase after treatment with EDTA and EPG increased the mechanical properties of fibers and fiber/epoxy composites. It is suggested that the improvement in mechanical properties was due to polymerization of lignin by laccase resulting in hemp fibers with a stiffer structure. Once part of lignin was removed prior to laccase treatment, a less marked increase in mechanical properties was observed.

Modelling of the changes in mechanical properties and physical properties of composites made with differently treated hemp fibers improved understanding of the effect of composite porosity on mechanical properties of unidirectional (UD) hemp fiber/epoxy composites. It was demonstrated that the applied

models provide a concept to be used for the evaluation of performance of differently treated fibers in composites.

This study has resulted in improved understanding of the role of different components in contributing to the tensile properties of hemp fibers and of fiber treatments to improve the mechanical properties of natural fiber reinforced composites.

DANSK SAMMENFATNING

Hampeplanten har det latinske navn *Cannabis sativa* og nogle sorter af denne er egnet til industriel brug. Sammenlignet med syntetiske fibre (fx glasfibre), har hampefibre mange fordele, såsom lav pris, lav densitet (1,5 g/cm^3) og høj specifik styrke og stivhed. Som følge af stigende miljøbevidsthed er interessen i hampefiberforstærkede polymer kompositmaterialer stigende. Disse kompositmaterialer har acceptable mekaniske egenskaber og lave fremstillingsomkostninger. For at fremskynde anvendelsen af polymere kompositmaterialer med hampefibre, skal fibrene behandles, før de kan anvendes samt for at optimere egenskaberne af fibrene. Det overordnede formål med denne undersøgelse var derfor at forstå sammenhængen mellem hampefibrenes fysisk-kemiske egenskaber, og de mekaniske egenskaber af hampefiberarmerede kompositmaterialer efter forskellige behandlinger af fibrene.

Den første del af dette studie undersøgte effekten af høsttidspunkt og top/midt/bund sektion af stænglerne på de mekaniske egenskaber af hampefibrene for endvidere at korrelere de mekaniske egenskaber til deres kemiske sammensætning og morfologi. Det blev fundet at de sekundære fibre i bundsektionen ved især sen høst reducerede de gunstige mekaniske egenskaber af hampefibrene. Højst styrke blev opnået med tidlig høst men gav intet udbytte af frø hvilket betød at sen høst blev testet i det videre forløb af studiet.

Det var vores hensigt at finde de vigtigste faktorer, der skader fibernes egenskaber under traditionel markrødning. For at sammenligne og demonstrere de signifikante effekter blev der udført kontrolleret svampebehandling med *Phlebia radiata* Cel 26 og *Ceriporiopsis subvermispora*. Disse behandlinger fjernede pektin mere effektivt end traditionel markrødning. Fibrene med de højeste mekaniske egenskaber blev opnået med *P. radiata* Cel 26. Dette resulterede samtidig i at kompositterne havde højere stivhed og trækstyrke. Forskellene i mekaniske egenskaber af fibrene og de resulterende kompositter var formodentlig på grund af cellulaseenzymaktivitet, der kan nedbryde cellulose og skader fibrene.

Yderligere arbejde blev udført for at undersøge tilstedeværelsen af forskellige enzymaktiviteter under markrødning og kontrolleret svampebehandling med *P. radiata* Cel 26. Cellulase, polygalacturonase, galactanase og xyloglucan (XG) samt specifik endoglucanaseaktivitet blev bestemt i de rå ekstrakter fra hampefibrene efter markrødning og behandling med *P. radiata* Cel 26 ved varigheder af 7, 14 og 20 dage. Celluaseaktiviteten viste sig at være den afgørende faktor for reduktionen i de mekaniske egenskaber.

Derimod gav behandlingen med *P. radiata* Cel 26 meget høj polygalacturonase aktivitet sammenlignet med markrødning.

Det er helt sikkert, at cellulaser har en negativ indvirkning på fibernes styrkeegenskaber. Mono-komponent pektinase enzymer blev derved testet på hampefibrene kombineret med hydrothermal behandling ved 110 - 131°C. Forbedret fjernelse af pektin fra hampefibrene viste sig at have positiv indvirkning på hampfiberkompositmaterialerne. Yderligere arbejde blev udført for at forstå betydningen af forskellige cellevægskomponenter (dvs. pektin, hemicellulose og lignin) på fibrenes trækstyrke. Pektinfjernelse øgede både composite stivhed og styrke. Hemicellulosefjernelse øgede komposit stivheden, men nedsatte styrken på grund af fjernelsen af xyloglucan. Ændringerne i mekaniske egenskaber af kompositmaterialerne korrelerede med den kemiske sammensætning og kompositternes porøsitet. Det kan give en måde at optimere de naturlige cellulosefibre til komposit brug på.

Oxidation af lignin ved anvendelse af laccase efter behandling med EDTA og EPG øgede de mekaniske egenskaber af fibre og fiber/epoxy kompositter. Forbedringen i de mekaniske egenskaber skyldes formentlig polymerisation af lignin ved laccase resulterende i en stivere kemisk struktur. Når en del af ligninen blev fjernet før laccasebehandling, blev der observeret en moderat stigning i de mekaniske egenskaber.

Modellering af ændringerne i mekaniske og fysiske egenskaber af kompositter lavet med de forskelligt behandlede hampefibre forbedrede forståelsen af effekten af porøsitet på de mekaniske egenskaber i de ensrettede hampefibre / epoxy kompositter. Det blev påvist, at de anvendte modeller giver et koncept, der skal anvendes til evaluering af ydeevnen af forskelligt behandlede fibre i kompositter. Denne undersøgelse har dermed resulteret i en bedre forståelse af den rolle, de forskellige komponenter bidrager med til trækstyrkeegenskaberne af hampefibrene. Samtidig er fiberbehandlingen optimeret resulterende i forbedrede mekaniske egenskaber af kompositmaterialerne.

LIST OF PUBLICATIONS

This PhD thesis is based on the following papers, which will be referred to by their roman numerals in the text:

I **Ming Liu**, Dinesh Fernando, Geffrey Daniel, Bo Madsen, Anne S. Meyer, Marcel Tutor Ale, & Anders Thygesen
Effect of harvest time and field retting duration on the chemical composition, morphology and mechanical properties of hemp fibers
Industrial Crops and Products, 2015, 69, 29-39

II **Ming Liu**, Dinesh Fernando, Anne S. Meyer, Bo Madsen, Geffrey Daniel, & Anders Thygesen
Characterization and biological depectinization of hemp fibers originating from different stem sections
Industrial Crops and Products, 2015, 76, 880-891

III **Ming Liu**, Marcel Tutor Ale, Barłomiej Kołaczkowski, Dinesh Fernando, Geffrey Daniel, & Anders Thygesen
Comparison of field retting with *Phlebia radiata* Cel 26 retting of hemp fibers for fiber-reinforced composites
Applied Microbiology and Biotechnology, 2016, (submitted 13th September 2016)

IV **Ming Liu**, Diogo Alexandre Santos Silva, Dinesh Fernando, Anne S. Meyer, Bo Madsen, Geffrey Daniel, & Anders Thygesen
Controlled retting of hemp fibers: Effect of hydrothermal pre-treatment and enzymatic retting on the mechanical properties of unidirectional hemp/epoxy composites
Composites Part A: Applied Science and Manufacturing, 2016, 88, 253-262

	Ming Liu, Anne S. Meyer, Dinesh Fernando, Diogo Alexandre Santos Silva, Geffrey Daniel, & Anders Thygesen
V	Effect of pectin and hemicellulose removal from hemp fibers on the mechanical properties of unidirectional hemp/epoxy composites *Composites Part A: Applied Science and Manufacturing*, 2016, 90, 724-735
	Ming Liu, Andrea Baum, Jürgen Odermatt, Jens Berger, Liyun Yu, Birgitte Zeuner, Anders Thygesen, Jesper Holck &Anne S. Meyer,
VI	Oxidation of lignin in hemp fibers by laccase: Effects on mechanical properties of hemp fibers and unidirectional fiber/epoxy composites *Composites Part A: Applied Science and Manufacturing*, 2016, (submitted 3rd September 2016)
	Ming Liu, Anders Thygesen, Anne S. Meyer, & Bo Madsen
VII	Modelling of volumetric composition and mechanical properties of unidirectional hemp/epoxy composites – Effect of enzymatic fiber treatment *IOP Conference Series: Materials Science and Engineering*, 2016, 139, 12-31

TABLE OF CONTENTS

CHAPTER I − Introduction

Hemp is the common name for *Cannabis sativa* cultivated for industrial use. Hemp cultivation allows a diversification of crop rotations in arable farming and has a low requirement for fertilizer and herbicide [1,2]. In addition, hemp is a fast growing crop, producing more fiber yield than most other plant sources, i.e. cotton and flax. More importantly, compared with synthetic materials (e.g. glass fiber), hemp fibers have many advantages such as low cost and low density together with their high stiffness and strength to weight ratio [3–6]. In the past, hemp fibers were widely used for carpets and rope. As environmental awareness has grown, the importance of sustainable, renewable and environmentally friendly materials has also increased considerably in recent years. The development of natural cellulosic fibers to replace synthetic materials in composite applications has in particular gained unprecedented interest [6–10].

1.1 Natural fiber

1.1.1 Physical structure

Hemp stems are 1.5 – 2.5 m tall and 5 – 15 mm in diameter. Hemp fibers produced from hemp stems, which contain 30 – 40% w/w fiber content, are organized in layers from the stem pith toward the surface by 1 – 5 mm xylem, 10 – 50 μm cambium, 100 – 300 μm cortex, 20 – 100 μm epidermis and 2 – 5 μm cuticle, as schematically shown in **Figure 1.1**.

At the microscopic level, primary and secondary single fibers are polygonal in shape, with 4 – 6 sides. The primary single fibers nearest the epidermis are larger and have a cell wall thickness of 6 – 11 μm, cell wall area of 330 – 1500 μm^2, and lumen area of 40 – 170 μm^2, and are formed at the early growth stage [4,11]. The secondary single fibers near the cambium layer are smaller and have a cell wall thickness of 2 – 7 μm, cell wall area of 100 – 260 μm^2, lumen area of 0 – 6 μm^2 [12] . The formation of secondary fibers occurs at the beginning of flowering [4,13]. The secondary fibers are then organized into bundles which produce a distinct layer in the mature stem, in contrast to the primary fibers. The secondary fibers in hemp are primarily located at the bottom of the plant stem and are much shorter (approx. 2 mm long) than the primary fibers (approx. 20 mm long) [12–14].

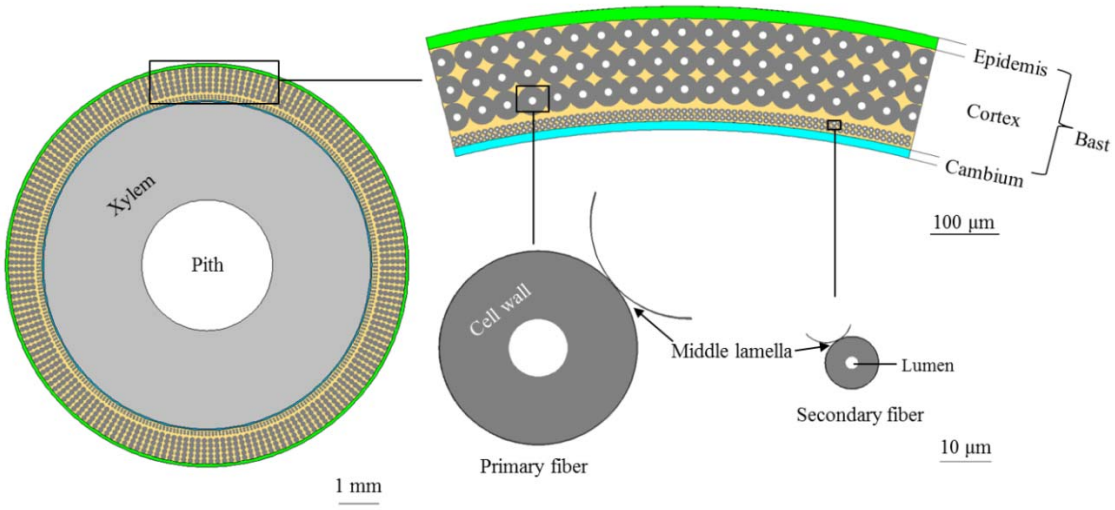

Figure 1.1 Schematic diagram of a transverse section of hemp stem showing the organization and morphology of a bast strip and single fiber (e.g. primary- and secondary fibers) in the bast layer [4].

Under TEM microscopy, single fiber cell walls are found to be mainly composed of primary wall and secondary cell wall. The primary wall has a thickness of 70 – 110 nm (**Figure 1.2**) [15]. The secondary cell wall is composed of a S1 layer (100 – 130 nm in thickness) and a S2 layer (3 – 13 µm in thickness) [15]. The thicker S2 layer has been observed to have a laminate structure consisting of 1 – 4 major concentric layers with a thickness of 1 – 5 µm (**Figure 1.2**) [15].

The cell wall is commonly considered as a composite, as shown in **Figure 1.2**, which is composed of cellulose microfibrils as reinforcements and non-cellulosic polymers, mainly including hemicellulose, pectin, lignin, as matrix polymers [16]. The construction varies greatly between the layers: the primary wall has loosely packed microfibrils which interweave randomly; in the secondary walls, the microfibrils are closely packed and parallel to each other [15,17]. Using X-ray diffraction, the cellulose microfibrils in the S1 layer have been shown to have S-helical orientation with microfibril angles (MFA) in the range of 70 – 90°, while in the outer and inner part of the S2 layer, the microfibrils have Z-helical orientation with MFA in the range of 25 – 30° and 0 − 2°, respectively [15].

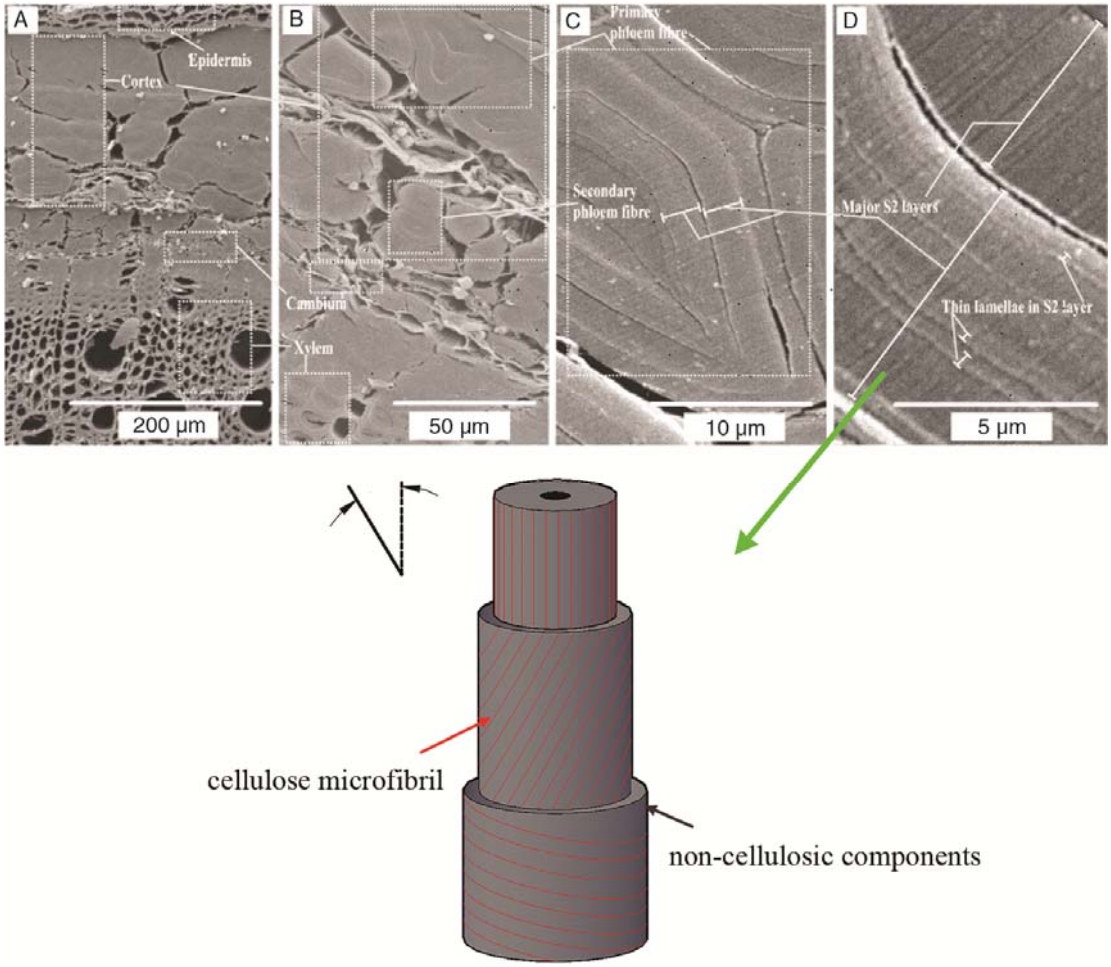

Figure 1.2 Hemp stem shown at increasing magnification using different transverse sections in SEM. A: Xylem + cambium + cortex + epidermis; B: Primary and secondary single fibers; C: Major layers in primary single fiber; D: Thin lamellae within the S2 layer (above) and a model of the microfibril orientation throughout the secondary cell wall (below) [15].

1.1.2 Chemical composition and structure

Hemp fibers, similarly to wood fibers, are mainly composed of cellulose, hemicellulose, lignin and pectin [12,18]. The chemical composition of untreated hemp bast fibers varies with the cultivar [19], harvest year [19], harvest time (or growing stage) [20], the location of fibers within hemp stems [21], and fiber processing [22,23]. The chemical composition of different cultivars hemp fibers reported in the literature is listed in **Table 1.1**. Hemp fibers are composed of 53-91% cellulose, 4-18% hemicellulose or pentosan, 1-17% pectin, and 1-21% lignin. Cellulose consists of linear chains of β-1,4- linked D-glucose units and is organized into microfibrils cross-linked by glycans (e.g. xyloglucan, glucuronoarabinoxylan,

galactomannan, mannan) [24,25]. The interlocked network of microfibrils and glycans is further embedded in a matrix of pectic substances and reinforced with structural aromatic substances (e.g. lignin and hydroxycinnamates) (**Figure 1.3**) [24,26,27]. The aromatic substances presumably add mechanical properties to the cell by interacting with polysaccharides via cross-linking reactions [28,29].

The chemical compositions of fibers and distribution of the constituents define the properties of fibers [30]. Hence, in previous studies, changes in chemical composition of natural fibers after different fiber processing have been commonly used to explain changes in the mechanical properties of fibers and fiber/matrix polymers composites [21,31,32].

Table 1.1 Chemical compositions of hemp fibers.

Cultivar	Cellulose (%)	Hemicellulose (%)	Pectin (%)	Lignin (%)	Reference
USO31	78.4-81.7	5.7-6.4	-	10-13	[19]
Unspecified	58.7	14.2	16.8	6	[33]
Fedora 17	65.6-84.9	6.0-8.1	9.4-25	2.7-4.5	[20]
Felina	57.1-61.8	8.3-14.3	2.8-8.6	1.2-7.3	[34]
Unspecified	76.1-89.2	1.9-12.3	-	2.1-5.7	[35]
Unspecified	82.0-88.9	4.1-8.4	-	2.2-3.8	[36]
Unspecified	88.3-91.0	6.5-9.8	-	1.4-2.1	[37]
Felina 34	64.0-83.0	11.0-15.0	1.0-6.0	1.0-4.0	[38]
USO	54.4	-	8.7	6.1	[39]
Fedora	55	16	8	4	[40]
Felina	64-76	15	1-6	2-4	[15]
Unspecified	53.9-57.6	16.3-18.2	6.5-7.1	20-21	[41]
Fibrimon 56	53.2	6.9	-	5.0	[14]
Fedora 19	58.6	9.3	-	5.0	[14]
Kompolti Sárgaszárú	68.2-69.2	6.7-8.5	-	3.5-5.5	[14]
Kompolti Hybrid TC	60.2-74.3	7.1-7.9	-	3.3-4.4	[14]
Unspecified	63.7-78.4	11.8-17.3	1.9-7.3	1.7-5.0	[42]

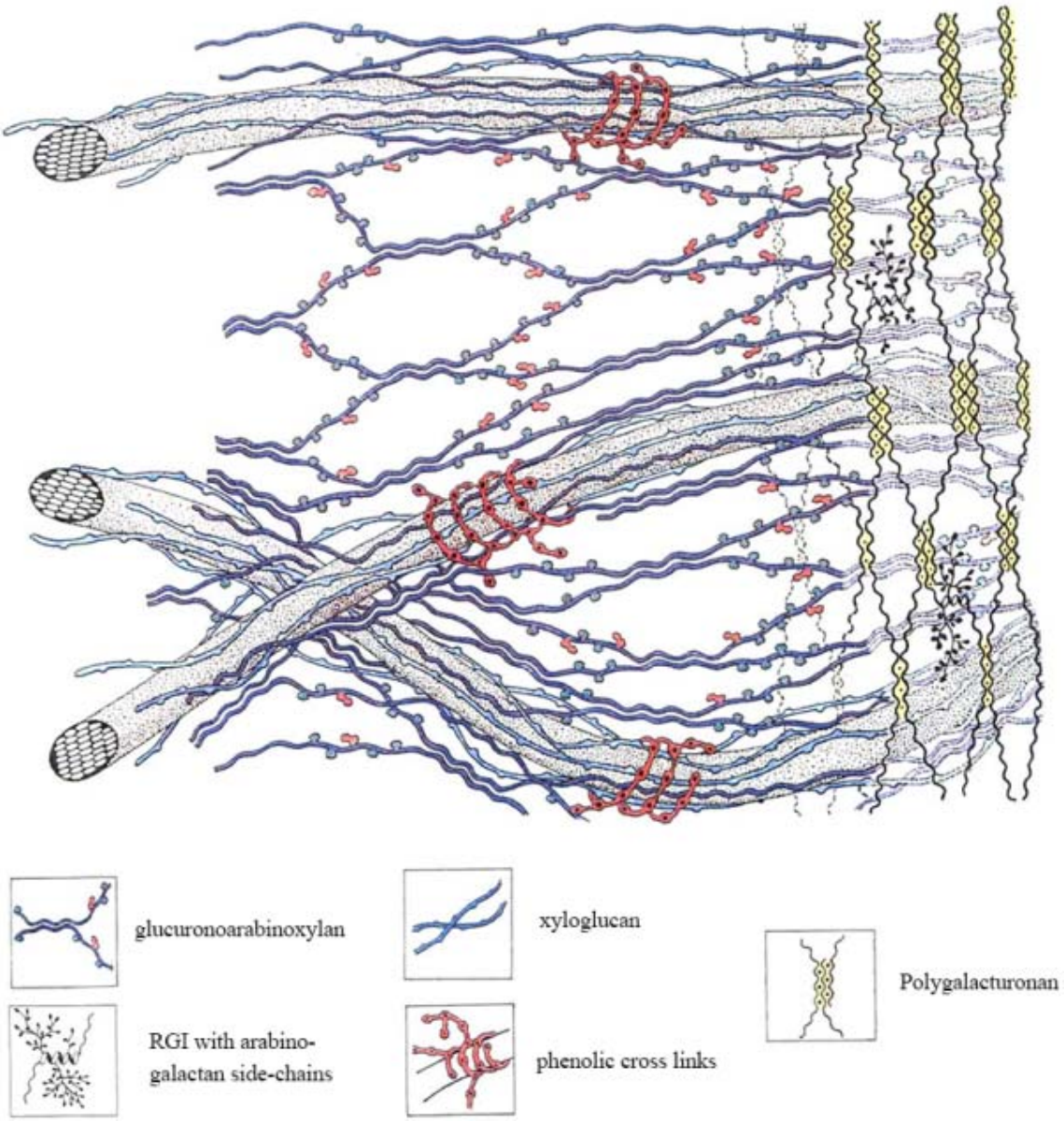

Figure 1.3. Structural model of primary cell walls [24].

1.1.2.1 Cellulose

Cellulose is a homogeneous linear polymer of glucan with repeating β-1,4-D-glucose units bound by glycosidic bounds, as illustrated in **Figure 1.4**. Covalent linkage is formed between the hydroxyl group of the C4 and the C1 carbon atom by water elimination. Cellulose is the most abundant and largest organic polymer in plant cell walls. The glucose monomers in cellulose form hydrogen bonds both within its own chain (intramolecular) to form elementary fibrils, and within neighboring chains (intermolecular) to form 3D- network microfibrils (**Figure 1.5**) [43,44]. Within the cellulose fibrils there are regions where the

cellulose chains are arranged in a highly ordered structure (crystalline), and regions that are disordered (amorphous) (**Figure 1.4**) [44].

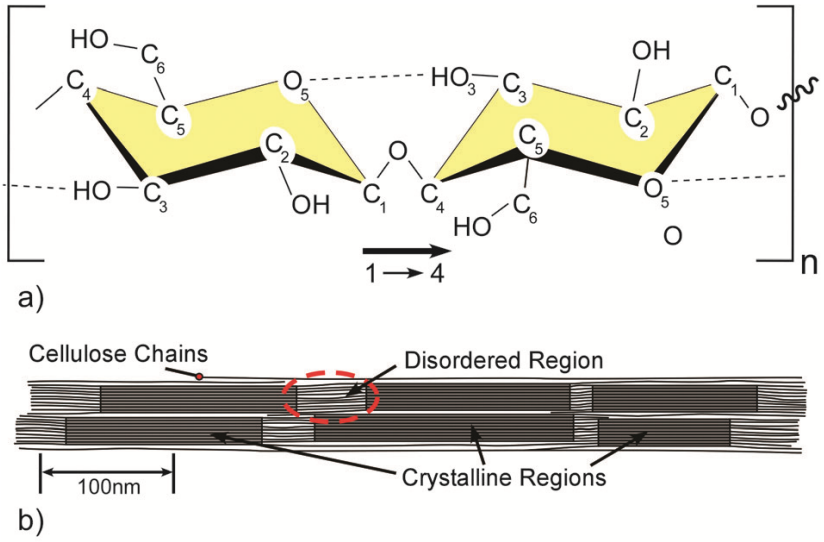

Figure 1.4. Molecular structure of a single cellulose chain (n= DP, degree of polymerization), showing the directionality of the 1→ 4 linkage and intrachain hydrogen bonding (dotted line) (a), schematics of an idealized cellulose microfibril showing one of the configurations of the crystalline and amorphous regions (b)[44].

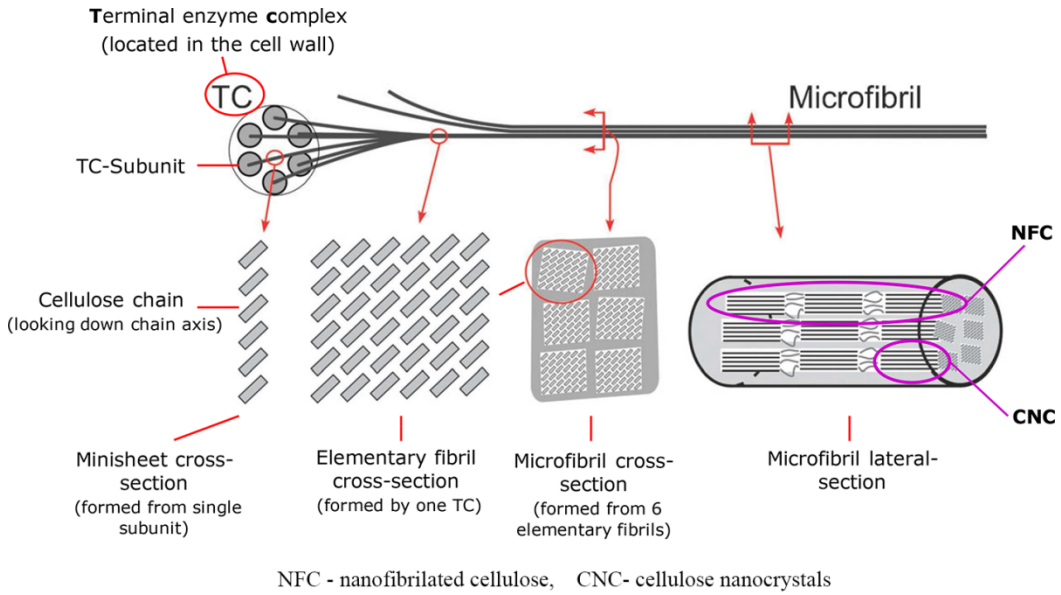

Figure 1.5. Schematic of the different levels of the formation of a microfibril [44].

1.1.2.2 Hemicellulose

Hemicellulose is a heterogeneous group of polysaccharides associated with lignin and cellulose in plant cell walls. Hemicellulose is characterized by having a β-1,4-linked backbone with an equatorial configuration. Hemicelluloses include arabinoxylan, xyloglucans, xylans, mannans and glucomannans, and galactoglucomannan etc. [24,25,45], as illustrated in **Figure 1.6**.

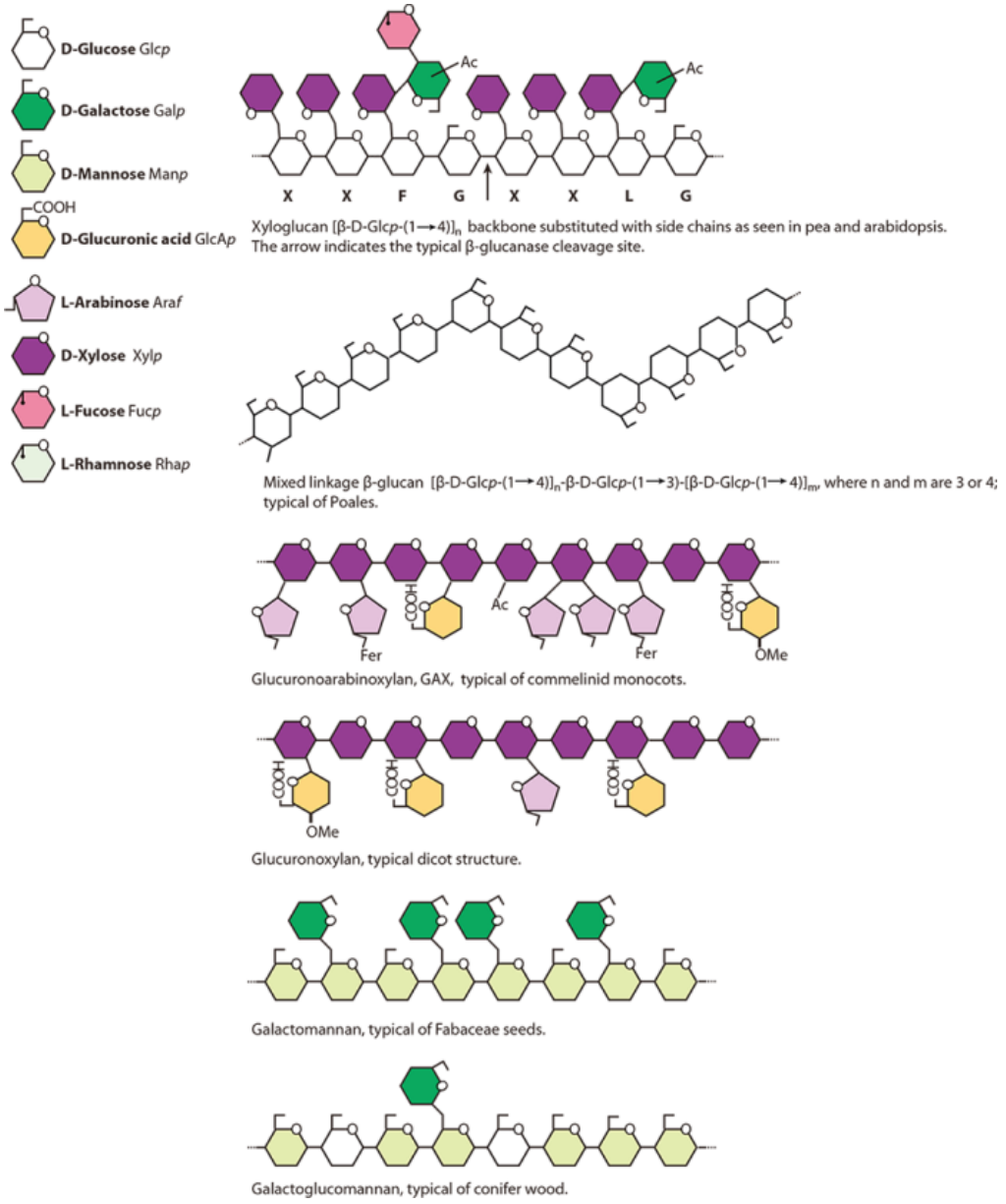

Figure 1.6. Schematic illustration of the types of hemicelluloses found in plant cell walls. ″Fer" represents esterification with ferulic acid (3-methoxy-4-hydroxycinnamic acid) [45].

The detailed structure and abundance of hemicelluloses vary widely between different species and cell types [45,46]. Previous studies have shown that hydroxycinnamic acids (e.g. ferulic acid) actively participate in the cross-linking of arabinoxylans in hemicellulose polymers of plant cell wall, where some arabinose residues are found esterified at the O-5 position with ferulic acid residues [47,48]. Other studies have demonstrated that hemicellulose polymers (e.g. arabinoglucuronoxylan) are linked to lignin by hydroxycinnamates, and that a fraction of the linkages involved a structure of polysaccharide-ester-hydroxycinnamic acid (e.g. ferulic acid)-ester-lignin[49,50]. The hemicelluloses are suggested to contribute to strengthening the cell wall by interaction with other components of plant cell walls [45].

1.1.2.3 Aromatic substances

Lignin is the main aromatic substance in plant cell wall. Lignin is a heterogeneous aromatic biopolymer forming a three-dimensional structure with ether and carbon-carbon linkage between different phenylpropanoid units (**Figure 1.7**) that have been identified as p-coumaryl (H type), coniferyl (G type) and sinapyl (S type) alcohols (**Figure 1.7**).

In addition, hydroxycinnamic acids are a class of aromatic acid, which are present in small quantities in the cell walls of hemp fibers [20]. As mentioned above, hydroxycinnamic acids are involved in the linkage between hemicellulose and lignin [49,50].

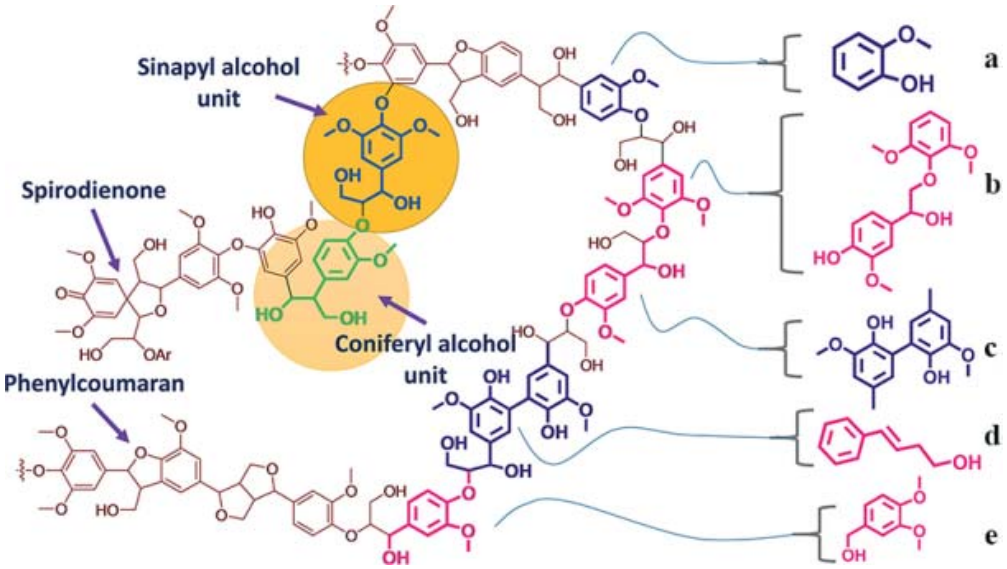

Figure 1.7. Schematic drawing of lignin showing various linkages and lignin model compounds. phenol and methoxy functionalities (a), a β-O-4 linkage (b), a 5-5′ linkage (c), a propyl side chain (d), and a benzylic group (e) [51].

1.1.2.4 Pectin

Pectin is a family of complex linear polysaccharides, which are responsible for the integrity and cohesion of plant cell walls [52–54]. Pectic polysaccharides are most abundant in the primary cell walls and middle lamella region. Pectin mainly contains four pectic polysaccharides including more than 70% homogalacturonan (HG), 20% rhamnogalacturonan I (RG I) and 10% rhamnogalacturonan II (RG II), and small quantities of other substituted galacturonans (e.g. xylogalacturonan) [53,55,56], as illustrated in **Figure 1.8a**.

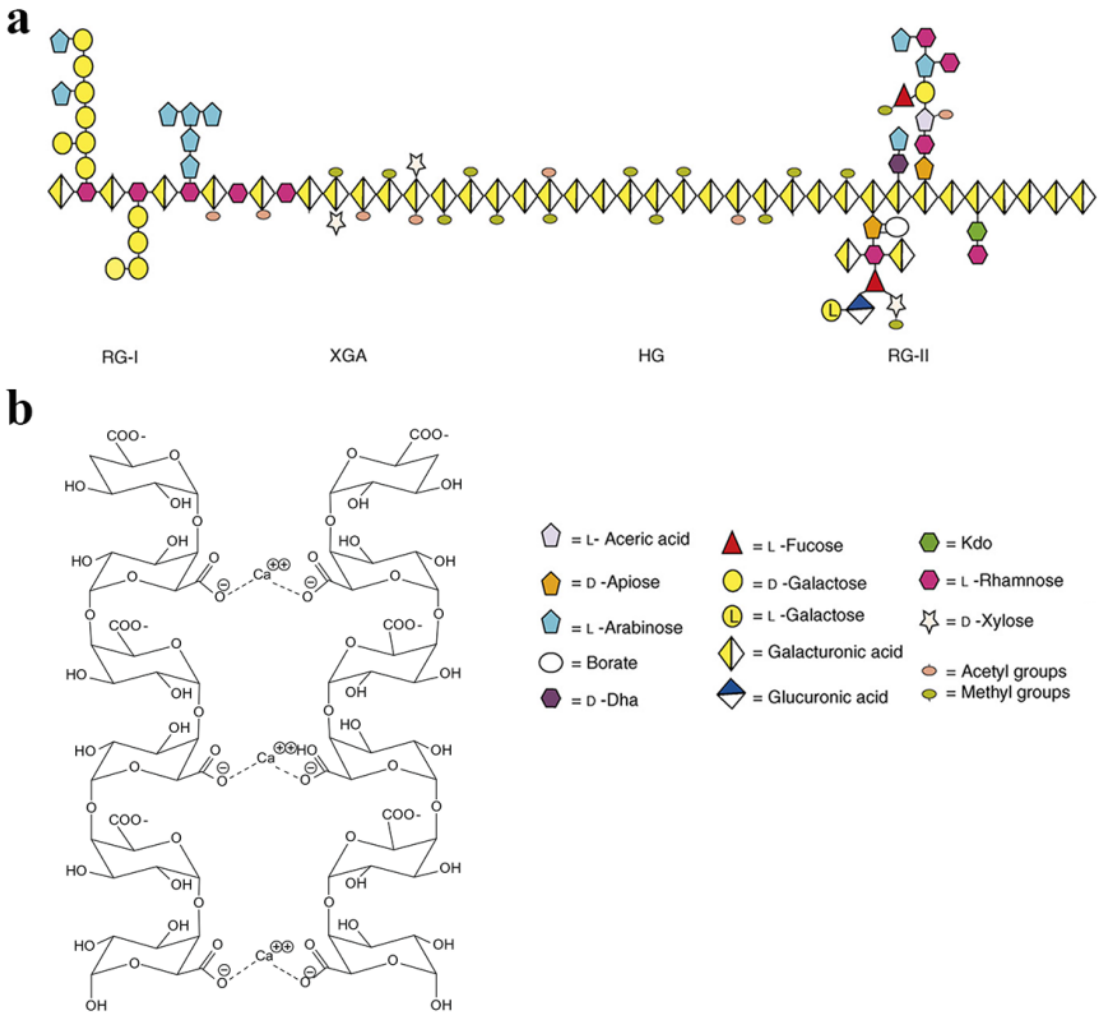

Figure 1.8. Schematic drawing of pectin showing the four pectic polysaccharides including homogalacturonan (HG), rhamnogalacturonan I (RG I), rhamnogalacturonan II (RG II) and xylogalacturonan (XGA) (a) [53], and the egg-box model of calcium crosslinking in HG polysaccharides (b) [56] showing Ca^{2+} involved interactions between two neighboring pectin chains.

The physicochemical properties of pectin are largely dependent on the degree of methyl and acetyl esterification. Low-methoxyl (LM) pectin (i.e. HG) has sufficient carboxyl groups for the formation of calcium-mediated interactions between two neighboring pectin chains, as described by the "egg-box″ model (**Figure 1.8b**) [56,57]. However, high-methoxyl (HM) pectin does not contain sufficient polygalacturonic acid residues unmethylated at the C-6 position to form a stable structure through calcium-mediated interactions. Instead, hydrogen bonding and hydrophobic interactions have been suggested as important forces in maintaining a stable structure for HM-pectin [58,59].

1.1.3 Mechanical properties

Hemp fibers are biodegradable polymers that have many unique advantages, such as low cost, low density, and moderate tensile strength and stiffness. Density and mechanical properties of different varieties of hemp fibers are listed in **Table 1.2**. As shown, the density of hemp fibers is approx. 1.5 g/cm^3. Tensile strength, stiffness and failure strain of hemp fibers are 200-1000 MPa, 18-66 GPa, and 2-4%, respectively.

Synthetic fibers (e.g. glass fiber and carbon fiber) have relatively high tensile strength and stiffness. By contrast, natural fiber has lower fiber density (1.5 g/cm^3) than glass fiber (2.55 g/cm^3). Thus, the specific tensile strength (133- 670 MPa) and stiffness (12-44 GPa) of hemp fibers are comparable to the specific tensile strength (approx. 760 MPa) and stiffness (approx. 30 GPa) of glass fibers. Hemp fibers therefore have potential as replacements for glass fiber as reinforcements for composite materials.

In addition, **Table 1.2** shows that there is large variability in the mechanical properties of hemp fibers. Many efforts have been made to understand better the scattered mechanical properties of hemp fibers [21,60]. A number of studies indicate that many inherent factors may affect the mechanical properties of natural fibers, such as chemical composition [21,61], microfibril angle [61–65], and structure of fiber cell walls [24,66]. These studies have demonstrated the importance of chemical composition and structure of fiber cell walls on the mechanical properties of hemp fibers [21,60,62].

Table 1.2 Mechanical properties of hemp fiber and synthetic fiber.

Fiber type	Density (g/cm^3)	Tensile strength (MPa)	Stiffness (GPa)	Failure strain (%)	Reference
Hemp	1.4-1.5	550-600	25-35	-	[67]
Hemp	1.5	310-750	30-60	2-4	[68]
Hemp		368-482	17.6-19.6	2.5-3	[69]
Hemp		889 ± 472	35.5 ± 17.3	2.6 ± 2.2	[60]
Hemp		699 ± 450	31.2 ± 19.7	3.3 ± 1.6	[60]
Hemp		489 ± 233	33.8 ± 12.2	2.5 ± 1.3	[60]
Hemp		857 ± 260	58	-	[10]
Hemp		886	66	-	[17]
Hemp		636 ± 253	27.6 ± 7.5	2.1 ± 0.7	[70]
Hemp	1.6	200-1000	-		[42]
Glass fiber	2.55	1956	79	-	[71]
Carbon fiber	1.30	3950	238	-	[71]

1.2 Natural fiber reinforced composite

1.2.1 Composite materials

Generally speaking, a composite is considered to be any multiphase material that exhibits a significant proportion of the properties of both constituent phases in such way that a better combination of properties is realized [72]. Many composite materials are composed of two phases only; one is termed the matrix, which is continuous (continuous phase) and surrounds the other phase, often called the dispersed phase or discontinuous phase.

Natural fiber reinforced polymer composites (NFCs) are a type of composites where natural fibers (also called cellulosic fibers) are used as reinforcements in the composite materials. As discussed above, natural fibers have many unique advantages, such as environmental sustainability, low cost, low density, together with high stiffness and strength to weight ratio [5,6]. Research interest has been shifting towards the use of natural fibers as a substitute for synthetic fibers in reinforced polymer composites. There are many reasons for this interest, including the unique advantages of natural fibers and their high potential to replace synthetic fiber for composites use with almost comparable mechanical properties at lower cost [73,74]. The advantages and disadvantages are summarized in **Table 1.3**.

Table 1.3 Advantages and disadvantages of NFCs [5,74,75].

Advantages	Disadvantages
➢ Low density	➢ Low durability compared to synthetic fiber composites, but can be improved with fiber treatments
➢ High specific stiffness and strength	➢ High moisture absorption can result in fiber swelling
➢ Biodegradability and production of natural fibers has low impacts on environment	➢ Lower strength and stiffness compared to synthetic fibers
➢ Fibers can be produced at lower cost than synthetic fibers	➢ Considerably higher variability in mechanical properties of fibers
➢ Low hazard manufacturing process	➢ Lower thermal stability
➢ Low emission of toxic fumes when subjected to heat and during incineration at the end of life	➢ Less stable when subjected to natural microorganisms because cellulose fibers are biodegradable

1.2.2 Mechanical properties

In principle, the mechanical properties of composite depend not only on the fiber themselves but also on the degree to which an applied load is transmitted to the fibers by the matrix polymers under stress [72]. The principle is illustrated in **Figure 1.9**, where several of important parameters are listed that influence mechanical properties of composites. As shown, the factors include: (a) fiber properties; (b) matrix properties; (c) fiber length; (d) fiber packing ability; (e) fiber orientation; (f) porosity; (g) fiber volume content; (h) fiber/matrix interface properties et al [74].

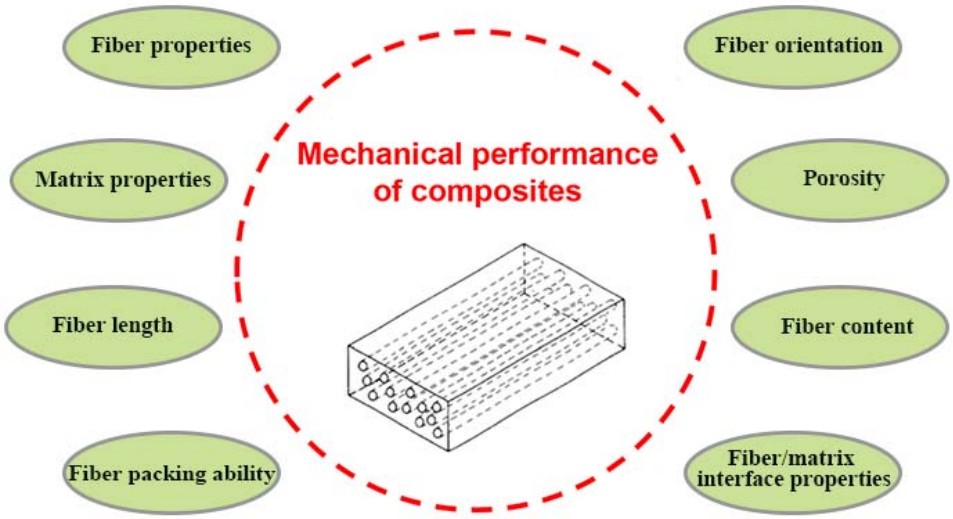

Figure 1.9. The performance of composites with fibers in a polymer matrix is governed by a range of parameters.

1.2.2.1 Mechanical properties of composites: stiffness and strength

A large number of modified rule of mixtures models for stiffness and strength of composites have been proposed in the literature [76,77]. In one of these models, through including the effect of porosity, the stiffness (E_c) and strength (σ_{cu}) of composites with a unidirectional fibers orientation and with continuous fibers can be expressed by Eq. 1 and Eq.2, respectively.

$$E_c = \left(V_f E_f + V_m E_m\right)\left(1 - V_p\right)^{n_E} \quad (1)$$

$$\sigma_{cu} = \left(V_f \sigma_{fu} + V_m \sigma_m^*\right)\left(1 - V_p\right)^{n_\sigma} \quad (2)$$

where E is the stiffness, V is the volume content, the subscripts c, m, f and p are composite, matrix, fiber and porosity, respectively. σ_{cu} is the composite strength, σ_{fu} is the fiber strength, and σ_m^* is the stress in the matrix at the failure strain of the composite, and n_E and n_σ are the porosity efficiency exponents (PEE) for stiffness and strength, respectively. When PEE =0, it is assumed that the porosity in the composites has no effect on the mechanical properties of the composites beyond lowering the load bearing volume. When PEE > 0, it is suggested that the porosity in the composites has an effect on the mechanical properties of composites by introducing stress concentrations [76].

As shown in Eq.1 and Eq.2, besides the effect of composite porosity, composite stiffness (E_c) and strength (σ_{cu}) are governed by the volume content of fibers (V_f) and of matrix (V_m) as well as the properties of the individual parts, E_f and σ_{fu} for fibers, and E_m and σ_m for matrix. The volume content of fibers (V_f) and of matrix (V_m) can be determined from the fiber mass to matrix mass ratio (or fiber weight content) that is the direct parameter used to manufacture composite, and from the properties of fibers and matrix polymers such as fiber and matrix density. Hence, composite stiffness (E_c) and strength (σ_{cu}) can be correlated with a simple parameter, i.e. fiber weight content that is used for composite manufacturing as input, as shown in **Figure 1.10**.

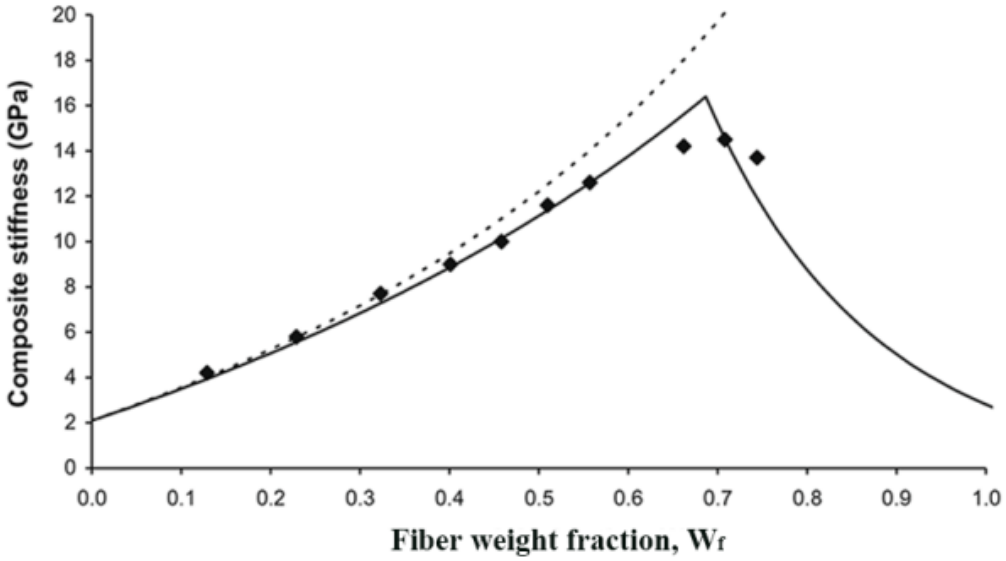

Figure 1.10. Stiffness of glass fiber reinforced polypropylene composites vs. glass fiber weight content [76], showing that the model line based on Eq.1 fits well with experimental data (♦) .

1.3 Effect of fiber treatment on properties of fibers and composites

As discussed in Section 1.2.1, NFCs have many disadvantages such as lower stiffness and strength compared to synthetic fibers (e.g. natural fibers) and large variability in their mechanical properties. But it has also been shown that those disadvantages can be more or less overcome by fiber treatment. In principle, the aim of fiber processing is to obtain more separated and cellulose rich fibers by removing non-cellulosic components and in that way to optimize the strength and form of the fibers before they are used as reinforcement in composites. Traditional cellulose fiber processing methods for hemp and flax fibers for use, mainly in yarn production, include field retting (also called dew retting) and water retting (**Figure 1.11**). This process has been studied and the local microbial communities has been shown to include fungi such as *Cladosporium* sp. and *Cryptococcus* sp. as well as bacteria including *Escherichia coli* [78,79]. These retting methods remove non-cellulosic components via spontaneously flourishing microbial activity, and these methods have been reported to have negative impacts on both fiber properties and the environment [36]. Many efforts have been made to develop new fiber processing methods to replace traditional field retting and water retting in order to obtain a high quality of natural fibers for NFCs application in recent years [15,22,38,80–84].

Figure 1.11. Image showing field retting (left, https://en.wikipedia.org/wiki/Retting) and water retting (right, http://www.thedailystar.net/jute-rotting-pollutes-chitra-44210).

Those studies have focused on development of new fiber treatment methods to replace conventional retting methods. According to the reagents used, the investigated fiber treatments can be divided into three categories: (1) controlled fungal retting [15,18,38,85]; (2) chemical treatment [22,33,86–89]; (3) enzyme treatment or retting [22,82,84,87,88,90,91].

1.3.1 Controlled fungal retting

An alternative retting method is the microbiologically controlled use of selected fungi to degrade non-cellulosic components in the fibers [15,18,38,85]. Thygesen et al. have investigated the effect of fungal defibration and depectinization selectivity of *Phlebia radiata* Cel 26 and *Ceriporiopis subvermispora*. They found that the mutated white rot fungus *P. radiata* Cel 26 can selectively degrade the epidermis and the lignified middle lamellae and thus facilitate production of small fiber bundles. Moreover, *P. radiata* Cel 26 exhibited a higher depectinization selectivity of 6.0 than *C. subvermispora* with a selectivity of 4.6 [18]. Composites with *P. radiata* Cel 26 treated hemp fibers exhibited a far fewer void content compared to composites with the other types of fibers (e.g. raw hemp fibers, water retted fibers and commercial hemp yarn) (**Figure 1.12**) [38]. Consequently, composites with *P. radiata* Cel 26 treated hemp fibers exhibited higher stiffness and tensile strength compared to composites with the other types of hemp fibers (**Figure 1.13**).

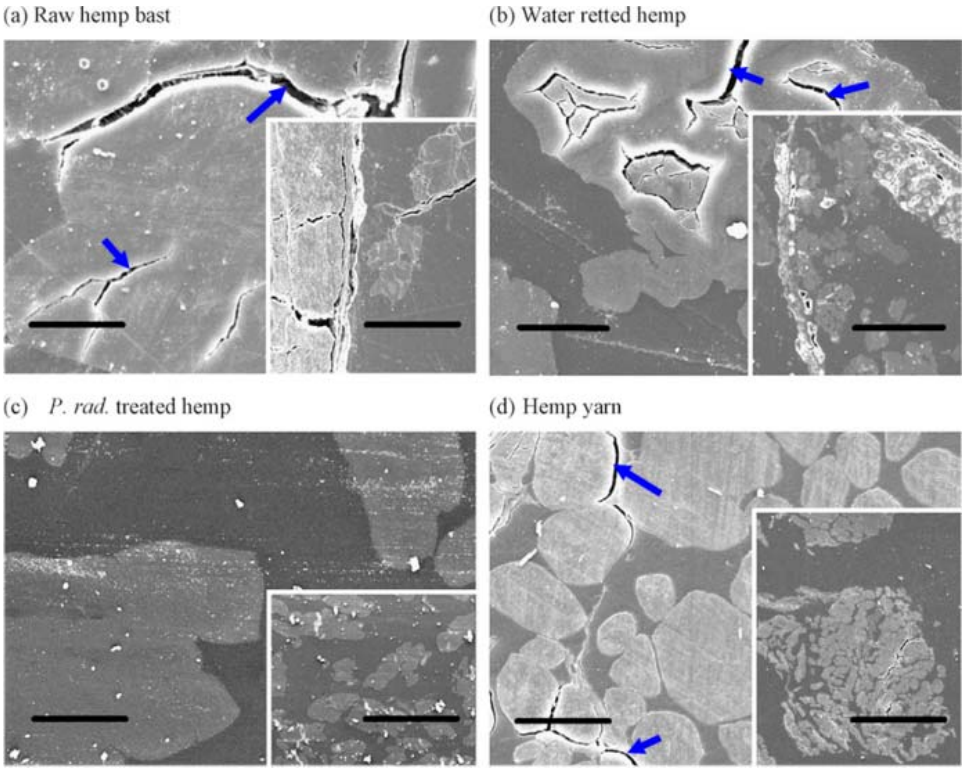

Figure 1.12. SEM microscopy images of transverse sections of composites with different type of hemp fibers [38]. The blue arrows show voids at fiber/epoxy interfaces. The scale bar in the left image is 20 µm and in the right image is 200 µm.

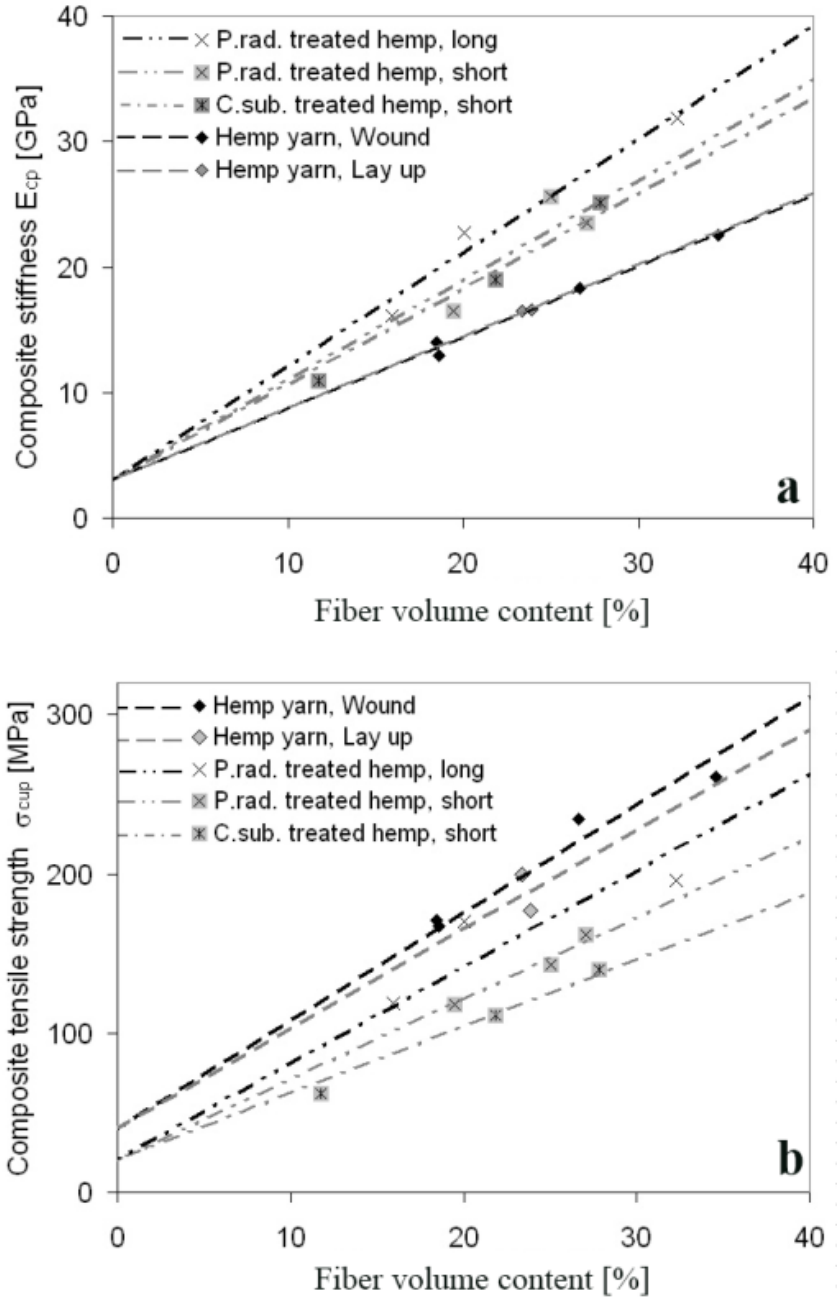

Figure 1.13. Stiffness (a) and tensile strength (b) of composites with differently treated fibers vs. fiber volume content [38].

In addition, compared to untreated hemp fibers, improved interfacial shear strength (IFSS) was found for hemp fibers treated with white rot fungi *Schizophyllum commune* when the fibers were used in fiber reinforced polypropylene (PP) composites [85]. The result indicates that the hemp fiber interfacial bonding with PP was improved by treatment with *Schizophyllum commune*.

1.3.2 Chemical treatment

Some research work has been conducted on non-cellulosic removal (e.g. removal of hemicellulose and pectin) and on the surface characteristics of chemically treated natural fibers. The physico-chemical and mechanical properties of natural fibers can be changed significantly by chemical treatments depending on the concentration of chemical agent and the duration of processing time [88].

Polymorphic transformation of cellulose I into cellulose II within the crystalline domains of flax fibers has been found to be determined by concentration of alkali. Alkali concentrations of 6-10% NaOH solution did not cause polymorphic changes within flax fiber cellulose, while increasing NaOH concentrations to more than 10% stimulated the polymorphic transformation of cellulose I into cellulose II [89]. The changes in polymorphic features of cellulose from cellulose I into cellulose II may alter the mechanical properties of natural fibers [92,93] due to differences in mechanical properties between cellulose I and cellulose II. Increased adhesion between flax fibers and unsaturated polyester was achieved using classical sodium hydroxyl plus acetic anhydride based treatments and with formic acid treatment [94].

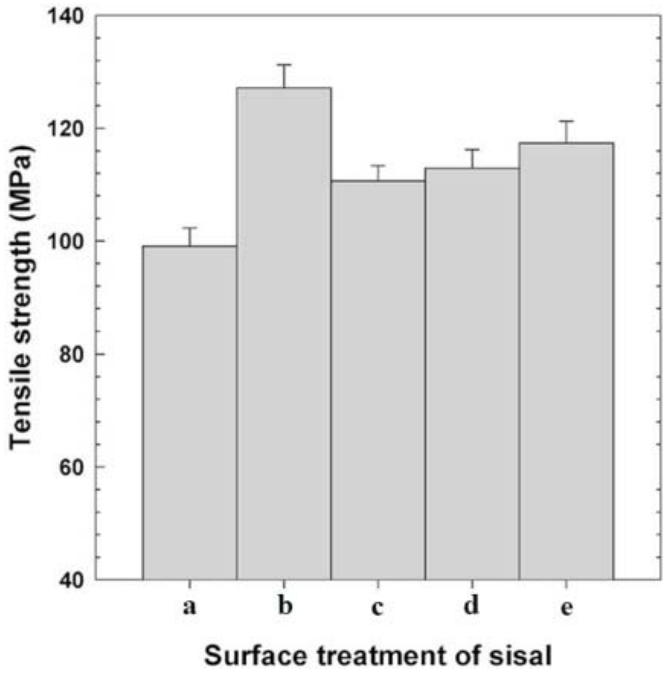

Figure 1.14. Effect of fiber treatment on the tensile strength of sisal/glass hybrid polyester composite (glass = 5.7 wt.%, total fiber content = 30% wt.%) [95]. Control (a); 5% NaOH (b); 10% NaOH (c); cyanoethylation (d); acetylation (e).

Mishra et al. have been reported that 5% NaOH treated sisal/glass hybrid polyester composite exhibited much higher tensile strength (approx. 130 MPa) compared to 5% untreated sisal/glass hybrid polyester composite (approx. 100 MPa) (Figure 1.14) [95]. The increase in the tensile strength of composites may be due to the improved adhesion between fibers and polyester polymers. However, when a high concentration of NaOH (e.g. 10%) was applied, the strength of the composites decreased (**Figure 1.14**) [95]. It has been suggested that this outcome is due to excess delignification of natural fibers resulting in weaker or damaged fibers [95,96].

1.3.3 Enzyme treatment

Enzyme treatment (also named as enzyme retting in the literature) involving treatment mainly with pectinolytic enzymes, offers an alternative method. This method would be both more controlled and would overcome the limitations of traditional methods with respect to time, efficiency and environmental impact. In enzyme treatment of fibers, pectic polymers are released from the middle lamella (ML) and fiber cell walls by using pectinases (e.g. endo-polygalacturonase) that randomly hydrolyze the glycosidic bonds of the homogalacturonan (HG) backbone to liberate monomeric, dimeric, or oligomeric fragments [97]. The degradation of pectin from ML allows fibers to be separated and improves adhesion between fibers and matrix polymers. Many efforts have been made to obtain optimum fibers for composite use by enzyme treatment [22,82,84,87,88,90,91].

A pectinase-rich commercial enzyme Viscozyme L was tested on flax fiber, but the mechanical properties were decreased after enzyme treatment [98]. Different crude polygalacturonases (PGases) were tested for flax fiber treatment; the crude PGases differed in their ability to ret flax fibers, with *A. niger* PGase being the best retting agent among all investigated PGases because it produced the fibers with the highest strength[82]. However, retting using PGases of *Rhizopus* produced the weakest fibers. Targeted enzymatic removal of pectin with commercial enzymes from hemp bast fibers has previously found to improve the coherence between fibers and matrix polymers and to produce positive effects on hemp fiber reinforced composites [84,99]. However, it appears that enzymes alone cannot penetrate the hemp fibers and efficiently degrade pectin [34].

The accessibility of the substrate surface to enzymes is of prime importance in enzymatic treatments involving insoluble substrates. Addition of chemical chelators (e.g. ethylenediaminetetraacetic acid (EDTA)) has been shown to promote enzyme catalyzed degradation of HG from cellulosic fibers during

enzymatic treatments [100,101]. The enhanced enzymatic degradation of HG results from the capacity of chemical chelators to form complexes particularly with calcium in pectin [102].

CHAPTER II − Hypotheses and Objectives

As briefly introduced in Chapter 1, many efforts have been made to promote the application of natural cellulose fibers in fiber reinforced composites. The negative impacts of traditional fiber treatments (e.g. field retting and water retting) on fiber properties and environment have been recognized even through these methods have been used for quite a long time. A series of experiments was conducted to understand the effect of different fiber treatments on the mechanical properties of fibers and fiber reinforced composites. However, the effects of traditional retting, fungal retting with some species of white rot fungi (e.g. *C. subvermispora*) and even with commercial enzymes on the properties of natural fibers has not been fully understood. To develop new fiber treatments, the key factors that influence the properties of fibers during those treatments must be well and systematically studied.

Cellulosic fibers are primarily composed of cellulose, hemicellulose, lignin and pectin. Understanding the contribution of different components to the tensile properties of cellulose fibers will greatly help to reshape and optimize cellulose fibers for application in composites. Hence, a deeper insight from the perspective of both basic and applied science is needed into the component interactions in the highly intermixed structure of natural fiber cell walls. In particular, a better understanding is needed into the role of different constituent of fiber cell wall in contributing to the mechanical properties of fibers.

Lastly, to optimize fiber treatments, the correlation between chemical composition of natural fibers, structural properties of natural fibers and fiber reinforced composites needs to be established. The PhD study was conducted in order to realize the above purpose and expedite the application of natural fibers in polymer matrix composites.

2.1 Hypotheses

Hemp fibers were selected as starting materials for fiber treatments in this study. This PhD study was built up based on the following hypotheses:

- Chemical composition, distribution of each constituent and structure of natural fibers affect the mechanical properties of hemp fibers;
- The negative impact of field retting (or water retting) on mechanical properties of hemp fibers is due to the action of cellulase enzyme activity during the retting period;

- The improved mechanical properties of hemp fiber reinforced polymer composites that results from fiber treatments is mainly due to the reduction in composite void content;
- The decrease in composite void content can be linked to the removal of non-cellulosic components by fiber treatments;
- Polymerization of aromatic substances in hemp fibers can further improve the mechanical properties of hemp fiber reinforced composites after pectin removal from hemp fibers;
- Modified rule of mixture models by including effect of composite voids provide a tool to assess the performance of differently treated hemp fibers in composites.

2.2 Objectives

The main objective of this study was to test the above hypotheses. The following specific objectives were constructed to meet this goal:

- To study and relate the mechanical properties of untreated hemp fibers with the chemical composition and morphology of natural fibers;
- To assess the effect of traditional field retting on chemical composition and mechanical properties of fibers and fiber reinforced composites;
- To investigate different enzyme activity, especially pectinase and cellulase enzyme activity, in extracts from field retted and controlled fungal retted fibers and establish the correlation between mechanical properties of differently treated fibers and different enzyme activity;
- To establish the correlation between mechanical properties of hemp fiber reinforced composites and composite void content;
- To establish the correlation between mechanical properties of hemp fiber reinforced composites and chemical composition of fibers after different treatments;
- To investigate the effect of polymerization of aromatic substances in hemp fibers by laccase treatment on mechanical properties of hemp fibers and hemp fiber reinforced composites;
- To investigate the changes in the content and structure of aromatic substances by laccase treatment.

- To compare the fit between experimental results of physical and mechanical properties of composites containing differently treated hemp fibers and results calculated from applied models.

CHAPTER III − Characterization of untreated hemp fibers: effect of harvest time and stem sections on properties of fibers

In order to know the characteristics of the untreated hemp fibers used as the starting materials for this study, the first requirement of this thesis was to characterize the starting materials. Harvest time and stem section were chosen as two parameters which might affect the mechanical properties of hemp fibers under investigation. To assess the effect of harvest time and stem section on fiber properties and on the later fiber processing, the chemical composition, morphology and mechanical properties of hemp fibers were analyzed.

3.1 Hypotheses

- Harvest time and stem section affect mechanical properties of hemp fibers through differences in chemical composition and morphology of hemp fibers;
- Cellulose is the main component strengthening fiber cell walls, so the higher the content of cellulose in hemp fibers, the higher mechanical properties they exhibit.

3.2 Related papers

This chapter was based on the following published papers.

I **Ming Liu**, Dinesh Fernando, Geffrey Daniel, Bo Madsen, Anne S. Meyer, Marcel Tutor Ale, & Anders Thygesen

Effect of harvest time and field retting duration on the chemical composition, morphology and mechanical properties of hemp fibers

Industrial Crops and Products, 2015, 69, 29-39

II **Ming Liu**, Dinesh Fernando, Anne S. Meyer, Bo Madsen, Geffrey Daniel, & Anders Thygesen

Characterization and biological depectinization of hemp fibers originating from different stem sections

Industrial Crops and Products, 2015, 76, 880-891

3.3 Significance of the study

Natural cellulosic fibers, such as hemp fibers, have moderate tensile strength (300 – 800 MPa) and stiffness (30 – 60 GPa), and high stiffness and strength to weight ratio [6], but their mechanical properties vary greatly [60]. It has previously been reported that many factors, including variety [60], growth stage of the plant [103], growth conditions [104], stem section [69], and harvest year [69] etc, can affect the physical properties of hemp fibers. Therefore, it is important to gain an improved understanding of the changes in mechanical properties of fibers in relation to morphological features and chemical composition of fibers at varied harvest time and from different stem sections.

3.4 Experimental consideration

The hemp (Cannabis sativa L.) variety USO-31 used was sown in France (N 48.8526°, E 3.0190° (WGS84)) on May 5th 2013. The hemp plants were harvested at two growth stages: (1) at the beginning of flowering (i.e. early harvest on July 18th 2013); and (2) at seed maturity (i.e. late harvest on Sep 6th, 2013). The late harvested hemp stems were selected for the investigation of stem section effects. Three stem sections were defined on one hemp stem: bottom (one third above the base of the stem), top (one third under the inflorescence base), and middle (between bottom and top sections).The hemp bast fibers strips were manually peeled from the hemp stems for chemical composition and mechanical properties tests.

Generally, for this study, there were three reasons for choosing two growth stages of hemp plants, namely at the beginning of flowering, and at seed maturity. First, at the beginning of flowering, fiber cell walls are almost mature and exhibit good mechanical properties with less lignin deposition on fiber cell walls [105]. Second, lignification proceeds rapidly after flowering [106], so late harvested fibers might have higher lignin content which may affect the mechanical performance of fibers. Third, hemp seeds could also be harvested as a product of hemp plants if fibers can be harvested at seed maturity stage.

3.5 Highlights

Reduction in bast content and thickness of the primary bast fiber layer in stems were found to be highly significant with plant maturity, but fiber lumen (%) did not change with plant maturity. A significant increase in the secondary fiber fraction occurred with fiber maturity, and reached a maximum value of 10% at seed maturity stage.

A reduction was detected in cellulose content (indicated by glucan content) of fiber cell walls from 66% for early harvested fibers to 61% for the late harvested fibers. A statistically significant increase in lignin deposition from 3.4% to 4.8%, and a slight decrease in pectin content of fiber cell walls with fiber maturity were observed. These changes in chemical composition of fibers with fiber maturity were further confirmed by microscopy observations and histochemical analyses (**Figure 3.1**). As a result of those differences in morphological features and chemical compositions, fibers harvested at the beginning of flowering were found to exhibit higher tensile strength of 950 MPa, stiffness of 35 GPa, and failure strain of 6.0%, which confirmed our hypotheses.

An effect of stem sections on chemical composition and morphology of fibers was confirmed. Pectin content of fibers was found to increase from the bottom to the top stem sections, while lignin content increased from the top to the bottom stem sections. The highest proportion of secondary fibers was mainly found at the bottom. Consequently, fibers from the top and middle stem sections exhibited better mechanical properties than those from the bottom stem sections (**Figure 3.2**).

Overall, the study showed that mechanical properties of untreated hemp fibers were related to the chemical compositional make-up and morphological properties of hemp fibers, notably the secondary fiber cell contents.

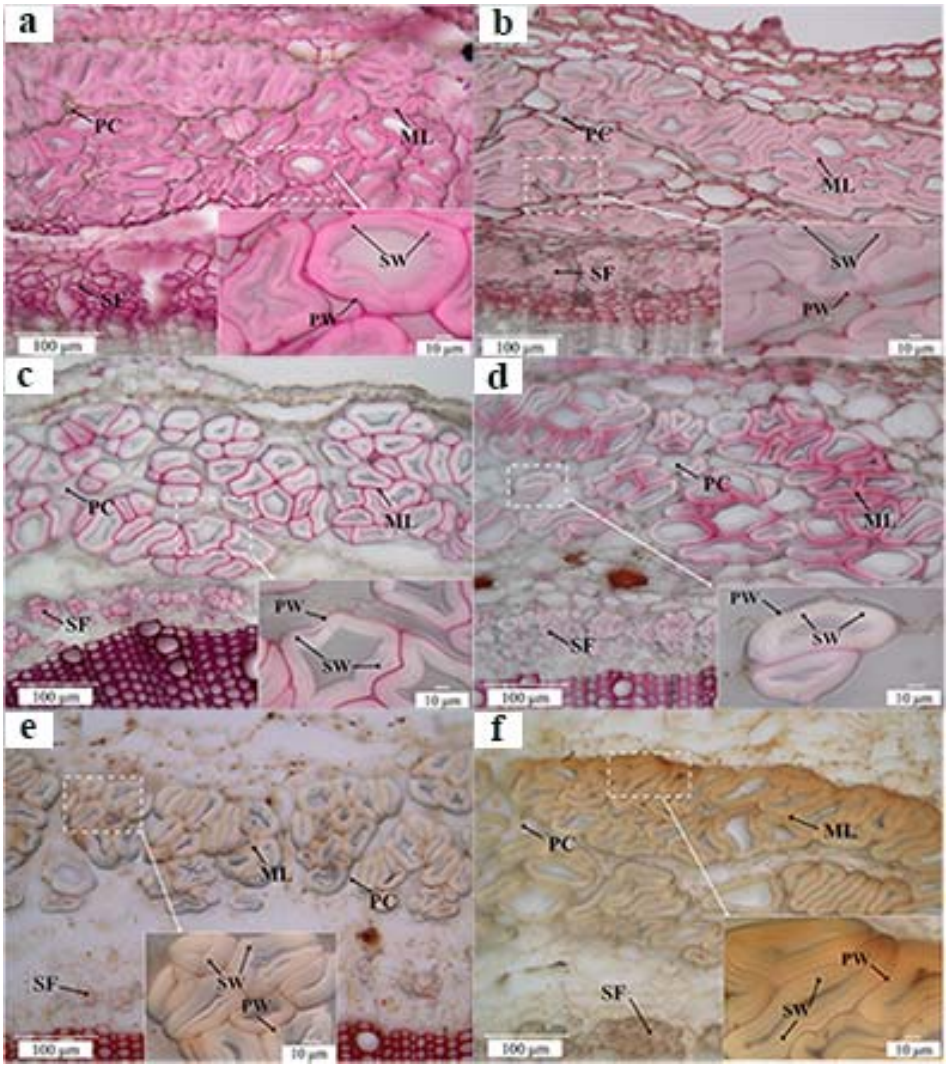

Figure 3.1. Micrographs showing transverse sections of hemp stems isolated from early- and late harvest samples after staining for pectin using ruthenium red (a-b) and for lignin using Wiesner (c-d) and Mäule reagents (e-f).

Ml- middle lamella; PC-parenchyma cell; PW-primary wall; SF-secondary fiber; SW- secondary wall.

(a) and (b): positive reaction for pectin in hemp stems from early harvest (a) and late harvest (b);

(c) and (d): positive reaction for guaiacyl lignin units in hemp stems from early harvest (c) and late harvest (d);

(e) and (f): positive reaction for syringyl lignin units in hemp stems from early harvest (e) and late harvest (f). (from Paper I)

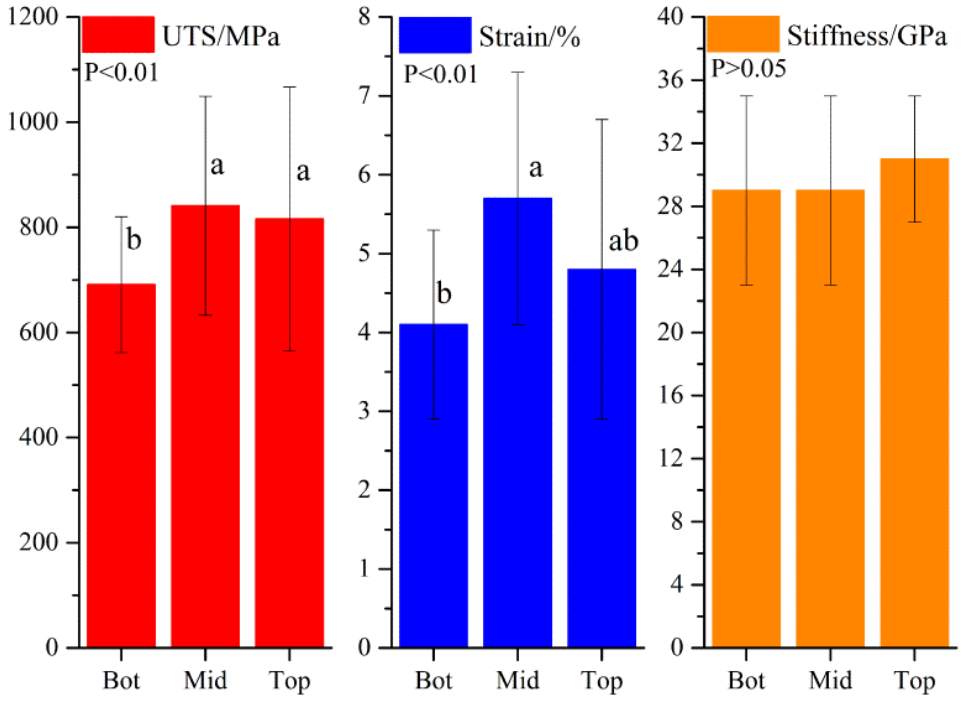

Figure 3.2. Ultimate tensile strength (UTS), strain and stiffness of untreated hemp fibers from bottom (Bot), middle (Mid) and top (Top) stem sections. Values within a group that do not share a letter are significantly different at the 5% level. (from Paper II)

CHAPTER IV Comparison of field retted and fungal retted hemp fibers for fiber reinforced composites

Fiber processing is necessary and important to produce suitable natural cellulosic fibers for application in high-grade biocomposite materials. In principle, the aim of fiber processing is to obtain more separated and cellulose rich fibers by removing non-cellulosic components and thus optimize the strength and form of the fibers before they are used as reinforcements in composites. Traditional retting processing, including field retting (also known as dew retting) and water retting, has been commonly used to remove non-cellulosic components from natural fibers. In field retting, hemp stems are spread out in the fields where they are attacked by spontaneous flourishing microbial activity. This process may potentially damage fibers due to the presence of cellulolytic enzyme activities. Despite its long use, the process is still largely empirical. To some extent, a more controlled retting process with selected fungi can overcome the disadvantages of the field retting process. This chapter describes comparisons of traditional field retting and more controlled fungal retting conducted to elucidate the effect of biological treatment of hemp fibers on mechanical properties of fibers and fiber reinforced composites.

4.1 Hypotheses

- Traditional field retting produces a negative impact on the mechanical properties of hemp fibers, and controlled retting with the mutated white rot fungus *P. radiata* Cel 26 produces better fibers with higher stiffness and strength;
- The mutated white rot fungus *P. radiata* Cel 26 has greater selectivity value (weight loss of pectin/weight loss of cellulose) in degrading pectin in hemp fibers than field retting or controlled retting with *C. subvermispora*;
- Effect of different fiber retting methods on properties of fibers can be explained by enzyme activity in extracts from differently retted hemp fibers.

4.2 Related papers

This chapter was based on the following published papers.

I **Ming Liu**, Dinesh Fernando, Geffrey Daniel, Bo Madsen, Anne S. Meyer, Marcel Tutor Ale, &

Anders Thygesen

Effect of harvest time and field retting duration on the chemical composition, morphology and mechanical properties of hemp fibers

Industrial Crops and Products, 2015, 69, 29-39

II **Ming Liu**, Dinesh Fernando, Anne S. Meyer, Bo Madsen, Geffrey Daniel, & Anders Thygesen

Characterization and biological depectinization of hemp fibers originating from different stem sections

Industrial Crops and Products, 2015, 76, 880-891

III **Ming Liu**, Marcel Tutor Ale, Barłomiej Kołaczkowski, Dinesh Fernando, Geffrey Daniel, & Anders Thygesen

Comparison of field retting with fungal retting using *P. radiata* Cel 26 for hemp fiber treatment aiming at fiber reinforced composites

Applied Microbiology and Biotechnology, 2016, (submitted)

4.3 Significance of the study

Traditional field retting is largely empirical and subject to weather conditions. The identification of microorganisms involved in field retting and assays of enzymes secreted by the microorganisms could improve understanding of changes in chemical composition and mechanical properties of fibers during field retting. Improved understanding would then help in optimizing retting processing and in avoiding severe degradation of cellulosic fibers.

The crucial factors involved in maintaining fiber mechanical properties may be revealed through a comparison of traditional field retting and more controlled fungal retting by assessing the different responses of hemp fibers to field retting and fungal retting with different selected fungi. The study can also help to develop new enzymatic fiber processing to obtain high mechanical properties of fibers for composite use.

4.4 Experimental consideration

During the retting process, it is hypothesized that cellulolytic enzyme activity is the crucial factor that affects the physical properties of hemp fibers. To verify this hypothesis, a wild-type white rot fungus (i.e. *Ceriporiopsis subvermispora*) and a mutated white rot fungus (i.e. *Phlebia radiata* Cel 26) were used for controlled fungal retting; the mutated white rot fungus *P. radiata* Cel 26 produces less cellulolytic enzymes than its wild types and other wild white rot fungi (e.g. *C. subvermispora*). Controlled fungal retting was carried out on hemp stems for 7, 14, and 20 days in the laboratory under controlled conditions. In order to compare with traditional retting process, field retting was carried out for 7, 14, and 20 days after harvest. The changes of microbial communities during field retting were analyzed, after which, enzyme activities (e.g. cellulolytic, hemicellulolytic, and pectinolytic enzymes activity) were measured in order to explain the changes in the mechanical properties of fibers and fiber reinforced composites.

The effect of starting materials on the performance of biological retting was considered. According to the findings in Chapter 1, chemical composition of fibers, and particularly lignin content, varies from the top to the bottom stem sections. Lignin is known as a barrier for the entry of microorganisms and inhibits fiber extraction and depectinization by biological methods. To investigate the effect of starting materials on the performance of fungal retting, stem pieces from different stem sections (i.e. top, middle and bottom) were selected for fungal retting. The response of hemp fibers from different stem sections to fungal retting was recorded and compared to optimize the fungal retting and obtain high quality hemp fibers.

4.5 Highlights

A negative effect of field retting on mechanical properties of hemp fibers was found with extended field retting, while the mechanical properties of fibers maintained during controlled fungal retting with *P. radiata* Cel 26. These results were confirmed by the differences in glucanase activity between field retted and fungal retted hemp fibers. Field retted fibers were shown to have higher glucanase activity. Glucanase activity reached the highest level of about 0.1U/ (g dry matter) at the second- week of field retting, while glucanase activity was half of that value (i.e. 0.05 U/ (g dry matter)) for fungal retted fibers using *P. radiata* Cel 26 at the same retting period (**Figure 4.1**). The results confirmed our previous hypotheses.

In comparison to field retted samples, higher polygalacturonase activity was detected in fungal retted fibers using *P. radiata* Cel 26. The highest polygalacturonase activity of about 0.6 U/ (g dry matter) was detected during the first week in fungal retted fibers, after which the activity gradually decreased (**Figure 4.1**). Due to the high polygalacturonase activity and low glucanase activity present during fungal retting with *P. radiata* Cel 26, fungal retted fibers exhibited much lower polygalacturonan content than field retted samples. Laccase activity was detected during fungal retting, but was not found during field retting (**Figure 4.1**). The result was confirmed by the degradation of lignin (indicated by Klason lignin) during fungal retting with *P. radiata* Cel 26. Consequently, composites with fungal retted fibers with *P. radiata* Cel 26 exhibited higher stiffness and UTS than composites with field retted fibers (**Figure 4.2**).

In comparison to retting with *C. subvermispora*, the mutated *P. radiata* Cel 26 offered more advantages such as high depectinization efficiency and high selectivity of depectinization (**Table 4.1**). The performance of fungal retting was found to be dependent on the starting materials (i.e. stem sections). The yield of fibers, degradation of cellulose, pectin and lignin, and selectivity of depectinization during fungal retting were found to decrease from the bottom to the top stem sections (**Table 4.1**). The different responses of starting materials (i.e. stem sections) were related to the differences in the chemical composition of fibers originating from different stem sections. The different responses could further change the initial variations in the mechanical properties of fibers among fibers originating from different stem sections. Therefore the effect of fiber processing and of the original differences in the material should be considered in the selection of fibers with fewer variations in mechanical properties.

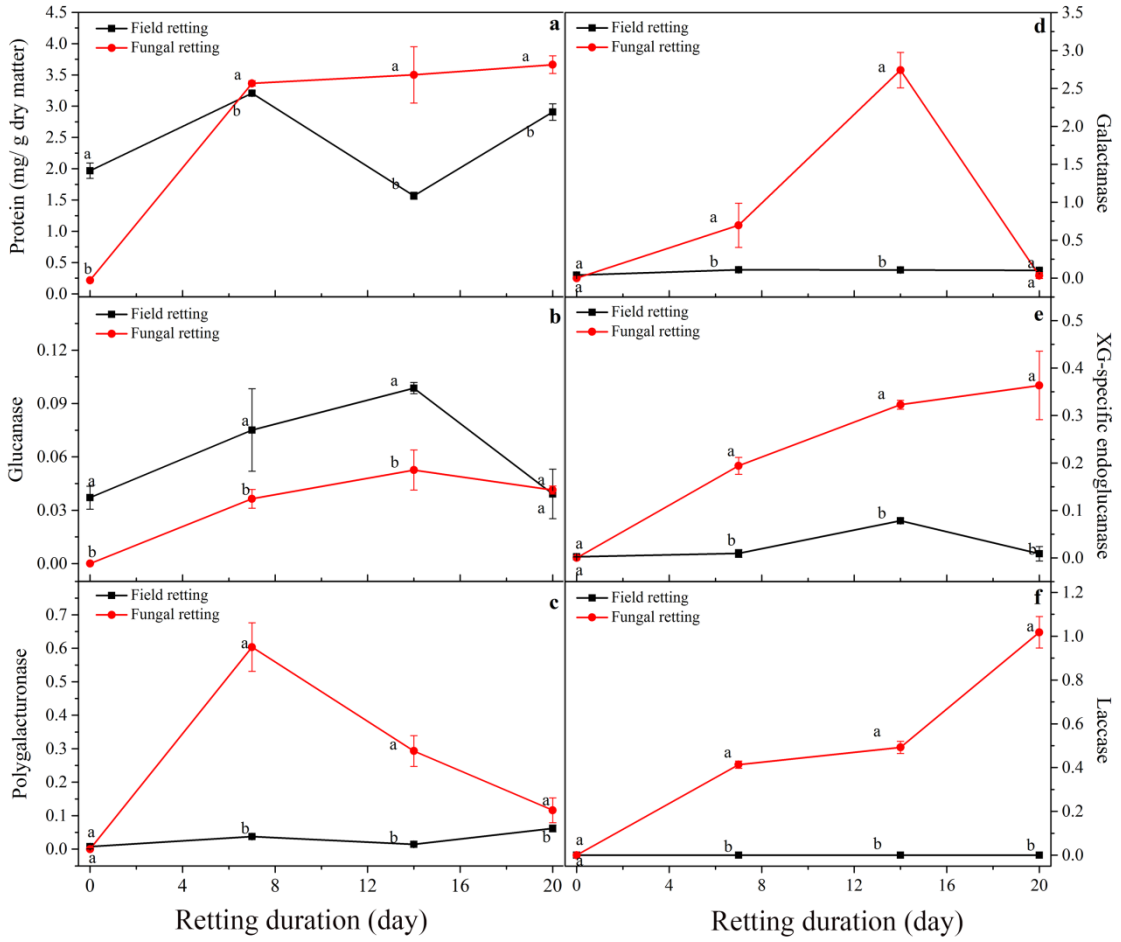

Figure 4.1. Protein content of enzyme extracts (a), and enzyme activities of glucanase (b), polygalacturonase (c), galactanase (d), XG-specific endoglucanase (e), and laccase (f) vs. retting durations (Unit of enzyme activities were shown as U/ (g dry matter hemp fibers)). (from paper III)

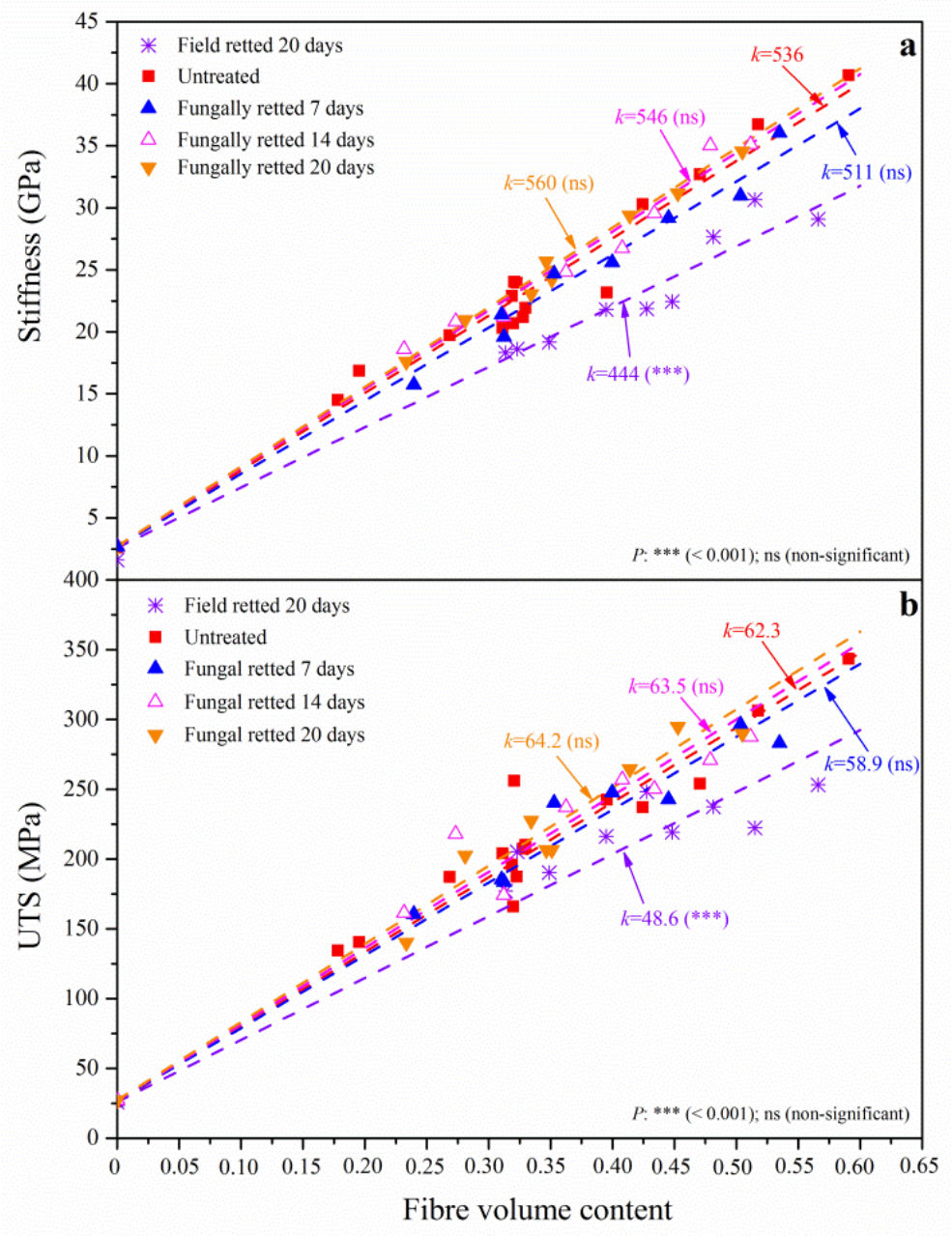

Figure 4.2. Stiffness (a) and UTS (b) of composites reinforced with untreated and treated fibers vs. fiber volume (V_f) contents (*k* is slope of linear regression model lines). (from paper III)

Table 4.1. Component losses, fiber yield and depectinization selectivity at different sections after cultivation with white rot fungi for 14 days (Control group was used as a baseline for the calculation of component losses and fiber yield). (from paper II)

Fungal retting	Stem section	Selectivity value	Yield %	Weight loss (%) [1,2]					
				Glu	GalA	Rha	Gal	Ara	Lignin
P. radiata Cel 26	bottom	36.1	88(5)	2(11)	71(5)	51(4)	26(9)	64(9)	3(8)
	middle	18.1	83(2)	4(10)	74(6)	57(9)	33(12)	63(25)	14(8)
	top	10.0	82(4)	7(9)	75(5)	60(13)	40(11)	69(11)	19(8)
C. subvermispora	bottom	8.2	92(1)	4(9)	46(8)	20(3)	15(14)	30(22)	-4(-3)
	middle	3.2	83(1)	14(9)	57(9)	31(15)	19(11)	46(24)	7(7)
	top	3.1	74(5)	20(9)	69(4)	50(5)	42(8)	70(10)	18(9)

[1] Glu: glucose, GalA: galacturonic acid, Gal: galctose, Ara: arabinose, Lignin: Klason lignin.

[2] Weight losses are shown as mean value ± uncertainty at the 95% confidence level, selectivity as mean values and yield as mean value ± standard deviation.

CHAPTER V − Hydrothermal pre-treatment and enzymatic retting of hemp fibers for the utilization in strong composites

To obtain high stiffness and strength of fibers, it is important to treat natural cellulosic fibers with mono-active enzymes (e.g. pectinase) to avoid any degradation of cellulose. Pre-treatment of hemp fibers is necessary to improve enzyme penetration and obtain good results. This chapter describes the assessment of hydrothermal pre-treatment at varied severity (i.e. 112 °C, 121 °C, and 134 °C) to improve enzymatic pectin removal from hemp fibers during enzymatic treatment with mono-component pectinases. Last, the hydrothermally pre-treated and enzymatically retted fibers were assessed in unidirectional fiber/epoxy composites.

5.1 Hypotheses

- Mild hydrothermal pre-treatment enhances enzymatic removal of pectin from hemp fibers, but pre-treatment itself does not damage fibers.
- Pectin removal by mono-component enzymes produces a positive impact on mechanical properties of hemp fiber reinforced composites;
- Improved mechanical properties of hemp fiber reinforced composites are due to lowered stress concentration effect resulted from decreased composite void content.

5.2 Related papers

Ming Liu, Diogo Alexandre Santos Silva, Dinesh Fernando, Anne S. Meyer, Bo Madsen, Geffrey Daniel, & Anders Thygesen

IV Controlled retting of hemp fibers: Effect of hydrothermal pre-treatment and enzymatic retting on the mechanical properties of unidirectional hemp/epoxy composites
Composites Part A: Applied Science and Manufacturing, 2016, 88, 253-262.

5.3 Significance of the study

The results presented in Chapter IV have shown that the presence of cellulolytic enzyme activities decreased the mechanical properties of fibers and lowered the mechanical properties of fiber reinforced composites, especially when fibers were treated by field retting. High mechanical properties of fibers and

fiber-reinforced composites were obtained by fungal retting with a mutated fungus (i.e. *P. radiata* Cel 26) due to low cellulolytic enzyme activity present during fiber retting with *P. radiata* Cel 26. Even though less decrease in mechanical properties of fibers was obtained, fungal retting is still a time-consuming process, which takes more than one month including the time for cultivating the fungus [38]. Therefore it is important to test mono-active enzymes for fiber treatment in order to obtain high quality fibers.

Treatment of hemp fibers by enzymes alone cannot achieve good results of pectin removal and fiber separation [22,34,107]. Pre-treatment of hemp fibers prior to enzymatic retting is therefore essential to achieve improved enzymatic pectin removal and fiber separation. Hydrothermal pre-treatment is commonly applied in biorefining schemes, such as 2nd generation bioethanol production, to obtain high cellulose convertibility in the subsequent enzymatic treatment with cellulase enzymes [108,109]. It is therefore important to assess whether mild hydrothermal pre-treatment at low temperature (112 – 134 °C) would enhance enzymatic pectin removal from hemp fibers and to produce cellulose rich fibers without any negative effect on fiber mechanical properties.

Increased mechanical properties of hemp fiber/polypropylene composites with randomly oriented fibers after pectin removal by chemical chelators and pectinase have been obtained in previous studies [84,99]. The improved mechanical properties of the composites was attributed to more separated fibers after pectinase treatments [84,99]. However, the relationships between composite properties and the changes in composite porosity after enzymatic treatments have not yet been established. Hence, it is important to study the changes in composite porosity and composite mechanical properties after pectin removal by hydrothermal pre-treatment and enzymatic retting.

5.4 Experimental consideration

Hydrothermal pre-treatment is commonly applied in biorefining schemes, such as 2nd generation bioethanol production, to obtain high cellulose convertibility in the subsequent enzymatic treatment with cellulase enzymes [108,109]. In this process, high temperature (170 – 220 °C) and pressure (1000 – 1600 kPa) are usually applied [108–110]. Under such high temperature and pressure, some of the hemicellulose can be degraded and the mechanical properties of hemp fibers will be negatively affected. In addition,

high temperature and pressure inevitably lead to high energy consumption. Therefore, low temperature (112 – 134 °C) and pressure (50 – 200 kPa) were applied in this study.

Hydrothermal pre-treatment at three different pressures or temperatures was assessed to see whether these treatments could improve enzymatic pectin removal from hemp fibers during the enzymatic retting step. The removal of pectin and mechanical properties of fibers were used as indicators to optimize the severity of the hydrothermal pre-treatment.

After pectin removal from hemp fibers by hydrothermal pre-treatment and enzymatic retting, fiber surface was expected to become cleaner and fibers more separated. The interfaces between fiber and matrix would also be improved. Hence, the porosity content of the composites would decrease. In this study, composite porosity was selected as a parameter to indicate the improvement in the interfaces between fiber and matrix. The changes in composite porosity could be further linked to the changes in the mechanical properties of the composites due to changes in stress concentrations.

5.5 Highlights

A decrease in pectin content with severity of pre-treatment was observed during hydrothermal pre-treatment. In addition, a reduction in arabinan, galactan, xylan and Klason lignin was noted with increasing severity of pre-treatment.

SEM micrographs showed that significant physical microstructural changes to hemp fibers occurred during hydrothermal pre-treatment at varied severity. Epidermal and parenchymal cells were seen to be partially degraded and removed from hemp fibers during hydrothermal pre-treatment.

Hydrothermal pre-treatment was associated with enhanced accessibility of pectin in hemp fibers to pectinases. This accessibility was indicated by increased enzymatic removal of pectin during enzymatic retting with hydrothermally pre-treated hemp fibers compared to untreated hemp fibers (**Figure 5.1**). The increased accessibility of pectin for pectinases was presumably due to the changes in fiber morphology observed in SEM micrographs.

No significant reduction in mechanical properties of fibers during hydrothermal pre-treatment was found. Hydrothermal pre-treatment at 100 kPa and 121 °C combined with 90-min enzymatic retting produced fibers with the highest ultimate tensile strength (UTS) of 780 MPa and stiffness of 36 GPa.

In a comparison of all fiber treatments, the combined treatment exhibited a positive effect on the mechanical properties of fiber/epoxy composites (**Figure 5.2**) with the lowest porosity factor of 0.08 (**Figure 5.3**), while traditional field retting exhibited a negative effect on the mechanical properties of fiber/epoxy composites (**Figure 5.2**) with the highest porosity factor of 0.16 (**Figure 5.3**). Composites containing hydrothermally pre-treated at 100 kPa combined with 90 min enzymatically treated fibers had the highest UTS of 325 MPa and stiffness of 38 GPa at fiber volume content of 50%, which was 31% and 41% higher, respectively, compared to composites made with field retted fibers (**Figure 5.2**).

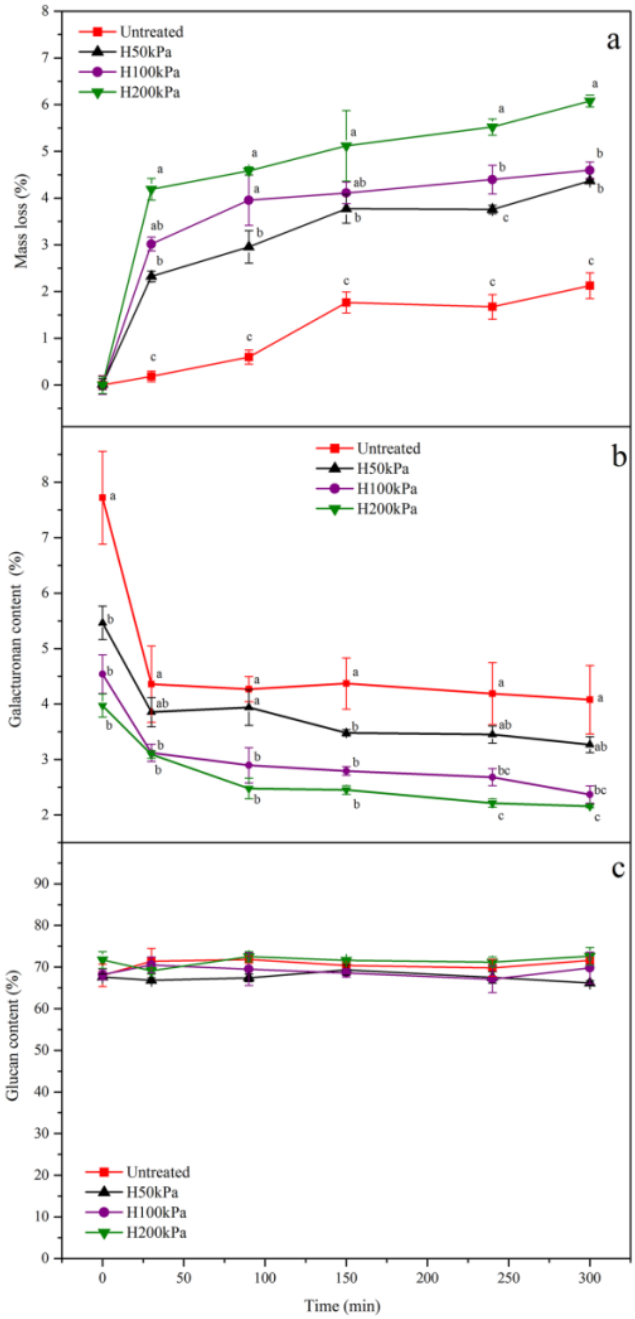

Figure 5.1. Mass loss of fibers (a), galacturonan content (b) and glucan content (c) of resultant fibers after enzymatic retting. For the same incubation time with enzymes, values that do not share a letter are significantly different at the 5% level. (from paper IV)

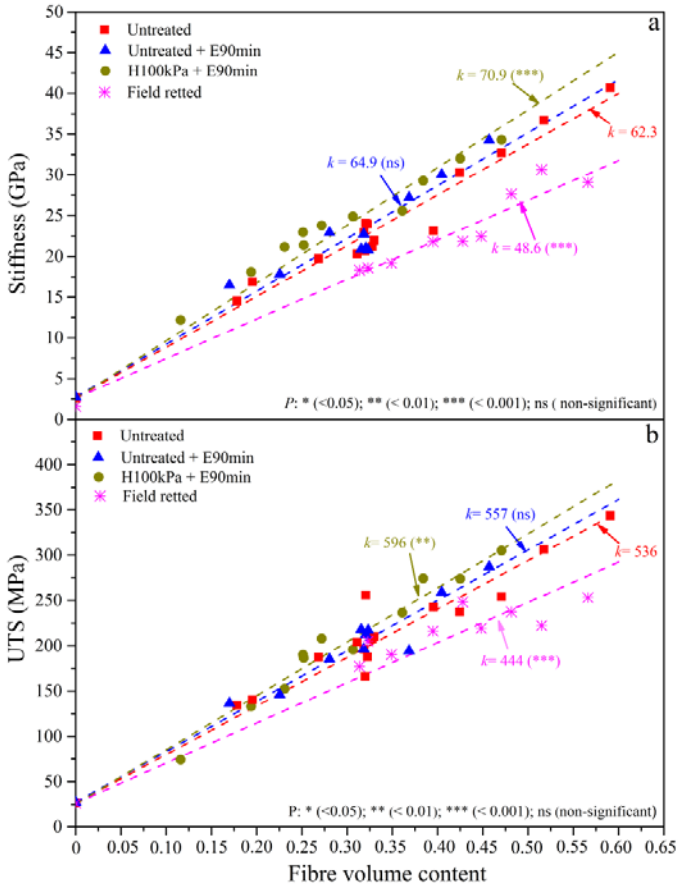

Figure 5.2. Stiffness (a) and UTS (b) of composites reinforced with untreated and treated fibers vs. fiber volume (V_f) content (k is slope of linear regression model lines). (from paper IV)

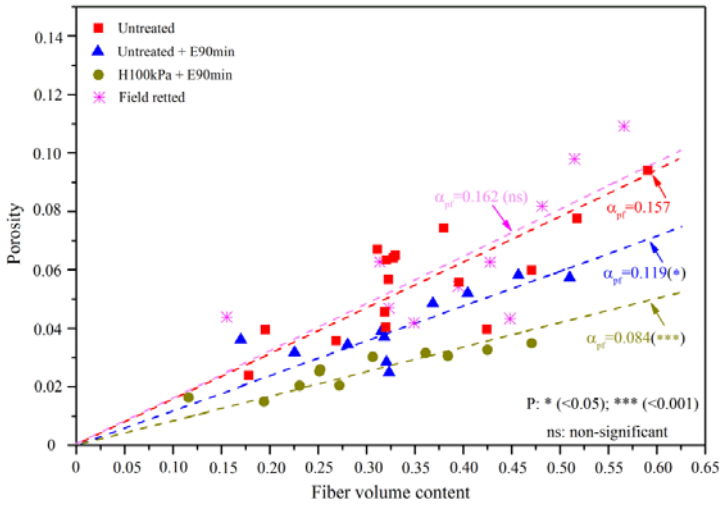

Figure 5.3. Porosity of composites reinforced with untreated and treated fibers vs. fiber volume (V_f) content. (from paper IV)

CHAPTER VI − Effect of pectin and hemicellulose removal from hemp fibers on the mechanical property of hemp fiber/epoxy composites

The effect of pectin and hemicellulose removal on the mechanical properties of fibers and fiber reinforced composites was investigated in order to understand the importance of pectin and hemicellulose compounds for the mechanical properties of fibers and fiber/epoxy composites. EDTA and pectinase was used to remove pectin from hemp fibers, and NaOH was used to remove hemicellulose. The effect of pectin and hemicellulose removal on the morphology of fibers and mechanical properties of fiber/epoxy composites was studied.

6.1 Hypotheses

- EDTA is capable of promoting enzymatic pectin degradation by removing calcium from hemp fibers;
- Pectin removal increases both stiffness and strength of hemp fibers/epoxy composites due to improved fiber incorporation in the epoxy matrix;
- Hemicellulose removal decreases the strength of hemp fibers and hemp fiber/epoxy composites;
- Composite stiffness correlates positively with the degree of non-cellulosic components removal by fiber treatments.

6.2 Related papers

Ming Liu, Anne S. Meyer, Dinesh Fernando, Diogo Alexandre Santos Silva, Geffrey Daniel, & Anders Thygesen

V Effect of pectin and hemicellulose removal from hemp fibers on the mechanical properties of unidirectional hemp/epoxy composites

Composites Part A: Applied Science and Manufacturing, 2016, 90, 724−735.

6.3 Significance of the study

Hemp fibers are mainly composed of three classes of polysaccharides: cellulose, hemicellulose and pectin. Cellulose consists of β-1, 4-linked glucan chains and is organized into microfibrils cross-linked by xyloglucan (XG). Pectin fills the spaces between cellulose and XG. The cellulose and the cross-linked

XG chains are commonly considered as the two main components which provide cell wall strength. Pectin mainly functions as glue that packs the cellulose microfibrils into individual fibers, and then into fiber bundles. It is therefore important to have an improved understanding of the role played by pectin and hemicellulose in the mechanical properties of fiber reinforced composites. The study can also help to optimize the mechanical properties of hemp fiber/epoxy composites.

6.4 Experimental consideration

Pectin was removed using EDTA and pectinase, and hemicellulose was removed using 10% NaOH. In Chapter 5, improved pectin removal was achieved by using hydrothermal pre-treatment and enzymatic retting. As mentioned, some degradation of hemicellulose was observed during hydrothermal pre-treatment, and therefore the combined treatment cannot fulfil the purpose of this study. Chemical chelators have also been known to enhance pectin removal by pectinases [100,101]. The enhanced enzymatic degradation of pectin by EDTA results from the capacity of chemical chelators to form complexes in particular with calcium in pectin. Alkali extraction with 10% NaOH is widely used for the isolation of hemicellulose from lignocellulosic biomass to obtain cellulose of high purity. Therefore 10% NaOH treatment was applied in this study to remove hemicellulose from hemp fibers after pectin removal.

6.5 Highlights

Pectin removal by EDTA and endo-polygalacturonase (EPG) removed the epidermal and parenchyma cells from hemp fibers and improved fiber separation (**Figure 6.1**). Hemicellulose removal by NaOH further improved fiber surface cleanliness (**Figure 6.1**).

The removal of epidermal and parenchyma cells and the improved fiber separation decreased composite porosity content. With the exception of field retted samples, the fiber correlated porosity factors of composites with differently treated fibers were found to be correlated with pectin and hemicellulose content of the fibers (**Figure 6.2**). As a result, pectin removal increased both composite stiffness and ultimate tensile strength (UTS) (**Figure 6.3**). Hemicellulose removal increased composite stiffness, but decreased composite UTS due to the removal of hemicellulose (**Figure 6.3**).

There is clear evidence that effective fiber stiffness and effective fiber strength correlate with the cellulose content of fibers (**Figure 6.2**). In a comparison of all fiber treatments, composites with 0.5%

EDTA + 0.2% EPG treated fibers had the highest UTS of 327 MPa at fiber volume content of 50%. Composites with 0.5% EDTA + 0.2% EPG → 10% NaOH treated fibers had the highest stiffness of 43 GPa (**Figure 6.3**) and the lowest porosity factor of 0.04 and the least amount of voids present at fiber/epoxy interfaces (**Figure 6.4**).

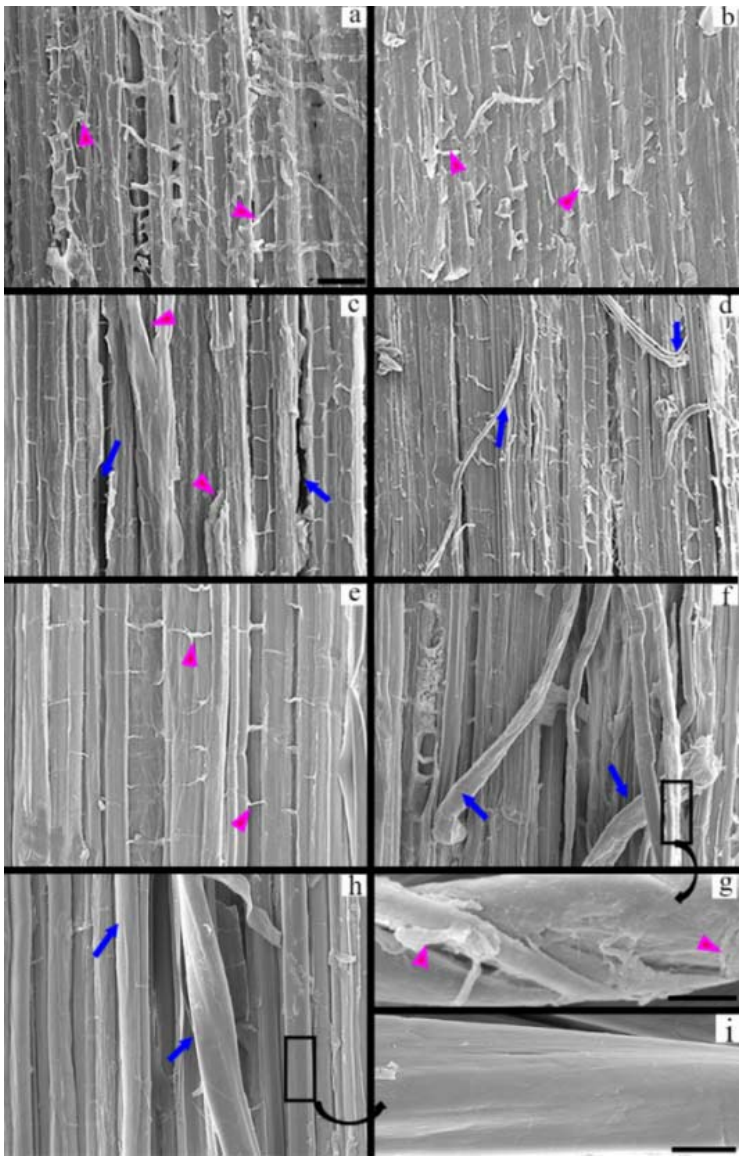

Figure 6.1. ESEM micrographs showing cross sections of hemp bast fiber strips: field retted (a), untreated (b), 1% EDTA treated (c), 2% EDTA treated (d), 0.2% EPG treated (e), 0.5% EDTA + 0.2% EPG treated (f)-(g), and 0.5% EDTA + 0.2% EPG → 10% NaOH treated (h)-(i). Magenta arrowheads show parenchyma cell residues on fiber surface; blue arrows show separated fibers and open spaces between fibers. Scale bar in (a) is 50 µm with the same magnification for (b)-(e). Scale bar in (g) and (i) is 10 µm. (from paper V)

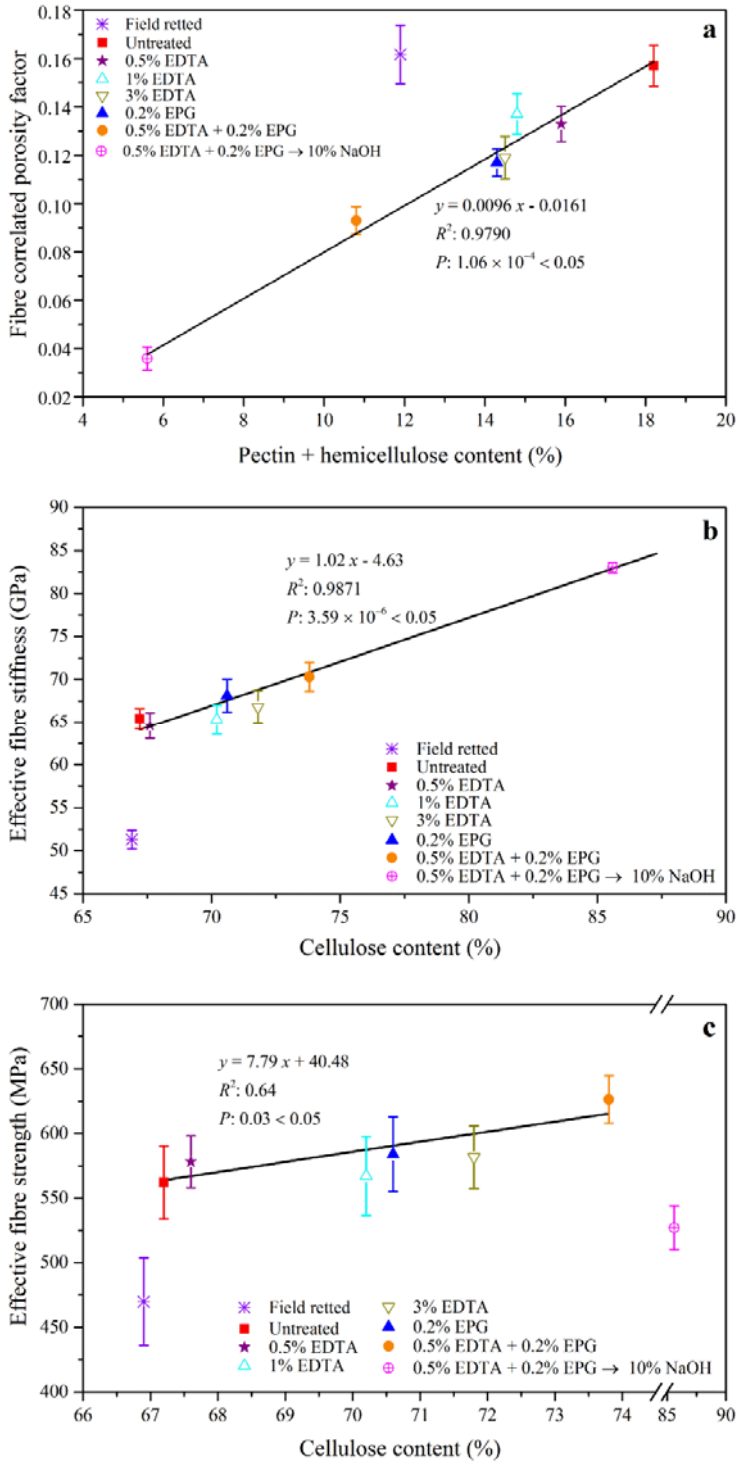

Figure 6.2. Fiber correlated porosity factor (α_{pf}) vs. pectin + hemicellulose content (a), effective fiber stiffness vs. fiber cellulose content (b), and effective fiber strength vs. fiber cellulose content (c). (from paper V)

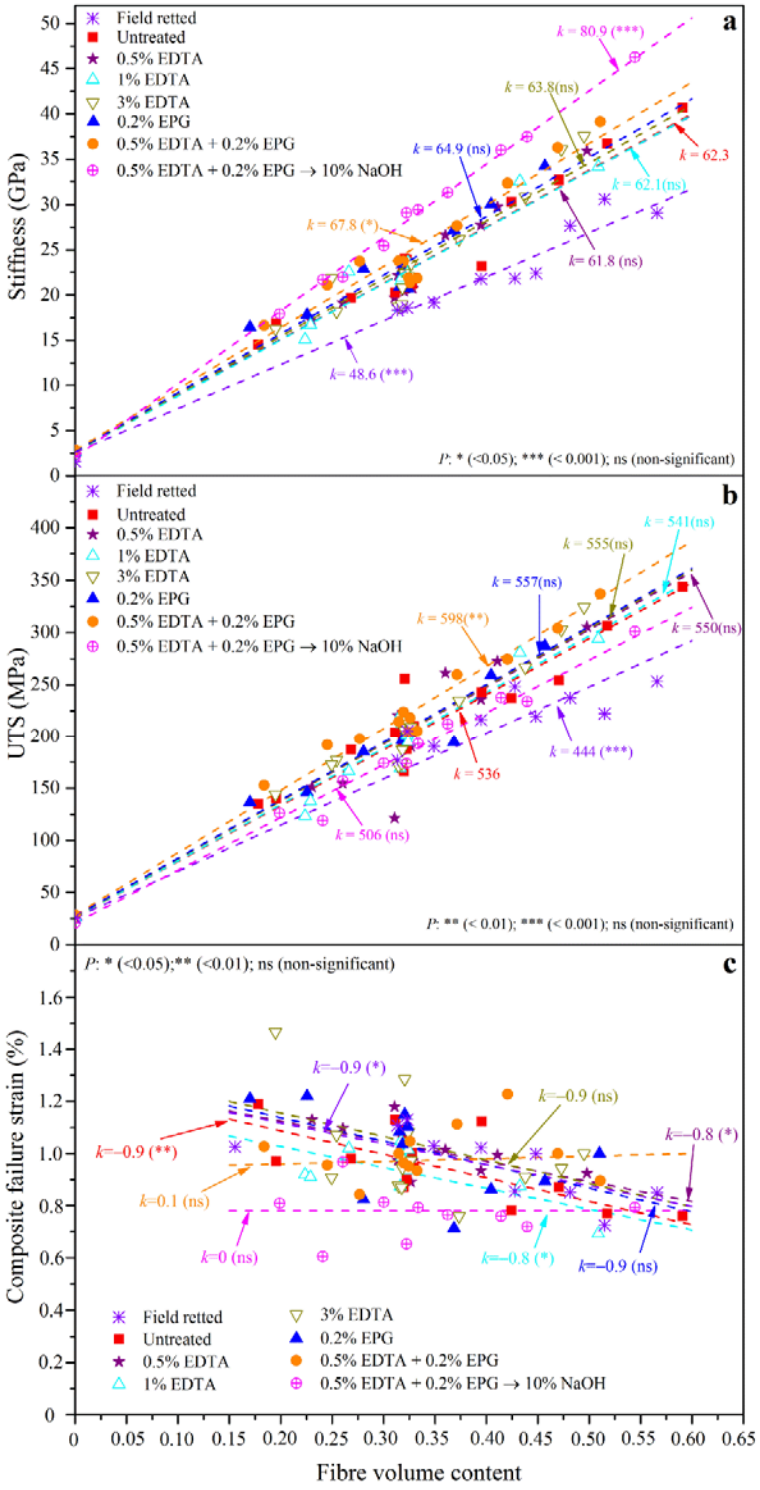

Figure 6.3. Stiffness (a), UTS (b) and failure strain (c) of composites reinforced with untreated and treated fibers vs. fiber volume contents (V_f). (In images a and b, the P value indicates the significant level for the slope of model lines between differently treated fibers vs. untreated fibers. In image c, the P value indicates the significance level for the slope of model lines vs. 0) (from paper V)

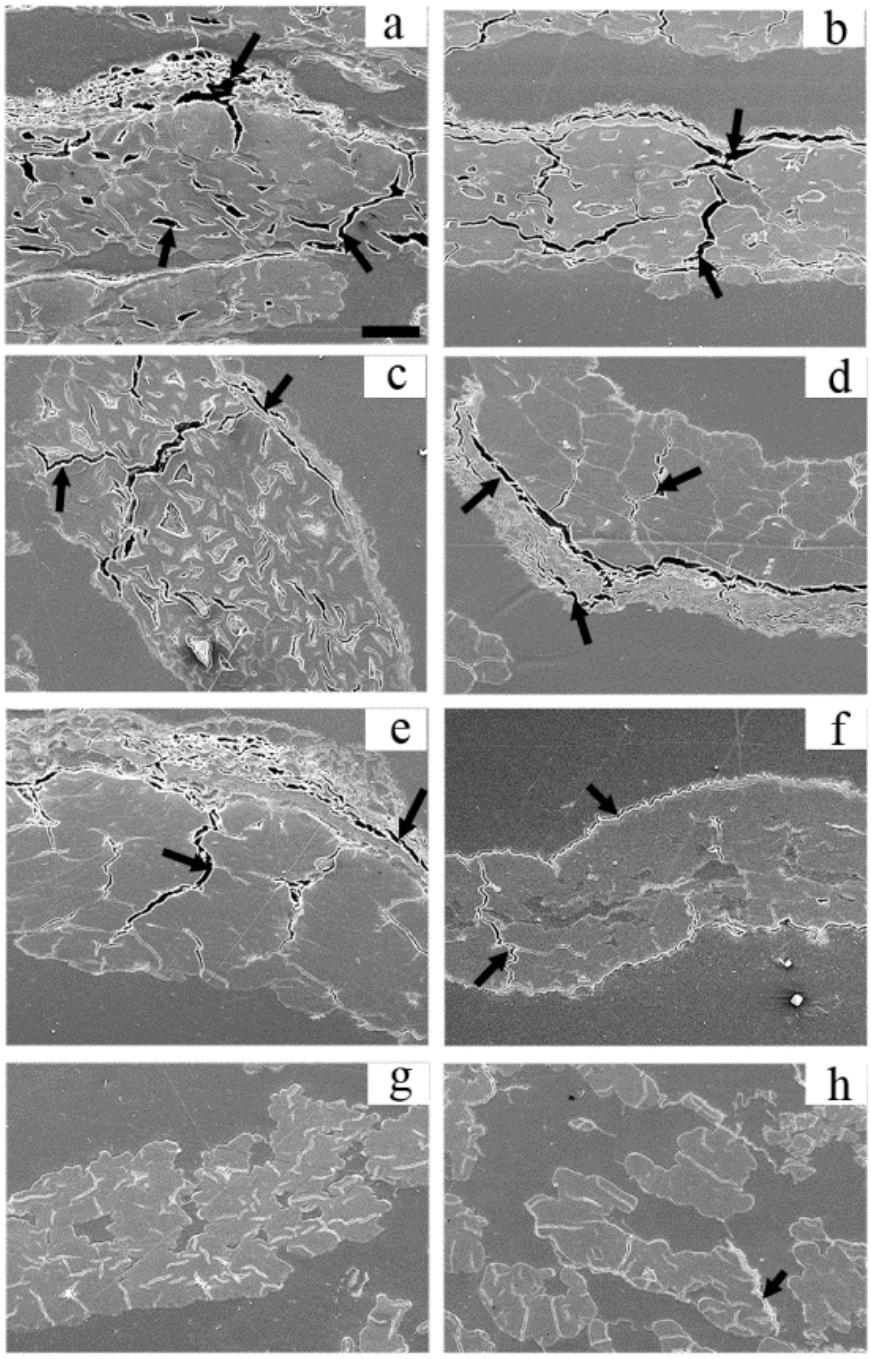

Figure 6.4. ESEM micrographs of polished hemp fiber/epoxy composites with field retted (a), untreated (b), 0.5% EDTA treated (c), 3% EDTA treated (d), 0.2% EPG treated (e), 0.5% EDTA + 0.2% EPG treated (f) and 0.5% EDTA + 0.2% EPG → 10% NaOH treated (g-h) fibers. Arrows show examples of porosities at epoxy/epidermis, epidermis/epidermis, epidermis/fiber, fiber/fiber and fiber/epoxy interfaces. Scale bar in (a) is 50 μm with the same magnification for (b) – (h). (from paper V)

CHAPTER VII − Oxidation of lignin in hemp fibers by laccase: effects on the mechanical property of hemp fibers and unidirectional fiber/epoxy composites

A deeper insight into the role of different matrix polymers within fiber cell walls is important. Further insight is especially needed with regard to how lignin contributes to the mechanical properties, and how the modification (i.e. polymerization) of lignin affects the mechanical properties of fibers. To improve the mechanical properties of fibers and fiber reinforced composites, laccase treatment was applied to hemp bast fibers to oxidize and polymerize phenols in hemp fibers and thus strengthen hemp structure. In this study, the resulting changes in phenol structures were analyzed to verify the following hypotheses.

7.1 Hypotheses

- Oxidation of aromatic substances in hemp fibers by laccase can improve mechanical properties of hemp fibers and hemp fiber reinforced composites;
- Once the aromatic substances have been removed prior to laccase treatment, less profound increases in mechanical properties of hemp fibers and hemp fiber reinforced composites will occur.

7.2 Related papers

Ming Liu, Jügen Odermatt, Andrea Baum, Birgitte Zeuner, Liyun Yu, Jens Berger, Anders Thygesen, &Anne S. Meyer,

VI Oxidation of lignin in hemp fibers by laccase: Effects on mechanical properties of hemp fibers and unidirectional fiber/epoxy composites

Composites Part A: Applied Science and Manufacturing, 2016, (submitted)

7.3 Significance of the study

The primary fibers of hemp are one of the most suitable, cellulose rich fibers for manufacturing strong biocomposite materials. The fibers are located in the outer part of the hemp stem beneath the epidermis. The primary fibers are mainly composed of cellulose, hemicellulose, lignin and pectin [18]. Cellulose consists of a linear chain of β-1,4-linked D-glucose units and is organized into microfibrils interlocked by glycans (e.g. xyloglucan, galactomannan) [24,25]. The cellulose microfibrils and the interlocked glycans are commonly considered as the two main components which provide cell wall strength. Furthermore, the

interlocked network of microfibrils and glycans is embedded in a matrix of pectic substances, and the network if further reinforced with structural protein and aromatic substances (e.g. lignin) [24,26,27].

Thus, a deeper insight into the role of different matrix materials within fiber cell walls is important, especially as regards how lignin contributes to the mechanical properties of fibers, and the possibility of polymerization of lignin to improve mechanical properties of fibers. The deeper understanding of the role of lignin can help to achieve strong fibers and fiber-reinforced composites.

7.4 Experimental consideration

It is recognized that aromatic substances can be polymerized or cross-linked to form complex structures by laccase enzymes [47,111,112]. In addition, laccase catalyzed cross-linking of ferulic acid has been observed in sugar beet [111,113]. In this study, the changes in lignin and hydroxycinnamates in hemp fibers after laccase treatment were characterized to explain the changes in mechanical properties of fibers and fiber reinforced composites due to laccase treatment. Changes in lignin-hydroxyl groups were characterized by near infrared (NIR) spectra, since NIR spectra provide information of the first and the combined overtones of phenol-OH groups. Changes in hydroxycinnamic acids were determined by reverse reversed phase high performance liquid chromatography (RP-HPLC).

Removal of lignin prior to laccase treatment was carried out to verify the above hypothesis. Changes in mechanical properties, lignin-OH groups and contents of hydroxycinnamic acids were analyzed in the same way as described above.

7.5 Highlights

Laccase treatment after 0.5% EDTA + 0.2% endo-polygalacturonase (EPG) treatments increased the mechanical properties of hemp fibers and fiber/epoxy composites without influencing composite porosity content (**Figure 7.1**). However, when hemp fibers were treated with NaOH prior to laccase treatment, no increase in mechanical properties of fibers and fiber/epoxy composites was noted (**Figure 7.1**). In a comparison of all samples, 0.5% EDTA + 0.2% EPG → 0.5% Laccase treated fibers had the best effective fiber properties with the highest stiffness of 82 GPa and strength of 630 MPa. In addition, composites with such treated fibers had the best mechanical properties with the highest stiffness of 42 GPa and strength of 330 MPa at fiber volume content of 50% (**Figure 7.1**).

The maximum decomposition temperature increased to 350.2 °C from 345.7 °C after fibers were treated with laccase after 0.5% EDTA + 0.2% EPG treatments. In addition, the maximum decomposition temperature increased to 367.9 °C from 360.8 °C after fibers were treated with laccase after 0.5% EDTA + 0.2% EPG → 10% NaOH treatments (**Figure 7.2**). The increased thermal stability of the laccase treated fiber maybe due to oxidation of lignin, and the oxidation of lignin can induce the further generation of covalent bonds and cross-linking of aromatic substances in the fiber.

As shown in NIR spectra after processing by standard normal variate (SNV) and mean centering, the peak shifted to 1432 nm from lower wavelengths (i.e. 1410 nm and 1421 nm) after fibers were treated with laccase, regardless of the prior treatments (**Figure 7.3**). The shifting of the peak in the NIR spectra was probably due to the oxidation of lignin hydroxyl groups by laccase.

The differences in the responses of mechanical properties of fibers and fiber/epoxy composites to the laccase treatments presumably resulted from the alkali treatments. FTIR spectra and chemical composition data showed that some lignin was removed during alkali treatments. As a result, less lignin was available for the catalyzed polymerization reactions with laccase. Therefore, no change in the mechanical properties of fibers and fiber/epoxy composites after laccase treatments was noticed when alkali treatment was applied prior to laccase treatments. The hypotheses were therefore confirmed.

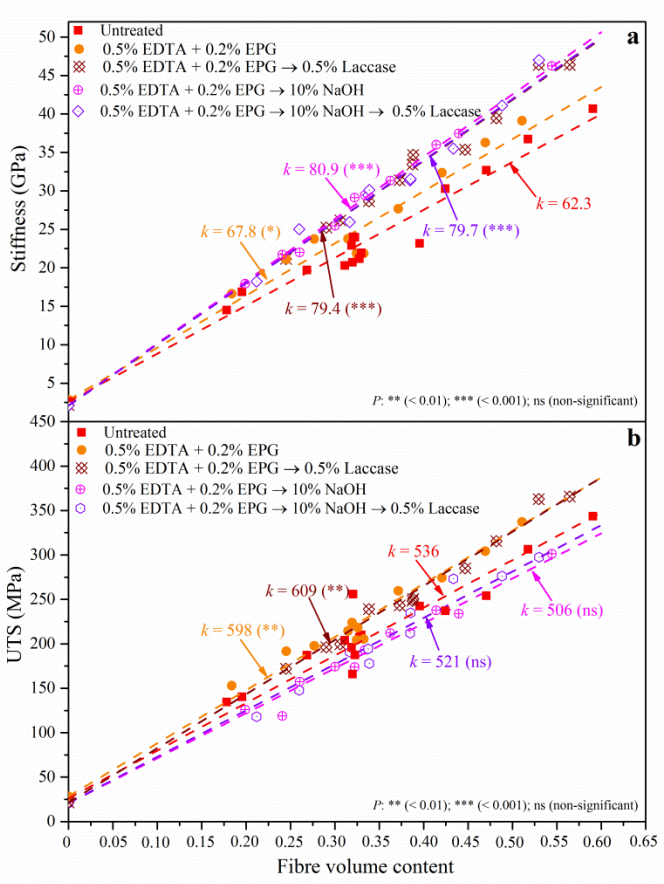

Figure 7.1. Stiffness (a) and UTS (b) of composites reinforced with untreated and treated fibers vs. fiber volume contents (V_f). (from paper VI)

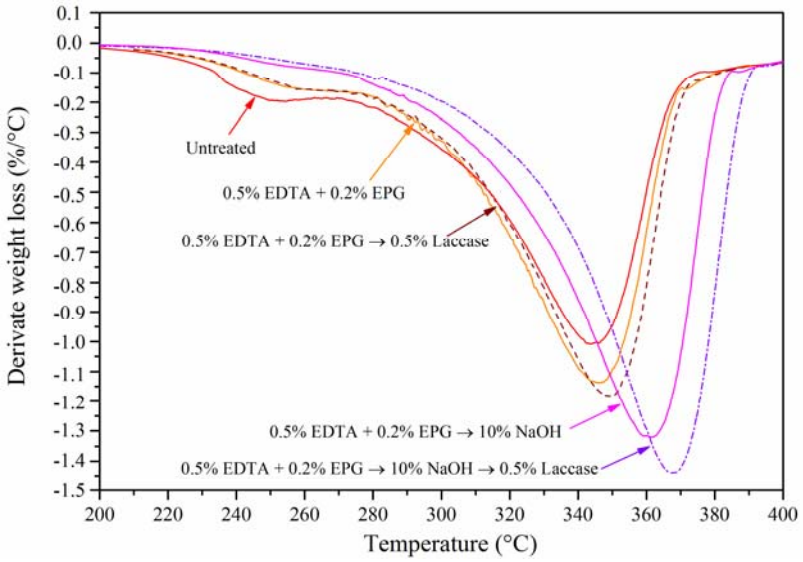

Figure 7.2. Thermogravimetric analysis for derivatives of weight (%) vs. temperature of untreated and differently treated fibers. (from paper VI)

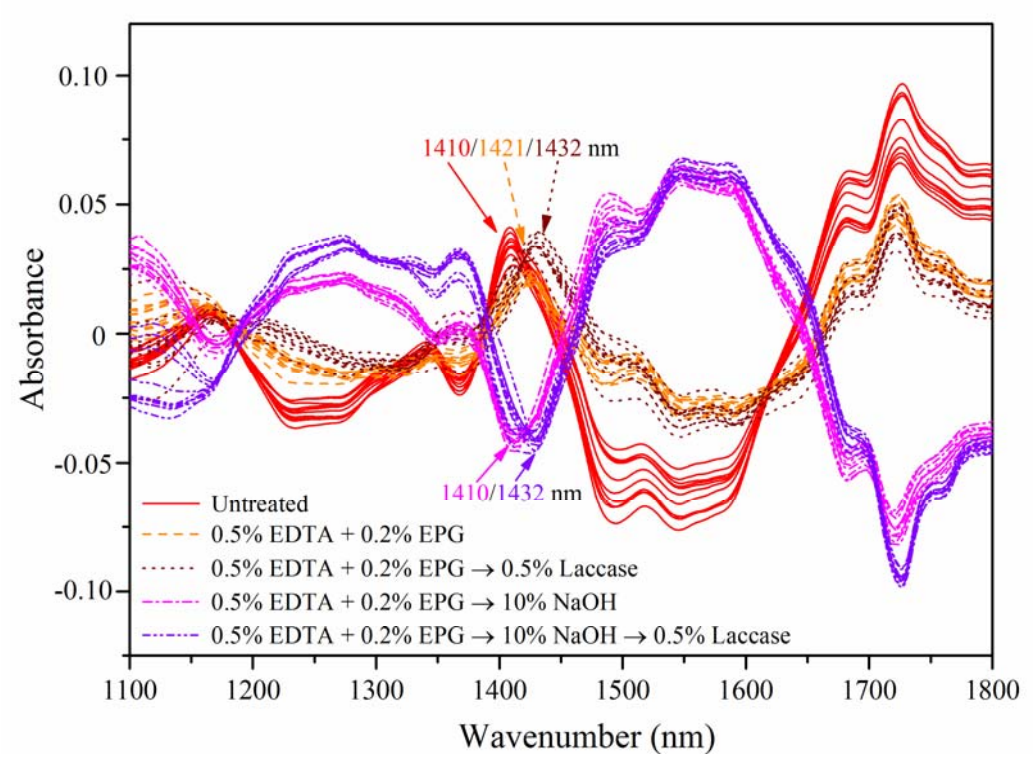

Figure 7.3. Near infrared spectra after processed by SNV and mean centering. (from paper VI)

CHAPTER VIII − Modelling of volumetric composition and mechanical properties of unidirectional hemp/epoxy composites- Effect of enzymatic fiber treatment

Composite porosity is a main parameter used to assess the quality of composites. The aim of this study was to determine the quantitative effect of porosity on composite mechanical properties and density and to obtain a tool to demonstrate the effect of fiber treatments on mechanical properties and density of fiber reinforced composites. Modified rule of mixture model by considering porosity effect on volumetric composition and mechanical properties of composites was applied in this study. The model was verified by comparing modeling results and experimental results of composites with respect to volumetric composition, mechanical properties and density of composites with differently treated hemp fibers.

8.1 Hypotheses

- The modified model from rule of mixture model through including effect of composite void, can fit well with experimental data for composite density and composite mechanical properties;
- The applied model provides a useful tool to assess the physical and mechanical properties of composites incorporated with differently treated hemp fibers.

8.2 Related paper

IV **Ming Liu**, Anders Thygesen, Anne S. Meyer, & Bo Madsen

Modelling of volumetric composition and mechanical properties of unidirectional hemp/epoxy composites – Effect of enzymatic fiber treatment

IOP Conference Series: Materials Science and Engineering, 2016, 139, 12-31

8.3 Significance of the study

A study of the relations between fiber processing routes and the volumetric composition and mechanical properties of composites is central to the goal of assessing the effect of various fiber treatments. Models that consider porosity effect on volumetric composition, density and mechanical properties (i.e. stiffness and strength) were applied this this study. The modelling could provide valuable understanding of the effect of fiber treatments on the properties of the composites. This approach is

shown to provide a tool to predict the properties of the composites with a certain type of treated fibers for the investigated fiber content.

8.4 Model selection

The rule of mixtures model (ROM) for stiffness of composites has been widely used [114–117]. This model has only considered the effect of fiber volume content on the mechanical properties of composite without including any parameters for the effect of other factors such as composite porosity (fiber correlated and matrix correlated porosity), fiber length, fiber orientation *etc*. In order to be more realistic, a large number of modified rule of mixtures models for stiffness and strength of composites have been proposed [76,77,118]. In order to demonstrate the effect of porosity on mechanical properties of fiber/epoxy composites, a model that included the effect of porosity was selected for modelling performed in this study.

8.5 Highlights

Composites with enzymatically treated fibers, particularly hydrothermally pre-treated and enzymatically treated fibers, exhibited clearly higher density due to their lower porosity contents and higher fiber volume contents. The model predictions of composite density in **Figure 8.1** show that the predicted composite density is in good agreement with the experimental data. Therefore, the density of composites with a given type of fiber treatment can be well predicted as a function of the fiber weight content.

The model lines in **Figures 8.2** and **8.3** were established by setting the porosity efficiency exponent (n) equal to 0 and 2. For n = 0, it is assumed that all the porosity is located inside the fibers, in the so-called lumen, and this is assumed to have no effect on the mechanical properties of the composites. For n = 2, it is assumed that all the porosity is located outside the fibers, e.g. at the fiber/matrix interface or in the fiber bundles to produce un-impregnated fibers. This is assumed to lead to stress concentrations, which are modelled by setting n equal to 2. When n = 0, as shown in **Figures 8.2a** and **8.3a**, composite stiffness and strength increase non-linearly with W_f with a upward curvature until $W_{f\,trans}$, after which, stiffness and strength are only slightly reduced. When n = 2, as shown in **Figures 8.2b** and **8.3b**, composite stiffness and strength increased non-linearly with W_f with a downward curvature until $W_{f\,trans}$, after which, stiffness

and strength are reduced radically. The downward curvature of the model lines is most obvious for the composites with the highest porosity content, such as the composites with field retted and untreated fibers. Generally, the model lines are in good agreement with the experimental data.

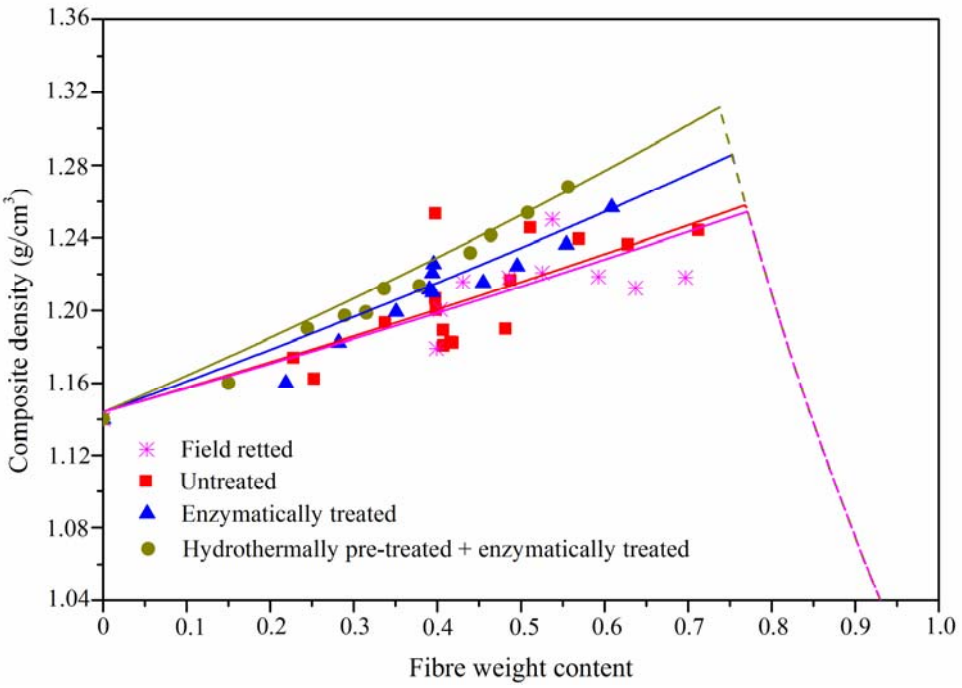

Figure 8.1. Composite density vs. fiber weight content. (from paper VII)

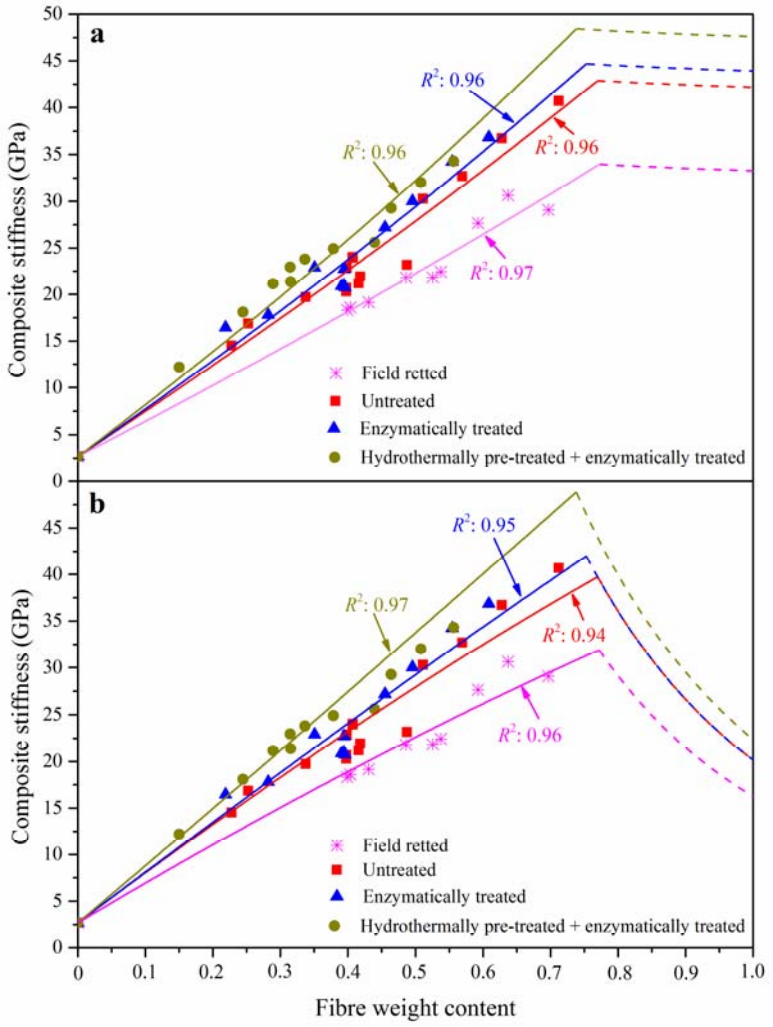

Figure 8.2. Composite stiffness vs. fiber weight content. Model lines are constructed using a porosity efficiency exponent of (a) 0 and (b) 2. Values of adjusted R-squared are shown next to the model lines. (from paper VII)

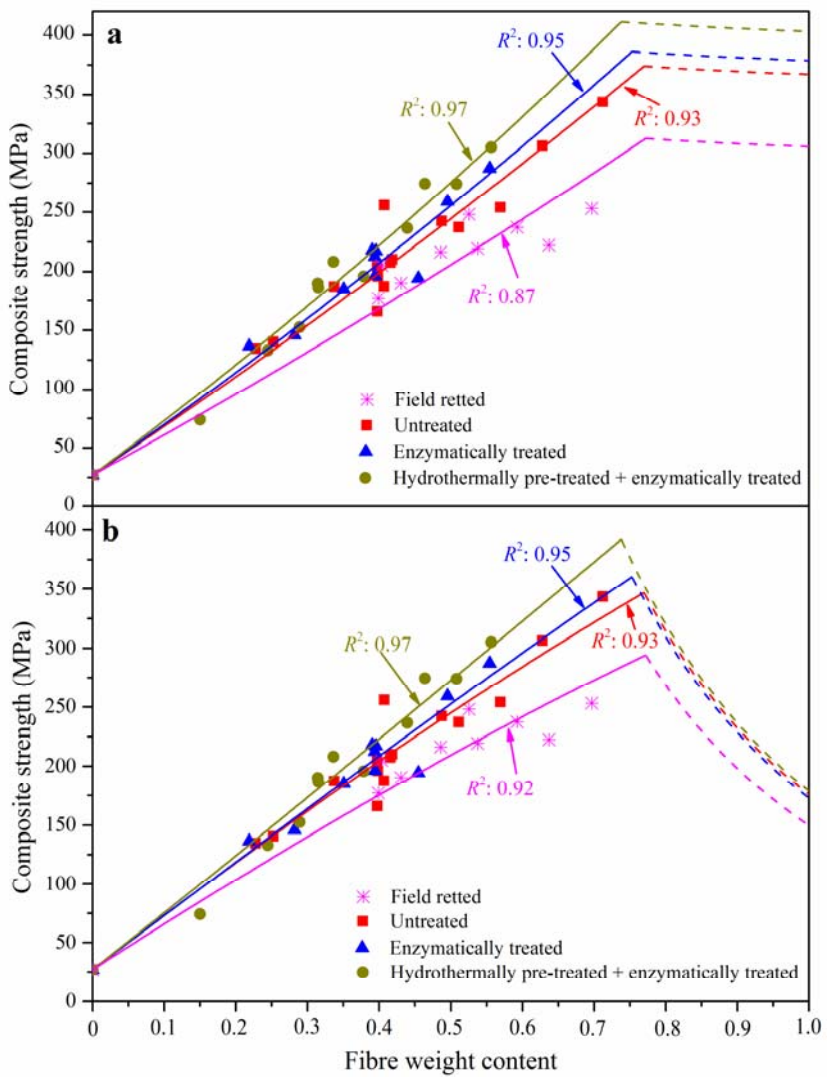

Figure 8.3. Composite strength vs. fiber weight content. Model lines are constructed using a porosity efficiency exponent of (a) 0 and (b) 2. Values of adjusted R-squared are shown next to the model lines. (from paper VII)

CHAPTER IX − Conclusions and Future perspectives

9.1 Conclusions

The overall aim of this PhD study was to improve mechanical properties of hemp fiber reinforced composites and obtain a better understanding of the roles of different fiber cell wall components in contributing to the mechanical properties of hemp fibers and fiber reinforced composites. A prerequisite for the PhD study was to have an overview of the different factors that influence of the mechanical properties of natural cellulosic fibers in order to select strong hemp fibers for composites (Chapter I). In addition, the factors that affect the mechanical properties of natural fiber reinforced composites were summarized to provide an inspiration for optimization of the mechanical properties of natural fiber reinforced composites through fiber processing such as chemical and enzymatic fiber processing.

The effect of harvest time and stem sections on chemical composition, morphology and mechanical properties of hemp fibers was investigated (papers I and II). The objective of this study was to find the correlation between chemical composition and morphology of hemp fibers and the mechanical properties of hemp fibers. Our initial hypothesis, based on the fact that cellulose is the main component that strengthens fiber cell walls, was that harvest time and stem sections influenced fiber properties through influencing fiber chemical compositions, and cellulose content in particular. The results of this study confirmed our initial hypothesis and showed that harvest time of hemp fibers and origin of stem section did affect chemical composition. A highly significant reduction in cellulose deposition and a slight decrease in pectin content, but a significant increase in lignin deposition in fiber cell walls, were noted with stem maturity (stem sections from the top to the bottom). Microscopy observations and histochemical analyses corroborated the results of the changes in fiber chemical compositions with maturity. The results showed that hemp fibers with lower maturity (i.e. harvested at the beginning of flowering or from top and middle stem sections) had higher stiffness and tensile strength than the fibers with higher maturity (i.e. harvested at seed maturity or from bottom stem sections).

Prior of manufacturing of high quality natural fiber reinforced composites, fiber processing to remove non-cellulosic components is usually needed to obtain more separated and cellulose rich fibers. Paper I also studied the effect of the traditional field retting method at varied retting durations on chemical composition and mechanical properties of hemp fibers. The results can be used a benchmark to assess the

other fiber processing methods described in the subsequent chapters of this PhD study. The results showed that traditional field retting damaged fiber properties due to the presence of cellulase activity (papers I and III). Consequently, composites with traditionally field retted fibers had much lower stiffness and strength than composites with untreated fibers (paper III). No improvement in fiber/matrix interfaces was noted by field retting, as indicated by similarly high porosity contents were present both in the composites with field retted fibers and in the composites with untreated fibers. Compared to traditional field retting based on local spontaneous microbial activities, fungal retting with the mutant *Phlebia radiata* Cel 26, which produces less cellulase than its wild type, can degrade pectin more efficiently and produced high quality fibers (papers II and III). As a result composites with *P. radiata* Cel 26 retted fibers had much high stiffness and strength compared to composites with field retted fibers.

The effect of field retting and fungal retting on chemical composition and mechanical properties of hemp fibers and hemp fiber/epoxy composites can be explained by the enzymes activity of enzyme extracts from field retted and *P. radiata* Cel 26 retted fibers at varied retting durations (paper III). The extracts from field retted fibers had much higher cellulase activity during the first 20 days of retting compared to extracts from *P. radiata* Cel 26 retted fibers. Extracts from *P. radiata* Cel 26 retted fibers exhibited much higher polygalacturonase, galactanase, xyloglucan (XG)-specific endo-glucanase and laccase activity (paper III). In a comparison of field retting and *P. radiata* Cel 26 retting, *P. radiata* Cel 26 retting demonstrated higher efficiency of pectin degradation, higher retting selectivity (ratio of pectin degradation and cellulose degradation), and produced stronger hemp fibers and hemp fiber reinforced composites (papers II and III). These results further confirmed our previous hypothesis that cellulase activity is the key factor that damages the quality of hemp fibers during retting.

To obtain high quality hemp fibers and fiber reinforced composites, mono-component pectinases were applied in hemp fiber processing so as to completely get rid of cellulase activities. Hydrothermal pre-treatment at mild conditions could improve enzyme accessibility of hemp fibers (paper IV). Consequently, improved pectin removal from hemp fibers by pectinases (e.g. endo-polygalacturonase) was obtained. Hydrothermal pre-treatment of hemp stems at 121 °C for 30 min followed by enzyme treatment of hemp bast fibers with pectinases produced the strongest fibers with a very low content of pectin (~ 3%). Last, an increase in both stiffness and UTS of the composites made with hydrothermally pre-treated and

enzymatically treated fibers was observed. The improved mechanical properties of fiber/epoxy composites were mainly due to the improved coherence between fibers and matrix polymers, as indicated by the decreased composite porosity content (paper IV).

The above studies showed that cellulase activity had a negative effect on fiber mechanical properties and pectin removal by using mono-component pectinases provided a way to obtain high quality hemp fiber reinforced composites. To further improve the mechanical performance of hemp fiber reinforced composites, it is important to understand the role of different components of fiber cell walls in contributing to the mechanical performance of hemp fibers and hemp fiber reinforced composites. To achieve this aim, a series of experiments were carried out (paper V). Pectin removal by EDTA and endo-polygalacturonase removed parenchyma and epidermal cells from hemp fibers, and the porosity content of the composites reinforced with the resultant fibers decreased. Stiffness and UTS of the composites with EDTA and endo-polygalacturonase treated fibers increased compared to composites with untreated fibers. Hemicellulose removal by sodium hydroxide improved the stiffness of composites due to the increase in cellulose content. But sodium hydroxide treatment decreased UTS of the composites due to the disrupted interlocked network as a result of the removal of hemicellulose, especially xyloglucans.

The interlocked network of cellulose and glycans is reinforced with aromatic substances. Modification of the aromatic substances in hemp fibers may further increase the mechanical properties of hemp fibers and hemp fiber reinforced composites. Laccase from *Trametes versicolor* was used to oxidize the aromatic substances in hemp fibers, and the results showed that laccase treatment can further strengthen the fiber network (paper VI). Stiffness and UTS of fibers and fiber/epoxy composites increased after fibers were treated by laccase after pectin removal by EDTA and endo-polygalacturonase. In addition, increased thermal resistance of hemp fibers was observed after laccase treatment. However, once aromatic substances were partially removed by alkali treatment prior to laccase treatment, no improvement in mechanical properties of fibers and fiber reinforced composites was noted. Small quantities of hydroxycinnamic acids in hemp fibers were found. Our initial hypothesis was that the improvement in mechanical properties of hemp fibers caused by laccase treatment was due to enzymatically catalytic cross-linking of hydroxycinnamic acids, especially ferulic acids. However, no noticeable changes in the content of hydroxycinnamic acids were observed before and after laccase treatments. This may be because the content of hydroxycinnamic acids monomers was very low, and the

changes could hardly be detected. Changes in lignin structures were revealed by NIR spectra and Py-GC/MS (paper VI). The results demonstrated that mechanical properties of hemp fibers can be manipulated by modifying the aromatic components in hemp fibers.

Lastly, the effect of enzymatic fiber treatments, especially pectinase enzymes treatments, on the fiber performance in unidirectional hemp fiber/epoxy composites was assessed by modelling the volumetric composition and mechanical properties of the composites using a modified rule of mixture model. The modelling study gave a better understanding of the effect of fiber treatments on mechanical properties of fibers and fiber/epoxy composites. The modified rule of mixture model, which introduced a fiber correlated porosity factor to consider the effect of porosity, fitted well with the experimental results of composite density and mechanical properties of composites. This study demonstrated that the applied model provides a concept for use in evaluation of the performance of treated fibers in composites.

9.2 Future perspectives

As we have shown in this study, hemp fibers have great potential for use as reinforcements in biocomposite materials. A series of chemical and enzymatic fiber processing approaches were conducted to improve the mechanical properties of hemp fibers and hemp fiber/epoxy composites. In principal, the studied fiber processing methods also are suitable for other lignocellulosic fibers for composite use. A lot of work can still be done to accelerate the application of natural fibers in polymer matrix composites.

Investigation of the effect of different polymer matrices on the mechanical properties of natural fibers is important to expand the application of natural fibers in biocomposite materials. Different polymer matrices may require additional fiber treatments to obtain the maximum mechanical properties of fiber reinforced composites. When hydrophobic polymers (e.g. polyester, polypropylene) in particular are used as matrix phase, fiber surfaces need to be treated to improve fiber/matrix interfaces. Alfa fiber surface modification by chemical reactions between chemical reagents (e.g. maleic anhydride, styrene and acrylic acid) and the OH group on fiber surfaces was conducted by Bessadok et al. (2009) [119]. Modification of flax fiber by grafting of various vinyl monomers mixtures such as methylmethacrylate (MMA)/ ethylacrylate (EA), MMA/acrylonitrile (AN) and MMA/acrylic acid (AA) has also been investigated to improve the mechanical or physical performance of natural fibers [120]. These techniques can possibly be applied to hemp fiber/ hydrophobic polymer composites.

As has shown in this study, without spinning into yarns, hemp bast fibers can be used for manufacturing strong biocomposites using different fiber processing methods. However, a continuous form of fibers (e.g. yarn) is required to up-scale industrial application. Traditional spinning techniques which involve decortication, scutching, carding, cottonization and spinning steps, can be applied to chemically and enzymatically treated fibers. However, traditional fiber processing was found to decrease the mechanical properties of hemp fibers dramatically [42]. Traditional fiber spinning is a part of the textile manufacturing process and produce yarn by twisting together of drawn out strands of fibers. The twisting angles depend on applied spinning method and can affect the mechanical properties of the composites [37]. New processing (e.g. dry-jet-wet spinning) for manufacturing regenerated fibers by using lignocellulosic materials has been intensively studied [121–124]. High-strength regenerated fibers have been obtained with UTS up to 800 MPa and stiffness of 30 GPa from cellulosic materials using ionic liquid (i.e. [DBNH][OAc]) as dissolution solvent. These techniques could be applied in this study. The structure of the regenerated fibers might be further reinforced by laccase treatments such as conducted in this study (paper VI).

With these considerations in mind, an interesting area for further study aimed at obtaining strong fibers for composite use could involve spinning cellulosic fibers or cellulosic materials into continuous forms of fibers (named regenerated fibers). This could be done using the dry-jet-wet spinning method using ionic liquids as dissolution solvent. Treatments of the regenerated fibers based on properties of the selected matrix polymers may be required to achieve the maximum mechanical properties of fibers and fiber reinforced composites.

CHAPTER X − REFERENCES

[1] Ranalli P, Venturi G. Hemp as a raw material for industrial applications. Euphytica 2004;140:1–6.

[2] Amaducci S, Scordia D, Liu FH, Zhang Q, Guo H, Testa G, et al. Key cultivation techniques for hemp in Europe and China. Ind Crops Prod 2014;68:2–16.

[3] Reddy N, Yang Y. Characterizing natural cellulose fibers from velvet leaf (*Abutilon theophrasti*) stems. Bioresour Technol 2008;99:2449–54.

[4] Liu M, Fernando D, Daniel G, Madsen B, Meyer A, Ale M, et al. Effect of harvest time and field retting duration on the chemical composition, morphology and mechanical properties of hemp fibers. Ind Crops Prod 2015;69:29–39.

[5] Faruk O, Bledzki AK, Fink HP, Sain M. Biocomposites reinforced with natural fibers: 2000-2010. Prog Polym Sci 2012;37:1552–96.

[6] Joshi S V., Drzal LT, Mohanty AK, Arora S. Are natural fiber composites environmentally superior to glass fiber reinforced composites? Compos Part A Appl Sci Manuf 2004;35:371–6.

[7] Fuqua MA, Huo S, Ulven CA. Natural Fiber Reinforced Composites. Polym Rev 2012;52:259–320.

[8] Van Vuure AW, Baets J, Wouters K, Hendrickx K. Compressive properties of natural fibre composites. Mater Lett 2015;149:138–40.

[9] Liu M, Silva DAS, Fernando D, Meyer AS, Madsen B, Daniel G, et al. Controlled retting of hemp fibres: Effect of hydrothermal pre-treatment and enzymatic retting on the mechanical properties of unidirectional hemp/epoxy composites. Compos Part A Appl Sci Manuf 2016;88:253–62.

[10] Pickering KL, Beckermann GW, Alam SN, Foreman NJ. Optimising industrial hemp fibre for composites. Compos Part A Appl Sci Manuf 2007;38:461–8.

[11] Schäfer T, Honermeier B. Effect of sowing date and plant density on the cell morphology of hemp (*Cannabis sativa* L.). Ind Crops Prod 2006;23:88–98.

[12] Liu M, Fernando D, Meyer AS, Madsen B, Daniel G, Thygesen A. Characterization and biological depectinization of hemp fibers originating from different stem sections. Ind Crops Prod 2015;76:880–91.

[13] Amaducci S, Zatta A, Pelatti F, Venturi G. Influence of agronomic factors on yield and quality of hemp (*Cannabis sativa* L.) fibre and implication for an innovative production system. Field Crop Res 2008;107:161–9.

[14] van der Werf HMG, van der Veen JEH, Bouma ATM, ten Cate M. Quality of hemp (*Cannabis sativa* L.) stems as a raw material for paper. Ind Crops Prod 1994;2:219–27.

[15] Thygesen A, Daniel G, Lilholt H, Thomsen AB. Hemp fiber microstructure and use of fungal defibration to obtain fibers for composite materials. J Nat Fibers 2006;2:19–37.

[16] Lefeuvre A, Bourmaud A, Morvan C, Baley C. Elementary flax fibre tensile properties: Correlation between stress-strain behaviour and fibre composition. Ind Crops Prod 2014;52:762–9.

[17] Fan M, Dai D, Yang A. High strength natural fiber composite: defibrillation and its mechanisms of nanocellulose hemp fibers. Int J Polym Mater Polym Biomater 2011;60:1026–40.

[18] Thygesen A, Liu M, Meyer AS, Daniel G. Hemp fibres: Enzymatic effect of microbial processing on fibre bundle structure. Risoe Int Symp Mater Sci Proc 2013;34:373–80.

[19] Jankauskienė Z, Butkutė B, Gruzdevienė E, Cesevičienė J, Fernando AL. Chemical composition and physical properties of dew- and water-retted hemp fibers. Ind Crops Prod 2015;75:206–11.

[20] Crônier D, Monties B, Chabbert B, Cronier, D ; Monties, B; Chabbert B. Structure and chemical composition of bast fibers isolated from developing hemp stem. J Agric Food Chem 2005;53:8279–89.

[21] Charlet K, Baley C, Morvan C, Jernot JP, Gomina M, Bréard J. Characteristics of Hermès flax fibres as a function of their location in the stem and properties of the derived unidirectional composites. Compos Part A Appl Sci Manuf 2007;38:1912–21.

[22] Korte S, Staiger MP. Effect of processing route on the composition and properties of hemp fibre. Fibers Polym 2008;9:593–603.

[23] Nykter M, Kymäläinen H-R, Thomsen AB, Lilholt H, Koponen H, Sjöberg A-M, et al. Effects of thermal and enzymatic treatments and harvesting time on the microbial quality and chemical composition of fibre hemp (*Cannabis sativa* L.). Biomass and Bioenergy 2008;32:392–9.

[24] Carpita NC, Gibeaut DM. Structural models of primary cell walls in flowering plants: consistency of molecular structure with the physical properties of the walls during growth. Plant J 1993;3:1–30.

[25] Peña MJ, Vergara CE, Carpita NC. The structures and architectures of plant cell walls define dietary fibre composition and the textures of foods. In: McCleary B V., Prosky L, editors. Adv. Diet. fibre Technol., Blackwell Science; 2008, p. 42–60.

[26] Chesson A, Gordon AH, Lomax JA. Substituent groups linked by alkali-labile bonds to arabinose and xylose residues of legume, grass and cereal straw cell walls and their fate during digestion by rumen microorganisms. J Sci Food Agric 1983;34:1330–40.

[27] Markwalder HU, Neukom H. Diferulic acid as a possible crosslink in hemicelluloses from wheat germ. Phytochemistry 1976;15:836–7.

[28] Ralph J. Hydroxycinnamates in lignification. Phytochem Rev 2010;9:65–83.

[29] Lupoi JS, Singh S, Parthasarathi R, Simmons BA, Henry RJ. Recent innovations in analytical methods for the qualitative and quantitative assessment of lignin. Renew Sustain Energy Rev 2015;49:871–906.

[30] Komuraiah A, Kumar NS, Prasad BD. Chemical composition of natural fibers and its influence on their mechanical properties. Mech Compos Mater 2014;50:359–76.

[31] Behazin E, Ogunsona E, Rodriguez-uribe A, Mohanty AK, Misra M, Anyia AO. Mechanical, chemical, and physical properties of wood and perennial grass biochars for possible composite application. Bioresources 2016;11:1334–48.

[32] Thuault A, Eve S, Blond D, Bréard J, Gomina M. Effects of the hygrothermal environment on the mechanical properties of flax fibres. J Compos Mater 2013;48:1699–707.

[33] Le Troedec M, Sedan D, Peyratout C, Bonnet JP, Smith A, Guinebretiere R, et al. Influence of various chemical treatments on the composition and structure of hemp fibres. Compos Part A Appl Sci Manuf 2008;39:514–22.

[34] Thygesen A, Madsen F, Lilholt H, Felby C, Thomsen A. Changes in chemical composition, degree of crystallisation and polymerisation of cellulose in hemp fibres caused by pre-treatment. Proc 23th Risø Int Symp Mater Sci Risø Natl Lab Denmark 2002:315–23.

[35] Kostic M, Pejic B, Skundric P. Quality of chemically modified hemp fibers. Bioresour Technol

2008;99:94–9.

[36] Di Candilo M, Bonatti PM, Guidetti C, Focher B, Grippo C, Tamburini E, et al. Effects of selected pectinolytic bacterial strains on water-retting of hemp and fibre properties. J Appl Microbiol 2010;108:194–203.

[37] Madsen B, Hoffmeyer P, Thomsen AB, Lilholt H. Hemp yarn reinforced composites - I. Yarn characteristics. Compos Part A Appl Sci Manuf 2007;38:2194–203.

[38] Thygesen A, Thomsen AB, Daniel G, Lilholt H. Comparison of composites made from fungal defibrated hemp with composites of traditional hemp yarn. Ind Crops Prod 2007;25:147–59.

[39] Pakarinen A, Zhang J, Brock T, Maijala P, Viikari L. Enzymatic accessibility of fiber hemp is enhanced by enzymatic or chemical removal of pectin. Bioresour Technol 2012;107:275–81.

[40] Bonatti PM, Ferrari C, Focher B, Grippo C, Torri G, Cosentino C. Histochemical and supramolecular studies in determining quality of hemp fibres for textile applications. Euphytica 2004;140:55–64.

[41] Zhang J, Zhang H, Zhang J. Evaluation of liquid ammonia treatment on surface characteristics of hemp fiber. Cellulose 2014;21:569–79.

[42] Thygesen A, Madsen B, Bjerre AB, Lilholt H. Cellulosic fibers: Effect of processing on fiber bundle strength. J Nat Fibers 2011;8:161–75.

[43] Klemm D, Heublein B, Fink HP, Bohn A. Cellulose: Fascinating biopolymer and sustainable raw material. Angew Chemie - Int Ed 2005;44:3358–93.

[44] Moon RJ, Martini A, Nairn J, Simonsen J, Youngblood J. Cellulose nanomaterials review: structure, properties and nanocomposites. Chem Soc Rev 2011;40:3941–94.

[45] Scheller HV, Ulvskov P. Hemicelluloses. Annu Rev Plant Biol 2010;61:263–89.

[46] Ochoa-Villarreal M, Aispuro-Hernández, Emmanuel Vargas-Arispuro I, Martínez-Téllez MÁ. Plant Cell Wall Polymers: Function, Structure and Biological Activity of Their Derivatives. In: Gomes ADS, editor. Polymerization, InTech; 2012, p. 63–86.

[47] Grabber JH, Hatfield RD, Ralph J, Zoń J, Amrhein N. Ferulate cross-linking in cell walls isolated from maize cell suspensions. Phytochemistry 1995;40:1077–82.

[48] Mueller-Harvey I, Hartley RD, Harris PJ, Curzon EH. Linkage of p-coumaroyl and feruloyl groups to cell-wall polysaccharides of barley straw. Carbohydr Res 1986;148:71–85.

[49] Iiyama K, Lam TBT, Stone BA. Phenolic acid bridges between polysaccharides and lignin in wheat internodes. Phytochemistry 1990;29:733–7.

[50] Lapierre C, Pollet B, Ralet MC, Saulnier L. The phenolic fraction of maize bran: Evidence for lignin-heteroxylan association. Phytochemistry 2001;57:765–72.

[51] Dutta S, Wu KC-W, Saha B. Emerging strategies for breaking the 3D amorphous network of lignin. Catal Sci Technol 2014;4:3785–99.

[52] Pedrolli D, Monteiro A. Pectin and pectinases: production, characterization and industrial application of microbial pectinolytic enzymes. Open Biotechnol J 2009;3:9–18.

[53] Mohnen D. Pectin structure and biosynthesis. Curr Opin Plant Biol 2008;11:266–77.

[54] Harholt J, Suttangkakul A, Vibe Scheller H. Biosynthesis of Pectin. Plant Physiol 2010;153:384–95.

[55] Vincken J-P, Schols HA, Oomen RJFJ, McCann MC, Ulvskov P, Voragen AGJ, et al. If homogalacturonan were a side chain of rhamnogalacturonan I. Implications for cell wall architecture. Plant Physiol 2003;132:1781–9.

[56] Caffall KH, Mohnen D. The structure, function, and biosynthesis of plant cell wall pectic polysaccharides. Carbohydr Res 2009;344:1879–900.

[57] Liners F, Letesson JJ, Didembourg C, Van Cutsem P. Monoclonal antibodies against pectin: recognition of a conformation induced by calcium. Plant Physiol 1989;91:1419–24.

[58] Davis MAF, Gidley MJ, Morris ER, Powell DA, Rees DA. Intermolecular association in pectin solutions. Int J Biol Macromol 1980;2:330–2.

[59] Walkinshaw MD, Arnott S. Conformations and interactions of pectins. II. Models for junction zones in pectinic acid and calcium pectate gels. J Mol Biol 1981;153:1075–85.

[60] Marrot L, Lefeuvre A, Pontoire B, Bourmaud A, Baley C. Analysis of the hemp fiber mechanical properties and their scattering (Fedora 17). Ind Crops Prod 2013;51:317–27.

[61] Bourmaud A, Morvan C, Bouali A, Placet V, Perré P, Baley C. Relationships between micro-fibrillar angle, mechanical properties and biochemical composition of flax fibers. Ind Crops Prod 2013;44:343–51.

[62] Neagu RC. Stiffness Contribution of Various Wood Fibers to Composite Materials. J Compos Mater 2005;40:663–99.

[63] Nilsson T, Gustafsson PJ. Influence of dislocations and plasticity on the tensile behaviour of flax and hemp fibres. Compos Part A Appl Sci Manuf 2007;38:1722–8.

[64] Baley C. Analysis of the flax fibres tensile behaviour and analysis of the tensile stiffness increase. Compos Part A Appl Sci Manuf 2002;33:939–48.

[65] Dai D. Characteristic and performance of elementary hemp fibre. Mater Sci Appl 2010;1:336–42.

[66] Álvarez C, Rojano B, Almaza O, Rojas OJ, Gañán P. Self-bonding boards from plantain fiber bundles after enzymatic treatment: adhesion improvement of lignocellulosic products by enzymatic pre-treatment. J Polym Environ 2011;19:182–8.

[67] Sawpan MA, Pickering KL, Fernyhough A. Effect of various chemical treatments on the fibre structure and tensile properties of industrial hemp fibres. Compos Part A Appl Sci Manuf 2011;42:888–95.

[68] Mwaikambo LY, Ansell MP. Mechanical properties of alkali treated plant fibres and their potential as reinforcement materials. I. hemp fibres. J Mater Sci 2006;41:2483–96.

[69] Duval A, Bourmaud A, Augier L, Baley C. Influence of the sampling area of the stem on the mechanical properties of hemp fibers. Mater Lett 2011;65:797–800.

[70] Placet V, Trivaudey F, Cisse O, Gucheret-Retel V, Boubakar ML. Diameter dependence of the apparent tensile modulus of hemp fibres: A morphological, structural or ultrastructural effect? Compos Part A Appl Sci Manuf 2012;43:275–87.

[71] Fu SY, Lauke B, Mäder E, Yue CY, Hu X. Tensile properties of short-glass-fiber- and short-carbon-fiber-reinforced polypropylene composites. Compos Part A Appl Sci Manuf 2000;31:1117–25.

[72] Callister WD. Materials science and engineering. 3rd ed. New York: John Wiley & Sons, INC.; 1994.

[73] Shah DU, Schubel PJ, Clifford MJ. Can flax replace E-glass in structural composites? A small wind turbine blade case study. Compos Part B Eng 2013;52:172–81.

[74] Pickering KL, Efendy MGA, Le TM. A review of recent developments in natural fibre composites and their mechanical performance. Compos Part A Appl Sci Manuf 2015;83:98–112.

[75] Oksman K, Skrifvars M, Selin JF. Natural fibres as reinforcement in polylactic acid (PLA) composites. Compos Sci Technol 2003;63:1317–24.

[76] Madsen B, Thygesen A, Lilholt H. Plant fibre composites – porosity and stiffness. Compos Sci Technol 2009;69:1057–69.

[77] Madsen B, Lilholt H. Physical and mechanical properties of unidirectional plant fibre composites-an evaluation of the influence of porosity. Compos Sci Technol 2003;63:1265–72.

[78] Brown AE, Sharma HSS. Production of polysaccharide-degrading enzymes by saprophytic fungi from glyphosate treated flax and their involvement in retting. AnnApplBiol 1984;105:65–74.

[79] Ribeiro A, Pochart P, Day A, Mennuni S, Bono P, Baret JL, et al. Microbial diversity observed during hemp retting. Appl Microbiol Biotechnol 2015;99:4471–84.

[80] Jankauskiene Z, Lugauskas A, Repeckiene J. New methods for the improvement of flax dew retting. J Nat Fibers 2007;3–4:59–69.

[81] Islam MS, Pickering KL, Foreman NJ. Influence of alkali fiber treatment and fiber processing on the mechanical properties of hemp/epoxy composites. J Appl Polym Sci 2011;119:3696–707.

[82] Evans JD, Akin DE, Foulk JA. Flax-retting by polygalaxturonase-containing enzyme mixtures and effects on fiber properties. J Biotechnol 2002;97:223–31.

[83] Evans JD, Akin DE, Morrison WH, Himmelsbach DS, Foulk JA. Modifying Dew-Retted Flax Fibers by Means of an Air-Atomized Enzyme Treatment. Text Res J 2002;72:579–85.

[84] Li Y, Pickering KL. Hemp fibre reinforced composites using chelator and enzyme treatments. Compos Sci Technol 2008;68:3293–8.

[85] Li Y, Pickering KL, Farrell RL. Determination of interfacial shear strength of white rot fungi treated hemp fibre reinforced polypropylene. Compos Sci Technol 2009;69:1165–71.

[86] Aziz SH, Ansell MP. The effect of alkalization and fibre alignment on the mechanical and thermal properties of kenaf and hemp bast fibre composites: Part 1 - polyester resin matrix. Compos Sci Technol 2004;64:1219–30.

[87] Hanana S, Elloumi A, Placet V, Tounsi H, Belghith H, Bradai C. An efficient enzymatic-based process for the extraction of high-mechanical properties alfa fibres. Ind Crops Prod 2015;70:190–200.

[88] Cao Y, Chan F, Chui YH, Xiao H. Characterization of flax fibres modified by alkaline, enzyme, and steam-heat treatments. BioResources 2012;7:4109–21.

[89] Jähn A, Schröder MW, Füting M, Schenzel K, Diepenbrock W. Characterization of alkali treated flax fibres by means of FT Raman spectroscopy and environmental scanning electron microscopy. Spectrochim Acta - Part A Mol Biomol Spectrosc 2002;58:2271–9.

[90] Foulk J, Akin D, Dodd R. Influence of pectinolytic enzymes on retting effectiveness and resultant fiber properties. BioResources 2008;3:155–69.

[91] Hu W, Ton-That MT, Denault J, Rho D, Yang J, Lau PCK. Comparison between dew-retted and enzyme-retted flax fibers as reinforcing material for composites. Polym Eng Sci 2012;52:165–71.

[92] Diddens I, Murphy B, Krisch M. Anisotropic elastic properties of cellulose measured using inelastic X-ray scattering. Macromolecules 2008:9755–9.

[93] Eichhorn SJ, Young RJ, Davies GR. Modeling crystal and molecular deformation in regenerated cellulose fibers. Biomacromolecules 2005;6:507–13.

[94] Baley C, Busnel F, Grohens Y, Sire O. Influence of chemical treatments on surface properties and adhesion of flax fibre-polyester resin. Compos Part A Appl Sci Manuf 2006;37:1626–37.

[95] Mishra S, Mohanty AK, Drzal LT, Misra M, Parija S, Nayak SK, et al. Studies on mechanical performance of biofibre/glass reinforced polyester hybrid composites. Compos Sci Technol 2003;63:1377–85.

[96] Li X, Tabil LG, Panigrahi S. Chemical treatments of natural fiber for use in natural fiber-reinforced composites: A review. J Polym Environ 2007;15:25–33.

[97] Benen JAE, Kester HCM, Visser J. Kinetic characterization of *Aspergillus niger* N400 endopolygalacturonases I, II and C. Eur J Biochem 1999;259:577–85.

[98] Akin DE, Foulk JA, Dodd RB, McAlister DD. Enzyme-retting of flax and characterization of processed fibers. J Biotechnol 2001;89:193–203.

[99] Saleem Z, Rennebaum H, Pudel F, Grimm E. Treating bast fibres with pectinase improves mechanical characteristics of reinforced thermoplastic composites. Compos Sci Technol 2008;68:471–6.

[100] Adamsen APS, Akin DE, Rigsby LL. Chelating agents and enzyme retting of flax. Text Res J 2002;72:296–302.

[101] Stuart T, Liu Q, Hughes M, McCall RD, Sharma HSS, Norton A. Structural biocomposites from flax - Part I: Effect of bio-technical fibre modification on composite properties. Compos Part A Appl Sci Manuf 2006;37:393–404.

[102] Griko Y V. Energetics of Ca(2+)-EDTA interactions: calorimetric study. Biophys Chem 1999;79:117–27.

[103] Mediavilla V, Leupin M, Keller A. Influence of the growth stage of industrial hemp on the yield formation in relation to certain fibre quality traits. Ind Crops Prod 2001;13:49–56.

[104] van der Werf HMG, van Geel WCA, van Gils LJC, Haverkort AJ. Nitrogen fertilization and row width affect self-thinning and productivity of fibre hemp (*Cannabis sativa* L.). Field Crop Res 1995;42:27–37.

[105] Keller A, Leupin M, Mediavilla V, Wintermantel E. Influence of the growth stage of industrial hemp on chemical and physical properties of the fibres. Ind Crops Prod 2001;13:35–48.

[106] Struik PC, Amaducci S, Bullard MJ, Stutterheim NC, Venturi G, Cromack HTH. Agronomy of fibre hemp (*Cannabis sativa* L.) in Europe. Ind Crops Prod 2000;11:107–18.

[107] Fischer H, Müssig J, Bluhm C. Enzymatic modification of hemp fibres for sustainable production of high quality materials. J Nat Fibers 2006;3:39–53.

[108] Larsen J, Haven MØ, Thirup L. Inbicon makes lignocellulosic ethanol a commercial reality. Biomass and Bioenergy 2012;46:36–45.

[109] Oh YH, Eom IY, Joo JC, Yu JH, Song BK, Lee SH, et al. Recent advances in development of biomass pretreatment technologies used in biorefinery for the production of bio-based fuels, chemicals and polymers. Korean J Chem Eng 2015;32:1945–59.

[110] Thomsen MH, Thygesen A, Thomsen AB. Hydrothermal treatment of wheat straw at pilot plant scale using a three-step reactor system aiming at high hemicellulose recovery, high cellulose digestibility and low lignin hydrolysis. Bioresour Technol 2008;99:4221–8.

[111] Zaidel DNA, Arnous A, Holck J, Meyer AS. Kinetics of enzyme-catalyzed cross-linking of feruloylated arabinan from sugar beet. J Agric Food Chem 2011;59:11598–607.

[112] Ikeda R, Uyama H, Kobayashi S. Novel synthetic pathway to a poly (phenylene oxide). laccase-catalyzed oxidative polymerization of syringic acid. Macromolecules 1996:3053–4.

[113] Oosterveld A, Grabber JH, Beldman G, Ralph J, Voragen AGJ. Formation of ferulic acid dehydrodimers through oxidative cross-linking of sugar beet pectin. Carbohydr Res 1997;300:179–81.

[114] Ku H, Wang H, Pattarachaiyakoop N, Trada M. A review on the tensile properties of natural fiber reinforced polymer composites. Compos Part B Eng 2011;42:856–73.

[115] Sanadi AR, Prasad S V., Rohatgi PK. Sunhemp fibre-reinforced polyester. J Mater Sci 1986;21:4299–304.

[116] Roe PJ, Ansell MP. Jute-reinforced polyester composites. J Mater Sci 1985;20:4015–20.

[117] Shah DU, Schubel PJ, Licence P, Clifford MJ. Determining the minimum, critical and maximum fibre content for twisted yarn reinforced plant fibre composites. Compos Sci Technol 2012;72:1909–17.

[118] Joffe R, Madsen B, Nattinen K, Miettinen A. Strength of cellulosic fiber/starch acetate composites with variable fiber and plasticizer content. J Compos Mater 2014;49:1007–17.

[119] Bessadok A, Roudesli S, Marais S, Follain N, Lebrun L. Alfa fibres for unsaturated polyester composites reinforcement: Effects of chemical treatments on mechanical and permeation properties. Compos Part A Appl Sci Manuf 2009;40:184–95.

[120] Kalia S, Kaith BS, Kaur I. Pretreatments of natural fibers and their application as reinforceing material in polymer composites-A review. Polym Eng Sci 2009;49:1253–72.

[121] Ma Y, Asaadi S, Johansson L-S, Ahvenainen P, Reza M, Alekhina M, et al. High-strength composite fibers from cellulose-lignin blends regenerated from ionic liquid solution. ChemSusChem 2015:1–11.

[122] Vehviläinen M, Kamppuri T, Rom M, Janicki J, Ciechańska D, Grönqvist S, et al. Effect of wet spinning parameters on the properties of novel cellulosic fibres. Cellulose 2008;15:671–80.

[123] Jiang G, Huang W, Li L, Wang X, Pang F, Zhang Y, et al. Structure and properties of regenerated cellulose fibers from different technology processes. Carbohydr Polym 2012;87:2012–8.

[124] Ingildeev D, Effenberger F, Bredereck K, Hermanutz F. Comparison of direct solvents for regenerated cellulosic fibers via the lyocell process and by means of ionic liquids. J Appl Polym Sci 2013;128:4141–50.

Paper I

Ming Liu, Dinesh Fernando, Geffrey Daniel, Bo Madsen, Anne S. Meyer, Marcel Tutor Ale, & Anders Thygesen

Effect of harvest time and field retting duration on the chemical composition, morphology and mechanical properties of hemp fibers

Industrial Crops and Products, 2015, 69, 29-39

Industrial Crops and Products 69 (2015) 29–39

Contents lists available at ScienceDirect

Industrial Crops and Products

journal homepage: www.elsevier.com/locate/indcrop

Effect of harvest time and field retting duration on the chemical composition, morphology and mechanical properties of hemp fibers

Ming Liu [a], Dinesh Fernando [b], Geoffrey Daniel [b], Bo Madsen [c], Anne S. Meyer [a], Marcel Tutor Ale [a], Anders Thygesen [a,*]

[a] Center for Bioprocess Engineering, Department of Chemical and Biochemical Engineering, Technical University of Denmark, Søltofts Plads 229, 2800 Lyngby, Denmark
[b] Department of Forest Products/Wood Science, Swedish University of Agricultural Sciences, Vallvägen 9d, 75651 Uppsala, Sweden
[c] Department of Wind Energy, Technical University of Denmark, Frederiksborgvej 399, 4000 Roskilde, Denmark

ARTICLE INFO

Article history:
Received 31 October 2014
Received in revised form 3 February 2015
Accepted 5 February 2015

Keywords:
Cannabis sativa L.
Hemp fiber
Fiber extraction
Field retting
Mechanical properties

ABSTRACT

The large variability in the mechanical properties of hemp fibers is an issue in relation to their use in high-grade composites. The objective of the present study was to determine the optimal growth stage for harvesting hemp fibers for use in composites and to evaluate the effect of field retting time on mechanical performance of the fibers. Reduction in bast content and thickness of the primary bast fiber layer in stems were found to be highly significant ($P < 0.01$) with plant maturity. A significant increase in the secondary fiber fraction occurred with maturity, reaching a maximum value of 10% at seed maturity. A highly significant reduction in cellulose deposition in fiber cell walls was reflected by reduced fiber wall thickness with plant maturity and was related to the development and ripening of hemp seeds. A statistically significant increase in lignin deposition and a slight decrease in pectins in hemp fiber cell walls were also noted with stem maturity. Microscopy observations and histochemical analyzes corroborated the results from the chemical analyzes and revealed variations in morphological aspects and spatial micro-distributions of carbohydrates and lignin within the cell structure of the hemp stems between early- and late growth phases. Fibers harvested at the beginning of flowering exhibited high tensile strength and strain, which decreased with plant maturity. Reduction in strength was related to the increase in proportion of secondary fibers and decrease in cellulose deposition leading to inferior properties of fibers. A negative effect of field retting occurred only after extended field retting (i.e., 70 days) which was presumably due to accelerated degradation of cellulose by the action of microorganisms.

1. Introduction

Hemp fibers are cellulose-rich cells that are attractive as reinforcement agents in composite materials due to their low cost and density, good mechanical properties and potential sustainability and biodegradability (Islam et al., 2011; Thygesen et al., 2005, 2011). The hemp fibers suitable for composites are the primary- and secondary fibers (i.e., bast fibers) situated in the cortex of the hemp plant stem. The bast fibers encircle the core xylem and originate from the procambium and correspond to sclerenchyma primary cells (Crônier et al., 2005; Esau, 1943). Their morphological features differ significantly from those of xylem fibers. In addition, the morphology and chemical composition of bast fibers vary with maturity (Charlet et al., 2007; Duval et al., 2011; Mediavilla et al., 2001). This results in large variations in the mechanical properties of the fibers (Placet et al., 2012), and these variations are generally considered a major barrier for using hemp fibers in composites where high reliability and stability of fiber properties are required.

The main chemical components of hemp fiber cell walls are cellulose, hemicelluloses, lignin and pectin and the fibers are bound together by a pectin and lignin-rich middle lamella (ML) (Love et al., 1994; Nykter et al., 2008). For high-grade composites, the ML-fiber-fiber bonding must be degraded to obtain individual fibers and/or small fiber bundles. Therefore to increase the ease of fiber extraction from plants and reduce fiber breakage, the stems are normally retted before mechanical separation (termed "decortication"). The retting stage is critical for the broad use of hemp fibers with respect to economic aspects and fiber quality (Keller et al., 2001; Mediavilla et al., 2001).

* Corresponding author. Tel.: +45 21326303.
E-mail address: athy@kt.dtu.dk (A. Thygesen).

http://dx.doi.org/10.1016/j.indcrop.2015.02.010
0926-6690/

In field retting (also known as dew-retting), plant stems are spread out in the fields where they are attacked mainly by fungi. The pectinolytic enzymes expressed by the fungi can degrade the pectin in the middle lamella regions between fibers (Henriksson et al., 1997). Field retting is still widely used due to its low cost (Bacci et al., 2010), but is limited to geographic regions where weather conditions are suitable for fungi proliferation. Field retting also causes many problems such as increased scattering of fiber properties, insecurity of fiber supply due to poor weather conditions and may also cause delays in the planting of subsequent crops. Due to these disadvantages, more efficient and controllable methods have been investigated, including chemical treatment (Song and Obendorf, 2006), mechanical defibration (Vignon et al., 1996), and enzymatic retting (Li and Pickering, 2008). However, those methods require high energy input or expensive enzymes and/or may generate costly wastes (Tahir et al., 2011).

For natural fibers, their mechanical performance (e.g., tensile strength) largely depends on a number of crucial physical and chemical parameters, and the mechanical performances of natural hemp fibers were recently shown to be highly dependent on fiber diameter (Duval et al., 2011; Marrot et al., 2013; Placet et al., 2012). Tensile strength is found to decrease as the fiber diameter increases and this diameter dependence is closely related to both the number of fiber defects (i.e., kinks or dislocations) and number of single fibers contained in the fiber bundles (Fan, 2010).

Hemp contains secondary bast fibers situated outside the vascular cambium. These secondary fibers are shorter (approx. 2 mm long) and thinner (approx. 15 μm in diameter) than primary fibers (i.e., tenths of mm in length and 18–24 μm in diameter) (Mishra 2009; Sankari 2000a). According to Amaducci et al. (2008), these secondary fibers are primarily located at the bottom of the plant stem. Their formation has been reported to cause a reduction in both fiber yield and quality after flowering (Mediavilla et al., 2001). Thus, the mechanical properties of hemp fibers are dependent on many parameters such as fiber diameter, defects, chemical composition, and the presence/proportion of secondary fibers.

The aims of the present work were to provide an improved understanding of the reduction of mechanical properties of hemp fibers in relation to morphological features and chemical composition during growth and field retting.

2. Materials and methods

2.1. Raw material

2.1.1. Cultivation and harvest

The hemp (*Cannabis sativa* L.), variety USO-31, was sown at a rate of 45 kg/ha on May 5th 2013 in France (N 48.85°, E 3.02° (WGS84)) by hemp cultivation companies (Planète Chanvre and Bafa Neu GmbH). The seeds were sown with the seed drill 3–4 inches deep. The hemp plants were fertilized with 80 kg/ha N, 45 kg/ha K and 45 kg/ha P. The monoecious hemp plants were harvested at two developmental stages: (1) at the beginning of flowering (i.e., early harvest on July 18th 2013); and (2) seed maturity (i.e., late harvest on Sep 6th 2013). Using the definition of hemp growth stages given by Mediavilla et al. (1998), the two stages selected correspond to codes 2101 and 2204. Precipitation was not well distributed over the season (beginning of May to the end of September, 2013). From sowing date to the early harvest date, the weather was cool with an average temperature of 14.5 °C and precipitation was relatively evenly distributed with a total of 115 mm. Between early and late harvest (first retting period for early harvest sample, 50 days in total), the weather was quite hot (especially during daytime) with an average temperature of 19.6 °C and dry with a precipitation of 52 mm. From late harvest to the end of field retting (20 days in total), the weather was humid with a total precipitation of 41 mm and cool with an average temperature of 14.2 °C (Fig. 1).

2.1.2. Sampling and storage

In this study, sampling involved a complete randomized block design with three replications. With each harvest (i.e., early- and late harvest), in every replicate, 10 m^2 above-ground part of hemp was harvested and the number of plants was determined. Considering the high dependence of morphological feature, chemical composition and mechanical properties on hemp stem sections, only the bottom section (one third above the base of the stem) of the plant was investigated (Charlet et al., 2007; Duval et al., 2011). A randomized sample of 20 bottom sections of plants per replication was used to determine the diameter of hemp stem and bast content.

A flow diagram of the setup for this study is presented in Fig. 2. For early harvest, a randomized sample of 80 plants per replication was divided into 4 groups (Group 1–Group 4). For late harvest, a randomized sample of 100 plants per replication was divided into 5 groups (Group 1–Group 5).

2.2. Cell wall isolation

The bast fibers were air-dried at 40 °C with an air flow of 150 $m^3/(m^2$ grid h) (Maskinfabrikken Thisted, Denmark Type 150) and ground with a crushing microfine grinder (IKA, MF 10.1) to a particle size of 1 mm. Samples of about 3 g were then extracted in a Soxhlet apparatus (Gerhardt EV6 All/16 No. 10-0012) for 5 h using a 300 mL solution of toluene-ethanol-acetone (4:1:1 by volume) (Sluiter et al., 2008; Özmen et al., 2013). For each sample, the final residue was dried at 50 °C for 12 h. and the resulting residue was designated as cell wall residue (CWR).

2.3. Chemical analysis of CWR

Chemical analyzes were done using two-step sulfuric acid hydrolysis at 72% and 4% (w/w), according to the method of the US National Renewable Energy Laboratory (Sluiter et al., 2011). After acid hydrolysis, the hydrolysate was collected for monosaccharide analysis. Hemp fibers are characterized by their low lignin content, and the lignin content of hemp bast fibers is usually characterized by Klason lignin. (Charlet et al., 2007; Gutiérrez et al., 2006). For Klason lignin analysis, a crucible with filtrated solids (i.e., acid-insoluble ash + acid–insoluble lignin) was dried in an oven at 105 °C for 12 h. After cooling to room temperature in a desiccator, the crucibles were weighed (W1). Subsequently, the crucibles were placed in a muffle furnace at 550 °C for 3 h, then cooled in the desiccator and reweighed as W2 (i.e., acid–insoluble ash). The amount of acid–insoluble lignin (also termed Klason lignin) was determined as W1–W2.

Monosaccharide analyzes were performed by HPAEC-PAD analysis using an ICS-3000 system consisting of a gradient pump (model DP-1), an electrochemical detector/chromatography module (model DC-1) and autosampler (Dionex Corp., Sunnyvale, CA). Separation was achieved using a CarboPacTM PA20 (3 mm × 150 mm) analytical column following that described by Arnous and Meyer (2008). Roughly, it is considered that arabinose, galactose, galacturonic acid and rhamnose are specific to pectins, and glucose belongs to the cellulose moiety (Crônier et al., 2005; Vignon and Garcia-Jaldon, 1996). The concentration of polymeric sugars was calculated from the concentration of the corresponding monomeric sugars, using an anhydrous correction of 0.88 for C-5 sugars and a correction of 0.9 for C-6 sugar (Sluiter et al., 2011).

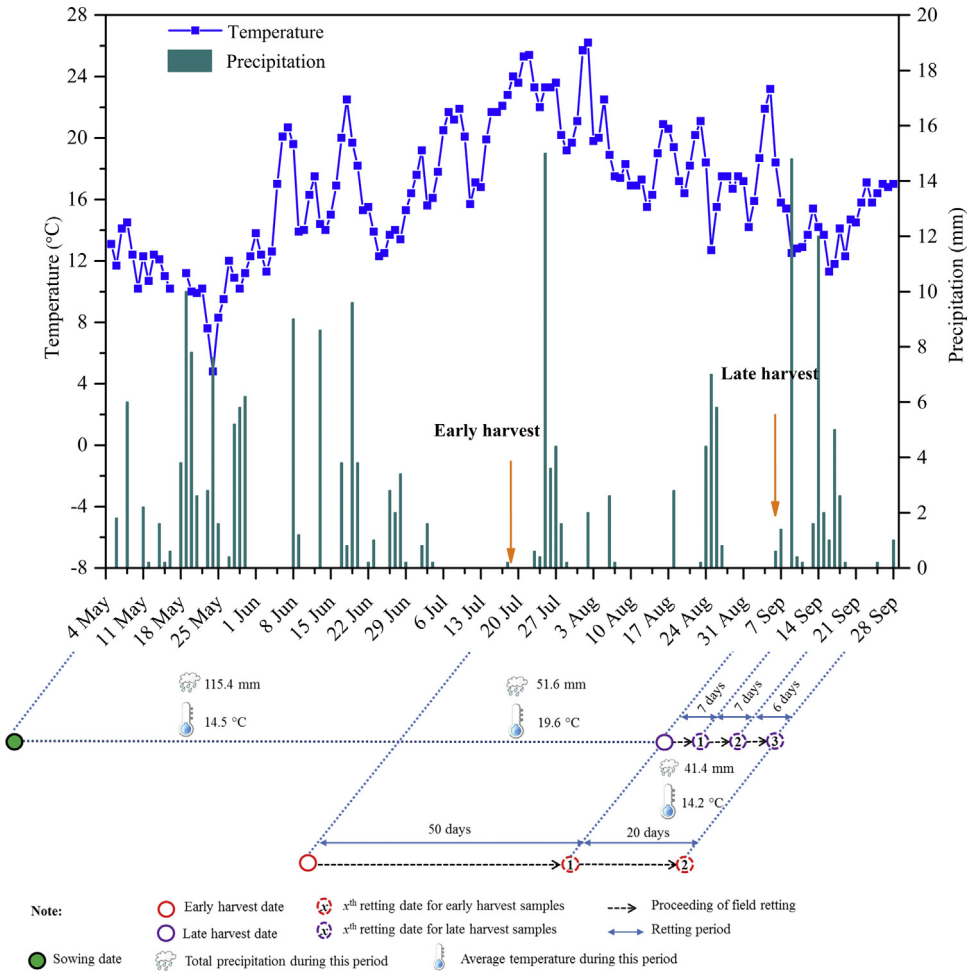

Fig. 1. Precipitation and daily average temperature in the trial location during the period of growth of the hemp plants and field retting (Meteo France, Weather station Mouroux no. 77320002).

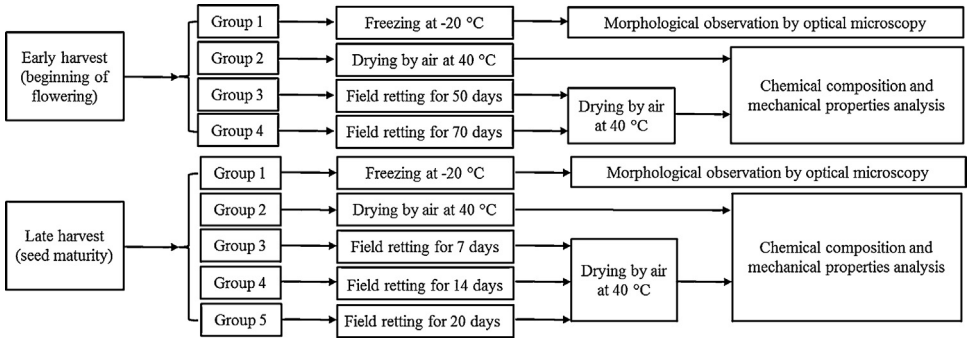

Fig. 2. Flow diagram showing sample preparation in this study.

2.4. Microscopic and histochemical observations

Fresh transverse sections were cut from the bottom regions of hemp stems using a stereo microscope (Wild Heerbrugg M8, Wild Leitz, Switzerland). Histochemical staining was performed on transverse hemp stem sections on glass slides followed by adding one drop of 50% (v/v) glycerol in water. Cover slips were placed on the stained sections, mounted in glycerol and examined immediately using a Leica DMLB light microscope (LM) with digital images recorded using an Infinity X-32 camera (DeltaPix Denmark). The following histochemical reactions were performed (Thygesen et al., 2005):

2.4.1. Lignin-hydroxycinnamyl aldehydes (Wiesner reaction)

The stem sections were stained with two drops of 10 g/L phloroglucinol in ethanol followed by the addition of one drop of 35% (v/v) HCl.

2.4.2. Syringyl lignin (Mäule reaction)

The stem sections were stained with one drop of 1% (w/v) aqueous $KMnO_4$ for 5 min. followed by three washes in water. The stem sections were then immersed in 3% (v/v) HCl for 1 min, washed with distilled water and immersed in 29% (v/v) NH_3 for 1 min, followed by washing with distilled water.

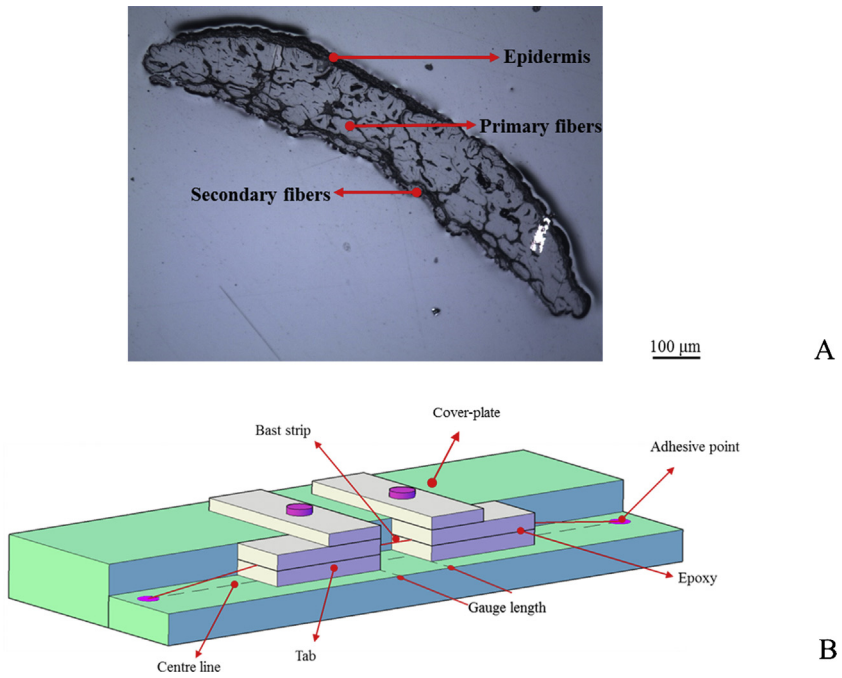

Fig. 3. The micrograph showing a transverse section of a bast fiber strip (A) and the setup used for sample preparation for tensile strength testing (B).

2.4.3. Pectin

The stem sections were stained with 0.02% (w/v) aqueous ruthenium red (JMC Specialty Products).

Due to the temporary nature of the staining reactions, all observations including digital image recording were performed within 10–15 mins of staining. A number of morphological features were measured using Image-Pro Plus (Media Cybernetics Inc., USA), including thickness and area of epidermis, primary fiber layer (PFL), secondary fiber layer (SFL), cambium, fiber cell walls and lumen. Thus the PF- (i.e., ratio of the PFL area to the bast area) and SF fractions (i.e., ratio of the SFL area to the bast area) could be determined.

Morphological features at hemp stem level were determined as the average of 4 measurements from 10 transverse sections from 3 bundles of each sample, which in total represented 120 measurements. At the single fiber level, an average of 4 measurements from 50 cells from 3 fiber bundles of each sample of bast fibers were made representing in total 600 measurements.

2.5. Tensile strength testing of fiber bundles

The bast fiber strips (80 mm long × 1 mm wide) were peeled manually from the hemp stem followed by minor modification of the strips with a razor blade to obtain constant width along the entire length of the bast fiber strips using a light microscope. The main part of the epidermis of each strip was removed using a razor blade and the center part of the strip, with length 60 mm, was excised for tensile testing. The other two pieces (each 10 mm in length) were embedded in epoxy resin and the cross-sectional area determined by optical microscopy combined with image analysis. The average cross-sectional area was applied in the further calculations. A sketch and a micrograph of a typical transverse section of the bast fibers are shown in Fig. 3A. Tensile tests were carried out on 20 specimens at each treatment level.

Test specimens were made by gluing tabs on each fiber tip with epoxy resin (DP 100) with a custom-made holder (Fig. 3B). Considering the short length of single fibers in test specimens, a gauge

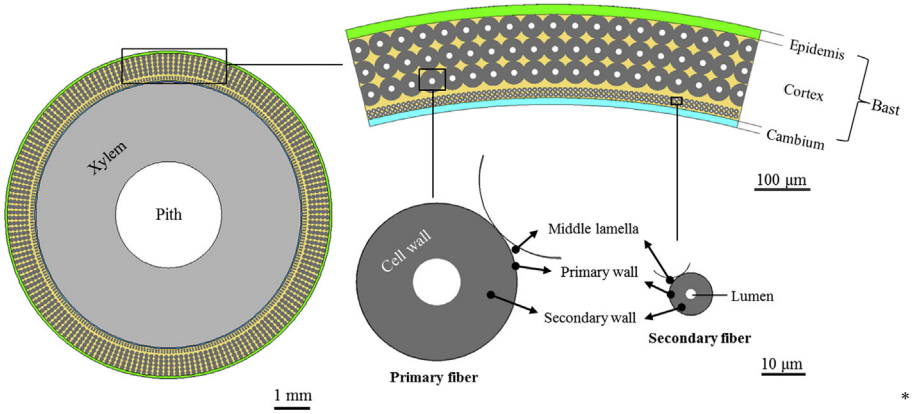

Fig. 4. Schematic diagram of a transverse section of hemp stem showing the organization and morphology of a bast strip and single fiber (e.g., primary- and secondary fibers) in the bast layer.

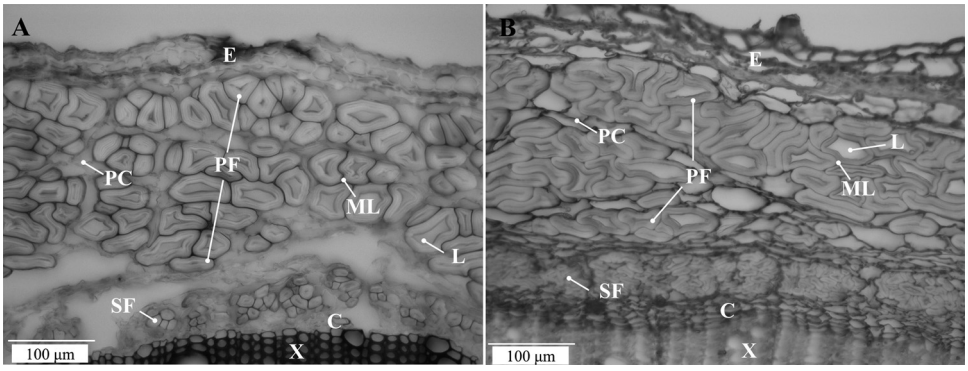

Fig. 5. Light micrographs of transverse sections from developing hemp stems: (A) early harvest; (B) late harvest.
E: epidermis; PF: primary fiber; X: xylem; PC: parenchyma cell; SF: secondary fiber; C: cambium; ML: middle lamella; L: lumen.

length of 10 mm was used. Bast fiber strips were first placed on the surface of the bottom tabs, aligned along the centerline and fixed at two adhesive points, keeping the test pieces straight. Then, a drop of epoxy resin was applied to the center of the bottom tabs and the upper tab placed on top. Finally a cover-plate was used to clamp the tabs using screw nuts. After curing at 20 °C for 24 h, the fixed samples were removed from the holder.

All samples were tensile tested using an Instron Testing Machine 2710-203 equipped with a 1000 N load cell, at a tensile speed of 0.5 mm/min at 25 °C and 50% humidity. The ultimate tensile strength (UTS) of the bast strips was defined as the ratio of failure load (N) and the cross-sectional area of the bast strips including the area of fiber cell walls and lumen.

2.6. Statistical analysis

Analysis of variance (ANOVA) for the two growth stages was performed on each measurement. For each morphological characteristic, chemical composition and mechanical properties, maturation effect was tested at a significance level of 5% (Minitab 16). For the mechanical properties of retted fibers, ANOVA was performed independently on the measurements of early- and late harvest samples and the field retting duration effect was tested. Differences between each retting time were evaluated using the Turkey multiple comparison test with a level of significance at 5%.

3. Results and discussion

3.1. Hemp stem morphology

The original hemp stems were 1.5–2.5 m tall and 5–15 mm in diameter. The stems contained 30–40% w/w bast fibers and were organized in layers from the stem pith toward the surface by 1–5 mm xylem, 10–50 μm cambium, 100–300 μm cortex, 20–100 μm epidermis and 2–5 μm cuticle at the macroscopic level. At the microscopic level, the bast fibers included primary- and secondary fibers. The definition of stem components was in accordance with that reported by Garcia-Jaldon et al. (1998) and Schäfer and Honermeier (2006) and shown schematically in Fig. 4. A large variation in the morphological features of hemp bast fibers from bottom section to top section was observed. Only the bottom section was therefore investigated in this study.

3.2. Microscopic observations of hemp bast fibers from different stem sections

A microscopic image of a transverse section illustrating the cellular structure of developing hemp stems is shown in Fig. 5 and morphological characteristics at stem- and single fiber levels shown in Tables 1 and 2, respectively. Great variations in the morphology of hemp stems were apparent with maturity providing interesting information on the variability at both bast fiber- and individual fiber levels. However, the same overall organization of layers from the innermost xylem toward the surface consisting of cambium, secondary- and primary fibers, epidermis and cuticle were observed for both developmental stages (Fig. 5A and B).

At the bast fiber level, there was a significant increase in thickness of secondary fiber layer (SFL) from 10 to 54 μm from early- to late harvest, but major reductions in the thickness of epidermis and primary fiber layer (PFL) were observed (Table 1). As a result, the primary fiber (PF) fraction decreased from 49 to 45% (non-significant at $P = 0.05$) and secondary fiber (SF) fraction increased significantly from 2 to 10%.

Hemp is characterized by the presence of secondary fibers which are shorter and thinner than primary fibers (Mishra 2009; Sankari 2000a). Amaducci (2008) reported the secondary fibers as primarily present in the bottom of plant stems. Besides the effect of fiber location inside hemp stems, Schäfer and Honermeier (2006) reported that the proportion of secondary fibers was affected by weather (i.e., dry conditions) and concluded that harsh weather results in more secondary fibers. According to our microscopy observations, the proportion of secondary fibers increased with period of growth. At the beginning of flowering, only a few secondary fibers surrounded by many parenchyma cells existed in the inner part of the bast fiber

Table 1
Morphological features of developing hemp stems analyzed from transverse sections of hemp stems (values in the table are shown as mean ± standard deviation).

Sample	Stem diameter (mm)	Bast content (%)	Xylem content (%)	EL thickness (μm)	PFL thickness (μm)	SFL thickness (μm)	PF fraction[b] (%)	SF fraction[b] (%)
Early harvest	7.2 ± 0.8	44 ± 1	56 ± 1	89 ± 23	184 ± 47	10 ± 3	49 ± 3	2 ± 3
Late harvest	8.6 ± 0.9	37 ± 1	63 ± 1	52 ± 21	119 ± 10	54 ± 4	45 ± 5	10 ± 6
F[a] value	4.0 ***	51.0 **	51.0 **	9.8 **	11 **	215 ***	ns	6 **

PFL: primary fiber layer, SFL: secondary fiber layer, EL: epidermis layer, ns: non-significant.
[a] F value for harvest time effect at $P < 0.05$ (*), $P < 0.01$ (**), and $P < 0.001$ (***).
[b] PF- and SF fractions were defined as the ratio of transverse area of primary- and secondary fiber in the fiber strip to the sum of the transverse area of epidermis layer, primary fiber layer, secondary fiber layer and cambium layer, respectively.

Table 2
Morphological features of developing hemp stems analyzed from transverse sections of fibers (values in the table are shown as mean ± standard deviation).

	Cell wall thickness (μm)	Cell area (μm^2)	Lumen area (μm^2)	Lumen (%)
Primary fiber				
Early harvest	12.2 ± 2.8	1416 ± 627	123 ± 125	8.2 ± 6.8
Late harvest	11.1 ± 2.0	1500 ± 772	173 ± 332	7.9 ± 9.4
P value[1]	<0.001	>0.05	>0.05	>0.05
Secondary fiber				
Early harvest	5.1 ± 1.4	193 ± 169	8 ± 8	7 ± 9
Late harvest	4.6 ± 1.2	178 ± 83	3 ± 3	2 ± 2
P value[*]	>0.05	>0.05	>0.05	>0.05

[*] *P* value: harvest time effect on the measurements of morphological features for primary- and secondary fibers.

layer showing a low abundance (Fig. 5A). In contrast, a distinct and thick secondary fiber layer arranged into separated fiber bundles was observed at seed maturity (Fig. 5B).

The results are consistent with previous studies (Mediavilla et al., 2001; Schäfer and Honermeier 2006), which show that the development of secondary fibers starts at the early flowering stage and more secondary fibers are formed during the latter part of seed ripening. In addition, it is interesting that the bast content was reduced from early- (44%) to late harvest (37%). In addition, the plant density of 250 per m^2 at emergence decreased to 140 per m^2 at early harvest and to 40 per m^2 at late harvest. This indicated that self-thinning occurred. This reduction in plant density may be ascribed to inter-plant competition, which is found to cause density-induced mortality resulting in a reduction of bast content in the stem (Van der Werf et al., 1995a,b)

At the single fiber level, morphological information with respect to primary- and secondary fiber were observed (Fig. 5). Results were consistent with previous studies on hemp bast fibers, where variations in fiber diameter have been reported (Crônier et al., 2005; Ouajai and Shanks, 2005; Placet et al., 2012; Schäfer and Honermeier, 2006; Wang et al., 2007). In Beckermann and Pickering (2008), the hemp fiber diameter was on average between 20 and 33 μm. However, since the fiber cells have different shapes (e.g., round, oval, polygonal), precise measurements of their diameter are almost impossible (Fig. 5). Therefore, in our study, the area of fiber cells was determined (Table 2). A reduction in the thickness of both primary- and secondary fiber cell walls with increasing maturity was found, whilst the reduction in the thickness of primary fiber cell walls was statistically significant ($P < 0.05$). However, the cell area of primary fibers was found to increase from 1416 to 1500 μm^2. Furthermore, the slight decrease in the proportion of lumen (i.e., porosity) from 8.2 to 7.9% indicated that the investigated fibers were already mature at the beginning of flowering. This is in agreement with the results reported by Amaducci et al. (2008) who found that hemp fibers from bottom sections of stems reached the highest maturity at the beginning of flowering.

It is interesting that the reduction in primary fiber- and secondary fiber cell wall thickness and area coincided with a reduction in bast content, while the proportion of secondary fibers showed a significant increase (Table 1). Presumably, inter-plant competition (indicated by a high decrease in plant density from 140 per m^2 to 40 per m^2 from early to late harvest), and the relatively dry and hot weather conditions between early and late harvest period (Fig. 1) are likely responsible for this results.

The foregoing description on variations in morphological characteristics for the two development stages shows that the morphological features of hemp fibers are strongly influenced by growth stages. It appears characterized by the non-terminating growth of fibers while new secondary fibers are continually generated from separated single cells at earlier growth stages (i.e., at the beginning of flowering). Secondary fibers are then organized into bundles which produced a distinct layer in the mature stem in contrast to that observed for primary fibers, which have been arranged into a layer since early harvest. In addition, the proportion of parenchyma cells among fiber bundles continued to increase (Fig. 5A and B). These changes were assumed associated with seed formation between early- and late harvest.

3.3. Chemical analysis and histochemical staining of transverse sections of hemp stems

The chemical components of bast fibers from early- and late harvest are presented in Table 3. Notably, the lignin content increased significantly from 3.4 to 4.8% over the growth period from the beginning of flowering to seed maturity. In contrast, a highly significant ($P < 0.01$) reduction in cellulose content (indicated by glucose content) and decrease in pectin deposition (indicated by galacturonic acid content) were noted from the beginning of flowering until seed maturity. The reduction in cellulose content was consistent with the morphological characteristics of bast fibers revealed by the microscopy investigations, which showed a decrease in cell wall thickness of both primary- and secondary fibers with maturity.

Histochemical analyzes were performed for visualizing the spatial micro-distribution of lignin and pectin in the wall structure of hemp cells. Pectins are non-cellulosic acidic polysaccharides that are found primarily in the compound middle lamellae (CML) of plant cell walls (i.e., between fibers, parenchyma etc.) with much lesser amounts in secondary walls. Ruthenium red staining has frequently been used for localizing pectin in plant/wood tissues and stains acidic pectins red/pink (Hou et al., 1999; Waller et al., 2004). The staining of transverse sections of hemp stem showed red/pink staining and presence of pectins in the CML region between all cell types (Fig. 6A and B) irrespective of the growth stage. In addition, greatest staining was shown in cell corner middle lamellae (ML) of hemp fibers indicating presence of pectins at high concentration. This suggests that fiber separation could be achieved by pre-treating pectin either by its partial removal or structural change in the ML region during retting. However, a difference in the staining intensity between the two developmental stages (Fig. 6A vs B), where early harvested hemp stems stained more strongly than late harvested stems were consistent with the chemical analysis during ripening of the hemp plants (Table 3).

The spatial micro-distribution of lignin within hemp cell walls during the two growth stages was determined using the Wiesner- and Mäule reactions (Fig. 6C–F). Phloroglucinol in the Wiesner reagent reacts with lignin guaiacyl units producing a deep red color while the Mäule reaction stains lignin brown/orange due to the reaction with syringyl units in lignin.

Although the xylem cell walls stained an intense red color with Wiesner reagent irrespective of the growth stage, differences in staining were observed in the bast region of the stem with respect to cell type and their growth phase (Fig. 6C and D). Similar observationfs were obtained with the Mäule reagent where a positive reaction for syringyl lignin was detected in the cell walls (Fig. 6E and

Table 3
Anhydrous monosaccharides and Klason lignin content of investigated hemp fibers (standard deviations of 3 replicates in parentheses)

Harvest time	Retting time	Amount (g/100 g dry matter)							
		Glu	GalA	Gal	Xyl	Man	Ara	Rha	Klason lignin
Early harvest	0	66.0 (1.5)	6.9 (0.4)	2.0 (0.2)	1.0 (0.0)	2.8 (0.3)	1.0 (0.l)	1.0 (0.1)	3.4 (0.5)
Late harvest	0	61.3 (0.4)	6.3 (0.3)	2.1 (0.1)	1.1 (0.2)	3.0 (0.3)	1.0 (0.1)	1.1 (0.0)	4.8 (0.5)
P value*		$P<0.01$	ns	ns	ns	ns	ns	ns	$P<0.05$
Early harvest	50	71.3 (0.5)	3.1 (0.3)	2.4 (0.1)	1.1 (0.1)	3.8 (0.4)	0.4 (0.0)	0.8 (0.0)	4.3 (0.1)
	70	65.1 (2.6)	4.1 (0.4)	2.0 (0.0)	1.5 (0.0)	4.9 (0.3)	0.6 (0.1)	0.8 (0.0)	7.4 (1.7)
Late harvest	7	63.9 (1.0)	5.4 (0.6)	2.0 (0.2)	1.1 (0.2)	4.0 (0.4)	0.7 (0.2)	1.0 (0.0)	5.3 (0.9)
	14	70.2 (0.5)	3.1 (0.4)	2.4 (0.2)	0.8 (0.2)	3.4 (0.1)	0.4 (0.0)	0.8 (0.0)	6.1 (0.9)
	21	66.9 (1.2)	3.6 (0.4)	2.0 (0.0)	1.0 (0.2)	3.9 (0.2)	0.6 (0.1)	0.8 (0.0)	8.1 (0.3)

Glu: glucose, GalA: galacturonic acid, Gal: galactose, Xyl: xylose, Man: mannose, Ara: arabinose, Rha: rhamnose.
* *P* value: the effect of harvest time on chemical composition of different samples, ns: non significant.

F). Although there was a positive reaction in both primary- and secondary fibers, both reagents stained the CML strongly and also the outermost layers of the secondary walls compared to inner regions which showed very pale or no staining (Fig. 6). This indicated that lignin is predominantly concentrated in CML regions of bast fibers with much lesser amounts in secondary walls. Results are consistent with the plant's classification as an Angiosperm, which are known to contain both guaiacyl and syringyl lignin units.

In addition, the bast fibers from the two growth stages stained differently according to plant growth stage. Despite positive

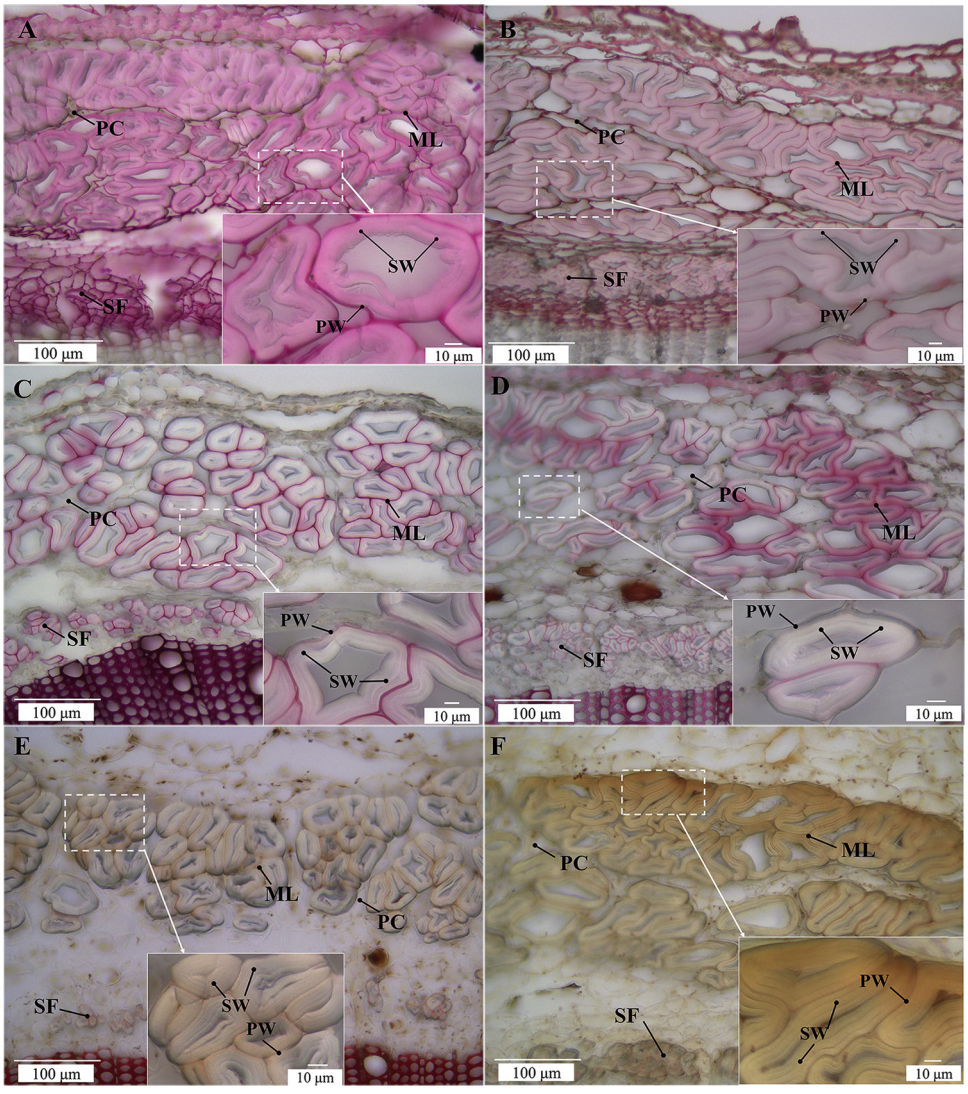

Fig. 6. Micrographs showing transverse sections of hemp stems isolated from early- and late harvest samples after staining for pectin (A and B) and guaiacyl lignin (C and D) and syringyl lignin (E and F).
ML: middle lamella; PC: parenchyma cell; PW: primary wall; SF: secondary fiber; SW: secondary wall.
(A) and (B): positive reaction for pectin in hemp stems from early harvest (A) and late harvest (B); (C) and (D): positive reaction for guaiacyl lignin units in hemp stems from early harvest (C) and late harvest (D); (E) and (F): positive reaction for syringyl lignin units in hemp stems from early harvest (E) and late harvest (F).

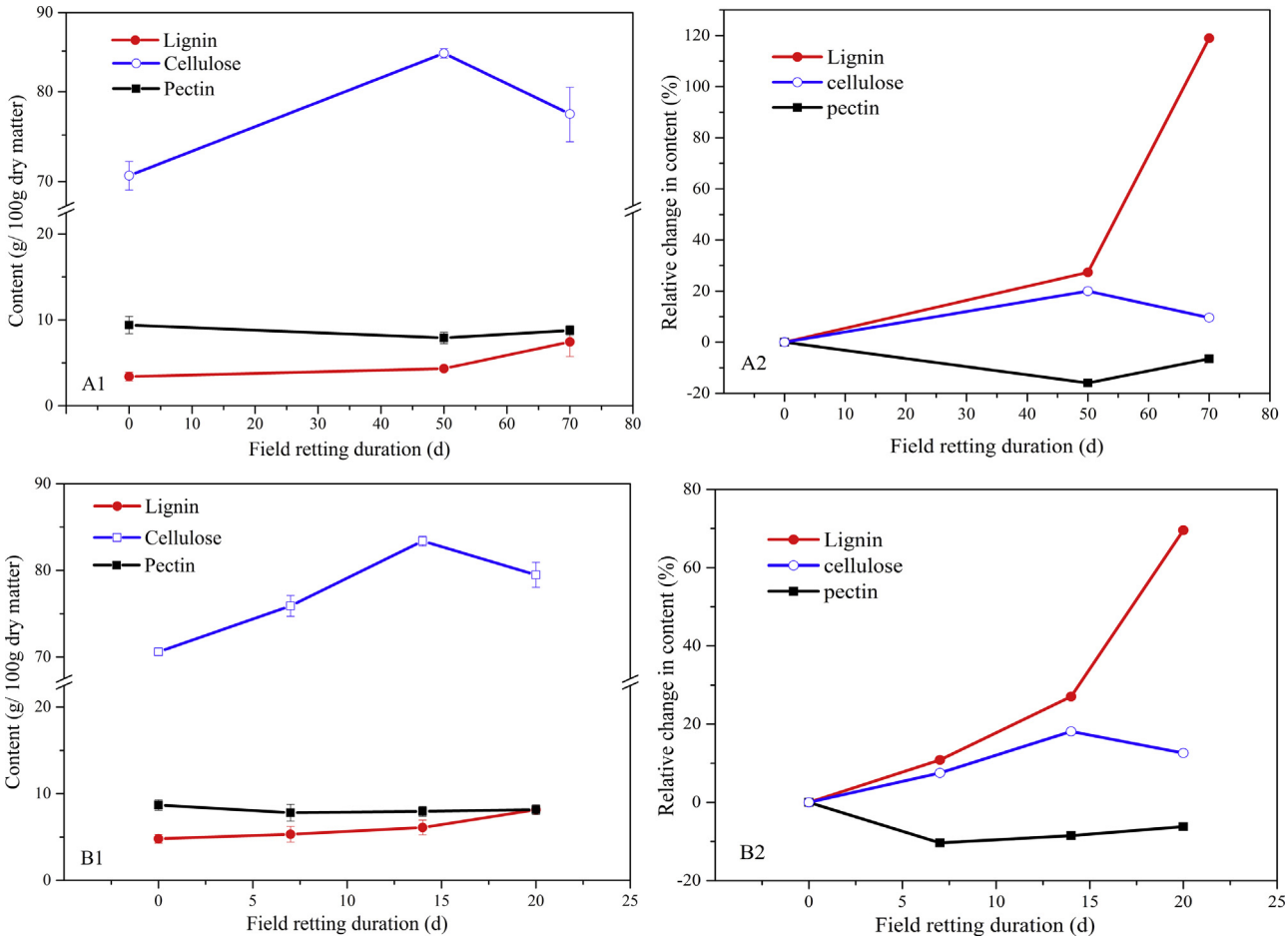

Fig. 7. Hemp stem content variations (A1: early harvest, B1: late harvest) and relative changes in content (A2: early harvest, B2: late harvest) of lignin, cellulose and pectin during field retting.

reactions for both primary- and secondary fibers as seen in Fig. 6C–F, the outermost primary fibers (close to epidermis) in stems at seed maturity stained with greater intensities indicating a higher lignin content in the most matured fibers presumably due to the deposition of lignin during the seed maturity stage. Results suggest that lignin deposition continued from the beginning of flowering to seed maturity thus correlating with the chemical composition analyzes.

Variations in relative carbohydrate and lignin components during field retting for both early- and late harvests were investigated. The relative and normalized content increase in lignin, pectin and cellulose are shown in Fig. 7. The cellulose content increased more than 10% during retting for both early- and late harvest, but decreased at later stages of the retting process. The pectin content decreased slightly at the beginning of retting and thereafter remained stable. In contrast, the lignin content increased steadily during the whole retting period for both early- and late harvested hemp. Results suggest that the cellulose content is highest at the early part of field retting whereas the lignin content becomes concentrated during the retting period. The results correlate with the normalized content increase (Fig. 7A2 and B2) and that cellulose, pectin and lignin are degraded at different rates. Pectin is removed at the highest rate, followed by cellulose and then lignin.

The changes in polymer composition can be explained by the action of microorganisms, which degrade and dissolve the cellular tissues and pectins surrounding the bast-fiber bundles (Fu et al., 2011), so facilitating further separation of the fibers from the stem (Di Candilo et al., 2010). When hemp stems start to degrade, fungal colonies appear as dark flecks on the surface of the bark and continue to develop until the surface turns to a steel-grey color (Jankauskienė and Gruzdevienė, 2013). At the initial stage of attack, growth of microorganisms is vigorous but as retting proceeds, the growth rate decreases (Donaghy et al., 1990). Therefore at the early stage of retting, pectins are degraded very rapidly (Fig. 7A2 and B2) with the rate of degradation decreasing as retting continues. In contrast, the rate of cellulose degradation increased gradually with period of retting. Presumably, as pectin is degraded and removed, the accessibility of cellulose for the microorganisms increases, and therefore a decrease in cellulose content is shown during the later stages of retting.

3.4. *Mechanical properties of non-retted and field retted hemp fibers*

The mean values for mechanical properties of the bast strips isolated from non-retted and field retted hemp stems are presented in Table 4. The mean values for ultimate tensile strength (UTS), elongation and stiffness were 683–954 MPa, 4.5–6.2%, and 27.5–34.9 GPa, respectively. Similar values for mechanical properties of hemp fibers are given in the literature (Table 5) with 489–899 MPa, 2.1–4.4%, and 27.6–66 GPa, respectively. Generally, the data verify that the method in this study for tensile testing gives reasonable values for UTS and stiffness, while the value for elongation is a little higher (Table 5).

Results indicate that the mechanical performance of hemp fibers was strongly influenced by harvest time. While fibers

Table 4
Mechanical properties of non-retted and retted hemp fibers from the field (standard deviations of 20 replicates in parentheses).

Retting duration (days)	Ultimate tensile strength(MPa)	Elongation at break(%)	Stiffness(GPa)
Early harvest			
0	954[a] (162)	6.2[a] (1.2)	34.9 (4.4)
50	822[b] (136)	5.4[ab] (1.5)	33.5 (8.1)
70	816[b] (128)	4.6[b] (1.4)	31.3 (4.0)
Late harvest			
0	812 [ab] (105)	4.6 (1.3)	31.1[ab] (5.6)
7	832[a] (198)	4.7 (1.8)	32.5[a] (4.8)
14	697[ab] (135)	4.5 (1.5)	30.7[ab] (4.5)
20	683[b] (107)	4.5 (1.2)	27.5[b] (4.6)
P value[*]	$P<0.05$	$P<0.001$	$P<0.05$

Values with different letters within a column for hemp harvested at the same time are significantly different ($P<0.05$).
[*] *P* value: harvest time effect on mechanical properties of non-retted hemp fibers.

Table 5
Mechanical properties of hemp fibers given in literature.

Hemp variety	Harvest year	Tensile strength at break (MPa)	Stiffness (GPa)	Elongation at break (%)	Gauge length (mm)	Tensile speed (mm/min)	Reference
Fedora 17	2011	889 ± 472	35.5 ± 17.3	2.6 ± 2.2	10	1	Marrot et al. (2013)
Felina 32	2009	699 ± 450	31.2 ± 19.7	3.3 ± 1.6	10	1	Marrot et al. (2013)
Fedora 17	2007	489 ± 233	33.8 ± 12.2	2.5 ± 1.3	10	1	Marrot et al. (2013)
Unknown	2002	857 ± 260	58	/	10	0.5	Pickering et al. (2007)
Unknown	/	886	66	/	/	/	Fan et al. (2011)
Unknown	/	636 ± 253	27.6 ± 7.5	2.1 ± 0.7	8	0.12	Placet et al. (2012)
USO-31	1995	830 (661, 1125)[a]	/	4.3 (3.2, 6.5)[a]	20	20	Sankari (2000b)
USO-31	1996	647 (478, 942)[a]	/	4.4 (2.6, 5.4)[a]	20	20	Sankari (2000b)

[a] Values denote median (25th percentile, 75th percentile).

from early harvest hemp stems exhibited significantly higher mechanical properties with an UTS and elongation at break and stiffness of 954 MPa, 6.2% and 34.9 GPa, respectively, those from the late harvest possessed 812 MPa, 4.6% and 31.1 GPa, respectively.

The variation of the mechanical properties of hemp fibers with harvest time can be explained by results from microscopy observations and chemical analyzes. A noticeable decrease in bast content and increase in the proportion of the secondary fibers (Table 1) during seed maturation were observed in the present study. The data obtained are in agreement with previously published reports where hemp fiber quality was found to be reduced with decreasing bast content, which may have resulted from self-thinning (Van der Werf et al., 1995a,b). In addition, Mediavilla et al. (2001) reported a reduction in fiber yield and quality after the flowering stage due to the formation of secondary fibers. Furthermore, the reduction of mechanical properties with maturity may also be closely related to the statistically significant decrease in cellulose deposition (Table 3) since the importance of cellulose on the tensile properties of hemp fibers is well known (Charlet et al., 2007; Marrot et al., 2013). Therefore, the significant decrease in tensile strength of hemp bast fibers can most likely be explained by the decrease in cellulose content (Table 3) and the increase in proportion of less valuable secondary fibers (Table 1) resulted from senescence and self-thinning of hemp plants from early to late harvest leading to inferior fiber quality.

Normally, retting precedes mechanical separation (decortication) of fibers from stems and is essential for the reduction of fiber damage. Field retting (or dew retting) is still widely used in industry because of its low cost. The effect of field retting duration on mechanical performance of hemp fibers is shown in Table 4. Early harvested hemp fibers had a longer period of field retting, which lasted 50 and 70 days, respectively because of the arid summer conditions compared to the colder and more rainy weather in September 2013 (Fig. 1). Their mechanical properties including UTS (Fig. 8), elongation at break and stiffness varied inversely with retting time. The UTS was greatly reduced compared with

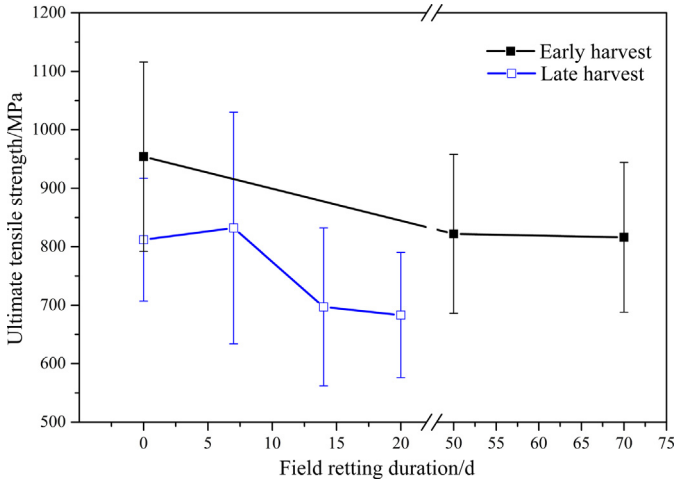

Fig. 8. The changes in ultimate tensile strength of hemp fiber strip with field retting duration.

non-retted samples and the reduction in elongation at break was not statistically significant until the period of retting reached 70 days. However, no significant decrease in stiffness was observed. These results may reflect the accelerated cellulose degradation during the latter part of field retting as indicated by the negative slope of the line for cellulose content in Fig. 7A1 and A2.

Results for the late harvest stems were similar to those from the early harvest although some interesting differences were noted. In particular, no statistical significant reduction in mechanical performance of fibers was observed compared with non-retted samples, although both UTS and stiffness decreased with the extended period of field retting. In addition, there was a slight increase in mechanical properties of fibers retted for 7 days in the field with respect to UTS and stiffness and then a notable reduction of both parameters with increasing retting time. This may be explained

by the significant increase in cellulose content in retted samples because of the microbial removal of pectins during field retting (see Fig. 7B1–B2). However, in later stages, cellulose degradation was accelerated after most of the non-cellulosic tissues were removed and accessibility of cellulose to the microorganisms was increased.

Together, the effect of field retting appears largely dependent on retting time. When retting duration was shorter, the mechanical properties of fibers with respect to UTS and stiffness may increase due to a continuous concentration of the cellulose content. However, the mechanical properties varied inversely with extended retting time probably due to accelerated cellulose degradation as a result of increasing accessibility of microorganisms to cellulose.

It should be noted that hemp fibers are categorized as "natural cellulosic fibers", whose properties can be influenced by many parameters during their growth and development (Duval et al., 2011). Furthermore, bast fiber strips can be regarded as fiber-reinforced composites, whose properties depend not only on those of the fibers themselves but also on the degree to which an applied load is transmitted to the fibers by the matrix phase under stress (Callister, 1994). The mechanical performances of the bast fiber strips therefore depend on both the mechanical properties of the individual fibers and coherence between fibers. Thus, the removal of non-cellulosic polymers during field retting results in lower coherence between fibers and thereby in lower mechanical properties.

4. Conclusions

The development of hemp fibers as reinforcement agents for composites and the requirement of high mechanical performance of cellulosic fiber reinforced materials require optimal fibers and a corresponding economical and accurate method for fiber extraction. Thus, an improved understanding of the properties of non-retted fibers and effects of field retting on the chemical composition and mechanical properties of fibers is of major importance.

Fibers harvested at seed maturity are significantly lignified and thus will be difficult to be extracted from hemp stems compared with fibers from the beginning of flowering. Furthermore, the important reduction in hemp bast mechanical properties with plant maturity may be attributed to the combined effect of the noticeable decrease in cellulose deposition, and the formation and increase in proportion of secondary fibers that caused deterioration of primary fiber quality regarding morphological and chemical characteristics. Highly lignified fibers are not desirable and favorable for retting. Considering the mechanical performance of hemp bast fibers, hemp harvested at the beginning of flowering is therefore recommended for use in strong composites.

In this study, the reduction in fiber quality caused by a long period of field retting was confirmed and may be related to a continuous increase in cellulose degradation, while no noticeable change in fiber quality was observed for short-periods of field retting. Consequently, traditional field retting may not be the optimal pretreatment for strong fibers and it is suggested that short-period field retting may be adopted to extract fibers more efficiently and accurately combined with other methods including the use of targeted enzymes, selected microbes or chemicals.

Acknowledgements

The authors are grateful to the Danish Council for Independent Research supporting the CelFiMat project (IP No. 12-127446: "High quality cellulosic fibers for strong biocomposite materials"). The financial support of China Scholarship Council (CSC, no. 201304910245) for Ming Liu's Ph.D. project is acknowledged. Tomas Fernqvist, Annette Eva Jensen and Jonas Kreutzfeldt Heininge are thanked for technical support.

References

Arnous, A., Meyer, A.S., 2008. Comparison of methods for compositional characterization of grape (*Vitis vinifera* L.) and apple (*Malus domestica*) skins. Food Bioprod. Process. 86 (C2), 79–86.
Amaducci, S., Zatta, A., Pelatti, F., Venturi, G., 2008. Influence of agronomic factors on yield and quality of hemp (*Cannabis sativa* L.) fibre and implication for an innovative production system. Field Crops Res. 107 (2), 161–169.
Bacci, L., Di Lonardo, S., Albanese, L., Mastromei, G., Perito, B., 2010. Effect of different extraction methods on fiber quality of nettle (*Urtica dioica* L.). Text. Res. J. 81 (8), 827–837.
Beckermann, G.W., Pickering, K.L., 2008. Engineering and evaluation of hemp fibre reinforced polypropylene composites: fibre treatment and matrix modification. Compos. Part A: Appl. Sci. Manuf. 39 (6), 979–988.
Callister, W.D., 1994. Materials Science and Engineering, third ed. John Wiley & Sons, New York, pp. 520–525.
Charlet, K., Baley, C., Morvan, C., Jernot, J.P., Gomina, M., Bréard, J., 2007. Characteristics of Hermès flax fibres as a function of their location in the stem and properties of the derived unidirectional composites. Compos. Part A: Appl. Sci. Manuf. 38 (8), 1912–1921.
Crônier, D., Monties, B., Chabbert, B., 2005. Structure and chemical composition of bast fibers isolated from developing hemp stem. J. Agric. Food Chem. 53 (21), 8279–8289.
Di Candilo, M., Bonatti, P.M., Guidetti, C., Focher, B., Grippo, C., Tamburini, E., Mastromei, G., 2010. Effects of selected pectinolytic bacterial strains on water-retting of hemp and fibre properties. J. Appl. Microbiol. 108 (1), 194–203.
Donaghy, J.A., Levett, P.N., Haylock, R.W., 1990. Changes in microbial population during anaerobic flax retting. J. Appl. Bacteriol. 69 (5), 634–641.
Duval, A., Bourmaud, A., Augier, L., Baley, C., 2011. Influence of the sampling area of the stem on the mechanical properties of hemp fibers. Mater. Lett. 65 (4), 797–800.
Esau, K., 1943. Vascular differentiation in the vegetative shoot of *Linum*. III. The origin of the bast fibers. Am. J. Bot. 30 (8), 579–586.
Fan, M., 2010. Characterization and performance of elementary hemp fibers: factors influencing tensile strength. Bioresources 5 (4), 2307–2322.
Fan, M., Dai, D., Yang, A., 2011. High strength natural fiber composite: defibrillation and its mechanisms of nano cellulose hemp fibers. Int. J. Polym. Mater. Polym. Biomater. 60 (13), 1026–1040.
Fu, J.J., Mueller, H., de Castro, J.V., Yu, C.W., Cavaco-Paulo, A., Guebitz, G.M., Nyanhongo, G.S., 2011. Changes in the bacterial community structure and diversity during bamboo retting. Biotechnol. J. 6 (10), 1262–1271.
Garcia-Jaldon, C., Dupeyre, D., Vignon, M.R., 1998. Fibres from semi-retted hemp bundles by steam explosion treatment. Biomass Bioenergy 14 (3), 251–260.
Gutiérrez, A., Rodriguez, I.M., del Rio, J.C., 2006. Chemical characterization of lignin and lipid fractions in industrial hemp bast fibers used for manufacturing high-quality paper pulps. J. Agric. Food Chem. 54 (6), 2138–2144.
Henriksson, G., Akin, D.E., Hanlin, R.T., Rodriguez, C., Archibald, D.D., Rigsby, L.L., Eriksson, K.E.L., 1997. Identification and retting efficiencies of fungi isolated from dew-retted flax in the United States and Europe. Appl. Environ. Microbiol. 63 (10), 3950–3956.
Hou, W.C., Chang, W.H., Jiang, C.M., 1999. Qualitative distinction of carboxyl group distributions in pectins with ruthenium red. Bot. Bull. Acad. Sinica 40 (2), 115–119.
Islam, M.S., Pickering, K.L., Foreman, N.J., 2011. Influence of alkali fiber treatment and fiber processing on the mechanical properties of hemp/epoxy composites. J. Appl. Polym. Sci. 119 (6), 3696–3707.
Jankauskienė, Z., Gruzdevienė, E., 2013. Physical parameters of dew retted and water retted hemp (*Cannabis sativa* L.) fibres. Zemdirbyste 100 (1), 71–80.
Keller, A., Leupin, M., Mediavilla, V., Wintermantel, E., 2001. Influence of the growth stage of industrial hemp on chemical and physical properties of the fibres. Ind. Crops Prod. 13 (1), 35–48.
Li, Y., Pickering, K.L., 2008. Hemp fibre reinforced composites using chelator and enzyme treatments. Compos. Sci. Technol. 68 (15–16), 3293–3298.
Love, G.D., Snape, C.E., Jarvis, M.C., Morrison, I.M., 1994. Determination of phenolic structures in flax fibre by solid-state C-13 NMR. Phytochemistry 35 (2), 489–491.
Marrot, L., Lefeuvre, A., Pontoire, B., Bourmaud, A., Baley, C., 2013. Analysis of the hemp fiber mechanical properties and their scattering (Fedora 17). Ind. Crops Prod. 51, 317–327.
Mediavilla, V., Jonquera, M., Schmid-slembrouck, I., Soldati, A., 1998. Decimal code for growth stages of hemp (*Cannabis sativa* L.). J. Int Hemp Ass. 5 (2), 68–74.
Mediavilla, V., Leupin, M., Keller, A., 2001. Influence of the growth stage of industrial hemp on the yield formation in relation to certain fibre quality traits. Ind. Crops Prod. 13 (1), 49–56.
Mishra, S., 2009. Understanding Plant Anatomy, first ed. Discovery Publishing House PVT. LTD., New Delhi India, pp. 97–100.
Nykter, M., Kymäläinen, H.R., Thomsen, A.B., Lilholt, H., Koponen, H., Sjöberg, A.M., Thygesen, A., 2008. Effects of thermal and enzymatic treatments and harvesting time on the microbial quality and chemical composition of fibre hemp (*Cannabis sativa* L.). Biomass Bioenergy 32 (5), 392–399.

Özmen, N., Cetin, N.S., Mengeloglu, F., Birinci, E., 2013. Vinyl acetate modified scots pine reinforced HDPE composites: influence of various levels of modification on mechanical and thermal properties. Bioresources 8 (1), 1361–1373.
Ouajai, S., Shanks, R.A., 2005. Morphology and structure of hemp fibre after bioscouring. Macromol. Biosci. 5 (2), 124–134.
Pickering, K.L., Beckermann, G.W., Alam, S.N., Foreman, N.J., 2007. Optimising industrial hemp fibre for composites. Compos. Part A: Appl. Sci. Manuf. 38 (2), 461–468.
Placet, V., Trivaudey, F., Cisse, O., Gucheret-Retel, V., Boubakar, M.L., 2012. Diameter dependence of the apparent tensile modulus of hemp fibres: a morphological, structural or ultrastructural effect? Compos. Part A: Appl. Sci. Manuf. 43 (2), 275–287.
Sankari, H.S., 2000a. Towards Bast Fiber Production in Finland: Stem and Fibre Yields and Mechanical Fiber Properties of Selected Fibre Hemp and Linseed Genotypes. University of Helsinki, Finland, pp. 18–20.
Sankari, H.S., 2000b. Comparison of bast fibre yield and mechanical fibre properties of hemp (*Cannabis sativa* L.) cultivars. Ind. Crops Prod. 11 (1), 73–84.
Schäfer, T.A., Honermeier, B., 2006. Effect of sowing date and plant density on the cell morphology of hemp (*Cannabis sativa* L.). Ind. Crops Prod. 23 (1), 88–98.
Sluiter, A., Ruiz, R., Scarlata, C., Sluiter, J., Templeton, D., 2008. Determination of extractives in biomass. In: NREL Technical Report. NREL, NREL/TP-510-42619.
Sluiter, A., Hames, B., Ruiz, R., Scarlata, C., Sluiter, J., Templeton, D., Crocker, D., 2011. Determination of structural carbohydrates and lignin in biomass. In: NREL Technical Report. NREL, NREL/TP-510-42618.
Song, K.H., Obendorf, S.K., 2006. Chemical and biological retting of kenaf fibers. Text. Res. J. 76 (10), 751–756.
Tahir, P.M., Ahmed, A.B., SaifulAzry, S.O.A., Ahmed, Z., 2011. Retting process of some bast plant fibers and its effect on fibre quality: a review. Bioresources 6 (4), 5260–5281.
Thygesen, A., Daniel, G., Lilholt, H., Thomsen, A.B., 2005. Hemp fiber microstructure and use of fungal defibration to obtain fibers for composite materials. J. Nat. Fibers 2 (4), 19–37.
Thygesen, A., Madsen, B., Bjerre, A.B., Lilholt, H., 2011. Cellulosic fibers: effect of processing on fiber bundle strength. J. Nat. Fibers 8 (3), 161–175.
Van der Werf, H.M.G., Wijlhuizen, M., de Schutter, J.A.A., 1995a. Plant density and self-thinning affect yield and quality of fibre hemp (*Cannabis sativa* L.). Field Crops Res. 40 (3), 153–164.
Van der Werf, H.M.G., Van Geel, W.C.A., Van Gils, L.J.C., Haverkort, A.J., 1995b. Nitrogen fertilization and row width affect self-thinning and productivity of fibre hemp (*Cannabis sativa* L.). Field Crops Res. 42 (1), 27–37.
Vignon, M.R., Dupeyre, D., Garcia-Jaldon, C., 1996. Morphological characterization of steam-exploded hemp fibers and their utilization in polypropylene-based composites. Bioresour. Technol. 58 (2), 203–215.
Vignon, M.R., Garcia-Jaldon, C., 1996. Structural features of the pectic polysaccharides isolated from retted hemp bast fibres. Carbohydr. Res. 296, 249–260.
Waller, L.N., Fox, N., Fox, K.F., Fox, A., Price, R.L., 2004. Ruthenium red staining for ultrastructural visualization of a glycoprotein layer surrounding the spore of *Bacillus anthracis* and *Bacillus subtilis*. J. Microbiol. Methods 58 (1), 23–30.
Wang, B., Sain, M., Oksman, K., 2007. Study of structural morphology of hemp fiber from the micro to the nanoscale. Appl. Compos. Mater. 14 (2), 89–103.

Paper II

Ming Liu, Dinesh Fernando, Anne S. Meyer, Bo Madsen, Geffrey Daniel, & Anders Thygesen

Characterization and biological depectinization of hemp fibers originating from different stem sections

Industrial Crops and Products, 2015, 76, 880-891

Industrial Crops and Products 76 (2015) 880–891

Contents lists available at ScienceDirect

Industrial Crops and Products

journal homepage: www.elsevier.com/locate/indcrop

Characterization and biological depectinization of hemp fibers originating from different stem sections

Ming Liu [a], Dinesh Fernando [b], Anne S. Meyer [a], Bo Madsen [c], Geoffrey Daniel [b], Anders Thygesen [a,*]

[a] Center for Bioprocess Engineering, Department of Chemical and Biochemical Engineering, Technical University of Denmark, 2800 Kongens Lyngby, Denmark
[b] Department of Forest Products/Wood Science, Swedish University of Agricultural Sciences, Vallvägen 9D, 750-07 Uppsala, Sweden
[c] Section of Composites and Materials Mechanics, Department of Wind Energy, Technical University of Denmark, 4000 Roskilde, Denmark

ARTICLE INFO

Article history:
Received 11 March 2015
Received in revised form 9 July 2015
Accepted 21 July 2015

Keywords:
Hemp fiber
Fungal retting
Mechanical properties
Depectinization selectivity
White rot fungi

ABSTRACT

The wide variation of mechanical properties of natural fibers limits their applications in matrix composites. The aim of this study is to evaluate the properties of hemp fibers from different stem sections (top, middle and bottom) and to assess fungal retting pretreatment of hemp from different stem sections with the white rot fungi *Phlebia radiata* Cel 26 and *Ceriporiopsis subvermispora*. For the untreated hemp fibers, no apparent difference in tensile behavior for fiber bundles from different stem sections was observed, and more than 90% tested samples demonstrated plastic flow behavior. Fiber strength and stiffness were highest for the fibers from the top and middle stem sections. These properties were related to the compositional make up and morphological properties of hemp fibers, notably the secondary fiber cell contents. In fungal retting, there was a strong dependence of depectinization selectivity on stem section, which decreased from bottom to top presumably due to the significantly higher lignin content in the bottom section than in the top section (middle section was in between). Consequently, the fungal retting caused a lower reduction in strength of fibers from the bottom section than in those from the top stem section, and essentially reversed the influence of stem section on fiber tensile strength through depectinization selectivity. At whole hemp stem level, the fungal retting with *P. radiata* Cel 26 exhibited better mechanical properties with an ultimate tensile strength, strain and stiffness of 736 MPa, 2.3% and 42 GPa, respectively, while fibers treated with *C. subvermispora* exhibited lower mechanical properties of 573 MPa, 1.9% and 40 GPa, respectively. The study thus also showed that less variable and high strength fibers may be produced using the dependence of depectinization selectivity on stem section for composite application.

1. Introduction

Natural cellulosic fibers, such as hemp and flax, are increasingly considered as important raw materials for the production of high quality textiles and potential reinforcement agents in composite materials due to their environmental sustainability and biodegradability. The potential use of natural cellulosic fibers in high grade composites as replacements for synthetic glass fibers, has gained renewed interest over the last decade. Replacing synthetic glass fibers with natural cellulosic fibers offers advantages including low cost, low density and desirable mechanical properties in the resulting composite materials (Fan et al., 2011). For example, cellulose rich bast fibers from hemp exhibit high tensile strength (300–800 MPa) and high stiffness (30–60 GPa) (Aslan et al., 2011).

The mechanical properties of bast fibers vary greatly, rendering them unsuitable for use in high grade composite materials where high reliability and stability are required. Typical parameters that affect the mechanical performance of bast fibers include the variety (Marrot et al., 2013), growth stage of the plant at harvesting (Liu et al., 2015; Mediavilla et al., 2001), growth conditions (van Der Werf et al., 1995), stem section (Duval et al., 2011), and fiber treatments (Evans et al., 2002; Islam et al., 2011; Morrison et al., 2000). Charlet et al. (2007) reported that the mechanical properties of flax fibers were highly dependent on the stem section used to obtain the fibers. Fibers from the middle section exhibited the highest strength of 1795 ± 1127 MPa and ultimate strain of $2.4 \pm 0.7\%$, while fibers from the bottom section showed the lowest strength and ultimate strain of 757 ± 249 MPa, and $1.6 \pm 0.5\%$, respectively.

As reported for flax, the effect of stem section on mechanical properties of hemp fibers is that fibers from middle of stems exhibited higher tensile strength and elongation than fibers from

* Corresponding author. Tel.: +45 21326303.
E-mail address: athy@kt.dtu.dk (A. Thygesen).

http://dx.doi.org/10.1016/j.indcrop.2015.07.046
0926-6690/

the bottom and the top (Duval et al., 2011). However, the reasons for the results were not further analyzed. Compared to flax, the most disadvantageous feature in hemp fibers is the presence of inferior secondary fibers (Mankowski et al., 2006). The secondary fibers in hemp are primarily located at the bottom of the plant stem (Amaducci et al., 2008) and are much shorter (approx. 2 mm long) and thinner (approx. 6 μm in diameter) than the primary fibers (approx. 20 mm long and 10–40 μm in diameter) (van der Werf et al., 1994). The presence of secondary fibers in bottom stem section may contribute to rendering fibers from bottom inferior. Besides that, fibers from different sections show different chemical composition (e.g. cellulose, pectin, and lignin) (Crônier et al., 2005), which may result in different mechanical properties, though homogeneous maturity can be obtained by delaying harvest time from beginning to full flowering (Amaducci et al., 2008). Furthermore, variations in chemical composition (e.g. lignin) of fibers along plant stem may affect fiber extraction with biological methods, resulting in different responses (e.g. depectinization efficiency and selectivity) at different stem sections.

Regarding to fiber extraction, retting, a process used to remove non-cellulosic compounds from cellulosic fibers, is a major challenge in the extraction of cellulosic fibers. Traditional methods of retting include field retting and water retting. Field retting is subject to weather conditions, and causes significant scattering of fiber properties and extended field retting can even damage the fibers (Liu et al., 2015), whereas water retting, subjected to geographic regions, is also uncontrolled with respect to the modification of the fibers and moreover causes serious ecological problems (Hu et al., 2012). An alternative retting method is controlled microbiological retting. Controlled microbiological retting uses specific enzymes secreted by microorganisms during cultivation to attack chemical components in the fibers under controlled conditions (Thygesen et al., 2007). Thygesen et al. (2005, 2013) investigated the effect of fungal defibration and depectinization selectivity of *Phlebia radiata* Cel 26 and *Ceriporiopsis subvermispora*. They found that the mutated white rot fungus *P. radiata* Cel 26 can selectively degrade the epidermis and the lignified middle lamellae and thus small fiber bundles can be produced. Moreover, *P. radiata* Cel 26 exhibited higher depectinization selectivity of 6.0 than *C. subvermispora* with a selectivity of 4.6 and fibers treated with *P. radiata* Cel 26 showed much cleaner surface than the ones treated with *C. subvermispora*.

Hemp fibers from different parts of the stem may have different morphology, chemical composition and lignification due to varied ripeness. Consequently, fibers from different parts of the stem exhibit variations in mechanical performances. The differences in chemical composition and structure of hemp fibers will affect depectinization efficiency of adapted microorganisms, resulting in inhomogeneity (i.e. more scattered mechanical properties) during controlled microbiological retting.

In the present study, morphological features, chemical composition and mechanical properties of hemp fibers from different sections of hemp stems were characterized. Subsequently, two species of white rot fungi, *P. radiata* Cel 26 and *C. subvermispora*, were incubated with fibers from different stem sections (i.e. top, middle, and bottom) under controlled conditions to evaluate the effect of stem section on the performance of depectinization.

2. Materials and methods

2.1. Plant material

Hemp (*Cannabis sativa* L.), variety USO-31, was sown in France (N 48.8526°, E 3.0190°(WGS84)) by hemp cultivation companies (Planète Chanvre and Bafa Neu GmbH) (Liu et al., 2015). The hemp plants were fertilized with 80 kg/ha N, 45 kg/ha K, and 45 kg/ha P. The monoecious hemp plants were harvested on Sep 6th 2013. On the basis of the definition of the growth stages of hemp given by Mediavilla et al. (1998), the growth stage of the hemp plants at harvest corresponded to code 2204. Except for the hemp stem samples to be used for microscopy, the stems were air-dried at 40 °C with an air flow of 150 $m^3/(m^2$ grid h) (Maskinfabrikken Thisted, Denmark Type 150). Three stem sections were defined on one hemp stem: bottom (one third above the base of the stem), top (one third under the inflorescence base) and middle (between bottom and top sections). In general bast fibers were obtained from the individual stem samples by manual peeling.

2.2. Chemical analysis of bast fibers

Untreated bast fiber strips (defined in Liu et al. (2015)) were analyzed directly whereas fiber strips previously subjected to fungal retting (see below) were dried at 50 °C for 12 h prior to chemical analysis. For analysis, bast fibers were ground with a microfine grinder (IKA, MF 10.1; IKA®-Werke GmbH) to a particle size of 1 mm. Small ground samples of about 3 g were extracted in a Soxhlet apparatus (Gerhardt EV6 ALL/16 No. 10-0012) for 5 h using a 300 mL solution of toluene-ethanol-acetone (4:1:1 by volume) (Sluiter et al., 2008; Özmen et al., 2013). For each sample, the final residue was dried again at 50 °C for 12 h prior to further analysis. Waxy substances in the extraction solution were concentrated by rotary evaporator and then dried at 50 °C overnight. Wax content was therefore determined by the weight increase in the corresponding boiling flasks (Browning, 1967; Sluiter et al., 2008). Chemical analysis was done using two-step sulfuric acid hydrolysis at 72% for 1 h (30 °C) and subsequently at 4% (w/w) for 1 h (121 °C), according to the method of the US National Renewable Energy Laboratory (Sluiter et al., 2011). After acid hydrolysis, the hydrolysate was collected for monosaccharide analysis. Klason lignin content was gravimetrically determined as the residue of the hydrolysis.

Monosaccharide analysis was performed by HPAEC-PAD analysis using an ICS-3000 system consisting of gradient pumps (model DP-1), an electrochemical detector/chromatography module (model DC-1) and an autosampler (Dionex Corp., Sunnyvale, CA). Separation was achieved using a CarboPacTM PA20 (3 mm × 150 mm) analytical column as described by Arnous and Meyer (2008). Roughly, it is considered that arabinose, galactose, galacturonic acid and rhamnose are specific to pectins, and glucose belongs to the cellulose moiety. The concentration of polymeric sugars was calculated from the concentration of the corresponding monomeric sugars, using an anhydrous correction of 0.88 for arabinose, 0.89 for rhamnose, 0.90 for glucose and galactose, and 0.91 for galacturonic acid.

2.3. Microscopy and histochemical observations

Fresh transverse sections were cut from each hemp stem section under a stereo microscope (Wild Heerbrugg M8, Wild Leitz, Switzerland). Histochemical staining was performed on the transverse hemp stem sections on glass slides followed by adding one drop of 50% (v/v) glycerol in water. Cover slips were placed on the stained sections, mounted in glycerol and examined immediately using a Leica DMLB light microscope (LM) with digital images recorded using an Infinity X-32 camera (DeltaPix, Denmark). Staining of pectins, syringyl lignin and guaiacyl lignin were performed as described by Thygesen et al. (2005).

Due to the temporary nature of the staining reactions, all observations including digital image recording were performed within 10–15 min of staining. Using the digital images obtained, a number of morphological features were measured using Image-Pro Plus (Media Cybernetics Inc, USA) image analysis software, including: thickness and area of epidermis, primary fiber layer (PFL), secondary fiber layer (SFL), and cambium layer, and thickness and area

of fiber cells and lumen. Thus the PF- (i.e. ratio of PFL area to the bast area), and SF fractions (i.e. ratio of SFL area to bast area) could be determined.

Morphological features at hemp stem level were determined as the average of 4 measurements from 10 transverse sections from 3 bast fiber strips of each sample, which in total represented 120 measurements. At the single fiber level, an average of 4 measurements from 50 cells from 3 bast fiber strips of each sample of bast fibers were made, making a total of 600 measurements.

2.4. Fungal retting

Cultures of the white rot fungi *P. radiata* Cel 26 and *C. subvermispora* were grown on hemp stems as described by Thygesen et al. (2007). The fungi were stored and pre-cultivated on 2% (w/v) malt agar plates at 20 °C. For inoculation, the mycelia grown on one agar plate was homogenized into 100 mL water. A solution of 1.5 g/L NH_4NO_3, 2.5 g/L KH_2PO_4, 2 g/L K_2HPO_4, 1 g/L $MgSO_4{\cdot}7H_2O$ and 2.5 g/L glucose was used as growth medium in the fungal retting experiments. For each section, both the fungal retting and the corresponding control treatment (without incubation of fungi) were performed in duplicate. The growth medium (190 mL) and hemp stem pieces from the bottom, middle and top sections of stems (approx. 8 cm in length, 15 g/flask) were sterilized in 1 L Erlenmeyer flasks at 121 °C for 60 min. After cooling to ambient temperature, the mycelium suspension (25 mL) was added aseptically and the fungal retting experiments conducted at 28 °C for 14 days. Following fungal retting, the hemp stem pieces were washed in water to remove epidermal and fungal material from the stem surfaces and to separate the fibers from the woody cores of the stems. The resulting fibers were then dried at 50 °C for 24 h. In the meantime, a control group (without cultivation with fungi) was performed under the same condition.

After biological retting, the weight loss of a monosaccharide is defined in the following equation

$$\text{Weight loss} = \frac{m_0 w_0 - mw}{m_0 w_0} \times 100\% \quad (1)$$

where m_0 and m are dry mass of bast fibers (g), and w_0 and w are relative amounts (given as mass fraction, g/100 g dry matter) of investigated monomeric sugars for bast fibers in control group and test group, respectively. The mean value for weight loss of the anhydrous monosaccharide was calculated from Eq. (1) by use of the mean value for m_0, m, w_0 and w. For the uncertainty calculation, the error propagation from these parameters was considered. Finally, a coverage factor of 1.96 was used to calculate the expanded uncertainty to give a level of confidence of approximately 95%. The depectinization selectivity value is defined as the ratio of pectin degradation to cellulose degradation in the following equation:

$$\text{Depectinization selectivity} = \frac{\left((m_0 \times w_0(\text{Pectin}) - m \times w(\text{Pectin}))/m_0 \times w_0(\text{Pectin})\right) \times 100}{\left((m_0 \times w_0(\text{Cellulose}) - m \times w(\text{Cellulose}))/m_0 \times w_0(\text{Cellulose})\right) \times 100} \quad (2)$$

where w_0(pectin) and w(pectin) are relative amount of pectins for fibers and w_0(cellulose) and w(cellulose) are relative amount of cellulose for fibers in control group and test group, respectively. The applied definitions of pectin and cellulose are included in Section 2.2.

2.5. Tensile strength test of bast fibers

The bast fiber strips (80 mm long × 1 mm wide) were peeled manually from the dried hemp stems followed by minor modifications of the strips with a razor blade to obtain a constant width along the entire length using a stereo microscope (Liu et al., 2015). The weight range of those bast fiber strips was between 5 and 20 mg and tensile tests were carried out on 20 specimens for each stem section.

The test specimens for tensile strength tests were made by gluing tabs on each fiber end using epoxy (DP 100) resin with a gauge length of 10 mm using a custom-made holder. After curing at 20 °C for 24 h, the fixed samples were removed from the holder. All samples were tested with an Instron Testing Machine 2710-203 equipped with a 1000 N load cell, at a tensile speed of 0.5 mm/min, at 25 °C and 50% humidity. The cross-sectional area (A) of test samples was determined by the following equation:

$$A = \frac{m}{(\rho \times l)} \quad (3)$$

where m, ρ, and l represent weight, density, and length of the test sample, respectively. The density of the bast fiber strips was chosen as $\rho = 1.50\ \text{g/cm}^3$ (Satlow et al., 1994). The ultimate tensile strength (UTS) of the bast fiber strips was defined as the ratio of failure stress and cross-sectional area (A). After obtaining mechanical properties (e.g. UTS, strain and elongation) for bast fiber strips from all investigated stem sections (e.g. top, middle and bottom), the mechanical properties at whole hemp stem level was calculated by the following equation:

$$X_W = w_T X_T + w_M X_M + w_B X_B \quad (4)$$

where X_W, X_T, X_M and X_B are mechanical property (e.g. strength, strain and stiffness) of fibers at whole stem level and at top, middle and bottom stem section, respectively. w_T, w_M and w_B are the corresponding weight fractions of untreated hemp fibers at top, middle and bottom, respectively (Table 1: Fiber yield). Mean value calculation for X_w can be done from Eq. (4) by use of the mean value for each parameter. For the uncertainty calculation, the error propagation from X_T, X_M and X_B was considered. Finally, the expanded uncertainty was calculated at a level of confidence of approximately 95% by use of a coverage factor of 1.96.

2.6. Statistical analysis

Analysis of variance (ANOVA) for the different stem sections was performed on each direct measurement. For each measurement of morphological features, chemical composition and mechanical properties, the stem section effect was tested at a significance level of 5% (Minitab 16). Differences between each stem section were evaluated using the Tukey multiple comparison test at a 5% significance level.

3. Results and discussion

3.1. Microscopic view of hemp stem in different sections

Transverse sections illustrating the cellular structure of hemp fibers from different stem sections are shown in Fig. 1 and morphological features at stem- and single fiber level in Table 1 and Fig. 2, respectively. Overall, the plant stems were 188 ± 43 cm tall and organized in layers from xylem towards the surface by 10–50 μm cambium, 100–200 μm cortex (including both primary fiber and secondary fiber), and 20–100 μm epidermis. Great variations in the morphological characteristics at bast fiber- and individual fiber level were apparent.

At the stem level, there was a significant decrease ($P < 0.001$) in stem diameter from 9 to 4 mm from the bottom towards the top of the stem, and a remarkably thinner cortex layer (indicated by sum of thickness of the PFL and SFL) observed in the top stem section, while the bottom and the middle stem sections exhibit comparable cortex layer thickness of 180 μm (Table 1 and Fig. 1). However,

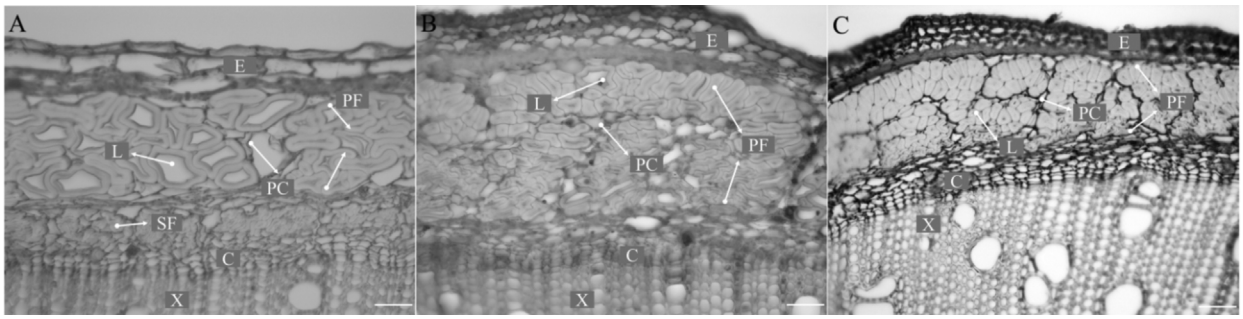

Fig. 1. Light micrographs of transverse sections from different hemp stem sections: (A) bottom; (B) middle; (C) top (the scale bar denotes 50 μm). E—epidermis; PF—primary fiber; X—xylem; PC—parenchyma cell; SF—secondary fiber; C—cambium; L—lumen.

Table 1
Morphological features of hemp stems at different sections.

Sample	Stem diameter (mm)	Fiber yield[1] (%)	Bast content[2] (%)	Xylem content (%)	EL[3] thickness (μm)	PFL[3] thickness (μm)	SFL[3] thickness (μm)	PF fraction[4] (%)
Bottom	8.6^{a} (0.9)	40^{a} (1)	37^{b} (1)	63^{a} (1)	52^{b} (21)	119^{b} (10)	54^{a} (4)	45 (6)
Middle	6.5^{b} (0.8)	36^{b} (0)	45^{a} (0)	55^{b} (0)	82^{a} (20)	188^{a} (29)	5^{b} (1)	53 (6)
Top	3.9^{c} (0.4)	24^{c} (1)	44^{a} (1)	56^{b} (1)	72^{ab} (16)	126^{b} (20)	0^{b} (0)	49 (8)
P value	*<0.001*	*<0.001*	*<0.001*	*<0.001*	*<0.05*	*<0.001*	*<0.001*	*ns.*[3]

[1] Fiber yield was defined as the ratio between the fiber content from one section to the fiber content from the whole stem.
[2] Bast content was defined as the ratio between the weight of fibers and the weight of the corresponding stems.
[3] EL: Epidermis layer; PFL: Primary fiber layer; SFL; Secondary fiber layer; ns: non-significant.
[4] PF fraction was defined as the ratio of the primary fiber layer and the sum area of layers of epidermis, primary fibers, secondary fibers and cambium.

especially the bottom section had a much thicker secondary fiber layer of 54 μm. As a result, the fiber yield decreased significantly ($P < 0.001$) from the bottom (40%), to the middle (36%), and to the top (24%) of the stems (Table 1). In contrast, hemp fibers from the middle and top sections exhibited significantly higher ($P < 0.001$) bast content (44–45%) than those from the bottom section (i.e. 37%). The lower bast content at the bottom section is presumably due to a thicker xylem layer (indicated by high xylem content of 63%).

At single fiber level, there was a decrease from stem bottom towards top in cell wall thickness from 11 to 6 μm, cell area from 1500 to 330 μm^2, and lumen area from 170 to 40 μm^2 (Fig. 2). The porosity (lumen, %) was found to be independent on stem section with a content of 8% (Fig. 2). Secondary fibers were most abundant in the bottom section of the hemp stems, but could also be observed in the middle section. In general, the values for morphological features of secondary fibers regarding cell wall thickness, cell wall area and porosity were much lower than the values for the primary fibers (Figs. 1 and 2).

Correlation between stem diameter (or cross sectional area of stem) and cell area, primary fiber layer thickness, and secondary fiber layer thickness were assessed in Fig. 3. For the whole stem, PFL thickness was found to be independent of the stem section (Fig. 3A). In contrast, secondary fiber layer thickness in the bottom sections of hemp stem, exhibited a tendency towards a positive correlation with stem section diameter (slope was not significantly different from 0; $P = 0.09 > 0.05$, Fig 3A). In addition, the primary fiber cell area (including cell wall area and lumen area) increased linearly versus the stem sections cross sectional area (Fig. 3B). The data indicated that after the late part of the flowering growth stage, when primary fibers from different stem sections have reached their highest maturity (Amaducci et al., 2008), secondary fibers start to develop and their proportion increased with stem diameter at the bottom section.

Recently, the tensile strength of natural fibers was found to decrease as their diameter increased and this dependence is attributed to both the number of fiber defects (i.e. kinks or dislocations) and the fiber configuration in tested specimens (Fan, 2010). The formation of secondary fibers in hemp stems was found to decrease fiber quality (Mediavilla et al., 2001). Based on previous studies on hemp, it is reasonable to assume that both larger fiber diameter (indicated by cell wall area and lumen area in Fig. 2) and a higher proportion of secondary fibers in the bottom section (Fig. 1) contributes to rendering fibers inferior (i.e. lower tensile strength).

3.2. Chemical composition of untreated hemp fibers and histochemical staining

3.2.1. Chemical composition

The chemical components of the bast fibers from different stem sections are shown in Table 2. Notably, fibers from top of stem have the lowest cellulose content (indicated by a glucose content of 55%), while these from the bottom and middle sections exhibit a statistically higher cellulose content of 61% and 62%, respectively. However, the difference between fibers from the middle and top stem sections was not significant ($P > 0.05$). Furthermore, the lignin content decreased significantly from 4.8 to 3.6% from bottom to the top section ($P < 0.01$) and wax content decreased significantly from 3.3 to 2.4% ($P < 0.05$). The variation in lignin content is in agreement with Crônier et al. (2005), who reported that hemp fibers from bottom have a higher lignin content of 4.0–4.5% than the ones from the top stems with 3.0–3.5%. On the other hand, a highly significant ($P < 0.01$) increase in pectin deposition indicated by a significant increase in galacturonic acid (GalA), rhamnose (Rha), galactose (Gal) and arabinose (Ara) contents from bottom to top section was noted.

The higher lignin content of fibers in the bottom section may be due to the higher proportion of secondary fibers (Fig. 1A) and that it reaches the highest ripeness compared with the two other sections (Amaducci et al., 2008). Compared to flax fibers, which were reported to contain 2.0–2.5% of Klason lignin from bottom to top stem section (Charlet et al., 2007), hemp fibers contain more lignin (Table 2), which is unfavorable for fiber extraction. Overall, the variation in the carbohydrate components with stem section is related to the ripeness of the hemp fibers and formation of secondary fibers in the bottom section.

It has been reported that the accumulation of wax on the cuticle forms a protective barrier against entry of infection agents into the plant (Foulk et al., 2001). The presence of wax on the cuticle

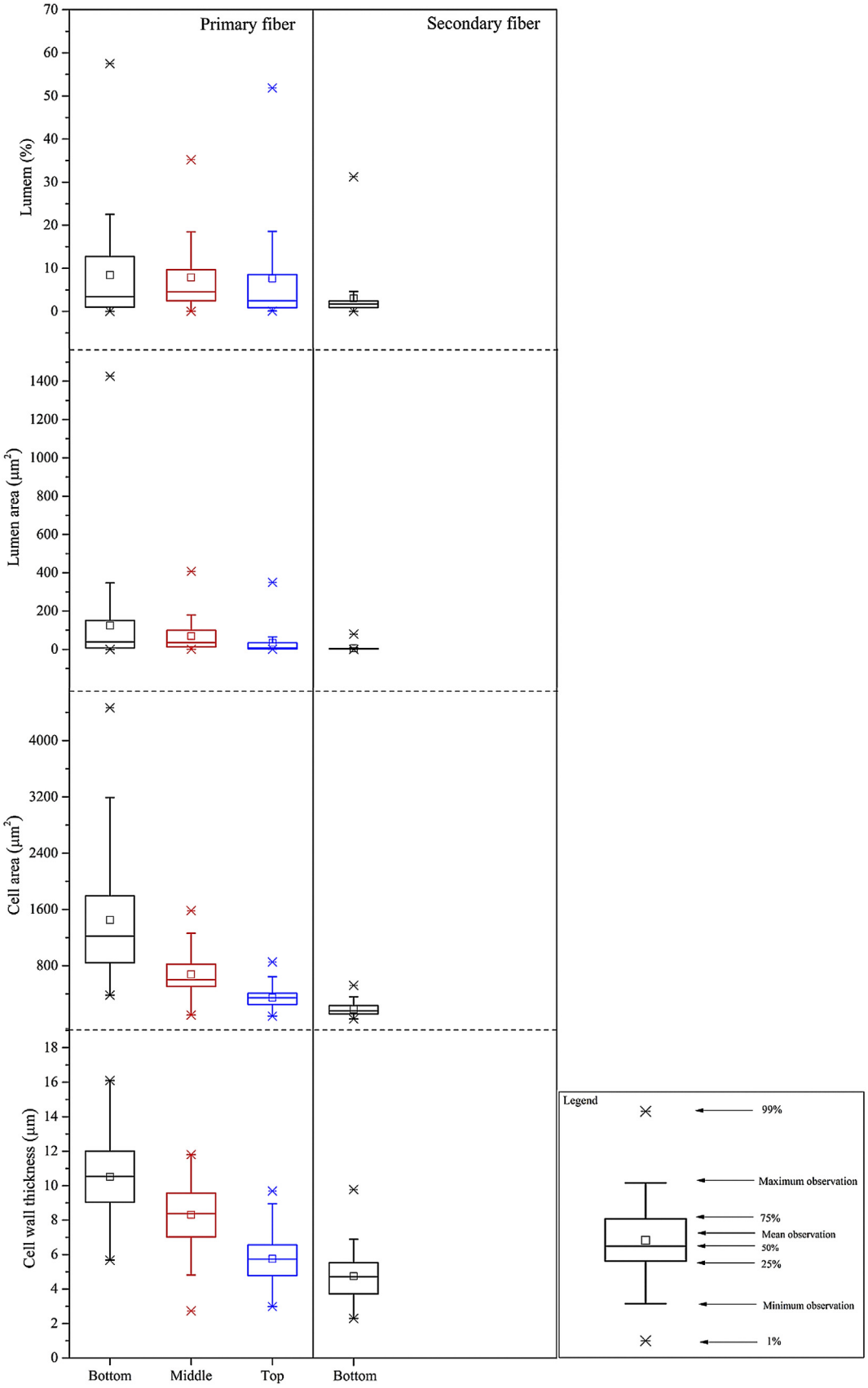

Fig. 2. Box plots of morphological feature data of hemp fibers from bottom, middle and top sections analyzed from microscopy recordings of transverse sections of fibers. (For the secondary fibers, reliable data was only obtained at the bottom sections).

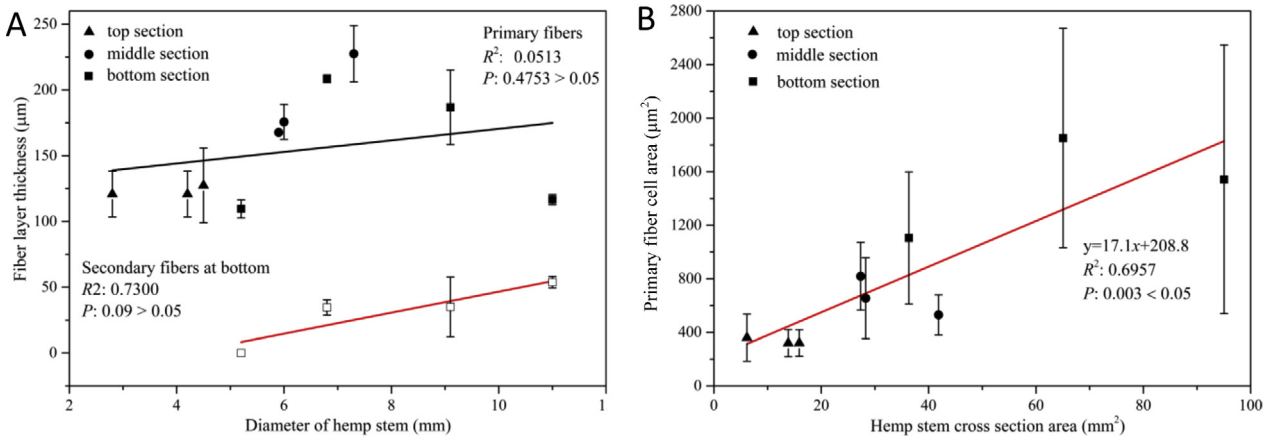

Fig. 3. Correlation between diameter of hemp stem sections and fiber layer thickness (A) and fiber cell area (B) from corresponding stem section.

Table 2
Anhydrous monosaccharides and lignin contents of hemp fibers from different stem sections.

Pretreatment[1]	Stem section	Amount (g/100 g dry matter)									
		Glu	GalA	Rha	Gal	Ara	Man	Xyl	Fuc	Lignin	Wax
Untreated	Bot	61.3^{aGH} (0.4)	6.3^{bBCD} (0.3)	0.9^{b} (0)	1.8^{b} (0.1)	1.1^{b} (0.1)	3.0^{ab} (0.3)	1.1^{b} (0.1)	0.6 (0.1)	4.8^{a} (0.5)	3.3^{a} (0.2)
	Mid	62.1^{aFG} (3.9)	7.3^{bB} (0.5)	1.0^{ab} (0.2)	2.0^{b} (0.2)	1.1^{b} (0.2)	3.4^{a} (0.4)	1.4^{a} (0.1)	0.5 (0)	4.4^{ab} (0.1)	2.9^{ab} (0.1)
	Top	54.8^{bH} (2.6)	9.0^{aA} (0.6)	1.2^{a} (0)	2.6^{a} (0.2)	1.8^{a} (0.2)	2.5^{b} (0.2)	1.0^{b} (0)	0.5 (0)	3.6^{b} (0.3)	2.4^{b} (0.1)
Control	Bot	68.1^{abDEF} (2.8)	5.1^{bD} (0.6)	0.9^{b} (0.2)	1.8^{b} (0.3)	1.0^{b} (0.2)	3.5 (0.6)	1.3 (0.2)	0.5 (0)	5.3^{a} (0.2)	/
	Mid	69.5^{aCDE} (2.7)	5.4^{abCD} (0.7)	1.0^{ab} (0.2)	2.0^{b} (0.3)	1.0^{b} (0.4)	3.4 (0.3)	1.5 (0.2)	0.5 (0.1)	4.9^{ab} (0.3)	/
	Top	65.3^{bEFG} (2.8)	6.5^{aBC} (1.3)	1.3^{a} (0.2)	2.7^{a} (0.3)	1.6^{a} (0.3)	3.5 (0.3)	1.5 (0.3)	0.4 (0.1)	4.6^{b} (0.3)	/
Pr-treated	Bot	76.5^{bAB} (2.8)	1.7^{bF} (0.2)	0.5 (0)	1.5^{b} (0)	0.4^{b} (0)	4.4 (0.4)	0.9^{b} (0.2)	0.5 (0.1)	5.9^{a} (0.2)	/
	Mid	80.5^{aA} (2.8)	1.7^{bF} (0.2)	0.5 (0.1)	1.6^{b} (0.2)	0.4^{ab} (0.1)	4.1 (0.3)	1.0^{b} (0.1)	0.6 (0.1)	5.1^{b} (0.2)	/
	Top	74.1^{bBC} (2.4)	2.0^{aEF} (0.2)	0.6 (0.1)	1.9^{a} (0.1)	0.6^{b} (0.1)	4.3 (0.9)	1.3^{a} (0.2)	0.6 (0.1)	4.5^{c} (0.2)	/
Cs-treated	Bot	70.9^{CD} (2.4)	3.0^{aE} (0.2)	0.8^{b} (0)	1.6^{b} (0.1)	0.8 (0.2)	3.8 (0.7)	1.1 (0.2)	0.5 (0.1)	6.0^{a} (0.1)	/
	Mid	72.4^{BCD} (2.8)	2.8^{abE} (0.2)	0.9^{a} (0)	1.9^{a} (0.1)	0.7 (0.1)	3.8 (0.2)	1.0 (0.2)	0.5 (0.1)	5.6^{b} (0.1)	/
	Top	70.7^{CD} (2.4)	2.7^{bEF} (0.1)	0.8^{a} (0)	2.1^{a} (0)	0.7 (0.2)	4.2 (0.4)	1.1 (0.3)	0.5 (0.1)	5.0^{c} (0.1)	/

[1] For one pretreatment, values for the same monosaccharide with different lowercase are significantly different at a confidence of 5%. In addition, values in the whole column for the same monosaccharide with different capital letters are significantly different at a confidence of 5%. (Glu-glucose, GalA-galacturonic acid, Rha-rhamnose, Gal-galactose, Ara-arabinose, Man-mannose, Xyl-xylose, Fuc-fucose, Lignin: Klason lignin, *Pr*-treated: samples treated with *P. radiata* Cel 26, *Cs*-treated: samples treated with *C. subvermispora*).

can also be a barrier for the retting process and thereby reduce its efficiency. Furthermore, the presence of wax affects downstream processes such as bleaching and dying (Kernaghan and Kiekens, 1992). Additionally, the high lignin concentration in the middle lamellae between individual fibers in the hemp bast was found to be an effective barrier to enzymatic retting (Morrison et al., 1999). Therefore, a higher content of waxy substances and lignin can inhibit depectinization of hemp stems with microorganisms during the retting process.

3.2.2. Histochemical analysis of transverse stem sections

Histochemical analysis was performed to visualize the spatial micro-distribution of pectin and lignin in hemp cells. Pectin consists of non-cellulosic acidic polysaccharides that are found mainly in the compound middle lamella (CML) regions of plant cell walls (e.g. fibers and parenchyma) with much lower amounts in secondary walls. Ruthenium red, which binds selectively to the intramolecular spaces of the carboxyl groups of pectin giving a red/pink color, has been widely used for visualizing pectin distributions in plant structures (Hou et al., 1999; Waller et al., 2004). Ruthenium red staining of transverse sections from hemp stems highlighted the presence of pectin as a red/pink color throughout cross sections (from Fig. 4A–C) irrespective of stem section origin. Greatest staining intensity was observed in the CML regions between all cell types (i.e. fiber–fiber cells, fiber–parenchyma cells and parenchyma–parenchyma cells) indicating the presence of pectin at high concentrations. There was a clear difference in the staining intensity among the investigated stem sections, especially in the CML regions between all cell types, with an increase in staining from the bottom to the top of the stems, consistent with the chemical composition of fibers from the different stem sections (Table 2).

The spatial micro-distribution of lignin within hemp cell walls in different stem sections was determined using Mäule- (Fig. 4D–F) and Wiesner reactions (Fig. 4G–I). The Mäule reagent reacts with lignin, giving a deep red color with syringyl lignin and yellow/orange color with guaiacyl lignin. The Wiesner reagent stains lignin deep red due to a reaction with the guaiacyl units in lignin. Though the whole xylem cell walls were stained an intense red color with Mäule reagent irrespective of the stem section, differences in staining were observed in the bast fiber region with respect to cell type and stem section (Fig. 4D–F). Similar results were also observed after staining with the Wiesner reagent (Fig. 4G–I). Both reagents stained the CML between fiber cells and the outermost layers of the secondary walls more strongly than the inner parts of the cells, where only faint staining was detected. The staining results indicate that lignin is primarily concentrated in the CML region between primary fiber cells, with much lower lignin contents in the secondary walls and regions between primary fiber cells and parenchyma cells. The staining results are consistent with the

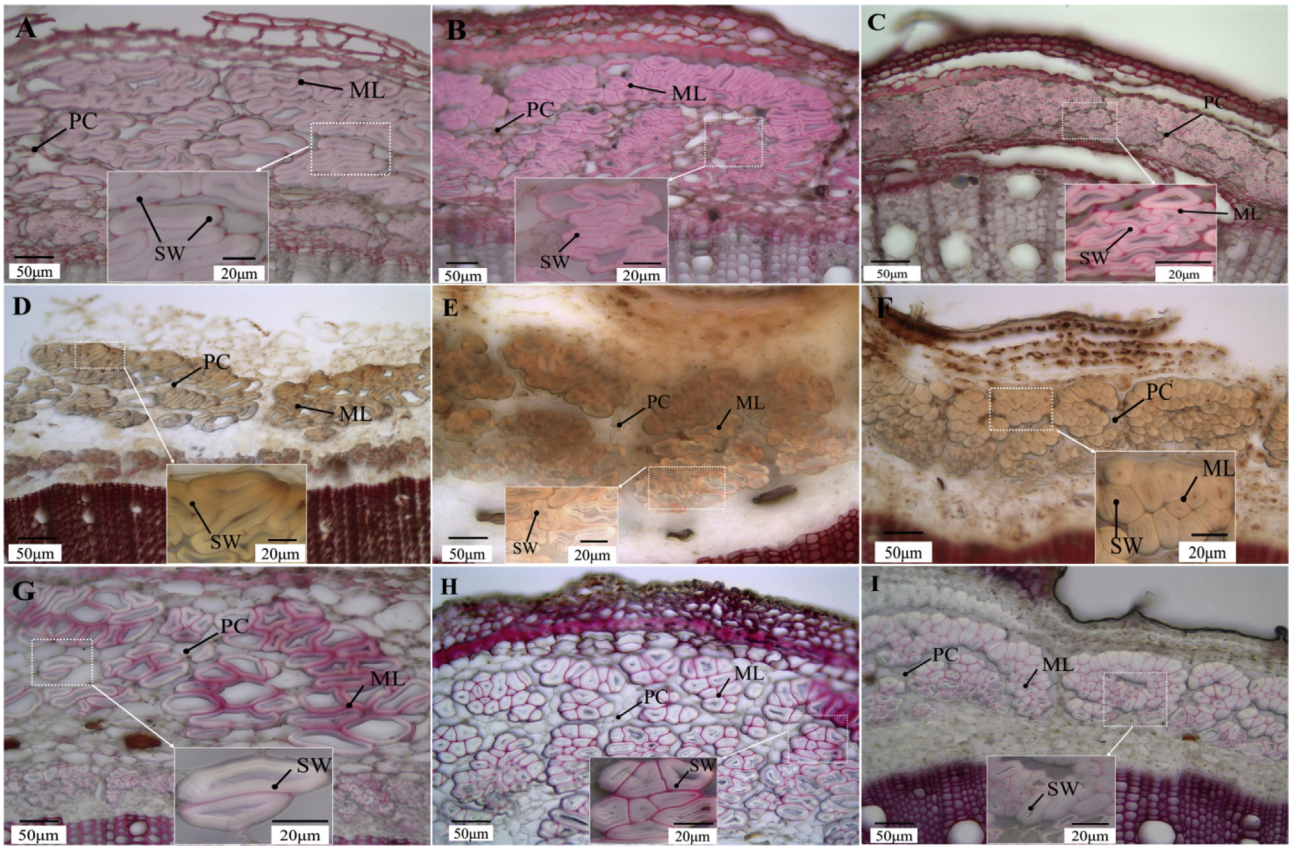

Fig. 4. Micrographs showing transverse sections of hemp stems from different stem sections after staining for pectin (A–C), syringyl lignin (D–F) and guaiacyl lignin (G–I) (ML—middle lamella; PC—parenchyma cell; SW—secondary wall). (A)–(C): positive reaction for pectin in the bottom (A), middle (B) and top (C) sections; (D)–(F): positive reaction for syringyl units in lignin from bottom (D), middle (E) and top (F) sections; (G)–(I): positive reaction for guaiacyl units in lignin from the bottom (G), middle (H) and top (I) sections.

classification of hemp as an Angiosperm, which are known to contain guaiacyl, *p*-hydroxyphenyl and syringyl lignin units (Gutiérrez et al., 2006).

The bast fibers from the different stem sections (i.e. top, middle and bottom) stained differently. Positive staining in both the primary- and secondary fibers along the entire stem was apparent (Fig. 4D–I), particularly with the outermost primary fibers (close to epidermis in Fig. 4D and G). From the top to the bottom stem section, the increase in staining intensity in the CML regions (between fiber cells and the outmost parts of secondary walls) presumably reflects the continuous deposition of lignin in hemp fibers where the fibers reach the highest maturity earlier (Amaducci et al., 2008; Crônier et al., 2005), thus correlating with the chemical composition data in Table 2.

3.3. *Mechanical properties of hemp fibers from different stem sections*

The typical stress–strain curves for all tested bast fiber strips and graphs with 10 representative stress–strain curves for each stem section are shown in Fig. 5a and Fig. 5b, respectively. The shape of the stress–strain curve was found to vary greatly between different bast fiber strips, even for those from the same hemp stem sections. As shown in Fig. 5a, two types of stress–strain curves for untreated hemp bast fiber were observed. One (type I) is linear elastic: the stress–strain curve is a straight line. The other (type II) is observed to include some plastic flow as indicated by the slightly bending progress curve.

The two types of stress–strain curves have been observed on single hemp fibers by Pickering et al. (2007) and Duval et al. (2011). For untreated hemp bast fiber, more than 90% tested samples demonstrated plastic flow behavior, as illustrated in Fig. 5b, and the rest (less than 10%) showed type I behavior. No apparent difference in tensile behavior of hemp bast fibers among top, middle and bottom stem sections was noticed.

The mean values and standard deviations of the mechanical properties of the hemp fibers including ultimate tensile strength (UTS), strain, and stiffness are presented in Fig. 6. The mechanical testing results indicate that the mechanical properties of hemp fibers were strongly influenced by stem section with respect to UTS and stiffness. Fibers from the middle section exhibited the best mechanical performance with the highest UTS and strain of 842 MPa and 5.7%, respectively, and a moderate stiffness of 28.8 GPa. Fibers from the top section showed moderate mechanical properties with UTS of 809 MPa, strain of 4.7%, and the highest stiffness of 31.5 GPa. However, fibers from the bottom section had the most inferior properties with the lowest UTS, strain, and stiffness of 686 MPa, 4.7% and 26.4 GPa, respectively. Furthermore, no noticeable differences in strain of these fibers were observed ($P > 0.05$).

The variation in mechanical properties of fibers with stem section can be explained by the differences in the morphological features (Figs. 1 and 2) and composition (Table 2). The diameter of hemp fibers (indicated by the area of fiber cell wall and lumen in Fig. 2) was found to vary markedly among top, middle and bottom stem sections, which can make mechanical properties of the fibers more scattered (Duval et al., 2011). In addition, a noticeable secondary fiber layer was present in the bottom section which has been found to reduce favorable mechanical properties. The slightly lower UTS of fibers from the top section might be due to the lower cellulose content (Table 2).

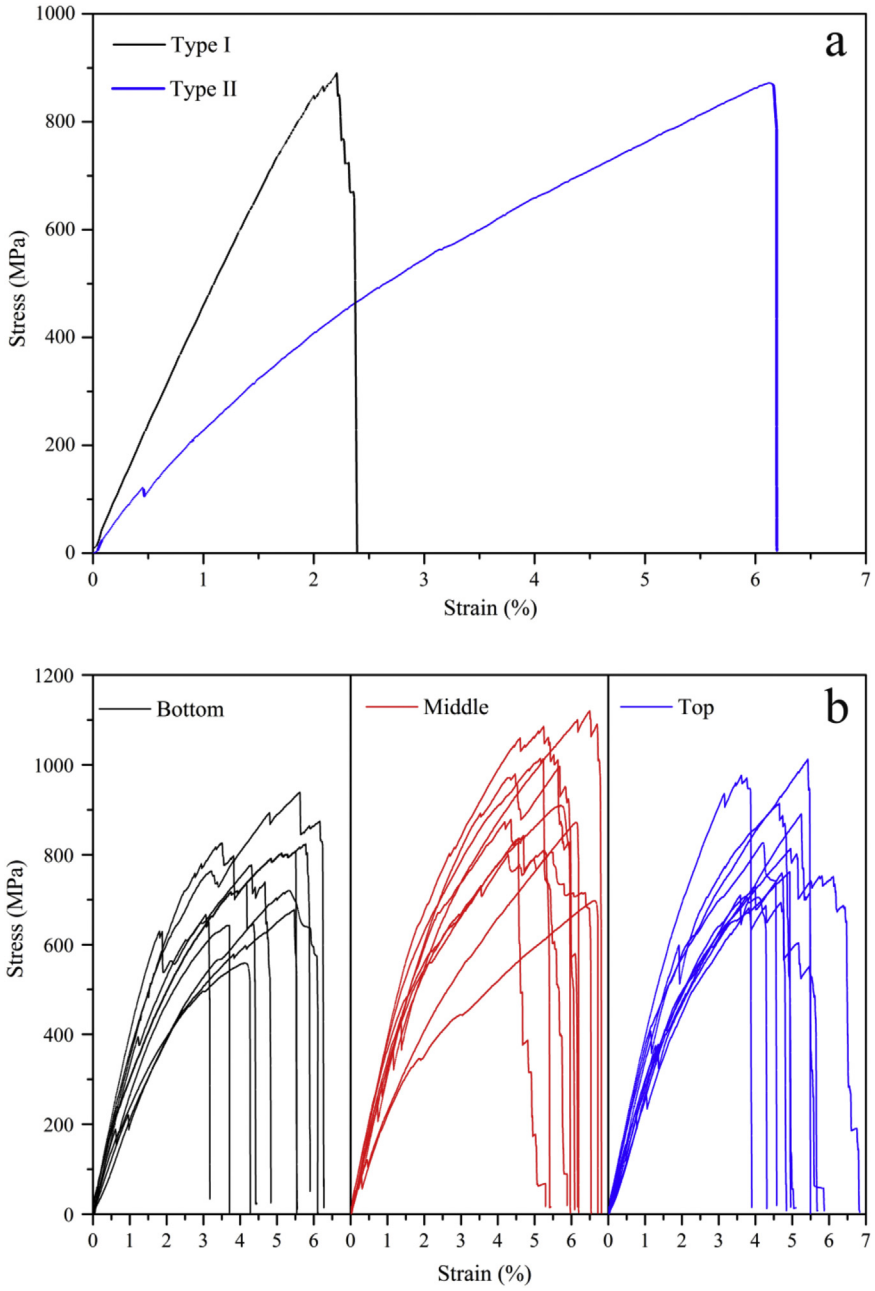

Fig. 5. The two observed stress–strain curve types I: linear elastic flow; II: plastic flow (a) and examples of stress–strain curves for untreated hemp bast fiber strips at bottom, middle and top stem sections (b).

3.4. *Effect of stem section on depectinization by fungal retting*

The effects of fungal retting on the chemical components of fibers from different stem sections are shown in Table 2. Surprisingly, a significant decrease in pectin content (indicated by GalA) happened to fibers in control group due to the removal of contamination on fiber surface and dissolution of water-soluble components during sterilizing (121 °C for 60 min) and 2-week incubation (about 14% dry matter weight loss in total). As a result, cellulose content (indicated by glucose content) was increased by about 10% (Table 2). For fungally treated samples, a significant ($P < 0.05$) amount of pectins (indicated by GalA and Ara) were degraded by cultivation with the fungi over 14 days. However, those cultivated with *P. radiata* Cel 26 exhibited much lower final levels of pectins than those incubated with *C. subvermispora*. This may be due to the high efficiency of *P. radiata* Cel 26 in degrading pectin, which is consistent with previous studies (Thygesen et al., 2013). Furthermore, cellulose content (indicated by glucose content) was concentrated to a significantly higher level for fibers after incubation with *P. radiata* Cel 26, particularly for fibers from the middle section, which increased from 70 to 81%. The cellulose content in the fibers treated with *C. subvermispora* increased to only 72%.

The effect of stem section on the performance of fungal retting on depectinization was evaluated by weight loss of cellulose (indicated by glucose), pectins (indicated by GalA, Rha, Gal, and Ara), and lignin (Klason lignin) after cultivation for 14 days, as shown in Table 3. For the characterization of the performance of fungi in depectinization, the depectinization selectivity was defined as the ratio between loss of pectins (%) and cellulose (%). According to the definition of depectinization selectivity, a higher selectivity

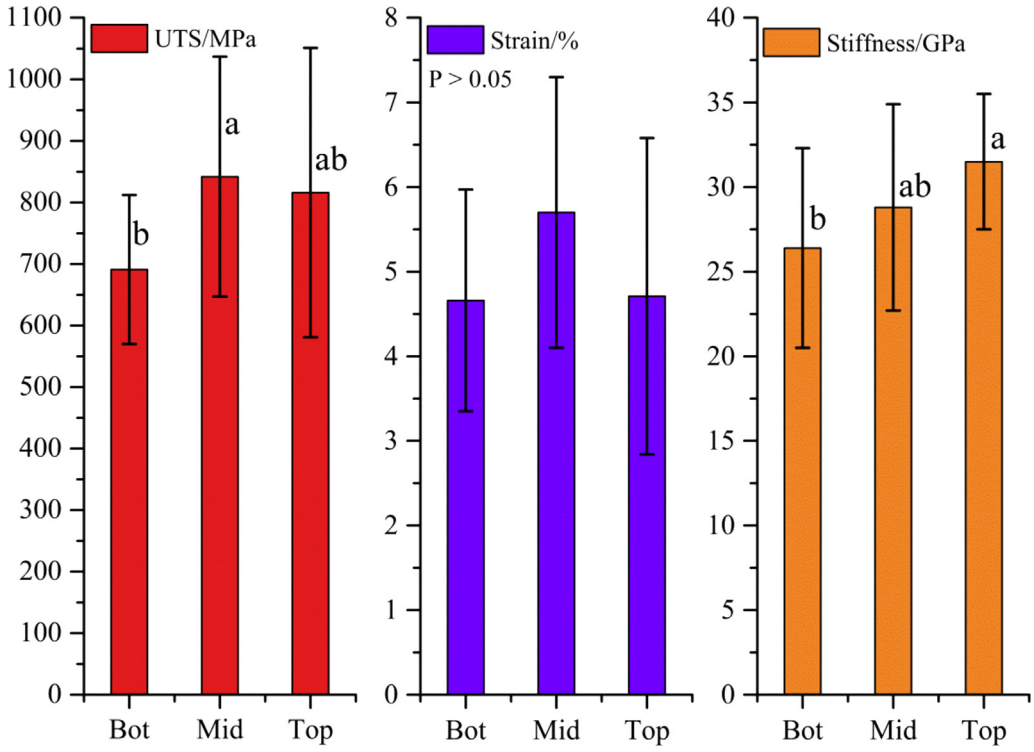

Fig. 6. Ultimate tensile strength (UTS), strain and stiffness of untreated hemp fibers from bottom (Bot), middle (Mid) and top (Top) stem sections. Values with different letters within a group are significantly different at $P = 0.05$.

Table 3
Component losses, fiber yield and depectinization selectivity at different sections after cultivation with white rot fungi for 14 days (Control group was used as baseline for the calculation of component losses and fiber yield).

Fungal retting	Stem section	Selectivity value	Yield %	Weight loss (%)[1,2]					
				Glu	GalA	Rha	Gal	Ara	Lignin
P. radiata Cel 26	Bottom	36.1	88 (5)	2 (11)	71 (5)	51 (4)	26 (9)	64 (9)	3 (8)
	Middle	18.1	83 (2)	4 (10)	74 (6)	57 (9)	33 (12)	63 (25)	14 (8)
	Top	10.0	82 (4)	7 (9)	75 (5)	60 (13)	40 (11)	69 (11)	19 (8)
C. subvermispora	Bottom	8.2	92 (1)	4 (9)	46 (8)	20 (3)	15 (14)	30 (22)	−4 (−3)
	Middle	3.2	83 (1)	14 (9)	57 (9)	31 (15)	19 (11)	46 (24)	7 (7)
	Top	3.1	74 (5)	20 (9)	69 (4)	50 (5)	42 (8)	70 (10)	18 (9)

[1] Glu: glucose, GalA: galacturonic acid, Gal: galctose, Ara: arabinose, Lignin: Klason lignin.
[2] Weight losses are shown as mean value ± uncertainty at a confidence of 95%, selectivity as mean values and yield as mean value ± standard deviation.

reflects improved preferential depectinization. In contrast, a lower selectivity indicates higher cellulose degradation.

It is noted that for both fungi, weight loss of cellulose, pectin and lignin increased from the bottom section of stem to the top section. However, the selectivity value for *P. radiata* Cel 26 decreased greatly from the bottom (36.1), to the middle (18.1) and to the top (10.0). In contrast, the apparent decrease in selectivity for *C. subvermispora* from the bottom (8.2), to the middle (3.2), and to the top (3.1) was about 3 times lower. The high depectinization selectivity for *P. radiata* Cel 26 was presumably due to its limited ability to degrade cellulose. For both fungi, the decrease in depectinization selectivity from the bottom to the top section was presumably due to variations in thickness of the bast fiber layer and chemical composition (particularly of lignin) with the stem section.

The thinner bast fiber layer, lower amount of waxy substances and lignin in fibers in the top section, may allow easier entry of microbes and their secreted enzymes and thus easier depectinization. Therefore weight loss of pectins (indicated by GalA, Rha, Gal and Ara in Table 3) increased from bottom to the top resulting in decreased fiber yield. As depectinization proceeds, most pectins surrounding the CML regions between the cell types (i.e. fiber cells and parenchyma cells) will be degraded and cellulose loss will increase (Table 3) as the accessibility of cellulose for fungi (or their enzymes) increases resulting in much lower fiber yield at top section after biological retting (indicated by much lower fiber yield of 74% at top section after retting with *C. subvermispora* compared with *P. radiata* Cel 26, shown in Table 3). As a result, for both fungi, the selectivity in the top section was lowest.

Differences in chemical composition of the untreated bast fibers from different stem sections, especially lignin, were found to influence the performance of depectinization by *P. radiata* Cel 26 and *C. subvermispora* with respect to selectivity and efficiency. The crucial role of lignin in lowering the accessibility of the components of fiber cell walls to fungi during the depectinization process was demonstrated. Generally, a higher lignin content of untreated fibers resulted in a higher efficiency of depectinization and lower cellulose degradation (Fig. 7). Thus, the efficiency of depectinization could be further improved by considering the differences in composition (e.g. lignin content) and structure of original materials.

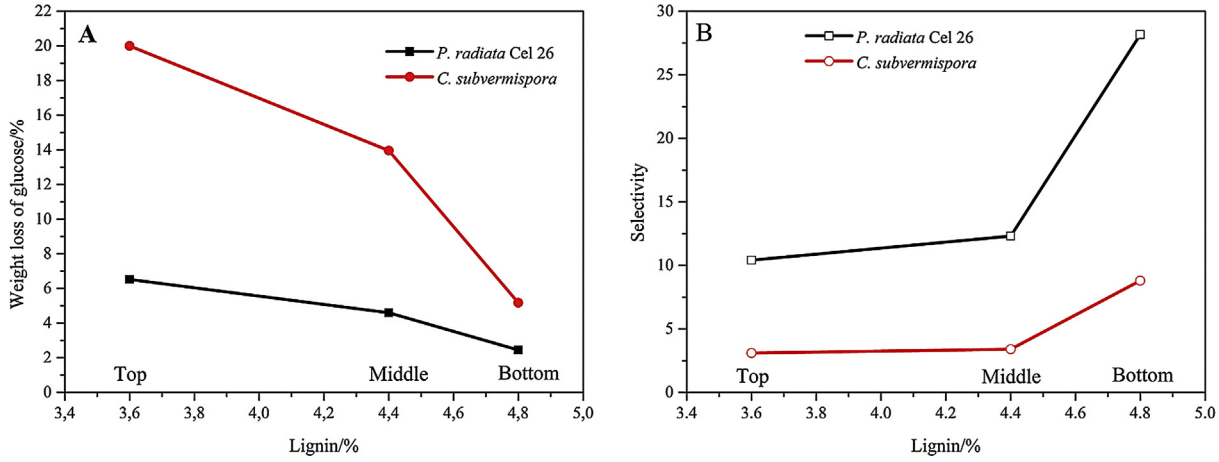

Fig. 7. Effect of lignin content of fibers on weight loss of cellulose caused by white rot fungi and their selectivity in depectinization.

Table 4
Mechanical properties of the investigated hemp fibers.

Parameter	Treatment	Stem section			*F* value[1]	Estimated for whole hemp stem
		Bottom[2]	Middle[2]	Top[2]		
UTS (MPa)	Untreated	686^{b} (126)	842^{a} (195)	809^{ab} (228)	3.83*	771 (204)
	Control	792 (146)	801 (151)	749 (172)	0.63	785 (180)
	Pr-treated[3]	770 (169)	743 (159)	671 (197)	1.72	736 (201)
	Cs-treated[3]	644^{a} (171)	574^{ab} (250)	456^{b} (155)	4.71*	573 (237)
Strain (%)	Untreated	4.66 (1.31)	5.70 (1.60)	4.71 (1.87)	2.70	5.04 (1.80)
	Control	2.97 (1.21)	2.70 (0.80)	2.60 (1.09)	0.56	2.78 (1.24)
	Pr-treated[3]	2.19 (0.72)	2.28 (0.91)	2.43 (0.87)	0.43	2.32 (0.97)
	Cs-treated[3]	2.22^{a} (0.54)	1.71^{b} (0.82)	1.50^{b} (0.48)	6.96**	1.86 (0.76)
Stiffness (GPa)	Untreated	26.4^{b} (5.9)	28.8^{ab} (6.1)	31.5^{a} (4.0)	4.57*	28.5 (6.7)
	Control	33.7 (7.2)	32.1 (9.7)	30.6 (6.5)	0.82	32.4 (9.5)
	Pr-treated[3]	42.4^{ab} (6.8)	45.7^{a} (10.3)	37.2^{b} (7.0)	5.57**	42.3 (9.8)
	Cs-treated[3]	34.5^{b} (5.1)	45.3^{a} (11.6)	39.4^{ab} (8.0)	7.92***	39.5 (10.0)

[1] *F* value for stem section affect at $P < 0.05^{*}$, $P < 0.01^{**}$, and $P < 0.001^{***}$.
[2] Values with different letters in the row are significantly different at $P = 0.05$ ($F_{0.05}(2, 57) = 3.16$, $F_{0.01}(2, 57) = 5.00$, $F_{0.001}(2, 57) = 7.82$).
[3] *Pr*-treated: samples retted with *P. radiata* Cel 26, *Cs*-treated: samples retted with *C. subvermispora*.

3.5. *Effect of stem section on mechanical properties of fungally treated hemp fibers*

Table 4 presents the mechanical properties of the bast fibers from different stem sections pretreated with *P. radiata* Cel 26 and *C. subvermispora* over 14 days, including UTS, strain and stiffness. It has been noticed that UTS of fibers from bottom section in control group increased from 686 ± 126 MPa to 792 ± 146 MPa compared to untreated hemp fibers, but strain of fibers from all investigated sections decreased significantly (Table 4). The increase in UTS can be explained by the separation of secondary fibers after steam sterilization (at 121 °C for 60 min) and cultivation for 2 weeks, and the significant decrease in strain may be due to the dissolution of water-soluble (i.e. non-cellulosic) components during sterilizing and incubation in culture indicated by the concentrated glucose content (Table 2). Moreover, compared to fibers in control group, the decrease in strain and increase in stiffness of pretreated fibers may be related to the degradation of non-cellulosic components during fungal retting.

Furthermore, it was found that fibers pretreated with *C. subvermispora* exhibit lower strength, strain and stiffness than fibers from the same stem section treated with *P. radiata* Cel 26. Notably, all the investigated fibers pretreated with *P. radiata* Cel 26, had comparable strengths (736 ± 201 MPa estimated for whole stem, $F = 1.72 < F_{0.05}$ (2, 57)) and strains (2.32 ± 0.97% estimated for whole stem, $F = 0.43 < F_{0.05}$ (2, 57)), though a significant difference ($P < 0.01$) in stiffness was observed (Table 4). However, fibers pretreated with *C. subvermispora* showed significant difference for all investigated parameters (i.e. UTS, strain, and stiffness) for the different sections at $P = 0.05$ (Table 4), and the *F* value for the effect of stem section on UTS, strain, and elongation was 4.71, 6.96 and 7.92 ($F_{0.05}(2, 57) = 3.16$, $F_{0.01}(2, 57) = 5.00$, $F_{0.001}(2, 57) = 7.82$), respectively. In addition, compared to fiber treated with *P. radiata* Cel 26, much lower strength of 573 MPa (estimated for whole hemp stem shown in Table 4), strain of 1.86% and stiffness of 39.5 GPa were obtained. According to this, it can be concluded that fibers pretreated with *C. subvermispora* caused the mechanical properties of fibers to be more scattered than *P. radiata* Cel 26.

By comparing the UTS of fibers pretreated with *P. radiata* Cel 26 and *C. subvermispora* to control group, an increase in reduction of UTS from bottom to top stem section for both fungi was observed (Fig. 8). The results suggested that the fibers responded differently to fungal retting with either *P. radiata* Cel 26 or *C. subvermispora* causing a variable change in mechanical properties (e.g. UTS in Fig. 8). As a result, the mechanical properties of fibers from different stem sections became more scattered, particularly for fibers treated with *C. subvermispora* (shown in Table 4). The strong dependence of responses of fibers to fungal retting with respect to mechanical properties on stem section was consistent with the stem section dependence of fungal selectivity of depectinization (Table 3). A high fungal selectivity of depectinization (e.g. at bottom section) resulting in less cellulose loss caused UTS of fibers to decrease slightly

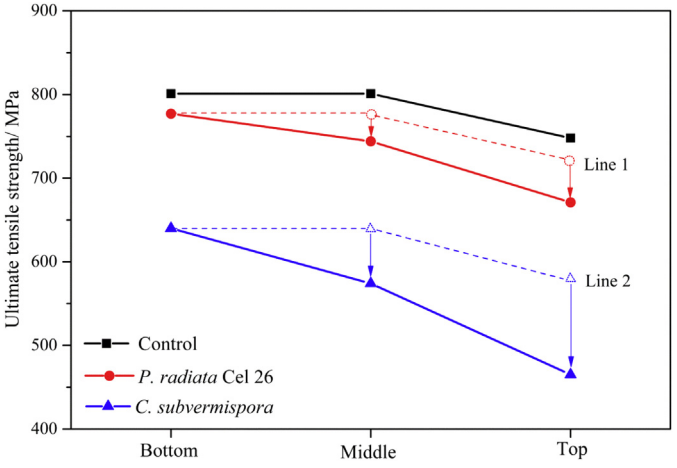

Fig. 8. Ultimate tensile strength of hemp fibers from the bottom, middle and top stem sections pretreated with *P. radiata* Cel 26 and *C. subvermispora* for 14 days. (Line 1: trend line showing changes in tensile strength for fibers treated with *P. radiata* Cel 26 if same decrease happened to middle and top sections as bottom section; Line 2: similar trend line showing changes for fibers treated with *C. subvermispora*).

(Fig. 8 for bottom stem section). In contrast, a lower fungal selectivity (e.g. at top section) resulting in a higher amount of cellulose loss (Table 4) consequently caused UTS of fibers to be reduced a lot (Fig. 8 for top stem section).

Previously, Duval et al. (2011) found that stem section influences the mechanical properties of hemp fibers. However, they concluded that as only low variations in the mechanical properties were observed, differentiation between stem sections is not necessary and the whole stem can be used for fiber extraction for manufacturing composites without restriction. Indeed, in this study, a dependence of mechanical properties of untreated fibers on stem section was confirmed (Fig. 6). Differences in mechanical properties of untreated fibers from different stem sections can be ascribed to the differences in the morphological features (e.g. transverse area of fiber cell, proportion of secondary fibers) and chemical compositions (e.g. cellulose) of the untreated hemp fibers. However, according to the present study, the effect of the differences in original materials, particularly in lignin content (Table 2), on biological defibration process should be considered in order to produce high grade fibers with high strength and low variation in mechanical properties.

4. Conclusions

Hemp stem section origin not only affects the mechanical properties of untreated fibers, but also the selectivity of depectinization. Autoclave treatment did cause some dissolution of pectin (indicated by galacturonic acid loss) and apparently removed secondary fibers to increase the tensile strength of fibers from bottom stem. Consequently, variation in the selectivity of depectinization changed the mechanical performance of fibers from different stem sections. Therefore, selection of fibers with fewer variations in mechanical properties should consider the influence of the differences in original materials on subsequent processes rather than only focus on the existing differences of the starting materials. Further insight into the biocatalytic mechanisms underlying the fungal retting selectivity may further improve treatment efficiency and mechanical properties of treated fibers.

Acknowledgements

The authors are grateful to the Danish Council for Independent Research supporting the CelFiMat project (IP No. 12-127446: "High quality cellulosic fibers for strong biocomposite materials"). The financial support of China Scholarship Council (CSC, no. 201304910245) for Ming Liu's Ph.D. project is acknowledged. The funding for an internship at Swedish University of Agricultural Sciences from Nordforsk Researcher Network to Ming Liu and from COST Action FP1205 to Anders Thygesen (ECOST-STSM-FP1205-020214-039501) is acknowledged. Annette Eva Jensen, Jan Sjølin, Jonas Kreutzfeldt Heininge and Marcel Tutor Ale are thanked for technical support.

References

Amaducci, S., Zatta, A., Pelatti, F., Venturi, G., 2008. Influence of agronomic factors on yield and quality of hemp (*Cannabis sativa* L.) fibre and implication for an innovative production system. Field Crops Res. 107 (2), 161–169.

Arnous, A., Meyer, A.S., 2008. Comparison of methods for compositional characterization of grape (*Vitis vinifera* L.) and apple (*Malus domestica*) skins. Food Bioprod. Process. 86 (C2), 79–86.

Aslan, M., Chinga-Carrasco, G., Sørensen, B.F., Madsen, B., 2011. Strength variability of single flax fibres. J. Mater. Sci. 46, 6344–6354.

Browning, B.L., 1967. Methods of Wood Chemistry. Interscience Publisher, John Wiley & Sons, New York, NY.

Charlet, K., Baley, C., Morvan, C., Jernot, J.P., Gomina, M., Bréard, J., 2007. Characteristics of Hermès flax fibres as a function of their location in the stem and properties of the derived unidirectional composites. Composites, A—Appl. Sci. Manuf. 38 (8), 1912–1921.

Crônier, D., Monties, B., Chabbert, B., 2005. Structure and chemical composition of bast fibers isolated from developing hemp stem. J. Agric. Food Chem. 53, 8279–8289.

Duval, A., Bourmaud, A., Augier, L., Baley, C., 2011. Influence of the sampling area of the stem on the mechanical properties of hemp fibers. Mater. Lett. 65 (4), 797–800.

Evans, J.D., Akin, D.E., Morrison III, W.H., Himmelsbach, D.S., Foulk, J.A., 2002. Modifying dew-retted flax fibers by means of an air-atomized enzyme treatment. Text. Res. J. 72, 579–585.

Fan, M., 2010. Characterization and performance of elementary hemp fibers: factors influencing tensile strength. Bioresources 5 (4), 2307–2322.

Fan, M., Dai, D., Yang, A., 2011. High strength natural fiber composite: defibrillation and its mechanisms of nano cellulose hemp fibers. Int. J. Polym. Mater. 60 (13), 1026–1040.

Foulk, J.A., Akin, D.E., Dodd, R.B., 2001. Processing techniques for improving enzyme-retting of flax. Ind. Crops Prod. 13 (3), 239–248.

Gutiérrez, A., Rodríguez, I.M., del Río, J.C., 2006. Chemical characterization of lignin and lipid fractions in industrial hemp bast fibers used for manufacturing high-quality paper pulps. J. Agric. Food Chem. 54 (6), 2138–2144.

Hou, W., Chang, W., Jiang, C., 1999. Qualitative distinction of carboxyl group distributions in pectins with ruthenium red. Bot. Bull. Acad. Sinca 40, 115–119.

Hu, W., Ton-That, M.T., Denault, J., Rho, D., Yang, J., Lau, P.C.K., 2012. Comparison between dew-retted and enzyme-retted flax fibers as reinforcing material for composites. Polym. Eng. Sci. 52 (1), 165–171.

Islam, M.S., Pickering, K.L., Foreman, N.J., 2011. Influence of alkali fiber treatment and fiber processing on the mechanical properties of hemp/epoxy composites. J. Appl. Polym. Sci. 119 (6), 3696–3707.

Kernaghan, K., Kiekens, P., 1992. Bleaching and dyeing of linen. In: Sharma, H.S.S., Van Sumere, C.F. (Eds.), The Biology and Processing of Flax. M Publications, Northern Ireland: Belfast, pp. 343–345.

Liu, M., Fernando, D., Daniel, G., Madsen, B., Meyer, A.S., Ale, M.T., Thygesen, A., 2015. Effect of harvest time and field retting duration on the chemical composition, morphology and mechanical properties of hemp fibers. Ind. Crops Prod. 69, 29–39.

Marrot, L., Lefeuvre, A., Pontoire, B., Bourmaud, A., Baley, C., 2013. Analysis of the hemp fiber mechanical properties and their scattering (Fedora 17). Ind. Crops. Prod. 51, 317–327.

Mankowski, J., Cierpucha, W., Kolodziej, J., Mankowski, T., 2006. Cottonized" flax and hemp fiber as a raw material for the production of blended yarns. In: Kozłowski, R., Zaikov, G.E., Pudel, F. (Eds.), Renewable Resources and Plant Biotechnology. Nova Science Publishers, Inc, Chicago, IL, pp. 63–65.

Mediavilla, V., Jonquera, M., Schmid-Slembrouck, I., Soldati, A., 1998. Decimal code for growth stages of hemp (*Cannabis sativa* L.). J. Int. Hemp Ass. 5 (2), 68–74.

Mediavilla, V., Leupin, M., Keller, A., 2001. Influence of the growth stage of industrial hemp on the yield formation in relation to certain fibre quality traits. Ind. Crops Prod. 13 (1), 49–56.

Morrison III, W.H., Archibald, D.D., Sharma, H.S.S., Akin, D.E., 2000. Chemical and physical characterization of water- and dew-retted flax fibers. Ind. Crops Prod. 12 (1), 39–46.

Morrison III, W.H., Akin, D.E., Archibald, D.D., Dodd, R.B., Raymer, P.L., 1999. Chemical and instrumental characterization of maturing kenaf core and bast. Ind. Crops Prod. 10 (1), 21–34.

Özmen, N., Cetin, N.S., Mengeloglu, F., Birinci, E., 2013. Vinyl acetate modified scots pine reinforced HDPE composites: influence of various levels

of modification on mechanical and thermal properties. Bioresources 8 (1), 1361–1373.
Pickering, K.L., Beckermann, G.W., Alam, S.N., Foreman, N.J., 2007. Optimising industrial hemp fibre for composites. Composites, A—Appl. Sci. Manuf. 38 (2), 461–468.
Satlow, G., Zaremba, S., Wulfhorst, B., 1994. Faserstoff-tabellen nach P.-A. Koch: flachs sowie andere bast- und hartfasern. Chemiefasern/Text 96 (44), 765–785.
Sluiter, A., Ruiz, R., Scarlata, C., Sluiter, J., Templeton, D. (2008). Determination of extractives in biomass. NREL Technical Report. NREL/TP –510-42619.
Sluiter, A., Hames, B., Ruiz, R., Scarlata, C., Sluiter, J., Templeton, D., Crocker, D., 2011. Determination of structural carbohydrates and lignin in biomass. In: NREL Technical Report NREL/TP-510-42619.
Thygesen, A., Liu, M., Meyer, A.S., Daniel, G., 2013. Hemp fibres: Enzymatic effect of microbial processing on fibre bundle structure. 34th Risø Int. Symp. Mater. Sci. vol. 34, 373–380.
Thygesen, A., Thomsen, A.B., Daniel, G., Lilholt, H., 2007. Comparison of composites made from fungal defibrated hemp with composites of traditional hemp yarn. Ind. Crops Prod. 25 (2), 147–159.
Thygesen, A., Daniel, G., Lilholt, H., Thomsen, A.B., 2005. Hemp fiber microstructure and use of fungal defibration to obtain fibers for composite materials. J. Nat. Fibers 2 (4), 19–37.
van der Werf, H.M.G., van der Veen, J.E.H., Bouma, A.T.M., ten Cate, M., 1994. Quality of hemp (*Cannabis sativa* L.) stems as a raw material for paper. Ind. Crops Prod. 2 (3), 219–227.
van Der Werf, H.M.G., Wijlhuizen, M., de Schutter, J.A.A., 1995. Plant density and self-thinning affect yield and quality of fibre hemp (*Cannabis sativa* L.). Field Crops Res. 40 (3), 153–164.
Waller, L.N., Fox, N., Fox, K.F., Fox, A., Price, R.L., 2004. Ruthenium red staining for ultrastructural visualization of a glycoprotein layer surrounding the spore of *Bacillus anthracis* and *Bacillus subtilis*. J. Microbiol. Methods 58 (1), 23–30.

Paper III

Ming Liu, Marcel Tutor Ale, Barłomiej Kołaczkowski, Dinesh Fernando, Geffrey Daniel, & Anders Thygesen

Comparison of field retting and *Phlebia radiata* Cel 26 retting of hemp fibers for fibre-reinforced composites

Applied Microbiology and Biotechnology, 2016, (submitted)

Comparison of traditional field retting and *Phlebia radiata* Cel 26 retting of hemp fibres for fibre-reinforced composites

Ming Liu [1], Marcel T Ale [1], Bartłomiej Kołaczkowski [1], Dinesh Fernando [2], Geoffrey Daniel [2], Anne S. Meyer [1], Anders Thygesen [1*]

[1] Center for Bioprocess Engineering, Department of Chemical and Biochemical Engineering, Technical University of Denmark, 2800 Kongens Lyngby, Denmark

[2] Department of Forest Products/Wood Science, Swedish University of Agricultural Sciences, Vallvägen 9D, 750-07 Uppsala, Sweden

* Corresponding author: athy@kt.dtu.dk; +45 21326303

Abstract

The effects of field retting versus fungal retting using *Phlebia radiata* Cel 26 (a mutant low in cellulose degrading ability) as hemp fibre treatment on chemical composition, mechanical properties of fibres and fibre/epoxy composites were studied. By phylogenetic frequency mapping, Ascomycota phylum were observed during the first 1-2 weeks of classical field retting, and thereafter, different types of bacteria, notably different Proteobacteria proliferated in field retted fibres. Extracts from field retted fibres exhibited high glucanase activities, while extracts from *P. radiata* Cel 26 retted fibres showed high polygalacturonase, galactanase, xyloglucan (XG)-specific endoglucanase and laccase activities. As a result, fungal retting gave a significantly higher glucan content in the fibres than field retting (~77% vs. 67%) and caused a higher removal of pectin from hemp fibres with a higher efficiency, as indicated by lower galacturonan content of fibres (1.6%) after fibres were retted for 3 weeks with *P. radiata* Cel 26 compared to a galacturonan content of 3.6% for field retted fibres. Fibre stiffness and ultimate tensile strength (UTS) were retained after retting with *P. radiata* Cel 26, but decreased after field retting. As a consequence, composites with fungal retted fibres had higher stiffness and UTS than composites with field retted fibres.

Keywords: Hemp fibre · Field retting · *Phlebia radiata* Cel 26 · Microbial community · Enzyme profiling · Composite strength

Introduction

The use of cellulosic fibres in high grade composites has gained increased interest over the last decade (Faruk et al. 2012; Liu et al. 2016b). Plant fibres originating from hemp (*Cannabis sativa* L.) are considered a particularly promising renewable raw material for production of high quality reinforcement of composite materials due to their high stiffness and strength to weight ratio (Faruk et al. 2012).

In order to isolate the cellulose-rich hemp fibres from the bast on the hemp stem surface, a retting process is needed. The retting process is used to separate the cellulosic fibres from the rest of the bast fibre material by degrading pectic substances located between the woody core (xylem) and the outer cortex layer, as well as in the middle lamella between fibres (Liu et al. 2015a). The main purpose of the retting is thus to degrade the pectins and other cementing compounds that bind the bast fibres and fibre bundles to other tissues and thereby separate the fibres (Liu et al. 2015a; Liu et al. 2015b). The removal of non-cellulosic components and separation of the cellulose fibers can improve interface bonding between fibers and matrix polymers and the mechanical properties of the fiber reinforced composites are therefore increased (Li et al. 2009; Liu et al. 2016a; Liu et al. 2016b).

During classic field retting, hemp stems are cut and spread on the field, and are then subjected to spontaneous, uncontrolled microbial proliferation to attain enrichment and separation of the cellulose rich fibres (Liu et al. 2015a). The resulting mechanical properties may however be reduced due to cellulase activity secreted by the proliferation of the native microorganisms on the hemp stems (Liu et al. 2015a). This process has been studied and local microbial communities shown to include fungi such as *Cladosporium* sp. and *Cryptococcus* sp. as well as bacteria including *Escherichia coli* have been found (Brown and Sharma 1984; Ribeiro et al. 2015). The identity and characteristics of different microorganisms involved in field retting, and their different enzymes activity should be studied to acquire a better understanding of the influence of classic field retting on chemical composition and mechanical properties of fibres during the field retting.

In order to avoid severe degradation of cellulose and reduction of fibre mechanical properties an alternative to field retting is the microbiologically controlled retting using selected fungi to degrade non-cellulosic components in the fibres (Thygesen et al. 2007; Liu et al. 2015b). *Phlebia radiata* Cel 26, belonging to the Basidiomycota phylum, produces less cellulase enzymes compared to its wild type (Nyhlen and Nilsson 1987). Nevertheless, the determination of enzyme activity in the extracts of *P. radiata* Cel 26 retted hemp fibres can provide knowledge on how the retting process can be optimized to produce high quality fibres.

The objective of this study was to compare the effect of field retting and *P. radiata* Cel 26 retting on mechanical properties of hemp fibre reinforced composites. It was hypothesized that higher

cellulase activities would be detected from enzyme extracts from field retted hemp fibres compared to *P. radiata* Cel 26 retted fibres and that any higher cellulase activity in field retted samples would correlate to decreased mechanical properties. As a result, it was expected that fibres with low mechanical properties should be obtained after field retting, while fibres with high mechanical properties and low pectin content would be obtained from *P. radiata* Cel 26 retting. Genetic identification and environmental scanning electron microscopy (ESEM) observation of bacteria and fungi was carried out during 3 weeks of retting to identify their abundance on hemp fibre surfaces. Enzymatic and microbial characteristics were linked to changes in chemical composition of fibres and mechanical properties of the fibres and fibre/epoxy composites.

Materials and methods

Raw materials and fibre treatments

Hemp (*Cannabis sativa* L.), variety USO-31, was sown on May 5th 2013 (N 48.8526°, E 3.0190° (WGS84)) by Bafa Neu GmbH) and harvested on Sep 6th 2013 (Liu et al. 2015a). Field retting was conducted for 7, 14 and 20 days after harvest as previously reported (Liu et al. 2015a). After field retting treatment, hemp stem samples were stored frozen until Deoxyribonucleic acid (DNA) extraction, enzyme extraction and fixation. Fungal retting with the white rot fungus *P. radiata* Cel 26 was carried out as previously reported (Liu et al. 2015b), In brief, hemp stem pieces were sterilized at 121 °C for 1 h, and the retting with *P. radiata* Cel 26 was then conducted for 7, 14 and 20 days on hemp stem pieces in 1 L Erlenmeyer flasks (15 g per flask, approx. 15 cm in length) at 28 °C (*P. radiata* Cel 26 was obtained from the Swedish Agricultural University, Uppsala, Sweden) (Nyhlen and Nilsson 1987). After fungal retting treatment, hemp stem samples were stored frozen until protein extraction for enzyme activity assay.

Fungal and bacterial classification by gene sequencing

Hemp fibres were isolated manually from stems by removing xylem using a scalpel. Approximately 50 mg of sample (2 mm^2) placed into 2 mL Eppendorf tubes was extracted directly for obtaining genomic DNA using PowerBiofilm™ DNA Isolation Kit (MO-BIO, Carlsbad, USA) according to the manufacturer's instructions. PCR amplification for both bacterial and fungal DNA was carried out using a C1000™ thermo-cycler (BIO-RAD, Hercules, USA). Each DNA sample (1 μL) was used as a template in a PCR reaction (Sun et al. 2015). The universal bacterial 16S ribosomal RiboNucleic Acid (RNA) primers used for PCR amplifications were 27F (5'-AGA GTT TGA TCA TGG CTC A-3') and 1492R (5'-CGGTTACCT TGTTACGACTT-3'), and the fungal primer sets were ITS5 (5'-GGAAGTAAAAGTCGTAACAAGG-3') and ITS4 (5'-TCCTCCGCTTATTGATATGC-3') (Eurofins Genomics, Ebersberg, Germany) (White et al. 1990; Gardes et al. 1991). The internally transcribed

spacer (ITS) is the spacer DNA situated between the small-subunit ribosomal RNA (rRNA) and the large-subunit rRNA genes in the chromosome or the corresponding transcribed region in the polycistronic rRNA precursor transcript). Extracted DNA (1 µL) was added to a PCR master mix (49 µL) containing 0.5 µM of primers, Phusion HF buffer (F-518), 200 µM dNTPs and 0.5 U Phusion Hot Start II DNA polymerase (#F-549L; Thermo Fisher Scientific, Wastham, USA) (Ale et al. 2016).

PCR products were purified using GFX PCR DNA and Gel Band Purification Kit (GE28-9034-70 Sigma-Aldrich, UK). Cloning was performed using the pJet1.2/Blunt cloning vector (50 ng/µL) and T4 DNA ligase (5 U/µL). Ligation was carried out according to the manufacturer's instructions (CloneJET PCR Cloning Kit #K1231, Thermo Scientific, USA) and the ligated product was used for transformation of electro-competent *E. coli* DH5α using BioRad Micropulser (BioRad, USA). Purified plasmids were sequenced using the 27F primer for bacteria and the ITS4 for fungi by the company Macrogen Europe (Amsterdam, The Netherlands). The unique sequences were submitted to EMBL Nucleotide Sequence Database with the submission code Hx2000055819 (anac) (SUB#924725).

A GenBank nucleotide database search was conducted using the BLAST algorithm (Basic Local Alignment Search Tool) to determine the closest relative of partial 16S gene sequences (Maidak et al. 1999). For each DNA sequence, a multiple alignment was created by Clustal W (Thompson et al. 1994). Evolutionary analysis and a phylogenic tree were constructed in Mega 6.0 (Kimura 1980), by the use of the Kimura 2 parameter model (Kimura 1980). The reliability of the branches was evaluated with non-parametric bootstrapping (100 replicates). All positions with less than 95% site coverage were eliminated (complete deletion option). That means that fewer than 5% alignment gaps, missing data and ambiguous bases were allowed at any position.

Protein extraction and enzyme activity assay

Hemp bast fibres were gently peeled from field retted and *P. radiata* Cel 26 retted hemp stems. For enzyme extraction, 4 g of bast fibres were submersed in 40 mL of 20 mM citrate buffer (pH 6.0) supplemented with 0.1% (v/v) Tween 20 and 0.25 mM dithiothreitol (DTT) in a glass tube, and the tube placed at 0 °C and shaken at 120 rpm for 1 h. The extraction and concentrating steps were performed as described previously (Suwannarangsee et al. 2014). For each sample, the crude enzyme extracts were concentrated until the volume was reduced to 3.0 mL. After concentrating, the concentrated enzyme extracts were kept at 4 °C for activity assay. Protein content of enzyme extracts were determined using Bovine serum albumin as standard (Bradford 1976).

The pectinolytic, cellulolytic and hemicellulolytic enzyme activities were determined in crude enzyme extracts from the field retted and *P. radiata* Cel 26 retted samples at 40 °C in 20 mM citrate buffer (pH 6.0). Glucanase, polygalacturonase, galactanase and xyloglucan (XG)-specific endoglucanase activities were determined by measuring formation of reducing ends. The substrates

used were for glucanase 10 g/L carboxymethyl cellulose (CMC) (Suwannarangsee et al. 2014), for polygalacturonase 2 g/L polygalacturonic acid (Thomassen et al. 2011), for galactanase 5 g/L potato galactan (Michalak et al. 2012) while for xyloglucan 10 g/L tamarind xyloglucan (Benko et al. 2008). Enzyme and substrate ratio of 5:1 (v/v) was used for all the enzyme activity assays. The amount of reducing sugars that were liberated was measured by using 4-hydroxybenzoic acid hydrazide (PAHBAH) as colorimetric agent (Lever 1973). One unit of the enzyme activity was defined as the volume of crude enzyme extracts (μL) required to liberate 1 μmol reducing ends (glucose equivalents) per minute under the assay conditions.

Laccase activity was measured by monitoring the oxidation of 2,2-azinobis (3-ethylbenz-thiazoline)-6 sulphonate (ABTS) by the enzyme extract at 420 nm (Li et al. 2008). *P. radiata* Cel 26 produces low levels of H_2O_2 and other peroxidases, which show activity with ABTS in the presence of H_2O_2 (Srinivasan et al. 1995). Therefore, catalase (Sigma Chemical Co.) was added at 1000 U/(mL of enzyme extracts) into crude enzyme extracts and incubated for 1 h at 37 °C to remove H_2O_2. One unit of laccase activity was defined as the volume of crude enzyme extracts (μL) required to oxidize 1 μmol ABTS per minute under the assay conditions.

Characterization of fibres

Chemical composition analysis

Dried bast fibres were ground with a microfine grinder (IKA, MF 10.1; IKA®-Werke GmbH) through a 1-mm screen. Ground samples were extracted in a Soxhlet apparatus (Liu et al. 2015a) and the extractive-free fibres hydrolysed using a two-step sulfuric acid process (Sluiter et al. 2011). After acid hydrolysis, the hydrolysate was collected for monosaccharide analysis, and Klason lignin (i.e. residue of the hydrolysis) content was gravimetrically determined. The chemical composition of the hydrolysate was analysed by high-performance anion-exchange chromatography with pulsed amperometric detection (HPAEC-PAD) and with recovery values of the monosaccharides estimated from parallel runs (Arnous and Meyer 2008).

Scanning electron microscopy of fibre surface

Samples (5 mm long × 2 mm wide) were cut from bast fibre strips under a stereo microscope and digital photos were taken using a Philips XL 30 ESEM microscope operated at 10 − 15 kV (Fernando and Daniel 2008). Preparation of samples for microscopy followed that described by (Fernando and Daniel 2008).

Tensile properties of fibres

Bast fibre strips (60 mm long × 1 mm wide) of mass in the range of 5 – 20 mg were used for tensile testing (Liu et al. 2015a). Tensile testing was performed using an Instron Testing Machine 2710-203

equipped with a 1kN load cell. The gauge length was 10 mm and the displacement rate 0.5 mm min^{-1} (corresponding to a strain rate of 5% min^{-1}). Tensile testing was performed on 20 specimens for each treatment. The cross-sectional area (A_f) was determined from measured fibre mass and length, and an assumed fibre density (i.e. 1.50 kg dm^{-3} (Cheung et al. 2009)). Stiffness (linear regression in the strain interval 0.05 – 0.25%), ultimate tensile strength (UTS), and failure strain were determined based on measured stress-strain curves.

Composites manufacturing and mechanical properties characterization

Manufacturing of fibre/epoxy composites

Composites were manufactured by manually aligning the treated hemp bast fibre strips resulting in unidirectional composites. Epoxy resin (Araldite® LY 1568) and its amine hardener (Aradur® 3489) were mixed at a 100/28 mass ratio and degassed in a vacuum oven. The setup for vacuum infusion and moulding processing has been described (Liu et al. 2016b). After demoulding, composite samples with dimensions 140 mm × 10 mm × 2 mm were obtained and then glass fibre/epoxy tabs with lengths of 50 mm mounted on composite specimens using epoxy glue (DP 460).

The volumetric composition of the composites was varied by varying the amount of fibres (m_f) in the mould chambers resulting in fibre weight contents (w_f) in the range 0 – 0.70. When the W_f was below 0.30, the composite specimens had irregular surfaces, and their thickness could not be measured accurately. For such cases, composite density (ρ_c) was determined by the buoyancy method (Archimedes principle) using water as the displacement medium. When W_f was above 0.30, the composites specimens had flat surfaces and ρ_c could be accurately calculated based on their dimensions (i.e. length, width and thickness). The volumetric composition of composite samples was determined from the equations described previously (Liu et al. 2016b). In the composites, the porosity (V_p) was assumed to be a linear function of the fibre volume content (V_f), where the established proportionality constant is equal to the fibre correlated porosity factor α_{pf} (Madsen et al. 2009) as expressed in Eq.1. The matrix correlated porosity factor (α_{pm}) was assumed to be zero.

$$V_p = \alpha_{pf} \times V_f \quad (1)$$

Tensile properties of composites

For tensile testing of the composite specimens, an Instron Testing Machine 5566 with a load cell of 10 kN was used. Strain measurements were conducted using two extensometers and the displacement rate was 1 mm min^{-1} (corresponding to a strain rate of 2.5% min^{-1}). Based on measured stress-strain curves, composite stiffness (E_c) (linear regression in the strain interval 0.05 – 0.25%) and UTS were determined. For each treatment, at least 10 specimens with varied fibre content were tested. The rule of mixtures (ROM) model (Madsen et al. 2009) was used to determine the effective fibre stiffness (E_f)

and fibre strength (UTS_{fu}) in the composites by linear regression versus fibre volume content (V_f) using Eqs.2 and 3, respectively. The intercept was set equal to the measured matrix stiffness (E_m) and strength (UTS_m^*) at the average failure strain of the composites.

$$E_c = V_f E_f + V_m E_m = E_m + V_f \left(E_f - E_m(1 + \alpha_{pf})\right) = E_m + kV_f \quad (2)$$

$$UTS_c = V_f UTS_{fu} + V_m UTS_m^* = UTS_m^* + V_f \left(UTS_{fu} - UTS_m^*(1 + \alpha_{pf})\right) = UTS_m^* + kV_f \quad (3)$$

where the subscripts c, f and m indicate composite, fibres, and matrix, respectively. *k* is the slope of the linear regression line, i.e. of E_c vs. V_f and UTS_c vs. V_f. Effective fibre stiffness (E_f) and tensile strength (UTS_{fu}) can thus be calculated from Eqs.2 −3 at $V_f = 1.0$ by linear extrapolation.

Results

Chemical composition of field retted and P. radiata Cel 26 retted fibres

Table 1 shows the changes in chemical composition of the hemp fibres after field - and *P. radiata* Cel 26 retting. A reduction in galacturonan, arabinan, and xylan content was noted with increasing retting duration during both treatments (Table 1). During field retting, the galacturonan content of fibres gradually decreased from 8.3% for untreated fibres, to 5.4% after 7 days, and to 3.1% after 14 days. After 20 days, no reduction in galacturonan content was found. In contrast, the galacturonan content decreased faster during retting with *P. radiata* Cel 26 and after 14 days, only 2% galacturonan remained. After 20 days of field retting arabinan and xylan contents decreased to 0.6 and 1.0%, repectively. The arabinan and xylan contents decreased similarly to 0.5 and 1.1% after 20 days of retting with *P. radiata* Cel 26.

In comparison to untreated fibres, no increase in glucan content was noted during field retting. In contrast, the relative glucan content in the hemp fibres increased after only 7 days of retting with *P. radiata* Cel 26 from 67 to 82% (Table 1). Besides these changes, a slight increase in lignin content (i.e. lignin to carbohydrate ratio), particularly during field retting was noted presumably due to a lack of lignin degrading enzymes produced by the microbial retting flora.

Establishment of microbial community during field retting

The changes in chemical composition of fibres during field retting (Table 1) were accompanied by changes in the microbial community versus time. Fig. 1 shows typical examples of the proliferation and pervasive action of fungi and bacteria on hemp fibre surfaces. In addition, gene sequencing provided identification and diversity of bacteria and fungi shown in Tables 2 and 3, respectively. Phylogenetic trees of the bacterial and fungal community evolution during field retting are shown in Fig. 2 and 3, respectively.

ESEM microscopy observation showed that neither bacteria nor fungal hyphae were present on the hemp fibre surface before field retting (Fig 1a). After 7 days of field retting fungal hyphae were abundant but very few bacteria were observed (Fig 1b). After 14 days, fungi were similarly frequent present on the hemp fibre surfaces as on fibres retted for 7 days, and bacteria were abundant and sometimes observed associated with fungal hyphae (Fig 1c). In addition, spots of local decay on the fibre surface were observed. After 20 days, a higher bacterial population was observed all over the fibre surfaces while fungal hyphae abundance was decreased (Fig 1d). In addition, severe degradation of the fibre surface was mainly observed at the locations with high bacterial colonization.

Bacterial community

16S rRNA from samples with different field retting durations was analyzed for bacterial diversity resulting in 81 sequences (Table 2). Sequences were grouped according to phylum affiliation including Chloroplast, α-ß-γ-Proteobacteria, Bacteroidetes and Firmicutes. In the unretted sample, the sequencing identified chloroplast originating from the outer part of the plant stem cells (Vergara et al 2016). From visual inspection, the green colour of chloroplast of the stems disappeared later. After 7 days retting, 14, 14, and 57% of the bacteria belonged to α-, ß-, and γ-Proteobacteria, respectively. After 20-days retting, the percentages of α- and ß- Proteobacteria were similar (19% and 16% of the bacteria) and that of γ-Proteobacteria decreased to 38%. Firmicutes bacteria were only identified after 7 days, while Bacteroidetes were identified after 14 and 20 days of retting with 8 and 25% of the bacteria, respectively.

The most frequent phylotype of bacteria was *Massilla aurea* (NR042502) between 7 and 14 days retting with 14 and 25%, respectively, decreasing to 16% after 20 days. *Rhizobium soli* (NR115996) was present at 14 – 17% of the bacteria during the whole retting period. *Pantoea agglomerans* (NR041978) was only present after 20 days of retting with 16%. The *Pseudomonas* fraction of the bacteria (including the species *argentinensis*, *rhizosphaera* and *syringae*) decreased from 28% after 7 days to 16% after 14 – 20 days. The *Shigella sonnei* part of the bacteria decreased from 29% after 7 days to 0% after 20 days. In addition minor but increasing percentages (0 → 3-10% of bacteria) were found for *Erwinia aphidicola*, *Chryseobacterium scophthalmum*, *Hymenobacter ginsengisoli*, *Hymenobacter norwichensis, Pedobacter hartonius* and *Pedobacter namyangjuensis.*

Figure 2 shows the genetic differences between the identified bacteria. It shows that few bacterial specie are present initially (7 days). It shows a more rich bacterial community after 14 days with 6 yellow lables and an even richer community after 20 days with 13 orange lables.

Fungal community

Sequences of the fungal community derived from the ITS genes corresponded to 6 genera distributed within the *Basidiomycota* phylum and to 7 genera within the *Ascomycota* phylum (Table 3). Between 0 and 7 days of retting, the fungal community was dominated by Ascomycota fungi with 74% increasing to 100% after 14 days of retting. *Ascomycota* was frequently represented by *Stemphylium globuliferum* with 18, 66 and 40% of the fungal community after 7, 14 and 20 days retting, respectively. The decrease in dominance of *S. globuliferum* after 14 days could be explained by increases in percentage of *Cladosporium uredinicola* (16 → 33%) and *Alternaria infectoria* (9 → 20%). However *C. uredinicola* dominated initially with 50% of the fungal community after 7 days. Low and decreasing percentage of *Cryptococcus* (including the species *carnescens*, *festucosus* and *victoriae*) and *Sphaerulina amelanchier* was observed with 10 and 7% of the fungal community after 0 days, respectively.

Figure 3 shows the genetic differences between the identified fungi and the extinction of Bacidiomycota after 14 days of retting, presumably as a result of faster growth of Ascomycota fungi. It also indicates that many widespread fungal specie are present initially (14 blue labels; high biodiversity) compared to 4 orange labels after 20 days represented by only *Alternaria*, *Stemphylium* and *Cladosporium*. This trend is opposite to the increasing richness of the bacterial community as illustrated in Figure 2.

Enzyme activity changes during field - and fungal retting

Figure 4 shows protein content and enzyme activities of the enzyme crude extracts from field retted and *P. radiata* Cel 26 at varied retting durations. As shown in Fig. 4a, enzyme extracts from *P. radiata* Cel 26 retted fibres had higher protein content compared to that from field retted fibres. Comparison of different enzyme activities in extracts from field - and *P. radiata* Cel 26 retted fibres, showed that field retted fibres had significantly higher glucanase activity up to 20 days. However, after 20 days, there was no difference in the glucanase activity present in both samples (Fig. 4b). High glucanase present in the extracts from field retted fibres corroborated with the chemical composition data (Table 1) and microbial community evolution during field retting (Table 2 and Table 3).

Much higher polygalacturonase activity in the extracts from *P. radiata* Cel 26 retted fibres was observed compared to that extracted from field retted fibres. Thereby the more efficient pectin degradation by fungal retting (Table 1) can be corroborated by the high polygalacturonase activity present in the enzyme extracts from *P. radiata* Cel 26 retted fibres (Fig. 4c). The highest polygalacturonase activity (0.6 U/g DM) was observed for 7 days *P. radiata* Cel 26 retted fibres. Thereafter, the activity gradually decreased to 0.1 U/g DM after 20 days.

Besides glucanase and polygalacturonase activities, galactanase, XG-specific endoglucanase, and laccase activities were determined for both field retted and *P. radiata* Cel 26 retted fibres. *P. radiata* Cel 26 retted fibres exhibited higher galactanase and XG-specific endo-glucanase activity than field retted fibres. Laccase activity was found to increase with extended *P. radiata* Cel 26 retting duration from 0.4 after 7 days to 1.0 U/g DM after 20 days, while no laccase activity was detected in the crude enzyme extracts from field retted fibres (Fig. 4f).

Mechanical properties of fibres and fibre/epoxy composites

The stiffness and UTS of the fibres are shown in Table 4. The untreated hemp fibres had stiffness of 29 GPa and UTS of 770 MPa. A decrease in fibre strength was observed with increased field retting duration to 683 MPa after 20 days (Table 4). The decrease in fibre strength with increased field retting duration can be explained by the loss of cellulose because of the presence of cellulase activities (Fig. 4b). For *P. radiata* Cel 26 retted fibres, the stiffness increased and UTS decreased slightly. After fibres were retted with *P. radiata* Cel 26 for 14 days, the stiffness and UTS of fibres were 42 GPa and 720 MPa.

All fungal retted and untreated fibres were assessed in hemp fibre/epoxy composites. In order to compare with traditional field retting, the 20-day field retted fibres were selected and also assessed in hemp fibre/epoxy composites. As shown in Fig. 5, the starting points of the ROM model lines at $V_f = 0$, showed the measured epoxy matrix stiffness (E_m) and UTS (UTS_m^*) of 2.7 GPa and 27 MPa, respectively, at the average failure strain of the composites of 1.0%. By comparison of the slopes (k) of model lines established by linear regression of E_c and UTS_c versus V_f, of composites with differently treated fibres, it can be seen that composites with *P. radiata* Cel 26 retted fibres, irrespective of retting duration, had much higher stiffness and strength than the composites with 20 days field retted fibres (Fig. 5). In addition, there were no statistical differences in neither stiffness nor strength between composites with *P. radiata* Cel 26 retted fibres and composites with untreated fibres (Fig. 5). The results are consistent with chemical composition, microbial community evolution and enzyme activity assay studies and demonstrated that *P. radiata* Cel 26 retting produced better fibres than field retting.

The effective fibre stiffness (E_f) and strength (UTS_{fu}) were established by using the ROM-model (Eqs. 2 −3). E_f was determined to be similar (65, 62, 66 and 67 GPa) for 0, 7-, 14-, and 20- days retted samples using *P. radiata* Cel 26, respectively. In contrast, 20 days field retted fibres showed that E_f was only 51 GPa. UTS_{fu} was determined to increase slightly (560, 548, 573, 587 MPa) for 0, 7-, 14-, and 20- days retted samples using *P. radiata* Cel 26, respectively. However, 20 days field retted fibres showed that UTS reduced to 470 MPa.

The porosity factors (α_{pf}) of composites with differently treated fibres were determined by Eq. (1) based on the experimental data of V_p versus V_f. In general, changes in the porosity factors indicate the variations in composite porosity. As shown in Fig. 6, composites with field retted and untreated fibres had the highest porosity factor (up to 0.16), followed by composites with *P. radiata* Cel 26 retted fibres (0.10 – 0.13). For composites made with *P. radiata* Cel 26 retted fibres, the composite porosity was found to decrease vs. the retting duration, as indicated by a decrease in the porosity factors vs. the retting duration (Fig. 7).

Discussion

Microbial community and enzyme expression

The changes in chemical composition of the hemp fibres was consistent with a previous study where field retting caused greater loss of cellulose with increased duration (Liu et al. 2015a), while fungal retting with *P. radiata* Cel 26 did not degrade the cellulose (Liu et al. 2015b). It is a strong indication for cellulase production during field retting due to the presence of wild microbial populations. Normally with these types of wild microbial populations, the bacteria associate with the fungal hyphae so that they can get access to carbohydrates released by the fungal attack of the plant cell wall. This kind of symbiosis has been proved in microbial conversion of phenolic compounds (Boonchan et al. 2000).

A similar phylum distribution of the field retting microbial community has been observed with water retting of jute (*Corchorus olitorius*) with Proteobacteria as the most abundant phylum of which γ was the main type (Munshi and Chattoo 2008). The γ-Proteobacteria was found to have ability to hydrolyze CMC and pectin owing to its cellulolytic and pectinolytic activity (Hrynkiewicz et al. 2010). The increased percentages of Bacteroidetes and α-Proteobacteria in the bacterial community with retting duration has also been observed in another study of field retting of hemp (Ribeiro et al. 2015). *Rhizobium* has been found to produce cellulase enzymes, which explains the cell wall degradation (Morales et al. 1984). The relatively abundant bacterial sequences of *Pantoea*, *Pseudomonas*, and *Massilia* have also been identified during field retting of hemp at varied durations in the previous study (Ribeiro et al. 2015). It has been found that *Massillia* species have cellulolytic activity (Hrynkiewicz et al. 2010) and *Pseudomonas* species were found to be particularly important in the decomposition of pectin in plant fibres during the process of retting, particularly under aerobic conditions (Betrabet and Bhat 1958; Rosemberg 1965).

Endophytic fungi such as *S. globuliferum* can penetrate the plant tissue while producing pectinase and cellulase enzymes (Wang and Dai 2011). *A. infectoria* has also been reported to perform

365 enzymatic hydrolysis of cellulose and hemicellulose (Silva et al. 2015). *Cladosporium* has been
366 reported to produce pectin lyase and cellulases (Brown and Sharma 1984). Presence of *Cladosporium*
367 and *Cryptococcus* genera have also been identified in field retted hemp fibres by Ribeiro et al.
368 (Ribeiro et al. 2015). *Cryptococcus* is known to produce cutinase enzymes (Masaki et al. 2005) that
369 are involved in cutin degradation in the cuticle on hemp stem surface. It can explain why
370 *Cryptococcus* dominated initially with 10% of the fungal community since cuticle is the outer and
371 most accessible layer of the hemp stem. The zero laccase activity is consistent with the lack of
372 Basidiomycota fungi in field retting. The higher Klason lignin of *P. radiata* Cel 26 retted fibres (Table
373 1) is presumably due to the lack of laccase activities (Table 3), and consistent with lack of lignolytic
374 Basidiomycotes during field retting, especially after 14 and 20 days (Table 3). These studies indicate
375 that an enzyme profile with pectin and carbohydrate degrading enzymes was produced during field
376 retting giving decay in the hemp fibre cell wall but with a weak decay on the lignin fraction. This
377 agrees with the fibre composition in Table 1.

378 *Fibre compositional changes and resulting composite properties*

379 Properties of composites depend not only on the fibre themselves but also on the degree to which an
380 applied load is transmitted to the fibres by the matrix phase under stress (Callister WD 1994). The
381 degree to which an applied load is transmitted to the fibres by matrix phase under stress largely
382 depend on the wettability of hemp fibres by matrix polymer (Gassan et al. 2000). High wettability of
383 the fibres by matrix polymer indicating improved interfaces between fibres and matrix phase, results
384 in improved interfacial shear strength (IFSS) (Li et al. 2009) and decreased composite porosity content
385 (Liu et al. 2016a; Liu et al. 2016b). The decreased composite porosity content lowers stress
386 concentrations and results in increased mechanical properties of the fibre reinforced composites
387 (Madsen et al. 2009; Liu et al. 2016c).

388 The decrease in composite porosity was primarily due to the removal of non-cellulosic components,
389 in particular the degradation of pectin and hemicellulose, and separation of cellulose fibers, improved
390 the bonding between fibres and matrix polymers (Liu et al. 2016a; Liu et al. 2016b). The fibre
391 correlated porosity factor was correlated with the galacturonan content of fibres after retting with *P.*
392 *radiata* Cel 26 at varied durations (Fig. 7). The decrease in composite porosity after retting with *P.*
393 *radiata* Cel 26 can also explain the better mechanical properties of the composites than composites
394 with field retted fibres (Fig. 5), due to the lowered effect of stress concentrations (Madsen et al. 2009).
395 Compared to composites with untreated fibres, decreased composite porosity for composites with
396 fungal retted fibres was observed (Fig. 6), but no differences between mechanical properties of the two
397 types of composites were found (Fig. 5). It indicated that some damages might also be introduced to *P.*
398 *radiata* Cel 26 retted fibres due to the presence of cellulase activity.

Overall concluding perspectives

Field retting based on natural microbial communities and *P. radiata* Cel 26 retting was assessed in hemp fibre treatment for fibre/epoxy composites use. It was found that both fungal and bacterial communities were involved in field retting. Ascomycota phylum were observed during the first 1-2 weeks of classical field retting, and thereafter, different types of bacteria, notably different Proteobacteria proliferated in field retted fibres. Field retted fibres exhibited much higher glucanase activities than *P. radiata* Cel 26 retted fibres, while the latter had higher polygalacturonase, galactanase, XG-specific endoglucanase and laccase activities. As a result, retting with *P. radiata* Cel 26 can degrade non-cellulosic components from hemp fibres at high efficiency compared to field retting. Composites with *P. radiata* Cel 26 retted hemp fibres had significantly higher stiffness and strength than composites made with field retted hemp fibres.

References

Ale MT, Barrett K, Addico GND, Knudsen NR, Johnson AAGJ, Meyer AS (2016) DNA-based identification and chemical characteristics of Hypnia musciformis from coastal sites in Ghana. Diversity 8:1–14.

Arnous A, Meyer ASS (2008) Comparison of methods for compositional characterization of grape (*Vitis vinifera* L.) and apple (*Malus domestica*) skins. Food Bioprod Process 86:79–86.

Benko Z, Siika-aho M, Viikari L, Réczey K (2008) Evaluation of the role of xyloglucanase in the enzymatic hydrolysis of lignocellulosic substrates. Enzyme Microb Technol 43:109–114.

Betrabet SM, Bhat J V (1958) Pectin decomposition by species of Pseudomonas and their role in the retting of Malvaceous plants. Appl Microbiol 6:89–93.

Boonchan S, Britz ML, Stanley GA (2000) Degradation and mineralization of high-molecular-weight polycyclic aromatic hydrocarbons by defined fungal-bacterial cocultures. Appl Environ Microbiol 66:1007–1019.

Bradford MM (1976) A rapid and sensitive method for the quantitation of microgram quantities of protein utilizing the principle of protein-dye binding. Anal Biochem 72:248–254.

Brown AE, Sharma HSS (1984) Production of polysaccharide-degrading enzymes by saprophytic fungi from glyphosate treated flax and their involvement in retting. AnnApplBiol 105:65–74.

Callister WD (1994) Materials science and engineering, 3rd edn. John Wiley & Sons, INC., New York

Cheung H, Ho M, Lau K, Cardona F, Hui D (2009) Natural fibre-reinforced composites for bioengineering and environmental engineering applications. Compos Part B Eng 40:655–663.

Faruk O, Bledzki AK, Fink HP, Sain M (2012) Biocomposites reinforced with natural fibers: 2000-2010. Prog Polym Sci 37:1552–1596.

Fernando D, Daniel G (2008) Exploring Scots pine fibre development mechanisms during TMP processing: Impact of cell wall ultrastructure (morphological and topochemical) on negative behaviour. Holzforschung 62:597–607.

Gardes M, White TJ, Fortin JA, Bruns TD, Taylor JW (1991) Identification of indigenous and introduced symbiotic fungi in ectomycorrhizae by amplification of nuclear and mitochondrial ribosomal DNA. Can J Bot 69:180–190.

Gassan J, Gutowski VS, Bledzki AK (2000) About the surface characteristics of natural fibres. Surf Eng 283:132–139.

Hrynkiewicz K, Baum C, Leinweber P (2010) Density, metabolic activity, and identity of cultivable rhizosphere bacteria on Salix viminalis in disturbed arable and landfill soils. J Plant Nutr Soil Sci 173:747–756.

Kimura M (1980) A simple method for estimating evolutionary rates of base substitutions through comparative studies of nucleotide sequences. J Mol Evol 16:111–120.

Lever M (1973) Colorimetric and fluorometric carbohydrate determination with p-hydroxybenzoic acid hydrazide. Biochem Med 7:274–281.

Li Y, Pickering KL, Farrell RL (2009) Determination of interfacial shear strength of white rot fungi treated hemp fibre reinforced polypropylene. Compos Sci Technol 69:1165–1171.

Li A, Zhu Y, Xu L, Zhu W, Tian X (2008) Comparative study on the determination of assay for laccase of Trametes sp. African J Biochem Res 2:181–183.

Liu M, Fernando D, Daniel G, Madsen B, Meyer A, Ale M, Thygesen A (2015a) Effect of harvest time and field retting duration on the chemical composition, morphology and mechanical properties of hemp fibers. Ind Crops Prod 69:29–39.

Liu M, Fernando D, Meyer AS, Madsen B, Daniel G, Thygesen A (2015b) Characterization and biological depectinization of hemp fibers originating from different stem sections. Ind Crops Prod 76:880–891.

Liu M, Meyer AS, Fernando D, Silva DAS, Geoffrey D, Thygesen A (2016a) Effect of pectin and hemicellulose removal from hemp fibres on the mechanical properties of unidirectional hemp/epoxy composites. Compos Part A Appl Sci Manuf 90:724–735.

Liu M, Silva DAS, Fernando D, Meyer AS, Madsen B, Daniel G, Thygesen A (2016b) Controlled

retting of hemp fibres: Effect of hydrothermal pre-treatment and enzymatic retting on the mechanical properties of unidirectional hemp/epoxy composites. Compos Part A Appl Sci Manuf 88:253–262.

Liu M, Thygesen A, Meyer AS, Madsen B (2016c) Modelling of volumetric composition and mechanical properties of unidirectional hemp/epoxy composites - Effect of enzymatic fibre treatment. IOP Conf Ser Mater Sci Eng 139:12–31.

Madsen B, Thygesen A, Lilholt H (2009) Plant fibre composites – porosity and stiffness. Compos Sci Technol 69:1057–1069.

Maidak BL, Cole JR, Parker CT, Garrity GM, Larsen N, Li B, Lilburn TG, McCaughey MJ, Olsen GJ, Overbeek R, Pramanik S, Schmidt TM, Tiedje JM, Woese CR (1999) A new version of the RDP (Ribosomal Database Project). Nucleic Acids Res 27:171–173.

Masaki K, Kamini NR, Ikeda H, Iefuji H (2005) Cutinase-Like Enzyme from the Yeast *Cryptococcus* sp. strain S-2 hydrolyzes polylactic acid and other biodegradable plastics. Appl Environ Microbiol 71:7548–7550.

Michalak M, Thomassen L V., Roytio H, Ouwehand AC, Meyer AS, Mikkelsen JD (2012) Expression and characterization of an endo-1,4-β-galactanase from *Emericella nidulans* in *Pichia pastoris* for enzymatic design of potentially prebiotic oligosaccharides from potato galactans. Enzyme Microb Technol 50:121–129.

Morales VM, Martinez-Molina E, Hubbell DH (1984) Cellulase production by Rhizobium. Plant Soil 80:407–415.

Munshi TK, Chattoo BB (2008) Bacterial population structure of the jute-retting environment. Microb Ecol 56:270–282.

Nyhlen L, Nilsson T (1987) Combined T.E.M. and UV-microscopy on delignification of pine wood by *Phlebia radiata* and four other white rotters. Lignin Enzym Microb Degrad 23–24:276–282.

Ribeiro A, Pochart P, Day A, Mennuni S, Bono P, Baret JL, Spadoni JL, Mangin I (2015) Microbial diversity observed during hemp retting. Appl Microbiol Biotechnol 99:4471–4484.

Rosemberg J a (1965) Bacteria responsible for the retting of Brazilian flax. Appl Microbiol 13:991–2.

Silva BMA, Prados-Rosales R, Espadas-Moreno J, Wolf JM, Luque-Garcia JL, Gonçalves T, Casadevall A (2015) Characterization of *Alternaria infectoria* extracellular vesicles. J Music Ther 52:202–210.

Sluiter A, Hames B, Ruiz R, Scarlata C, Sluiter J, Templeton D, Crocker D (2011) Determination of

492 structural carbohydrates and lignin in biomass. In: NREL Technical Report, NREL/TP-510-
493 42618

494 Srinivasan C, D'Souza T, Boominathan K, Reddy C (1995) Demostration of laccase in the white-rot
495 basidiomycete *Phanerochaete chrysosporium* BKM-F-1767. Appl Environ Microbiol 61:4274–
496 4277.

497 Sun G, Thygesen A, Meyer AS (2015) Acetate is a superior substrate for microbial fuel cell initiation
498 preceding bioethanol effluent utilization. Appl Microbiol Biotechnol 4905–4915.

499 Suwannarangsee S, Arnthong J, Eurwilaichitr L, Champreda V (2014) Production and characterization
500 of multi-polysaccharide degrading enzymes from *Aspergillus aculeatus* BCC199 for
501 saccharification of agricultural residues. J Microbiol Biotechnol 24:1427–1437.

502 Thomassen L V., Larsen DM, Mikkelsen JD, Meyer AS (2011) Definition and characterization of
503 enzymes for maximal biocatalytic solubilization of prebiotic polysaccharides from potato pulp.
504 Enzyme Microb Technol 49:289–297.

505 Thompson JD, Higgins DG, Gibson TJ (1994) Clustal W: improving the sensitivity of progressive
506 multiple sequence alignment through sequence weighting, position-specific gap penalties and
507 weight matrix choice. Nucleic Acids Res 22:4673–4680.

508 Thygesen A, Thomsen AB, Daniel G, Lilholt H (2007) Comparison of composites made from fungal
509 defibrated hemp with composites of traditional hemp yarn. Ind Crops Prod 25:147–159.

510 Vergara D, White KH, Keepers KG, Kane NC (2016) The complete chloroplast genomes of *Cannabis*
511 *sativa* and *Humulus lupulus*. Mitochondrial DNA 27:3793–3794.

512 Wang Y, Dai CC (2011) Endophytes: A potential resource for biosynthesis, biotransformation, and
513 biodegradation. Ann Microbiol 61:207–215.

514 White TJ, Bruns T, Taylor J (1990) Amplification and direct sequencing of fungal ribosomal RNA
515 Genes for phylogenetics. In: Innis MA, Gelfand DH, Sninsky JJ, White TJ (eds) PCR Protocols:
516 A Guide to Methods and Applications. Academic Press, New York, pp 315–322

517

Figure captions

Fig. 1. ESEM microscopy images showing presence of bacteria and fungi in field retted hemp after 0 (a), 7 (b), 14 (c) and 20 days (d). Scale bars: a,b, 20 μm; c,d, 10 μm.

Fig. 2. Phylogenetic tree of bacterial community present in the hemp fibre samples. The numbers show the similarity between the branches in %. α-Proteobacteria have blue branches, ß-Proteobacteria have brown branches, γ-Proteobacteria have purple branches while Bacteroidetes have green branches. Samples are sorted according to retting time (7 days = green; 14 days = yellow; 20 days = orange). Relative abundance is shown in % calculated based on the number of bacterial clones at each retting time.

Fig. 3. Phylogenetic tree of fungal community present in the hemp fibre samples. The numbers show the similarity between the branches in %. Ascomycota fungi have brown branches while Basidiomycota fungi have blue branches. Samples are sorted according to retting time (0 days = blue; 7 days = green; 14 days = yellow; 20 days = orange). Relative abundance is shown in % calculated based on the number of fungal clones at each retting time.

Fig. 4. Protein content of enzyme extracts (a), and enzyme activities of glucanase (b), polygalacturonase (c), galactanase (d), XG-specific endoglucanase (e), and laccase (f) versus retting duration (Units of enzyme activities were shown as U per g dry of matter hemp fibres).

Fig. 5. Stiffness (a) and UTS (b) of composites reinforced with untreated and treated fibres versus fibre volume (V_f) contents (*k* is slope of linear regression model lines).

Fig. 6. Porosity of composites reinforced with untreated and treated fibres versus fibre volume (V_f) content.

Fig. 7. Correlation between fibre correlated porosity factor (α_{pf}) and galacturonan content of fibres after different treatments.

542 **Table 1.** Chemical composition of hemp fibres after different treatments. Values are means
543 (standard deviation) for 3 replicates. In each column, values that do not share a letter are significantly
544 different at the 5% level.

Treatment	Retting period (days)	Amount[A] (%)						
		Glu	GalA	Gal	Ara	Xyl	Man	Lignin
Untreated	0	67.2(2.6)^{b}	8.3(0.4)^{a}	2.1(0.1)^{bc}	1.2(0.1)^{a}	1.3(0.2)^{a}	4.6(0.2)^{a}	5.3(0.2)^{b}
Field retting	7	63.9(1.0)^{b}	5.4(0.6)^{b}	2.0(0.2)^{c}	0.7(0.2)^{bc}	1.1(0.2)^{bc}	4.0(0.4)^{a}	5.3(0.9)^{ab}
	14	70.2(0.5)^{b}	3.1(0.4)^{c}	2.4(0.2)^{ab}	0.4(0.0)^{c}	0.8(0.2)^{c}	3.4(0.0)^{a}	6.1(0.9)^{ab}
	20	66.9(1.2)^{b}	3.6(0.4)^{c}	2.0(0.0)^{c}	0.6(0.1)^{bc}	1.0(0.2)^{bc}	3.9(0.2)^{a}	8.1(0.3)^{a}
Fungal retting	7	81.8(1.6)^{a}	4.2(0.2)^{c}	2.4(0.1)^{a}	0.7(0.0)^{b}	1.3(0.1)^{abc}	4.7(0.3)^{ab}	6.1(1.1)^{ab}
	14	83.4(3.8)^{a}	2.0(0.2)^{d}	2.3(0.2)^{a}	0.5(0.1)^{bc}	1.3(0.1)^{ab}	4.4(0.3)^{b}	5.3(0.1)^{b}
	20	76.7(1.5)^{a}	1.6(0.0)^{d}	2.0(0.0)^{c}	0.5(0.0)^{bc}	1.1(0.0)^{bc}	4.5(0.4)^{ab}	6.7(0.5)^{ab}

545

546 [A] Glu: glucan, GalA: galacturonan, Gal: galactan, Ara: arabinan, Xyl: xylan, Man: mannan, Lignin:
547 Klason lignin.

548

549 **Table 2.** Phylogenetic frequency and affiliation of bacteria based on the 16S rRNA gene on hemp
550 fibres retted for different time.

Phylum	Bacterial species		% of total bacterial community[1]				Accession no.[2]
	Genus	Species	Field retting time (day)				
			0	7	14	20	
α-Proteobacteria	*Rhizobium*	*soli*	0	14[1]	17[2]	16[5]	NR115996 (99%)
	Sphingomonas	*aerolata*	0	0	8[1]	3[1]	NR042130 (98%)
	Uncultured		0	0	8[1]	0	NR115822 (99%)
ß-Proteobacteria	*Massilia*	*aurea*	0	14[1]	25[3]	16[5]	NR042502 (99%)
γ-Proteobacteria	*Erwinia*	*aphidicola*	0	0	8[1]	3[1]	NR104724 (99%)
	Pantoea	*agglomerans*	0	0	0	16[5]	NR041978 (99%)
		brenneri	0	0	0	3[1]	NR116748 (99%)
	Pseudomonas	*argentinensis*	0	14[1]	0	10[3]	NR043115 (97%)
		rhizosphaera	0	14[1]	8[1]	3[1]	NR029063 (99%)
		syringae	0	0	8[1]	3[1]	NR074597 (99%)
	Shigella	*sonnei*	0	29[2]	8[1]	0	NR074894 (97%)
Bacteroidetes	*Chryseobacterium*	*scophthalmum*	0	0	0	6[2]	NR025386 (99%)
	Hymenobacter	*ginsengisoli*	0	0	0	3[1]	NR108904 (99%)
		norwichensis	0	0	0	10[3]	NR042172 (99%)
	Pedobacter	*hartonius*	0	0	8[1]	3[1]	NR104917 (97%)
		namyangjuensis	0	0	0	3[1]	NR113980 (99%)
Firmicutes	*Paenibacillus*	*hordei*	0	14[1]	0	0	NR109318 (99%)
Totals % [no. clones]			0[0]	100[7]	100[12]	100[31]	

551 [1] Percentage based on total number of sequences for each retting period. Bracket is the number of
552 clones identified.

553 [2] Similarity between identified sequence and published sequence.

554 [3] Reference: Vergara et al. 2015

555

556

557

558

559 **Table 3.** Phylogenetic frequency and affiliation of fungi based on the ITS gene from hemp fibres
560 retted at different time.

561

Phylum	Fungal species		% of fungal community[1]				Accession no.[2]
	Genus	Species	Field retting time (day)				
			0	7	14	20	
Ascomycota	*Alternaria*	*brassicae*	0 [0]	4 [1]	0 [0]	3 [1]	KM396418.1 (92-100%)
		infectoria	2 [1]	7 [2]	9 [3]	20 [6]	KC254057.1 (95-100%)
	Cladosporium	*antarcticum*	7 [3]	0 [0]	0 [0]	0 [0]	NR121332.1 (99-100%)
		macrocarpum	9 [4]	0 [0]	0 [0]	3 [1]	KC311478.1 (96-100%)
		uredinicola	21 [9]	50 [14]	16 [5]	33[10]	KP216999.1 (100%)
	Gibellulopsis	*nigrescens*	0 [0]	0 [0]	3 [1]	0 [0]	HE972037 (99%)
	Leptospora	*rubella*	2 [1]	0 [0]	0 [0]	0 [0]	HE774478.1 (95%)
	Pleospora	*herbarum*	0 [0]	0 [0]	3 [1]	0 [0]	KM272370.1 (93%)
	Sphaerulina	*amelanchier*	7 [3]	0 [0]	0 [0]	0 [0]	KF251596.1 (99%)
	Stemphylium	*globuliferum*	26 [11]	18 [5]	66 [21]	40[12]	KF479193.1 (94-99%)
Basidiomycota	*Bulleromyces*	*albus*	2 [1]	4 [1]	0 [0]	0 [0]	KC455879.1 (99%)
	Cryptococcus	*carnescens*	5 [2]	0 [0]	0 [0]	0 [0]	JX188120.1 (99-100%)
		festucosus	0 [0]	4 [1]	0 [0]	0 [0]	FR717832.1 (98%)
		victoriae	5 [2]	11 [3]	0 [0]	0 [0]	KM376379.1 (99-100%)
	Dioszegia	*hungarica*	2 [1]	0 [0]	0 [0]	0 [0]	EU286794.1 (99%)
	Entyloma	*microsporum*	2 [1]	0 [0]	0 [0]	0 [0]	KC311478.1 (94%)
	Rhodotorula	*aurantiaca*	2 [1]	0 [0]	0 [0]	0 [0]	AB093528.1 (99%)
	Sporobolomyces	*coprosmae*	7 [3]	4 [1]	0 [0]	0 [0]	AM160645.1 (99-100%)
Totals % [no. clones]			100 [43]	100 [28]	100 [32]	100 [30]	

562

563 [1] Percentage based on total number of sequences for each retting period. Bracket is the number of
564 clones identified.

565 [2] Similarity between identified sequence and published sequence.

566

567 **Table 4.** Mechanical properties of hemp fibres after different treatments. Values are means
568 (standard deviation) for 3 replicates. In each column, values that do not share a letter are significantly
569 different at the 5% level.

Treatment	Retting period (days)	Stiffness (GPa)	UTS (MPa)	Strain (%)
Untreated	/	29(5)^{bc}	770(100)^{a}	5.1(1.0)^{a}
Field retting	7	33(5)^{b}	832(198)^{a}	4.7(1.8)^{a}
	14	31(5)^{bc}	697(135)^{a}	4.5(1.5)^{ab}
	20	28(5)^{bc}	683(107)^{b}	4.5(1.2)^{ab}
Fungal retting	7	27(5)^{c}	707(130)^{a}	3.6(0.9)^{bc}
	14	42(5)^{a}	720(150)^{a}	2.3(0.5)^{cd}
	20	31(7)^{bc}	714(145)^{a}	3.1(0.8)^{d}

570
571

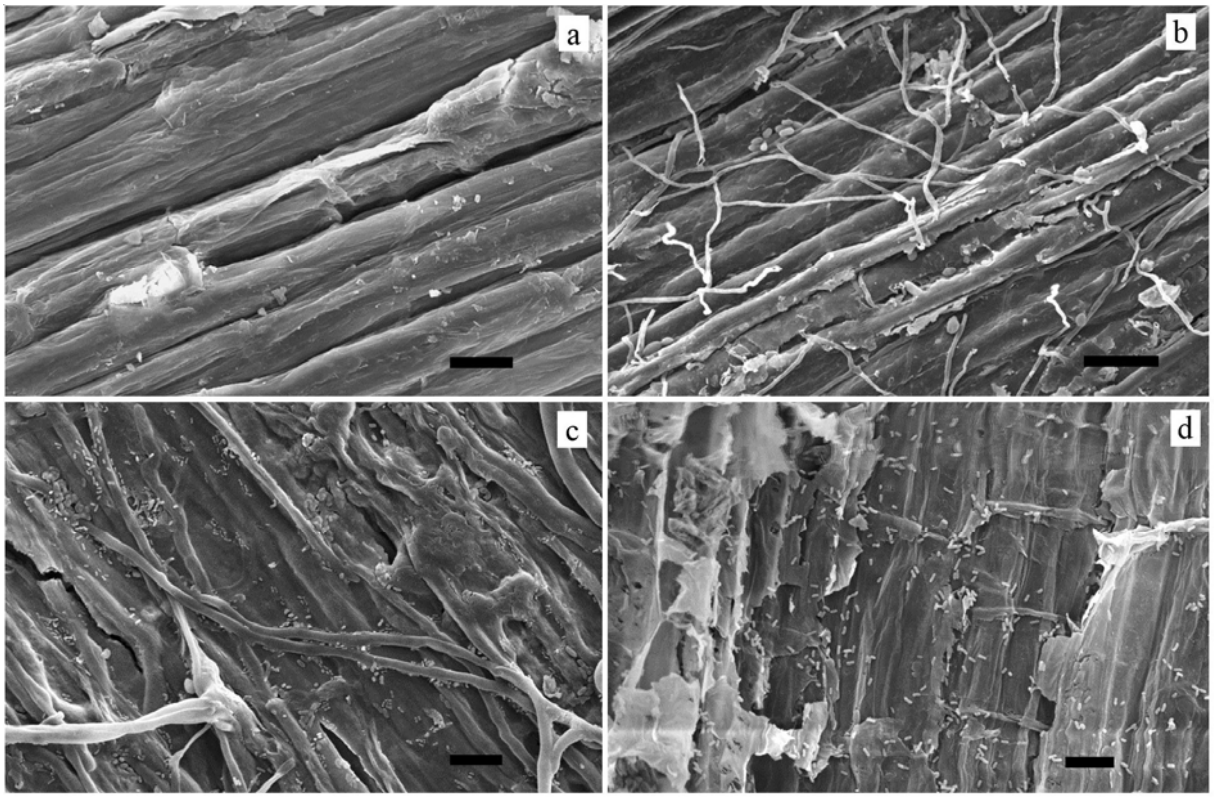

Fig.1.

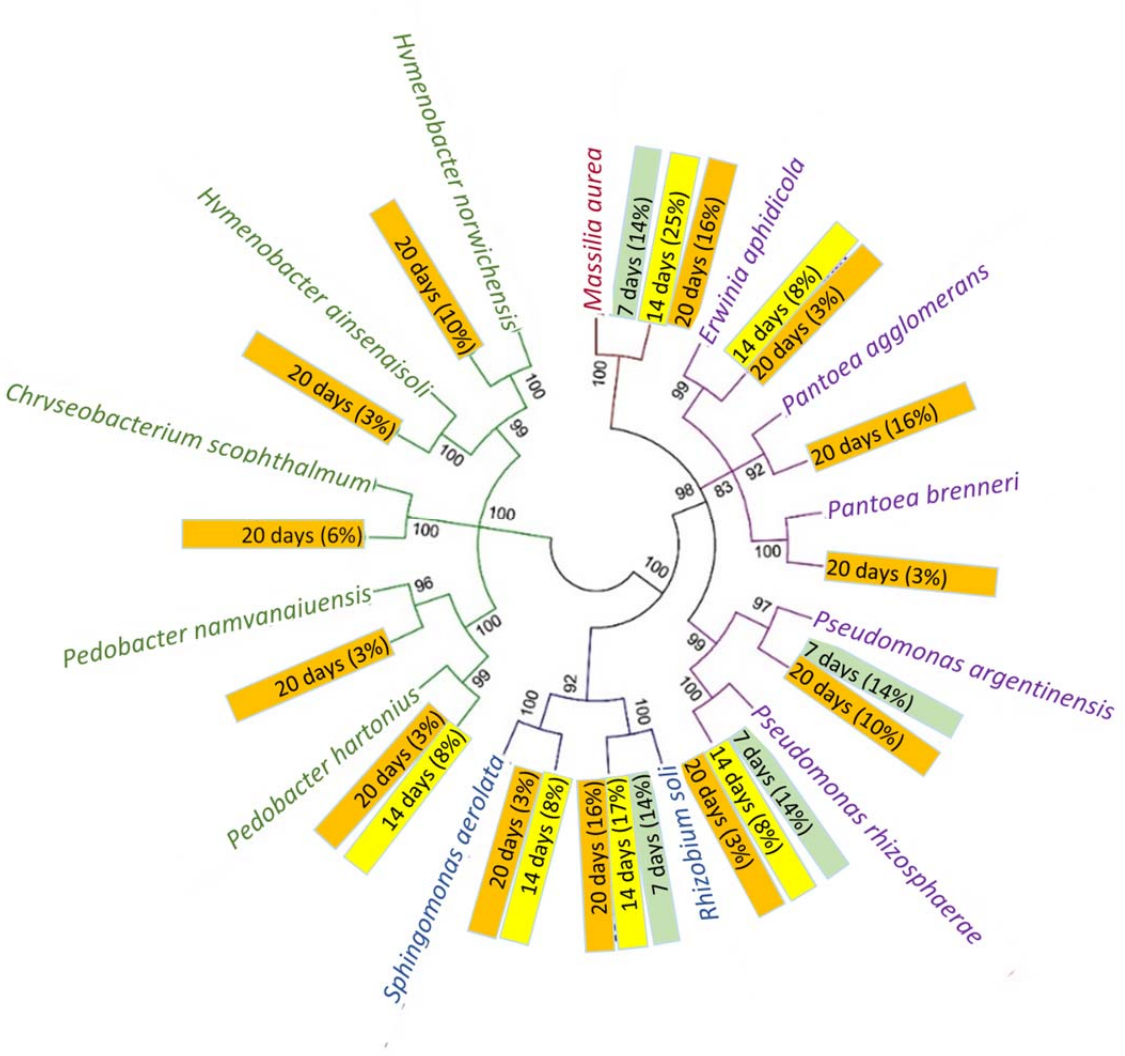

575

576 **Fig.2.**

577

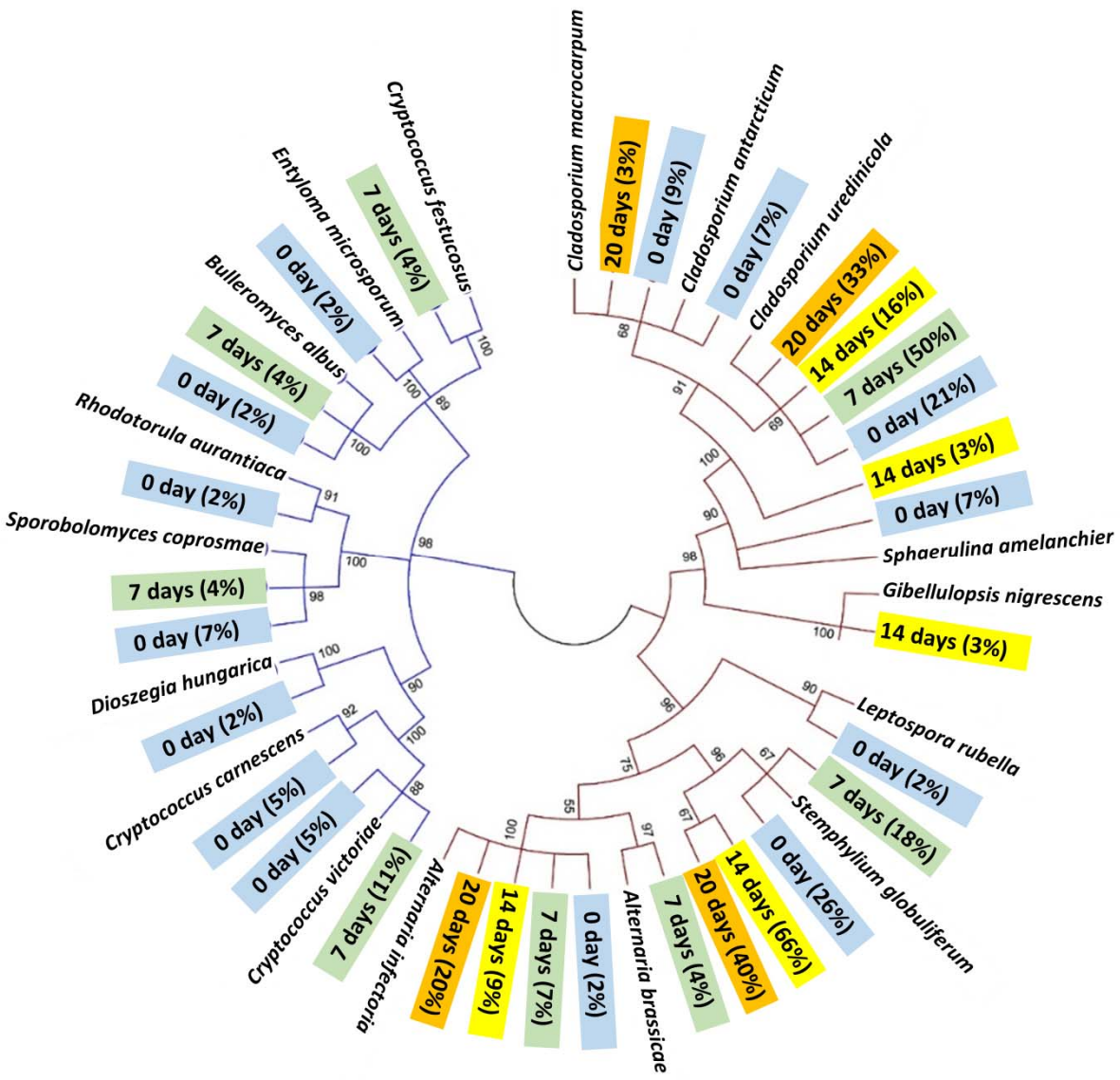

578

579 **Fig.3.**

580

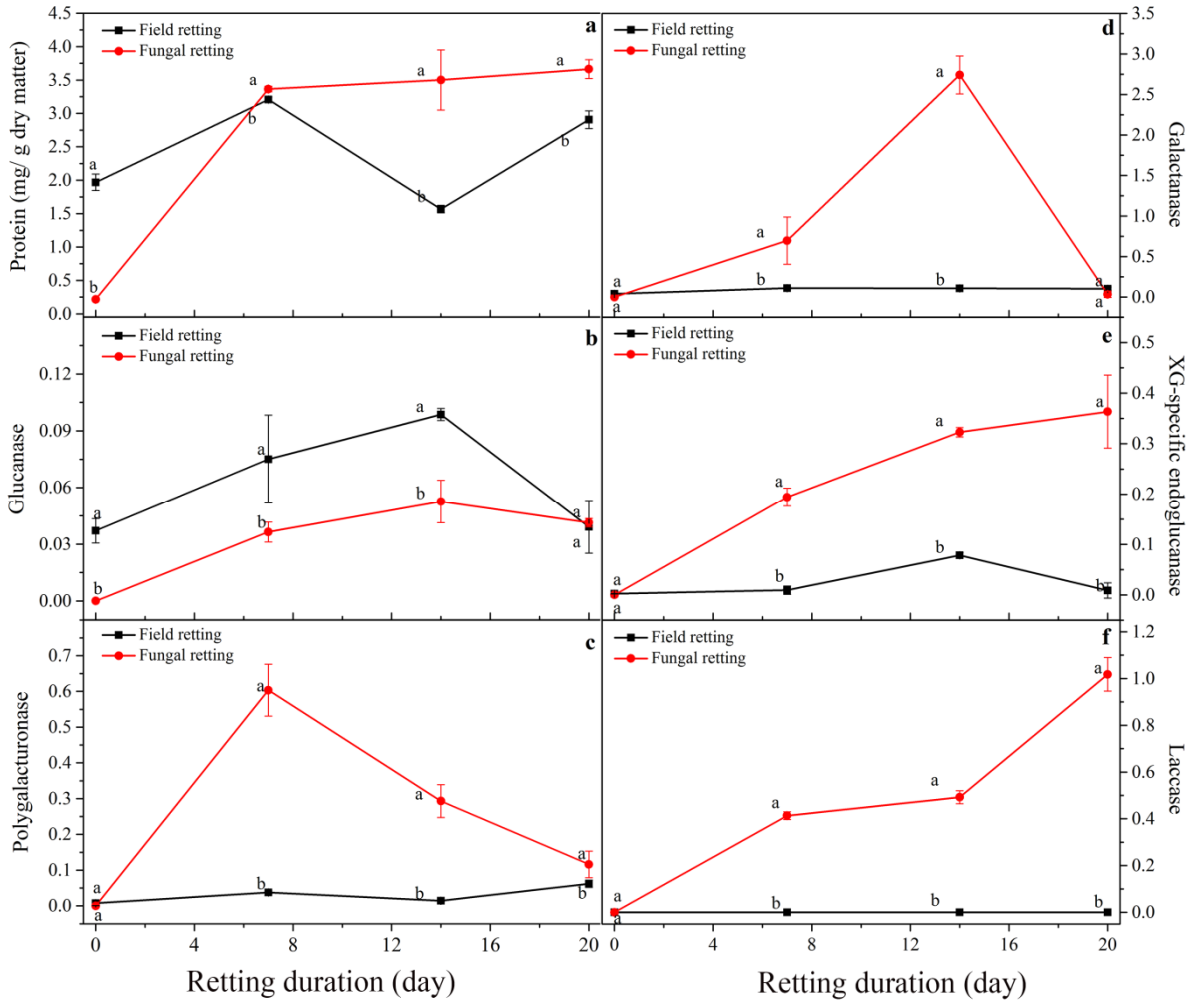
Field retting
Fungal retting
a
b
c
d
e
f
Protein (mg/ g dry matter)
Glucanase
Polygalacturonase
Galactanase
XG-specific endoglucanase
Laccase
Retting duration (day)
Retting duration (day)

Fig.4.

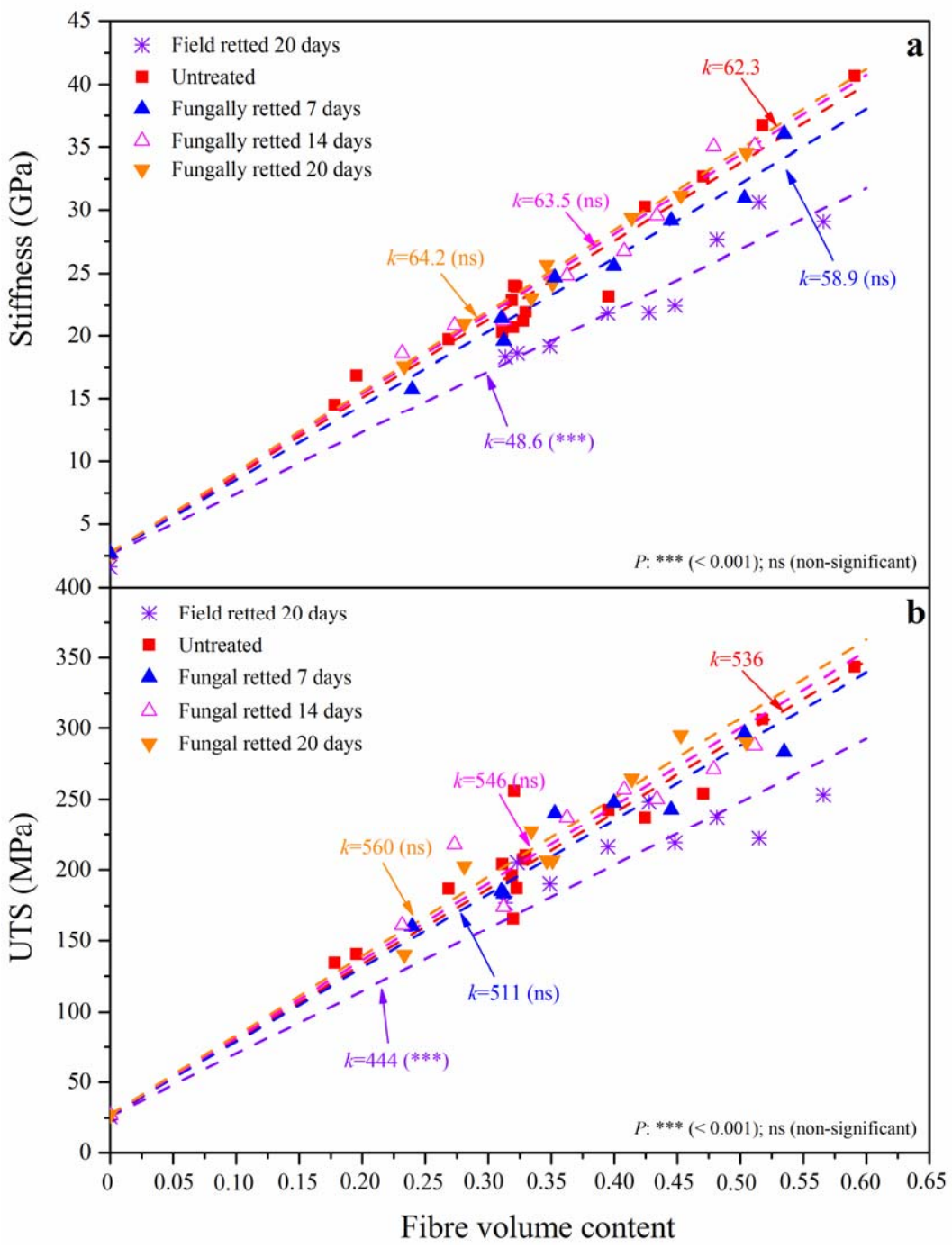

584

585 **Fig.5.**

586

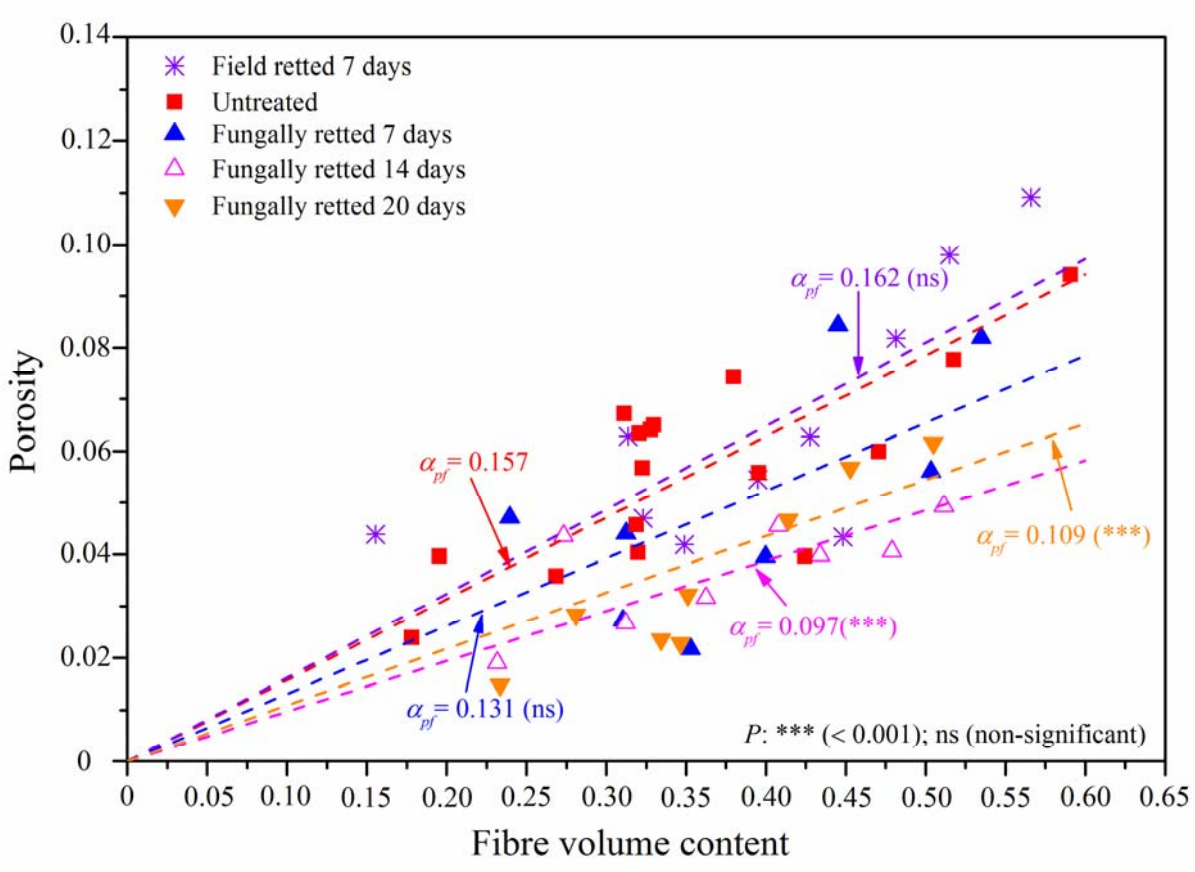

587

588 **Fig.6.**

589

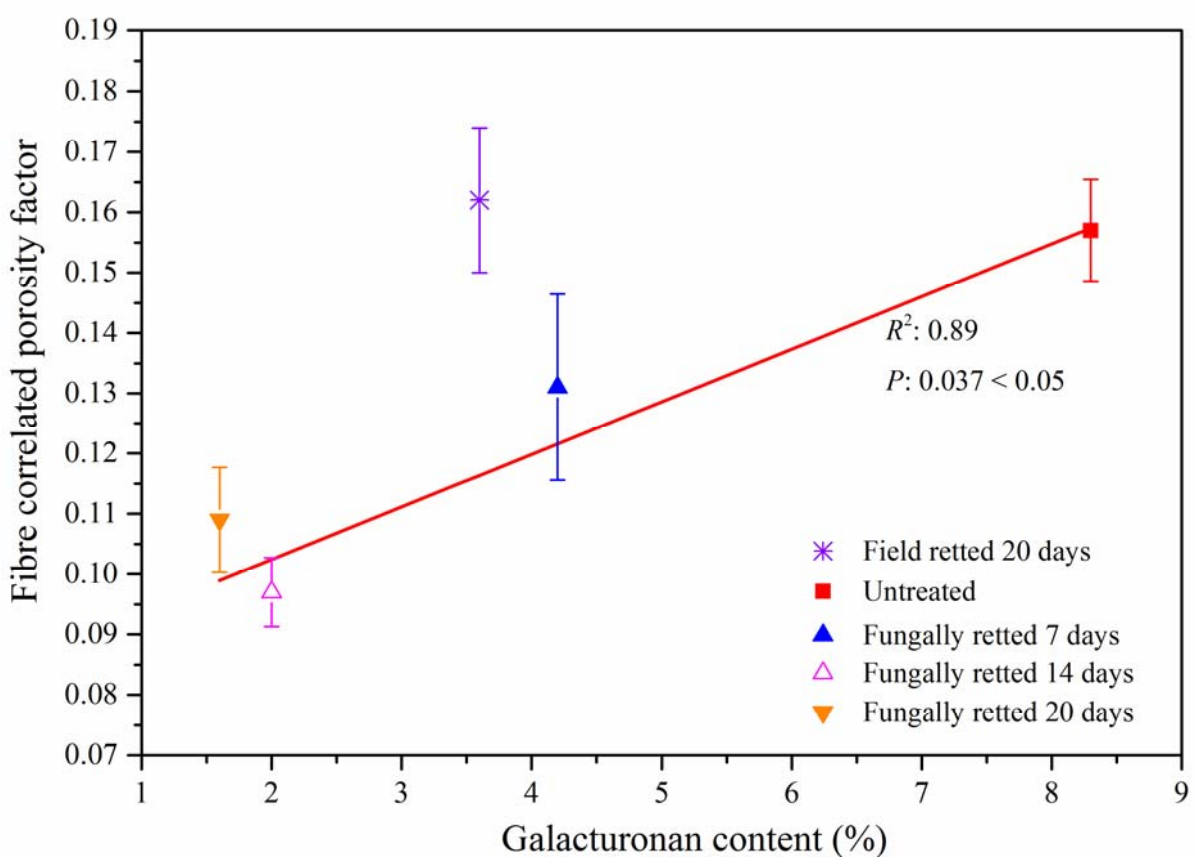

590

591 **Fig.7.**

592

593

Paper IV

Ming Liu, Diogo Alexandre Santos Silva, Dinesh Fernando, Anne S. Meyer, Bo Madsen, Geffrey Daniel, & Anders Thygesen

Controlled retting of hemp fibers: Effect of hydrothermal pre-treatment and enzymatic retting on the mechanical properties of unidirectional hemp/epoxy composites

Composites Part A: Applied Science and Manufacturing, 2016, 88, 253-262

Composites: Part A 88 (2016) 253–262

Contents lists available at ScienceDirect

Composites: Part A

journal homepage: www.elsevier.com/locate/compositesa

Controlled retting of hemp fibres: Effect of hydrothermal pre-treatment and enzymatic retting on the mechanical properties of unidirectional hemp/epoxy composites

Ming Liu [a], Diogo Alexandre Santos Silva [a], Dinesh Fernando [b], Anne S. Meyer [a], Bo Madsen [c], Geoffrey Daniel [b], Anders Thygesen [a,*]

[a] Center for BioProcess Engineering, Department of Chemical and Biochemical Engineering, Technical University of Denmark, Building 229, 2800 Kgs. Lyngby, Denmark
[b] Department of Forest Products/Wood Science, Swedish University of Agricultural Sciences, Vallvägen 9D, 750-07 Uppsala, Sweden
[c] Section of Composites and Materials Mechanics, Department of Wind Energy, Technical University of Denmark, Frederiksborgvej 399, 4000 Roskilde, Denmark

ARTICLE INFO

Article history:
Received 24 March 2016
Received in revised form 2 June 2016
Accepted 4 June 2016
Available online 6 June 2016

Keywords:
A. Natural fibres
A. Polymer-matrix composites (PMCs)
B. Mechanical properties
B. Porosity

ABSTRACT

The objective of this work was to investigate the use of hydrothermal pre-treatment and enzymatic retting to remove non-cellulosic compounds and thus improve the mechanical properties of hemp fibre/epoxy composites. Hydrothermal pre-treatment at 100 kPa and 121 °C combined with enzymatic retting produced fibres with the highest ultimate tensile strength (UTS) of 780 MPa. Compared to untreated fibres, this combined treatment exhibited a positive effect on the mechanical properties of hemp fibre/epoxy composites, resulting in high quality composites with low porosity factor (α_{pf}) of 0.08. Traditional field retting produced composites with the poorest mechanical properties and the highest α_{pf} of 0.16. Hydrothermal pretreatment at 100 kPa and subsequent enzymatic retting resulted in hemp fibre composites with the highest UTS of 325 MPa, and stiffness of 38 GPa with 50% fibre volume content, which was 31% and 41% higher, respectively, compared to field retted fibres.

1. Introduction

As a result of increasing environmental awareness, the use of sustainable, renewable and environmentally friendly materials is currently gaining interest. The development of natural cellulosic fibres to replace synthetic materials in composites is an important example of sustainable materials application. Compared with synthetic materials (e.g. glass fibre and polyepoxides), cellulosic fibres have many advantages such as low cost, low density with high tensile strength (300–1200 MPa) and high stiffness (30–70 GPa) [1,2]. However, natural cellulosic fibres also have some inherent disadvantages, including large variability in their mechanical properties resulting from biological variation and processing technology effects [2]. Most importantly, they are accompanied by non-cellulosic components when produced naturally in plants and these non-cellulosic components must be at least partially removed to obtain cellulosic fibres for impregnation in composites.

Hemp is a fast growing crop, producing higher cellulosic fibre yields than other non-wood plant sources, i.e. cotton and flax. The most suitable hemp fibres for composites are the primary fibres, which are situated in the cortex of the hemp stems. The primary fibres mainly consist of cellulose and are encased in fibre bundles with each individual fibre surrounded by middle lamellae (ML) composed of pectin and lignin [3]. When hemp stems are viewed cross-sectionally, the fibre bundles made up of the primary fibres form a fibre layer inside the cortex. The principle for fibre processing is to remove the lignin and pectin from the ML to obtain cellulose rich fibres, without decreasing the mechanical properties of the fibres.

Traditional fibre extraction methods include field retting and water retting. These treatments remove pectin via spontaneous flourishing (uncontrolled) microbial activity to produce cellulose rich fibres. Field retting is subject to weather conditions (esp. rainfall and temperature) and may result in scattered fibre mechanical properties and over retting can damage the fibres [3]. Water retting has also drawbacks with negative environmental impact such as water pollution. Enzyme retting, involving treatment mainly with pectinolytic enzymes, offers an alternative method, and may be more controlled in addition to overcoming the limitations of traditional methods with respect to time, efficiency and environmental impact.

* Corresponding author.
E-mail address: athy@kt.dtu.dk (A. Thygesen).

http://dx.doi.org/10.1016/j.compositesa.2016.06.003
1359-835X/

Targeted enzymatic removal of pectin from untreated hemp bast fibres has previously been found to improve the coherence between fibres and matrix, producing positive effects on randomly orientated hemp fibre/polypropylene composites [4,5]. Direct treatment of hemp stems with commercial enzyme mixtures, usually consisting of pectinases, hemicellulases and cellulases, has been examined for accomplishing controlled fibre retting. However, it appears that enzymes alone cannot penetrate the hemp stems to degrade pectins efficiently [6]. The accessibility of the substrate surface to enzymes is of prime importance in enzymatic treatments involving insoluble substrates. Pre-treatment of hemp fibres prior to enzymatic retting is thus essential to achieve good retting results.

Hydrothermal pre-treatment of hemp stems prior to enzymatic retting is more environmentally friendly than combining enzymes and ethylenediamine-tetra-acetic acid (EDTA), as water is the only reagent used in the process. Hydrothermal pre-treatment is a well-known pre-treatment method in biorefining schemes, including 2nd generation bioethanol production, where hydrothermal pre-treatment (Temperature = 170–200 °C, Vapor pressure = 1000–1600 kPa) is typically applied to obtain high cellulose convertibility in the subsequent enzymatic treatment with cellulase enzymes [7,8].

The scope of the study was to assess whether the mild hydrothermal pre-treatment of hemp stems would impart better enzymatic pectin removal from hemp fibres, to produce cellulose rich fibres with improved mechanical properties for unidirectional fibre/epoxy composites.

2. Materials and methods

2.1. Raw material and processing

2.1.1. Plant material

Hemp (*Cannabis sativa* L.), variety USO-31, was sown in France (N 48.8526°, E 3.0190° (WGS84)) as described in detail by Liu et al. [3] and supplied by the companies Planète Chanvre and Bafa Neu GmbH. The whole hemp stem under the inflorescence base was used as the starting material in the study. Hemp stem pieces with a length of approx. 15 cm were randomly collected from the chopped stems. Before treatment, the stem pieces were gently rinsed with warm water (40 °C) to remove dirt and then they were dried at 50 °C for 12 h. In order to compare the treatments with traditional field retting, field retting was carried out on the whole stems for 20 days after harvest [2].

2.1.2. Hydrothermal pre-treatment

Hydrothermal pre-treatment was carried out on the dried hemp stem pieces in 1 dm^3 Erlenmeyer flasks (100 cm^3 water and 15 g stems in each flask) at three different water vapour pressures (above the atmospheric pressure of 101.3 kPa) (50 kPa at 112 °C; 100 kPa at 121 °C; 200 kPa at 134 °C) for 30 min in an autoclave (LaM-4-20-MCS-J, SANOclav GmbH, Germany). In order to determine the mass loss of fibres during the hydrothermal pre-treatment, for each replicate, 6 g of bast fibres peeled from untreated hemp stems were hydrothermally treated at the same conditions as the hemp stems. A control (untreated sample) was performed at room temperature. After the hydrothermal pre-treatment, the hydrolysates were collected and filtered with a 0.22 μm syringe filter. When the filtered hydrolysates were cooled to room temperature, pH value was measured. Bast fibre strips were then manually peeled from the stems and thoroughly rinsed with warm water (40 °C). Afterwards, the fibres were dried at 50 °C for 12 h. The severity of the hydrothermal treatment was quantified by the P-factor (P), a parameter quantifying the combined effect of time and temperature, which can be calculated using Eq. (1) [9].

$$P = \int_0^t e^{40.48 - \frac{15{,}106}{T}}\, dt \quad (1)$$

where t is duration of the hydrothermal treatment in h, T is temperature in K, and 40.48 and 15,106 are constants derived from an activation energy on 125.6 kJ mol^{-1} for the fast-reacting xylan from *Eucalyptus saligna* [9].

2.1.3. Enzymatic retting

After hydrothermal pre-treatment, enzymatic retting was performed on the dried bast fibre strips for 0, 30, 90, 150, 240 and 300 min at a pH of 6.0 using a 25 mmol dm^{-3} citrate buffer, a temperature of 40 °C, and an agitation of 100 rpm. Monoactive recombinant *endo*-polygalacturonase and pectin lyase were applied at dosages of 0.2% and 0.1% (g protein per g dry matter), respectively. *endo*-polygalacturonase (EC 3.2.1.15) from *Emericella nidulans* was produced by fermentation of a *Pichia pastoris* clone transformed (principally as described previously [11,12]) with the gene AN4372.2 from the Fungal Genetic Stock Center, Kansas State University, USA [10]. Pectin lyase (EC 4.2.2.10) was produced and fermented in the same way with the gene AN2569.2 from the Fungal Genetic Stock Center, Kansas State University, USA. At the conditions applied for the enzymatic retting, the activity of *endo*-polygalacturonase and pectin lyase were 945 U cm^{-3} (17 U mg^{-1}) and 40 U cm^{-3} (3 U mg^{-1}), respectively.

At the end of the enzyme retting, the wet bast fibre strips were removed from the enzyme solution, and rinsed thoroughly with warm water (40 °C). Afterwards, the fibres were dried at 50 °C for 12 h. For all treatments, the liquid (cm^3) to fibre dry matter (g) ratio was 40:1 (4 g fibres per replicate, and in triplicate). Control treatments (without enzymes) were performed under the same conditions to determine the influence of non-enzymatic processes.

2.1.4. Manufacturing of composites

The treated bast fibre strips were manually untangled and aligned to allow the fibres to be processed into unidirectional composites. An epoxy resin (Araldite® LY 1568) and its amine hardener (Aradur® 3489) were mixed at a 100/28 mass ratio, and degassed in a vacuum oven. Fig. 1 shows a drawing of the moulding device used for manufacturing the composites. Firstly, bundles of fibre strips were cut to a length of 140 mm. The bundles were aligned in the mould chambers, and a press beam was placed on top of the fibres in each chamber (Fig. 1a). Two insert beams (fixed onto the mould) were used to fix the height of the mould chambers to 2 mm (Fig. 1b). The compaction of the fibres in the chambers by the press beams was conducted by using manual clamps. Thereafter, the entire mould was enclosed in a vacuum bag, and epoxy resin was infused into the mould chambers at room temperature (Fig. 1b). After curing for 12 h at 80 °C, the composite specimens with dimensions of 140 mm × 10 mm × 2 mm were demoulded. Tabs with lengths of 50 mm were mounted on the composite specimens using epoxy glue (DP 460) (Fig. 1c). The applied method for manufacturing composites is a modification of a method used by Martin et al. [13].

By varying the amount of fibres (m_f) in the mould chambers, the fibre weight content in the composites was varied in the range 0–0.7 (0–70% w/w). The absolute volume of the composite specimens (v_c) was calculated based on their dimensions (length, width and thickness). The density of the specimens (ρ_c) was then determined from their weight (m_c). The fibre volume content (V_f) was determined from the absolute fibre volume (v_f) using Eq. (2).

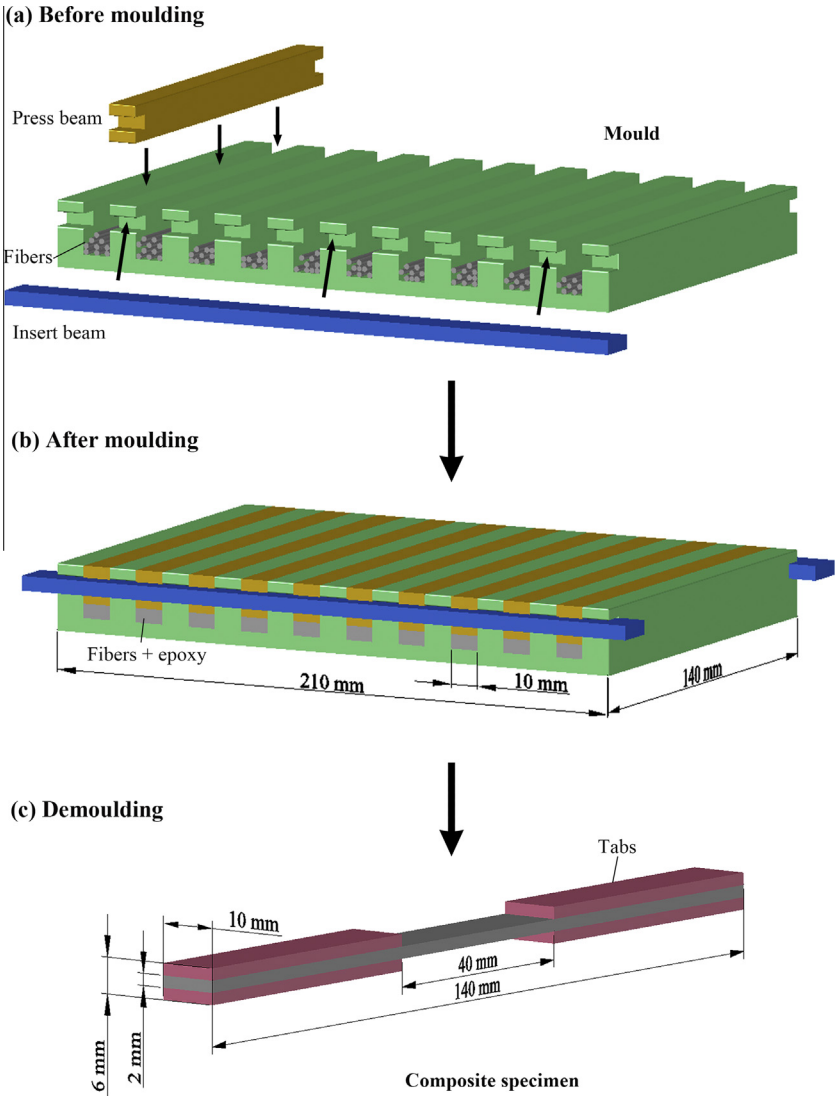

Fig. 1. Schematic drawings of the moulding tool and procedure used for manufacturing of unidirectional hemp fibre/epoxy composite specimens. (For interpretation of the references to color in this figure legend, the reader is referred to the web version of this article.)

$$V_f = \frac{v_f}{v_c} = \frac{\frac{m_f}{\rho_f}}{\frac{m_c}{\rho_c}} = \frac{m_f}{m_c} \times \frac{\rho_c}{\rho_f} \tag{2}$$

where the density of fibres was chosen as $\rho_f = 1500\ \mathrm{kg\ m^{-3}}$ [14]. The matrix volume content (V_m) was determined from the absolute matrix volume (v_m) using Eq. (3).

$$V_m = \frac{v_m}{v_c} = \frac{\frac{m_m}{\rho_m}}{\frac{m_c}{\rho_c}} = \frac{m_m}{m_c} \times \frac{\rho_c}{\rho_m} \tag{3}$$

where the density of matrix was measured to be $\rho_m = 1140\ \mathrm{kg\ m^{-3}}$. The porosity ($V_p$) was then determined using Eq. (4).

$$V_p = 1 - V_f - V_m \tag{4}$$

In the composites, the porosity V_p was assumed to be a linear function of the fibre volume content V_f, where the established proportionality constant is equal to the so-called fibre correlated porosity factor α_{pf} [15]. This is expressed in Eq. (5).

$$V_p = \alpha_{pf} \times V_f \tag{5}$$

2.2. Characterization and testing of fibres and composites

2.2.1. Mass loss of fibres

The mass loss of fibres after the treatments was calculated using Eq. (6).

$$\text{Mass loss}\ (\%) = \frac{m_0 \times w_0 - m \times w}{m_0 \times w_0} \times 100\% \tag{6}$$

where m is mass (g), w is dry matter content (%), and the subscript 0 designates the condition before the treatments. The dry matter content (w, %) was determined using a HR83 Halogen Moisture Analyser (Mettler Toledo).

2.2.2. Chemical composition of fibres

The dried bast fibres were ground with a microfine grinder (IKA, MF 10.1; IKA®-Werke GmbH) to a particle size of 1 mm. Ground samples of about 3 g were extracted in a Soxhlet apparatus (Gerhardt EV6 ALL/16 No. 10-0012) for 5 h using a 300 cm^3 solution of toluene-ethanol-acetone (4:1:1 by volume). The extractive-free fibres were dried at 50 °C for 12 h. The chemical compositions of the extractive-free fibres were analysed after acid hydrolysis by high-performance anion-exchange chromatography with pulsed amperometric detection (HPAEC-PAD), as described in details by

Liu et al. [2]. In this study, it is considered that galacturonic acid, rhamnose, galactose, and arabinose are specific to pectins, that glucose belongs to the cellulose moiety, and that xylose and mannose belong to the hemicellulose moiety.

2.2.3. Morphology of fibres

Samples with a size of 5 mm long × 2 mm wide were cut from the bast fibre strips under a stereo microscope for surface and cross sectional observations by environmental scanning electron microscopy (ESEM). The preparation of samples for microscopy followed the procedure described in detail by Fernando and Daniel [16]. Observations were performed using a Philips XL 30 ESEM operated at 10–15 kV.

2.2.4. Water retention value of fibres

The water retention value (WRV) of the fibres was determined by subjecting water-saturated samples to a centrifugal force under standard conditions using a 15 mm diameter centrifuge tube with a special spacer and diameter of 1 mm drainage hole at the bottom [17]. WRV is defined as the mass ratio of water retained in a sample after centrifugation to the dry mass of the sample. Measurements were performed for each treatment in triplicate (0.5 g dry fibres per replicate).

2.2.5. Tensile properties of fibres

Bast fibre strips (60 mm long × 1 mm wide) with masses in the range of 5–20 mg were used for tensile testing. Tabs were glued at the end of each fibre strip using epoxy resin (DP 100) to have a controlled gauge length. The preparation of specimens has been described in detail by Liu et al. [3]. Tensile testing was done using an Instron Testing Machine 2710-203 equipped with a 1 kN load cell. The gauge length was 10 mm, and the displacement rate was 0.5 mm min^{-1} (corresponding to a strain rate of 5% min^{-1}). Tensile tests were carried out on 20 specimens for each treatment. The cross-sectional area (A_f) of the fibre strips was determined using Eq. (7).

$$A_f = \frac{m_f}{\rho_f \times l_f} \tag{7}$$

where l_f is the length of the fibre strip specimens. Based on the measured stress-strain curves, stiffness (linear regression in the strain interval 0.05–0.25%), ultimate tensile strength (UTS), and failure strain were determined.

2.2.6. Tensile properties of composites

For tensile testing of the composite specimens, an Instron Testing Machine 5566 with a load cell of 10 kN was used. Two extensometers were used for strain measurements at a displacement rate of 1 mm min^{-1} (corresponding to a strain rate of 2.5% min^{-1}). Based on the measured stress-strain curves, stiffness (linear regression in the strain interval 0.05–0.25%) (E_c) and strength (UTS_c) were determined. For each treatment, at least 10 specimens with varied fibre content were tested. The rule of mixtures (ROM) model was used to determine the effective fibre stiffness (E_f) and fibre UTS (UTS_f) or σ_f in the composites by linear regression versus V_f using Eqs. (8) and (9), respectively [15], where the intercept was set equal to the measured matrix stiffness (E_m) and UTS_m at the average failure strain of the composites. Eqs. (4) and (5) were used to include V_p in the calculation of V_m.

$$\begin{aligned} E_c &= V_f E_f + V_m E_m \\ &= E_m + V_f(E_f - E_m(1+\alpha_{pf})) \\ &= E_m + V_f k \end{aligned} \tag{8}$$

$$\begin{aligned} UTS_c &= V_f UTS_f + V_m UTS_m \\ &= UTS_m + V_f(UTS_f - UTS_m(1+\alpha_{pf})) \\ &= UTS_m + V_f k \end{aligned} \tag{9}$$

where the subscripts c, f and m indicate composite, fibres (effective), and matrix, respectively. k is the slope of the linear regression line, i.e. of E_c vs. V_f and UTS_c vs. V_f.

3. Results and discussion

3.1. Hydrothermal pre-treatment

3.1.1. Mass loss and chemical composition

Compared with the untreated samples, mass loss (%) of hemp fibres during hydrothermal pre-treatment increased significantly with treatment severity indicated as water vapour pressure above the atmospheric pressure of 101.3 kPa (also mentioned as operating pressure) from 3% at 50 kPa, 4% at 100 kPa to 6% at 200 kPa (Table 1). The data confirmed that as the operating pressure increased from 50 to 200 kPa, pre-treatment became harsher (indicated by the corresponding P-factor in Table 1 increasing from 1.8 to 14.7 h), which in itself increased removal of polysaccharides from hemp fibres. A significant decrease in galacturonan content in the pre-treated hemp fibres was observed with increasing pre-treatment severity, from 8% for the untreated fibres to 6% at 50 kPa, 5% at 100 kPa and 4% at 200 kPa (Table 2).

In addition, a reduction in arabinan, galactan, xylan and Klason lignin was noted with increasing pre-treatment severity (Table 2). A gradual decrease in pH of the hydrolysates was noted with increased pre-treatment severity (Table 1) from 6.0 at 50 kPa, 5.8 at 100 kPa, to 5.2 at 200 kPa. Acetic acid can be liberated from the plant acetylated polysaccharides and galacturonic acid released from pectins at elevated temperatures, which may result in a decrease in the pH of the hydrolysates [18]. No or negligible removal of cellulose (indicated by glucan content) was observed after the hydrothermal treatment (Table 2). Overall, changes in the chemical compositions of the fibres during hydrothermal treatment mainly involved monomers of pectin at all the investigated conditions.

3.1.2. Morphology

ESEM micrographs of untreated and hydrothermally pre-treated hemp bast fibres showing fibre morphology changes at transverse and longitudinal surfaces are depicted in Figs. 2 and 3, respectively.

Fig. 2a shows transverse sections from untreated hemp stem samples with intact bast fibres and, native cellular structures with all the layers of epidermis and cortex (i.e. collenchyma cells, parenchyma cells and bast fibres) well organized and packed into a rigid structure. In addition, intact parenchyma cells interspersed among bast fibres and fibre bundles can clearly be seen holding fibres together as in the living plant (indicated by black arrowheads). In contrast, for the hydrothermally treated hemp samples, the epidermis was partly and/or completely gone (white double-

Table 1
Mass loss and WRV of fibres after hydrothermal pre-treatment at 50, 100 and 200 kPa. Values are means (standard deviation) for 3 replicates. Shown are also the P-factor of the treatments, and the pH of the hydrolysates. In each column, values that do not share a letter are significantly different at a level of 5%.

Hydrothermal pre-treatment	P-factor (h)	pH	Mass loss (%)	WRV (%)
Untreated	0	6.5	0.0 (0)^{c}	150 (20)^{b}
H50 kPa	1.8	6.0	2.7 (0.6)^{b}	330 (20)^{a}
H100 kPa	4.3	5.8	4.4 (1.1)^{ab}	320 (10)^{a}
H200 kPa	14.7	5.2	6.0 (0.2)^{a}	260 (10)^{a}

Table 2
Chemical composition of hemp fibres after hydrothermal pre-treatment of hemp stems at different operating pressures. Values are means (standard deviation) for 3 replicates. In each column, values that do not share a letter are significantly different at a level of 5%.

Pre-treatment	Amount[A] (%)							
	Glu	GalA	Rha	Gal	Ara	Man	Xyl	Lignin
Untreated	67.2 (2.6)^{a}	8.3 (0.4)^{a}	0.7 (0.1)^{a}	2.1 (0.1)^{a}	1.2 (0.1)^{a}	4.6 (0.2)^{a}	1.3 (0.2)^{a}	5.3 (0.2)^{a}
H50 kPa	67.6 (0.4)^{a}	5.8 (0.5)^{c}	0.8 (0.0)^{a}	2.1 (0.1)^{a}	1.0 (0.2)^{ab}	4.8 (0.1)^{a}	1.1 (0.1)^{b}	5.0 (0.1)^{a}
H100 kPa	67.0 (1.3)^{a}	4.5 (0.4)^{c}	0.8 (0.0)^{a}	1.8 (0.1)^{b}	0.8 (0.1)^{b}	4.5 (0.2)^{a}	1.1 (0.1)^{b}	4.6 (0.2)^{a}
H200 kPa	71.7 (0.2)^{a}	4.0 (0.1)^{c}	0.5 (0.0)^{b}	1.7 (0.1)^{b}	0.7 (0.2)^{b}	4.5 (0.1)^{a}	1.1 (0.2)^{b}	4.4 (0.2)^{a}

[A] Glu – glucan, GalA – galacturonan, Rha – rhamnan, Gal – galactan, Ara – arabinan, Man – mannan, Xyl – xylan, Lignin – Klason lignin.

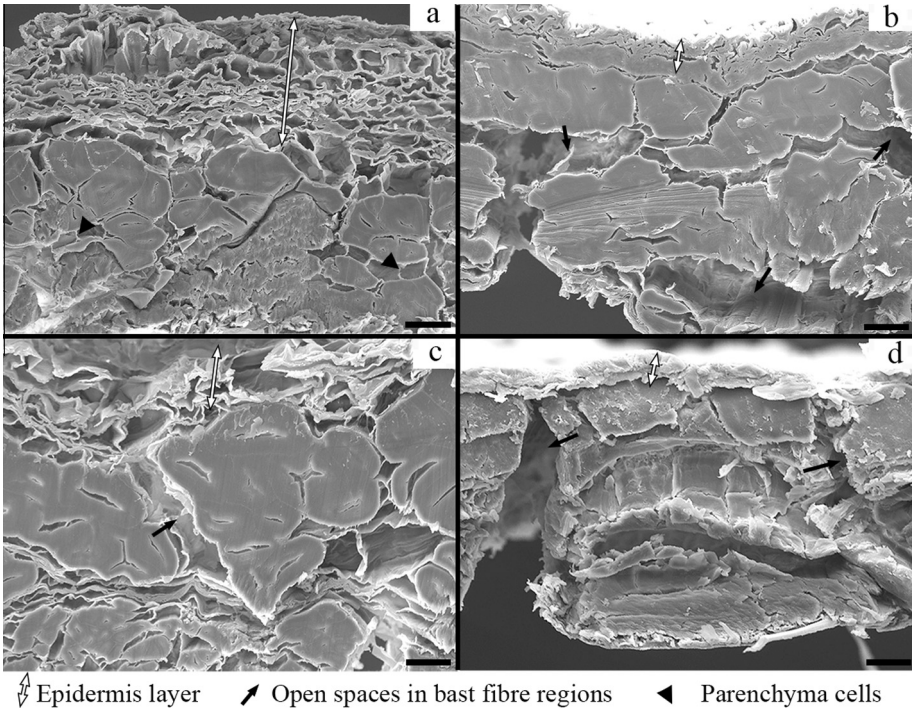

Fig. 2. ESEM micrographs showing cross sections of hemp bast fibre strip: (a) untreated, and after hydrothermal pre-treatments at (b) 50 kPa, (c) 100 kPa, and (d) 200 kPa. Scale bar length = 25 μm.

head arrows in Fig. 2b–d) and the bast regions (e.g. epidermis, cortex and cambium) were opened up considerably (black arrows). Opening of the bast regions was caused by changes to the cellular structure, where disintegration of cells/tissues appeared to increase with pre-treatment severity. Those changes in cellular structure led to adjacent layers separating with intact native fibre bundles.

Fig. 3 reveals significant physical microstructural changes to the fibre surface during hydrothermal treatment. For untreated samples, fibre surfaces were fully covered with parenchyma cells/cell residues (black arrowheads in Fig. 3a) with no or few voids between fibres and/or fibre bundles. In contrast, hemp fibres hydrothermally treated at 50 kPa (Fig. 3d) were covered with parenchyma cells that were partially broken down leading to the formation of agglomerates (white arrows). The agglomerates gave the appearance of impurities over the fibre surfaces (Fig. 3d).

In contrast to the samples treated at 50 kPa, fewer parenchyma cell residues and smoother fibre surfaces were observed for samples treated at 100 kPa (Fig. 3g). The fibres treated at 200 kPa (Fig. 3j) had very smooth and clean surfaces, with almost no impurities. In general, the changes in hemp fibre morphology and chemical structure during hydrothermal treatment may be attributed to thermal softening of cell wall polymers, leading to loosening/weakening and subsequent degradation in the water saturated environment. Lignin in the outer plant cell wall is known to make strong covalent cross-links with both protein and pectin, while pectin links to proteins via ionic bonds [19].

As the temperature during the hydrothermal treatments was above the glass transition temperature of in-situ lignin (the lignin-softening temperature of wood in a wet environment is ~80–100 °C) [20], lignin softening and thermal degradation of cell wall proteins and pectins presumably played a major role in loosening and breaking up the rigid cell wall structure of the hemp fibres. These structural alterations in turn presumably promoted water uptake in hemicellulose and pectins in the loosened and altered cell wall structure, leading to increased fibre swelling, observed as increasing WRVs (Table 1). A similar cascade of events has been reported for spruce fibre pulps [21]. Fibre swelling favours thermal lignin-softening [22] and this combination of events appears to have contributed to de-polymerization/decon struction and removal of chemical components from the hemp fibres.

3.1.3. Tensile properties of fibres

The mechanical properties shown in Table 3 suggest that hydrothermal pre-treatment did not negatively impact the ultimate tensile strength (UTS) of the hemp fibres until the operating pressure reached 200 kPa (134 °C), indicated by the significant

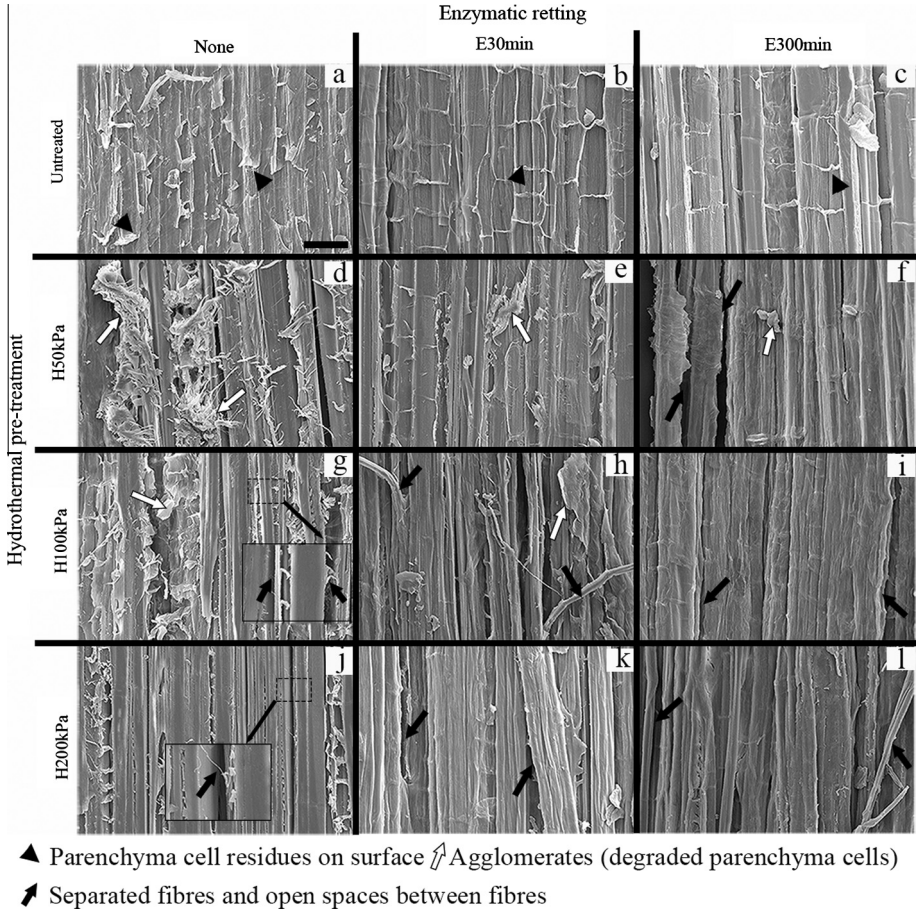

Fig. 3. ESEM micrographs showing surfaces of hemp bast fibre strips after hydrothermal pre-treatment at different operating conditions and after enzymatic retting for 30 min (E30 min) and 300 min (E300 min). Scale bar length = 50 μm.

Table 3
Mechanical properties of fibres after hydrothermal pre-treatment at different conditions and enzymatic retting for 90 min. Values are means (standard deviation) for 20 replicates. For the same hydrothermal pre-treatment, values that do not share a capital letter are significantly different at a level of 5%. For the same incubation time with enzymes during enzymatic retting, values that do not share a small letter are significantly different at a level of 5%.

Hydrothermal pre-treatment	Enzymatic retting	Stiffness (GPa)	UTS (MPa)	Failure strain (%)
Untreated	None	29 (5)$^{ab\ A}$	770 (100)$^{a\ A}$	5.1 (1.0)$^{a\ A}$
H50 kPa	None	31 (5)$^{ab\ A}$	720 (80)$^{a\ A}$	3.1 (1.0)$^{b\ A}$
H100 kPa	None	31 (6)$^{a\ B}$	690 (120)$^{ab\ A}$	2.9 (0.7)$^{b\ A}$
H200 kPa	None	28 (8)$^{b\ A}$	660 (100)$^{b\ A}$	2.9 (0.9)$^{b\ A}$
Untreated	E90 min	18 (4)$^{c\ B}$	640 (60)$^{b\ B}$	3.8 (0.9)$^{a\ B}$
H50 kPa	E90 min	29 (6)$^{b\ A}$	670 (80)$^{b\ A}$	2.9 (0.7)$^{b\ A}$
H100 kPa	E90 min	36 (5)$^{a\ A}$	780 (120)$^{a\ A}$	2.6 (0.9)$^{b\ A}$
H200 kPa	E90 min	26 (7)$^{b\ A}$	650 (220)$^{b\ A}$	3.0 (1.5)$^{b\ A}$

decrease in UTS from 770 MPa for untreated samples to 660 MPa. No significant effect of hydrothermal treatment on fibre stiffness was noticed, while a significant reduction in failure strain was found after hydrothermal treatment, irrespective of operating pressures from 5% for untreated samples to about 3% for all hydrothermally treated samples (Table 3).

These results were consistent with the morphology and structural changes during hydrothermal treatment (Figs. 2 and 3). During the hydrothermal pre-treatment, pectin and lignin were depolymerized and/or removed from the fibre structure, particularly in the ML between hemp fibres and/or fibre bundles; therefore, partial breakdown of the parenchyma holding the bast fibres was initiated. Compared to untreated fibres, the fibres became more disintegrated after hydrothermal pre-treatment. Thus, the binding between individual fibres or fibre bundles became weaker, leading to the decrease in UTS and failure strain (Table 3).

3.2. The effect of hydrothermal pre-treatment on subsequent enzymatic retting

3.2.1. Mass loss and chemical composition

After hydrothermal pre-treatment, retting with pectinolytic enzymes was conducted. As shown in Fig. 4a, the mass loss of the hydrothermally treated samples during enzymatic retting was significantly higher than that of untreated samples at a given incubation time. Mass loss during enzymatic retting was also found to increase with operating pressure of the hydrothermal pre-treatment. No significant difference in the mass loss between the samples that were hydrothermally pre-treated at 100 and 200 kPa was observed until enzymatic retting time reached 240 min. At 300 min, there was no apparent difference in mass loss between the samples pre-treated at 50 and 100 kPa.

Hemp fibres hydrothermally pre-treated at 100 and 200 kPa showed significantly lower ($P < 0.05$) galacturonan contents in comparison with untreated samples at all investigated enzymatic retting incubation durations (Fig. 4b). The most intensive reduction of galacturonan content in the hemp fibres occurred during the initial 30 min of enzymatic retting (indicated by the slope of the curves). Thereafter a slight decrease in galacturonan content was

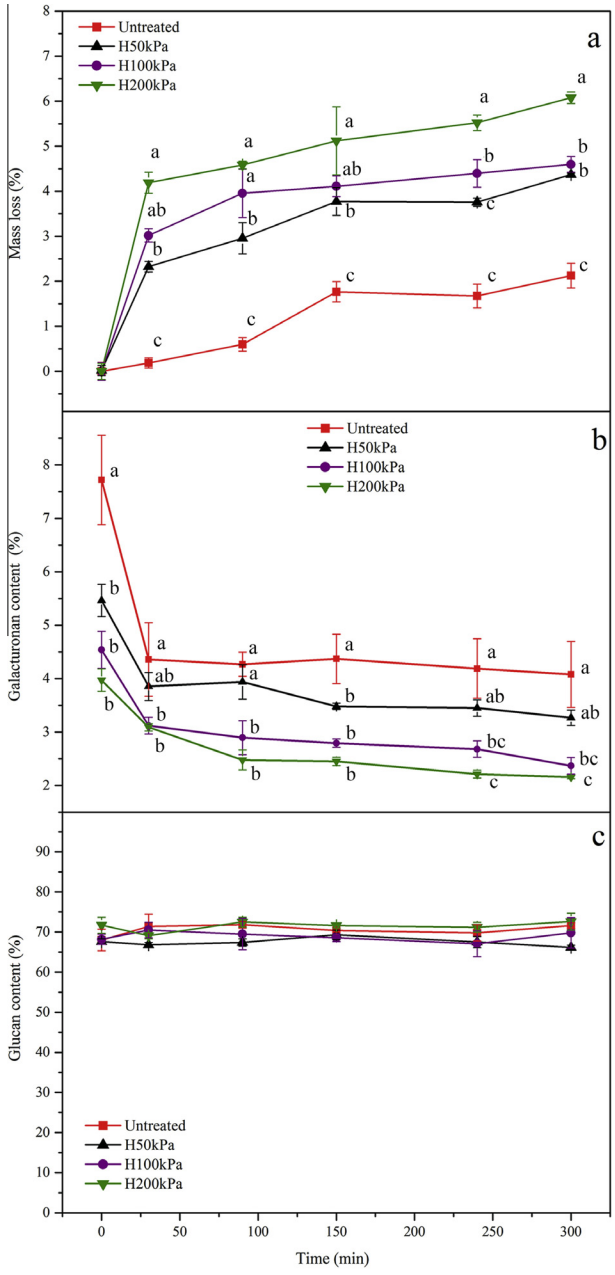

Fig. 4. Mass loss of fibres (a), galacturonan content (b) and glucan content (c) of resultant fibres after enzymatic retting. For the same incubation time with enzymes, values with different letters are significantly different at a level of 5%. (For interpretation of the references to color in this figure legend, the reader is referred to the web version of this article.)

observed for all studied samples. Moreover, except for the apparent changes in galacturonan contents, no noticeable changes in glucan content were found (Fig. 4c). Previously reported hemp fibres showed galacturonan contents of 3.6% after 20-day field retting [2], while our samples hydrothermally pre-treated at 100 and 200 kPa, even after only 90 min enzymatic retting, exhibited lower galacturonan contents of 3% (Fig. 4b).

Overall, the results presented in Fig. 4 reveal that the accessibility of pectin in the hemp structure for pectinases was significantly enhanced by the hydrothermal pre-treatment. For untreated hemp fibres, the rigid intact cellular structure with little or no void spaces in the stem structure (Fig. 3a) hindered enzyme access to the substrates (e.g. pectin). However, once the barriers, such as parenchyma cells were removed by hydrothermal treatment, the void spaces between fibre bundles (Fig. 3) allowed enzymes to penetrate and access the fibre surface. When harsher conditions were applied (200 kPa), increased removal of cell wall polymers and structural changes resulted in enhanced enzymatic degradation due to increasing substrate availability for the enzymatic reaction (Fig. 4).

Enhanced enzyme accessibility in the hydrothermally pre-treated samples was further corroborated by the increase in water retention values (WRV) after hydrothermal treatment (Table 1). The changes in WRV reflect the variations in the porous structure of the cell walls, concerning both the size and volume of the pores in the hemp bast structures created during hydrothermal treatment [23,24]. A high WRV represents an enhanced porosity, with large macro-pores within cell walls leading to improved enzyme penetration, thereby increasing substrate accessibility. In contrast, a low WRV indicates limited accessibility. As shown in Table 1, WRVs for all the hydrothermally pre-treated samples were significantly higher ($P < 0.05$) than the untreated samples, supporting this interpretation.

3.2.2. Morphology

ESEM micrographs indicated that there were no clear morphological changes in the untreated samples during enzymatic retting, irrespective of incubation time, reflected by the equally abundant presence of parenchyma cells on the fibre surfaces (black arrowheads in Fig. 3a–c). However, differences in the morphology during enzymatic retting within the samples hydrothermally pre-treated were observed: fibre surfaces had less surface impurities and fibre separation became greater, as the durations of enzymatic retting increased (Fig. 3d–l).

For samples hydrothermally pre-treated at 50 kPa, fewer impurity residues were observed even after only 30 min of enzyme retting. After enzymatic retting for 300 min, clean and smooth surfaces with well separated fibres were observed. These effects were more pronounced for samples treated at 100 kPa, with dirt free fibre surfaces resulting from a gradual decrease in the amount of parenchyma cells and an increased number of loosened bast fibres (Fig. 3h and i). Similar results were obtained for samples treated at 200 kPa, while propagation of fractures between the bast fibres and fibre separation appeared much greater (black arrows in Fig. 3k and l).

3.2.3. Tensile properties of fibres

No clear changes in glucan and galacturonan contents were recorded in the fibres after 90 min incubation with enzymes (Fig. 4). Therefore, samples enzymatically treated for 90 min were selected to investigate the effect of enzymatic retting on mechanical properties as shown in Table 3. Enzymatic retting on untreated (non-pretreated) fibres reduced the fibre strength from 770 MPa to 640 MPa and the stiffness from 29 GPa to 18 GPa. However, for hydrothermally pre-treated fibres, the enzymatic retting did not decrease the fibre strength. The hydrothermal pre-treatment at 100 kPa (H100 kPa) followed by enzymatic retting even increased the strength to 780 MPa and stiffness to 36 GPa (Table 3). This result indicated that the combination of 100 kPa hydrothermal pre-treatment and enzymatic retting was optimal (Table 3). In comparison, field retted fibres exhibited lower UTS of 680 MPa and stiffness of 28 GPa [3].

The data in Table 3 showed thereby a systematic trend that gradually more severe hydrothermal pretreatment induced a lowering of the UTS. It was also evident that the H200 kPa hydrothermal pretreatment caused the lowest UTS and stiffness for the fibres both when no enzymatic treatment was employed and with the subsequent enzymatic fibre treatment (Table 3). Untreated fibres had good mechanical properties, but enzymatic treatment of untreated fibres appeared to induce significant decreases in both

stiffness and UTS (Table 3). Differences in the responses to enzyme retting between hydrothermally treated and untreated fibres may have been caused by the curing of depolymerized low molecular aldehyde and phenolic functionalities acting as resins [25] and redistribution/re-deposition of gel materials of pectin during drying. The resins and pectin can glue cellulose microfibrils together, leading to a strong interface. On the other hand, these act as a barrier, blocking large macro-pores created in the cell walls during hydrothermal pre-treatment and thereby prevent enzymes penetration and substrate degradation inside individual fibres. Consequently, during enzymatic retting, the removal of pectin primarily happened in ML, without dramatic effect on the binding between the cellulosic microfibrils and non-cellulosic matrixes.

3.3. Tensile properties of hemp fibre/epoxy composites

Since the samples that had been hydrothermally pre-treated at 100 kPa and enzymatically treated for 90 min exhibited the highest UTS and stiffness, these samples were assessed in hemp fibre/epoxy composites. In Fig. 5, the start points of the ROM model lines at $V_f = 0$ are showing the measured epoxy matrix stiffness (E_m) and UTS (UTS_m) of 2.7 GPa and 27 MPa (at the average failure strain of the composites of 1.0%), respectively. In comparison of the slopes (k) established by linear regression of E_c and UTS_c versus V_f, of the composites with differently treated fibres, it was evident that the composites containing hydrothermally pre-treated and enzymatically treated fibres (sample code H100 kPa + E90 min) had the highest stiffness and UTS for all the tested V_f (Fig. 5). The tensile property data of the composites also revealed that the composites with field retted hemp fibres had the lowest stiffness and UTS; even lower than the composites containing the untreated hemp fibres (Fig. 5). The effective fibre stiffness (E_f) and strength (UTS_f) was established via the ROM-model (Eqs. (8) and (9)). E_f was determined to be 65, 68, 74 and 51 GPa for the samples Untreated, Untreated + E90 min, H100 kPa + E90 min, and Field retted, respectively. UTS_f was determined to be 560, 580, 620 and 470 MPa, respectively.

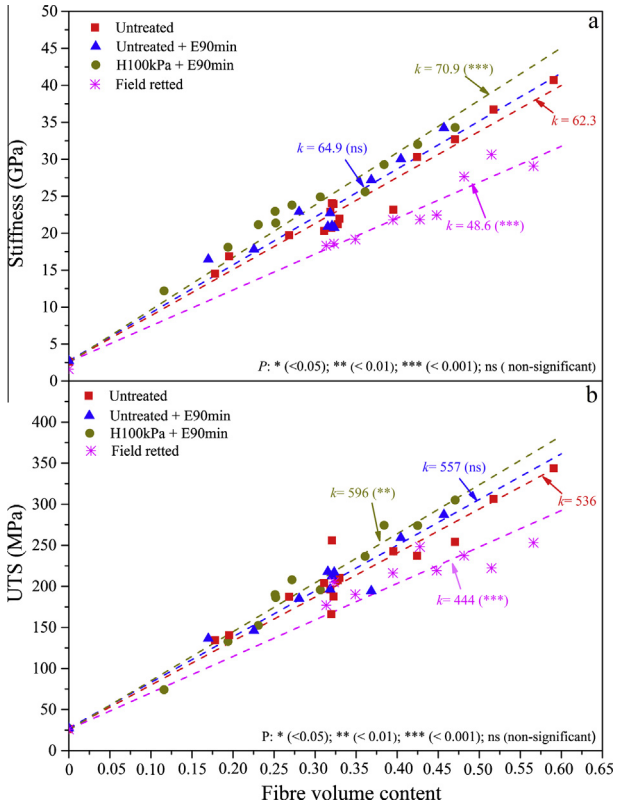

Fig. 5. Stiffness (a) and UTS (b) of composites reinforced with untreated and treated fibres versus fibre volume (V_f) contents (k is slope of linear regression model lines). (For interpretation of the references to color in this figure legend, the reader is referred to the web version of this article.)

Since enzymatic retting after hydrothermal pre-treatment produced higher improvement in the mechanical properties of the hemp fibre/epoxy composites than the other fibre processing methods, it indicates that the enzymatic removal of pectin improved the effective mechanical properties of the hemp fibres in the composites. At a fibre volume content of 0.50, the composites containing fibres hydrothermal pre-treated at 100 kPa and enzymatically retted exhibited the highest tensile strength of 325 MPa and stiffness of 38 GPa, 31% and 41% higher, respectively, compared to the field retted fibre composites (Table 4).

After pectin removal from hemp fibres, the improved mechanical properties of randomly oriented hemp fibre/polypropylene composites have been reported [4,5]. In those studies, different chemical and enzymatic treatments resulted in composites with a tensile strength of 40–48 MPa at fibre weight content of 0.40 compared to >205 MPa in this study (Fig. 5 at $V_f = 0.4$). The improvement in the composite mechanical properties was due to both the use of epoxy and unidirectional composites in this study.

3.4. Porosity in composites

Low porosity is a commonly applied criterion for high quality composites. The porosity factors (α_{pf}) of the composites produced with each type of hemp fibre were determined by Eq. (5) based on the experimental values of V_p versus V_f. The model lines were in good agreement with the experimental data points (Fig. 6). As shown, field retted and untreated samples had the highest porosity factors (up to 0.16), followed by enzymatically treated samples (0.12) (Fig. 6). The composite made with hydrothermally pre-treated and enzymatically retted fibres had the lowest porosity factor of 0.08 (Fig. 6), indicating the best impregnation of the hemp fibres by the epoxy matrix.

Overall, the variation of the composite porosity factors with fibre treatments was consistent with the observed morphology (Figs. 2 and 3). The porosity of plant fibres is due to cell lumens in fibre cells and parenchyma cells (Fig. 2) [15,26]. During enzymatic retting, parenchyma cells on the surface were partially removed and the epidermis layer was eliminated, particularly for the fibres treated with combined hydrothermal pre-treatment and enzymatic retting. These changes in fibre morphology presumably improved coherence between the matrix and the fibres; porosity was thus reduced.

3.5. Environmental and economic consideration

Environmental and economic factors should be considered when hemp fibre treatments are used on an industrial scale. Table 4 gives an assessment of environmental and economic factors, galacturonan content and mechanical properties for each fibre type and their fibre/epoxy composites. Enzymatic retting alone, combined hydrothermal pre-treatment and enzymatic retting, and field retting have relatively low environmental impacts. Traditional field retting is normally the cheapest hemp fibre treatment method, followed by enzymatic retting. The most effective method to remove pectins from hemp structure (indicated by GalA) was hydrothermal pre-treatment (100 kPa) combined with enzymatic retting (90 min), which resulted in composites with the highest tensile strength (325 MPa) and stiffness (38 GPa) at a fibre volume content of 0.50 (Fig. 5 and Table 4).

Table 4
Estimated relative environmental impact and economic costs for the treatments, and the resulting galacturonan content and mechanical properties of composites.

Treatment	Environmental impact	Economic costs			GalA (%)	Composite properties[a]	
		Enzyme	Energy	Equipment		Stiffness (GPa)	UTS (MPa)
Untreated	Low	None	Low	Low	7–9	34	295
Untreated + E90 min	Low	High	Medium	Medium	4–5	35	306
H100 kPa + E90 min	Low	High	High	High	2–3	38	325
Field retting	Low	None	Low	Low	4–5	27	249

[a] Mechanical properties were determined from the model lines in Fig. 5 at a fibre volume content of 0.50.

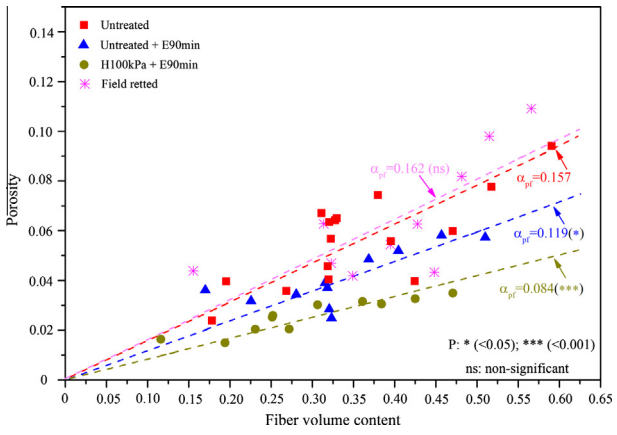

Fig. 6. Porosity of composites reinforced with untreated and treated fibres versus fibre volume (V_f) contents. (For interpretation of the references to color in this figure legend, the reader is referred to the web version of this article.)

Hydrothermal pre-treatment is commonly applied in biorefining schemes, such as 2nd generation bioethanol production. In 2nd generation bioethanol production, much higher pre-treatment temperatures (170–200 °C) and pressures (1000–1600 kPa) are usually applied [7,8] compared to the hydrothermal pre-treatment conditions (121 °C, 100 kPa) employed in this study. The hydrothermal pre-treatment used here is therefore considered as an inexpensive pre-treatment compared to the one used in the production of 2nd generation bioethanol.

4. Conclusion

An efficient methodology combining hydrothermal pre-treatment and subsequent enzymatic retting for the production of cellulose rich fibres from hemp without damaging fibre mechanical properties was reported in this study. Hydrothermal pre-treatment at 100 kPa for 30 min, followed by a 90 min pectinolytic enzyme treatment resulted in hemp fibres with low pectin contents (3%), high UTS (780 MPa) and high stiffness (36 GPa). These fibres could be used to make fibre/epoxy composites with UTS of 325 MPa and stiffness of 38 GPa at a fibre volume content of 0.50, which was the best mechanical properties produced in this study.

Acknowledgements

The authors are grateful to the Danish Council for Independent Research, Denmark supporting the CelFiMat project (No. 0602-02409B: "High quality cellulosic fibres for strong biocomposite materials"). The financial support of China Scholarship Council, China (CSC, no. 201304910245) for Ming Liu's Ph.D. project is acknowledged. The support for short-term scientific mission from Nordforsk Researcher Network, Norway, to Ming Liu in June 2015 is acknowledged. Annette Eva Jensen, Jonas Kreutzfeldt Heininge, Jan Sjølin and Michael Krogsgaard Nielsen from Technical University of Denmark are thanked for technical support.

References

[1] Bourmaud A, Morvan C, Bouali A, Placet V, Perré P, Baley C. Relationships between micro-fibrillar angle, mechanical properties and biochemical composition of flax fibers. Ind Crops Prod 2013;44:343–51.
[2] Liu M, Fernando D, Meyer AS, Madsen B, Daniel G, Thygesen A. Characterization and biological depectinization of hemp fibers originating from different stem sections. Ind Crops Prod 2015;76:880–91.
[3] Liu M, Fernando D, Daniel G, Madsen B, Meyer AS, Ale MT, et al. Effect of harvest time and field retting duration on the chemical composition, morphology and mechanical properties of hemp fibers. Ind Crops Prod 2015;69:29–39.
[4] Li Y, Pickering KL. Hemp fibre reinforced composites using chelator and enzyme treatments. Compos Sci Technol 2008;68(15–16):3293–8.
[5] Saleem Z, Rennebaum H, Pudel F, Grimm E. Treating bast fibres with pectinase improves mechanical characteristics of reinforced thermoplastic composites. Compos Sci Technol 2008;68(2):471–6.
[6] Thygesen A, Madsen FT, Lilholt H, Felby C, Thomsen AB. Changes in chemical composition, degree of crystallisation and polymerisation of cellulose in hemp fibres caused by pre-treatment. In: Lilholt H, Madsen B, Toftegaard H, Cendre E, Megnis M, Mikkelsen LP, et al., editors. Sustainable natural and polymeric composites – science and technology. Proc 23rd Risø Int Symp Mater Sci. Denmark: Risø National Laboratory; 2002. p. 315–23.
[7] Larsen J, Haven MØ, Thirup L. Inbicon makes lignocellulosic ethanol a commercial reality. Biomass Bioenerg 2012;46:36–45.
[8] Oh YH, Eom IY, Joo JC, Yu JH, Song BK, Lee SH, et al. Recent advances in development of biomass pretreatment technologies used in biorefinery for the production of bio-based fuels, chemicals and polymers. Korean J Chem Eng 2015;32(10):1945–59.
[9] Sixta H. Kraft pulping kinetics. In: Sixta H, editor. Handbook of pulp. Weinheim (Germany): WILEY-VCH; 2006. p. 185–365.
[10] Bauer S, Vasu P, Mort AJ, Somerville CR. Cloning, expression, and characterization of an oligoxyloglucan reducing end-specific xyloglucanobiohydrolase from *Aspergillus nidulans*. Carbohydr Res 2005;340(17):2590–7.
[11] Stratton J, Chiruvolu V, Meagher M. High cell-density fermentation. In: *Pichia* protocols, 103rd ed., Totowa (NJ): Humana Press; 1998. p. 107–20.
[12] Michalak M, Thomassen LV, Roytio H, Ouwehand AC, Meyer AS, Mikkelsen JD. Expression and characterization of an endo-1,4-β-galactanase from *Emericella nidulans* in *Pichia pastoris* for enzymatic design of potentially prebiotic oligosaccharides from potato galactans. Enzyme Microb Technol 2012;50(2):121–9.
[13] Martin N, Davies P, Baley C. Comparison of the properties of scutched flax and flax tow for composite material reinforcement. Ind Crops Prod 2014;61:284–92.
[14] Cheung HY, Ho MP, Lau KT, Cardona F, Hui D. Natural fibre-reinforced composites for bioengineering and environmental engineering applications. Compos Part B 2009;40(7):655–63.
[15] Madsen B, Thygesen A, Lilholt H. Plant fibre composites – porosity and stiffness. Compos Sci Technol 2009;69(7–8):1057–69.
[16] Fernando D, Daniel G. Exploring Scots pine fibre development mechanisms during TMP processing: impact of cell wall ultrastructure (morphological and topochemical) on negative behavior. Holzforschung 2008;62(5):597–607.
[17] ASTM Standard D2402-07. Standard test method for water retention of textile fibers (centrifuge procedure). West Conshohocken (PA): ASTM Internal.; 2012.
[18] Garrote G, Domínguez H, Parajó JC. Mild autohydrolysis: an environmentally friendly technology for xylooligosaccharide production from wood. J Chem Technol Biotechnol 1999;74(11):1101–9.
[19] Stevanic JS, Salmén L. The primary cell wall studied by dynamic 2D-FT-IR: interaction among components in Norway spruce (*Picea abies*). Cellul Chem Technol 2006;40(9–10):761–7.
[20] Salmén L. Viscoelastic properties of in situ lignin under water-saturated conditions. J Mater Sci 1984;19(9):3090–6.
[21] Eriksson I, Haglind I, Lidbrandt O, Sahnén L. Fiber swelling favoured by lignin softening. Wood Sci Technol 1991;25:135–44.
[22] Goring DAI. Thermal softening of lignin, hemicellulose and cellulose. Pulp Pap Mag Can 1963;64(12):T517–27.

[23] Andreasson B, Forsström J, Wågberg L. The porous structure of pulp fibres with different yields and its influence on paper strength. Cellulose 2003;10 (2):111–23.
[24] Chandra RP, Esteghlalian AR, Saddler JN. Assessing substrate accessibility to enzymatic hydrolysis by cellulases. In: Hu TQ, editor. Characterization of lignocellulosic materials, 1st ed., Wiley-Blackwell; 2008. p. 60–80.
[25] Stamboulis A, Baillie CA, Garkhail SK, Van Melick HGH, Peijs T. Environmental durability of flax fibres and their composites based on polypropylene matrix. Appl Compos Mater 2000;7(5–6):273–94.
[26] Madsen B, Thygesen A, Lilholt H. Plant fibre composites – porosity and volumetric interaction. Compos Sci Technol 2007;67(6–7):1584–600.

Paper V

Ming Liu, Anne S. Meyer, Dinesh Fernando, Diogo Alexandre Santos Silva, Geffrey Daniel, & Anders Thygesen

Effect of pectin and hemicellulose removal from hemp fibers on the mechanical properties of unidirectional hemp/epoxy composites

Composites Part A: Applied Science and Manufacturing, 2016, 90, 724-735

Composites: Part A 90 (2016) 724–735

Contents lists available at ScienceDirect

Composites: Part A

journal homepage: www.elsevier.com/locate/compositesa

Effect of pectin and hemicellulose removal from hemp fibres on the mechanical properties of unidirectional hemp/epoxy composites

Ming Liu [a], Anne S. Meyer [a], Dinesh Fernando [b], Diogo Alexandre Santos Silva [a], Geoffrey Daniel [b], Anders Thygesen [a,*]

[a] Center for Bioprocess Engineering, Department of Chemical and Biochemical Engineering, Technical University of Denmark, 2800 Kongens Lyngby, Denmark
[b] Department of Forest Products/Wood Science, Swedish University of Agricultural Sciences, Vallvägen 9D, 750-07 Uppsala, Sweden

ARTICLE INFO

Article history:
Received 1 July 2016
Received in revised form 30 August 2016
Accepted 31 August 2016
Available online 4 September 2016

Keywords:
A. Natural fibres
A. Polymer-matrix composites (PMCs)
B: Mechanical properties
B. Porosity

ABSTRACT

The objective of this study was to investigate the effect of pectin and hemicellulose removal from hemp fibres on the mechanical properties of hemp fibre/epoxy composites. Pectin removal by EDTA and endo-polygalacturonase (EPG) removed epidermal and parenchyma cells from hemp fibres and improved fibre separation. Hemicellulose removal by NaOH further improved fibre surface cleanliness. Removal of epidermal and parenchyma cells combined with improved fibre separation decreased composite porosity factor. As a result, pectin removal increased composite stiffness and ultimate tensile strength (UTS). Hemicellulose removal increased composite stiffness, but decreased composite UTS due to removal of xyloglucans. In comparison of all fibre treatments, composites with 0.5% EDTA + 0.2% EPG treated fibres had the highest tensile strength of 327 MPa at fibre volume content of 50%. Composites with 0.5% EDTA + 0.2% EPG → 10% NaOH treated fibres had the highest stiffness of 43 GPa and the lowest porosity factor of 0.04.

1. Introduction

Cellulosic fibres are natural resources with important properties such as low density, high specific tensile strength and stiffness, and a high aspect ratio (average length over diameter of the fibres) [1]. Due to these properties and concerns about the environment, the application of natural cellulosic fibre reinforced polymer composites has received considerable attention in recent years [2,3].

Hemp (*Cannabis sativa*) is a fast growing crop, which produces strong fibres that primarily lie beneath the epidermis in the cortex and form a ring in the phloem parenchyma [4]. Like wood fibres, hemp fibre cell walls are natural composites composed mainly of three classes of polysaccharides: cellulose, hemicellulose and pectins. Cellulose consists of β-1,4-linked glucan chains and is organized into microfibrils interlocked by xyloglucan (XG) [5]. The cellulose microfibrils and the cross-linked XG chains are generally considered as the two main components which provide cell wall strength. Pectins fill the spaces between cellulose and XG [5]. The pectins function as glue packing the microfibrils into final fibres that are approx. 20 mm in length and 10–40 μm in diameter [6]. The fibres make up the fibre bundles with varied sizes which are in turn organized into a fibre layer inside the cortex. Pectins and lignin in the middle lamellae (ML) join the fibres together [4,7].

The most abundant pectic polysaccharide in plant cell walls is homogalacturonan (HG), which is a linear homopolymer of α-1,4-linked galacturonic acid that comprises approx. 70% of pectin. Besides HG, the pectic polysaccharides are mainly comprised of rhamnogalacturonan I (RG I) and rhamnogalacturonan II (RG II). RG I represents 20–35% of pectic substrates and consists of a backbone of alternating α-1,4-D-galacturonic acid and α-1,2-L-rhamnose units; the latter are usually decorated with homopolymeric side chains of β-D-galactose and α-L-arabinose [8]. RG II makes up 5–10% of the pectin, and consists of a HG backbone of 1,4-linked α-D-galacturonic acid residues decorated with different types of side branches [9].

The physicochemical properties of pectin are largely dependent on the degree of methyl and acetyl esterification. Low-methoxyl (LM) pectin (i.e. HG) has sufficient carboxyl groups for the formation of calcium-mediated interactions between two neighbouring pectin chains, as described by the "egg-box" model [10]. However, high-methoxyl (HM) pectin does not contain sufficient polygalacturonic acid residues un-methylated at the C-6 position to form a stable structure through calcium-mediated interactions. Instead, hydrogen bonding and hydrophobic interactions have been

* Corresponding author.
E-mail address: athy@kt.dtu.dk (A. Thygesen).

http://dx.doi.org/10.1016/j.compositesa.2016.08.037
1359-835X/

suggested important forces in maintaining a stable structure for HM-pectin [11,12].

The principle behind fibre processing for the application of natural fibres in composites is to remove the non-cellulosic components (e.g. pectin, hemicellulose and lignin) to obtain well separated and cellulose rich fibres before use as reinforcement in composites. Traditional fibre processing methods such as field retting and water retting, however, are largely dependent on weather conditions (especially rainfall and temperature) and may damage the fibres if fibres are over retted [4,13]. Enzymatic treatment, involving mainly pectinolytic enzymes, may offer an alternative method to degrade pectin from hemp fibre strips and provide a solution to the limitations of traditional fibre retting methods.

In treatment of fibre with enzymes, pectic polymers are released from ML and fibre cell walls by using pectinases (e.g. endo-polygalacturonase) that randomly hydrolyze the glycosidic bonds of the HG backbone to liberate monomeric, dimeric or oligomeric fragments [14]. Addition of chemical chelators (e.g. ethylenediaminetetraacetic acid (EDTA)) has been shown to promote enzyme catalyzed degradation of HG from cellulosic fibres during enzymatic treatments [15,16]. The enhanced enzymatic degradation of HG results from the capacity of chemical chelators to form complexes particularly with calcium in pectin [17]. Furthermore, alkaline extraction with 10% NaOH is widely used for the isolation of hemicellulose from lignocellulosic biomass to obtain cellulose of high purity [18].

The objective of this study was to investigate the effect of sequential removal of pectin (e.g. homogalacturonan) and hemicellulose (e.g. xyloglucan) on the mechanical properties of fibres and their subsequent use in unidirectional hemp fibre/epoxy composites. Pectin removal from hemp fibres was carried out using EDTA alone and in combination with monoactive pectinase enzyme. In some experiments hemicellulose was also sequentially removed using 10% NaOH.

2. Materials and methods

2.1. Raw material and processing

2.1.1. Plant material

Hemp (*Cannabis sativa* L.), variety USO-31, was grown in France (N48.8526°, E3.0190°(WGS84)) as described in detail by Liu et al. [4]. Hemp stem pieces with a length of 150 ± 10 mm were randomly collected from the stems. Before treatment, hemp bast fibre strips were manually peeled from the stem pieces, gently rinsed with warm water (40 °C) to remove dirt and then dried at 50 °C for 12 h. Field retting was carried out on whole stems for 20 days after harvest [4] as a comparison to the treatments investigated in this study.

2.1.2. EDTA treatment

EDTA treatment was carried out on bast fibre strips using different concentrations of EDTA ($C_{10}H_{14}N_2Na_2O_8{\cdot}2H_2O$) (0.5, 0.75, 1, 2, and 3%, w/v) for 4 h in a water bath at 40 °C and agitation of 100 rpm. The liquid (cm^3) to fibre (g) ratio was 40:1. Before treatment, the pH of the EDTA solution was adjusted to 6.0 with 5 mol dm^{-3} NaOH. Each treatment was done in triplicate (4 g bast fibre strips/replicate). At the end of each treatment, the wet bast fibre strips were rinsed with MilliQ water and then dried at 50 °C for 12 h.

2.1.3. Enzymatic treatment

Enzymatic treatments using monoactive endo-polygalacturonase (EPG) with and without EDTA were performed on hemp bast fibre strips. The enzymatic treatments were carried out for 4 h at pH 6.0 in 25 mmol dm^{-3} citrate buffer in a water bath at 40 °C and agitation of 100 rpm. The liquid (cm^3) to fibre (g) ratio was maintained at 40:1. For enzymatic treatment in the presence of EDTA, 0.5% EDTA was added to enzyme solutions, and pH of the mixture was adjusted to 6.0 with 5 mol dm^{-3} NaOH.

The recombinant EPG was applied at a dosage of 0.2% (g protein/g dry matter). The EPG, derived originally from *Emericella nidulans*, was produced by fermentation of a *Pichia pastoris* clone (principally as described previously [19]) transformed with the gene AN4372.2 obtained from the Fungal Genetic Stock Center, Kansas State University, USA [20]. After the fermentation, the supernatant was recovered by centrifugation, and then subjected to a 0.4-μm sterile filtration, and finally the concentrated enzymes (or crude enzyme) after ultrafiltration with a 10 kDa cutoff membrane (Millipore, Sartorius) were used. At the end of enzyme treatment, the wet bast fibre strips were rinsed with MilliQ water and then dried at 50 °C for 12 h. Control treatments (i.e. without enzymes) were performed under the same conditions to determine the influence of non-enzymatic processing.

Using the above conditions, the activity of EPG was 945 U cm^{-3} (17 U mg^{-1} protein). The EPG activity was determined by measuring formation of reducing ends using 2 g dm^{-3} polygalacturonic acid as substrate [21] with enzyme to substrate ratio of 5:1 (v/v). The amount of reducing sugars that were liberated was measured by using 4-hydroxybenzoic acid hydrazide (PAHBAH) as colorimetric agent and glucose as standard [22]. One unit (1 U) of EPG activity is defined as the volume of the crude enzyme solution (cm^3) required to liberate 1 μmole reducing ends (glucose equivalents) per minute under the conditions applied in enzyme treatment. Protein content of the crude enzyme solutions was determined according to Bradford [23] using Bovine serum albumin as standard.

2.1.4. Sodium hydroxide treatment

After treatment with 0.5% EDTA and 0.2% EPG, the bast fibres were treated with 10% NaOH in tight plastic bags and held for 4 h in a water bath at 60 °C and agitated of 100 rpm. The liquid (cm^3) to fibre (g) ratio was 40:1. At the end of each treatment, the wet bast fibre strips were rinsed with MilliQ water and dried at 50 °C for 12 h.

2.1.5. Manufacturing of composites

The treated hemp bast fibre strips were manually aligned to allow the fibres to be processed into unidirectional composites. Bundles of fibre strips were firstly cut to a length of 140 mm, and the fibre strips were then justified to a bunch of fibre strips with masses in the range 0.6–2.3 g. Bunches of fibre strips were then put in each mould chamber. Afterwards, a press beam was placed on the top of the fibre strips in each chamber, and two insert beams were used to fix the height of the mould chambers to 2 mm. Epoxy resin (Araldite® LY 1568) and its amine hardener (Aradur® 3489) were mixed at a 100/28 mass ratio and degassed in a vacuum oven. The setup for the vacuum infusion and moulding processing has been described by Liu et al. [24]. After demoulding, composite samples with dimensions 140 mm × 10 mm × 2 mm were obtained and then glass fibre/epoxy tabs with lengths of 50 mm were mounted on composite specimens using epoxy glue (DP 460).

2.2. Characterization and testing of fibres and composites

2.2.1. Chemical composition analysis

The dried bast fibres were ground with a microfine grinder (IKA, MF 10.1; IKA®-Werke GmbH) to a particle size of 1 mm. Ground samples were extracted in a Soxhlet apparatus as described by Liu et al. [4], and then the extractive-free fibres were hydrolysed

using a two-step sulfuric acid process [25]. The chemical composition of the hydrolysates was analysed by high-performance anion-exchange chromatography with pulsed amperometric detection (HPAEC-PAD) [26]. Generally, arabinose, galactose, galacturonic acid and rhamnose were considered to be specific to pectins, xylose and mannose to the hemicellulose moiety and glucose to the cellulose moiety.

2.2.2. Calcium content determination

After EDTA treatment, the solution collected was analyzed with a Perkin-Elmer (Model 200) atomic absorption spectrometer (AAS) in emission mode (wavelength 422.7 nm, air-acetylene flame) to determine the amount of calcium released during treatment. Calcium standard solutions over the range 0–5 mg dm^{-3} of Ca^{2+} were used for calibration. For both samples and standards, 0.175 mol dm^{-3} HNO_3 and 0.1% La/Cs were added before analysis.

2.2.3. Morphology of fibres and composite specimens

Fibre samples of size 5 mm × 2 mm (long × wide) were cut from bast fibre strips under a stereo microscope for subsequent observations of fibre surface and cross section using environmental scanning electron microscopy (ESEM). Preparation of samples for microscopy followed the procedure described by Fernando and Daniel [27]. Observations were performed using a Philips XL 30 ESEM operated at 10–15 kV. The observation of composite specimens was performed in the same way as fibre samples.

2.2.4. Tensile properties of fibres

Bast fibre strips (60 mm long × 1 mm wide) of mass in the range of 5–20 mg were used for tensile testing. The preparation of test specimens has been described by Liu et al. [4]. Tensile testing was performed using an Instron Testing Machine 2710-203 equipped with a 1 kN load cell. The gauge length was 10 mm and the displacement rate was 0.5 mm min^{-1} (corresponding to a strain rate of 5% min^{-1}). Tensile testing was performed on 20 specimens for each treatment. The cross-sectional area (A_f) was determined from measured fibre mass and fibre length, and an assumed fibre density (i.e. 1.5 kg dm^{-3} [28]). Stiffness (linear regression in the strain interval 0.05–0.25%), ultimate tensile strength (UTS) and failure strain were determined based on the measured stress-strain curves.

2.2.5. Volumetric composition of composites

By varying the amount of fibres (m_f) in the mould chambers, the fibre weight content (w_f) in the composites was varied in the range 0–0.70. When W_f was below 0.30, the composite specimens were found to have irregular surfaces, and their thickness could not be measured accurately. For these cases, composite density (ρ_c) was determined by the buoyancy method (Archimedes principle) using water as displacement medium. When W_f was above 0.30, the composite specimens had flat surfaces, and ρ_c could be accurately calculated based on their dimensions (i.e. length, width and thickness).

The volumetric composition of composite samples was determined as described by Liu et al. [24]. In the composites, the porosity (V_p) was assumed to be a linear function of the fibre volume content (V_f), where the established proportionality constant is equal to the fibre correlated porosity constant α_{pf} [1]. This is expressed in Eq. (1). The matrix correlated porosity factor (α_{pm}) was assumed to be zero.

$$V_p = \alpha_{pf} \times V_f \tag{1}$$

2.2.6. Tensile properties of composites

For tensile testing of the composite specimens, an Instron Testing Machine 5566 with a load cell of 10 kN was used. Strain measurements were conducted using two extensometers and a displacement rate of 1 mm min^{-1} (corresponding to a strain rate of 2.5% min^{-1}). Based on the measured stress-strain curves, composite stiffness (E_c) (linear regression in the strain interval 0.05–0.25%) and tensile strength (σ_c or UTS) were determined. For each treatment, at least 10 specimens with varied fibre content were tested. The rule of mixtures (ROM) model [1] was used to determine the effective fibre stiffness (E_f) and strength (σ_{fu}) in the composites by linear regression versus fibre volume content (V_f) using Eqs. (2) and (3), respectively. The intercept was set equal to the measured matrix stiffness (E_m) and strength (σ_m^*) at the average failure strain of the composites.

$$E_c = V_f E_f + V_m E_m = E_m + V_f\left(E_f - E_m(1+\alpha_{pf})\right) = E_m + kV_f \tag{2}$$

$$\sigma_c = V_f \sigma_{fu} + V_m \sigma_m^* = \sigma_m^* + V_f\left(\sigma_{fu} - \sigma_m^*(1+\alpha_{pf})\right) = \sigma_m^* + kV_f \tag{3}$$

where the subscripts c, f and m indicate composite, fibre, and matrix, respectively. k is the slope of the linear regression line, i.e. of E_c vs. V_f and σ_c vs. V_f. Effective fibre stiffness (E_f) and tensile strength (σ_{fu}) can thus be calculated from Eqs. (2) and (3) at $V_f = 1.0$ by linear extrapolation.

3. Results and discussion

3.1. Pectin and hemicellulose removal from hemp fibres

Galacturonan content (GalA) of untreated hemp fibres of 8% was significantly decreased to 6% for 0.5% EDTA treated fibres, to 5% for 0.75% EDTA treated fibres, and finally to a little below 5% for 2% EDTA and 3% EDTA treated fibres (Table 1). In addition, there was a slight decrease in arabinan content, irrespective of the concentration of EDTA used in the treatments. No significant changes occurred to other components (Table 1).

The results are presumably due to the gradual increase in the removal of Ca^{2+}. During EDTA treatment, Ca^{2+} in the hemp structure will tend to bind with EDTA through proton displacement from the nitrogen atoms in preference to the carboxylate of pectin because there are two strong electron donors of nitrogen atoms for each EDTA molecule [17,29]. As a result of the competition between EDTA (in its alkaline salt form, EDTA-2Na·$2H_2O$) and non-esterified carboxyl groups of pectin in binding calcium, more calcium was released with increase in the concentration of EDTA from 6 (mg/100 g dry matter) for the control treatment, to 490 (mg/100 g dry matter) for 0.5% EDTA treatment, and finally to about 800 (mg/100 g dry matter) for 2% and 3% EDTA treatments (Fig. 1a), respectively. When Ca^{2+} was gradually removed from the hemp fibres, the structure of pectin became unstable, resulting in partial removal of pectin from hemp bast fibre strips and in particular removal of the low-methoxyl pectins (LM-pectin).

In general, the results shown in Table 1 demonstrate that EDTA treatment mainly affects homogalacturonan (HG) through calcium removal. Results shown in Fig. 1b further confirm that GalA removal correlates linearly with calcium removal by EDTA and has a slope of 1.0. The ratio of released calcium during EDTA treatment and the total galacturonan content in hemp fibres was found to increase from 0 for the control treatment (0% EDTA) to 0.30 for 0.5% EDTA treatment, and finally to approx. 0.47 for 2% and 3% EDTA treatment (Fig. 1c). According to the interaction between pectin and divalent cations, which mainly refers to calcium described by the "egg-box" model, the calcium to galacturonan ratio would be 0.50 for non-acetylated HG [30,31]. The results shown in Table 1 and Fig. 1 demonstrate that pectin could only be partially removed by EDTA treatment under the conditions applied, even though most of the calcium in hemp fibres was removed by EDTA. Furthermore, results shows that non-

Table 1
Chemical composition of hemp fibres treated with different concentrations of EDTA. Values are means (standard deviation) for 3 replicates. Values in each column that do not share a letter are significantly different at the 5% level.

Fibre sample	Amount (%)[1]					
	Ara	Gal	Glu	Xyl	Man	GalA
Field retted	0.6^{cd} (0.1)	2.0^{a} (0)	66.9^{b} (1.2)	1.0 (0.2)^{a}	3.9^{b} (0.2)	3.6^{d} (0.4)
Untreated	1.2^{a} (0.1)	2.1^{a} (0.1)	67.2^{b} (2.6)	1.3 (0.2)^{a}	4.6^{ab} (0.2)	8.3^{a} (0.4)
0.5% EDTA	0.8^{bc} (0.1)	2.1^{a} (0.1)	67.6^{b} (1.6)	1.0 (0.1)^{a}	5.2^{a} (0.1)	5.9^{b} (0.3)
0.75% EDTA	1.0^{ab} (0.0)	2.0^{a} (0.1)	72.5^{b} (4.7)	1.3 (0)^{a}	4.9^{ab} (0.1)	5.3^{bc} (0.2)
1.0% EDTA	0.9^{b} (0.0)	2.0^{a} (0.1)	70.2^{b} (4.3)	1.1 (0.1)^{a}	5.4^{a} (0.1)	4.7^{cd} (0.2)
2.0% EDTA	1.0^{b} (0.1)	2.0^{a} (0.0)	70.0^{b} (3.6)	1.0 (0.1)^{a}	5.0^{a} (0.1)	4.6^{cd} (0.4)
3.0% EDTA	1.0^{b} (0.1)	2.1^{a} (0.1)	71.8^{b} (1.6)	1.3 (0.1)^{a}	5.0^{a} (0.1)	4.4^{cd} (0.2)
0.2% EPG	0.9^{b} (0.1)	1.9^{ab}(0.1)	70.6^{b} (0.5)	1.1 (0.1)^{a}	5.0^{a} (0.1)	4.8^{c} (0.4)
0.5% EDTA + 0.2% EPG	0.8^{bc} (0.1)	1.7^{b} (0.3)	73.8^{b} (3.0)	1.0 (0.1)^{a}	4.6^{ab} (0.4)	2.1^{e} (0.4)
0.5% EDTA + 0.2% EPG → 10% NaOH	0.5^{d} (0.1)	1.7^{b} (0.1)	85.6^{a} (0.6)	0.2 (0)^{b}	1.7^{c} (0.1)	1.5^{e} (0.1)

[1] Ara-arabinan, Gal-galactan, Glu-glucan, Xyl-xylan, Man-mannan, GalA-galacturonan.

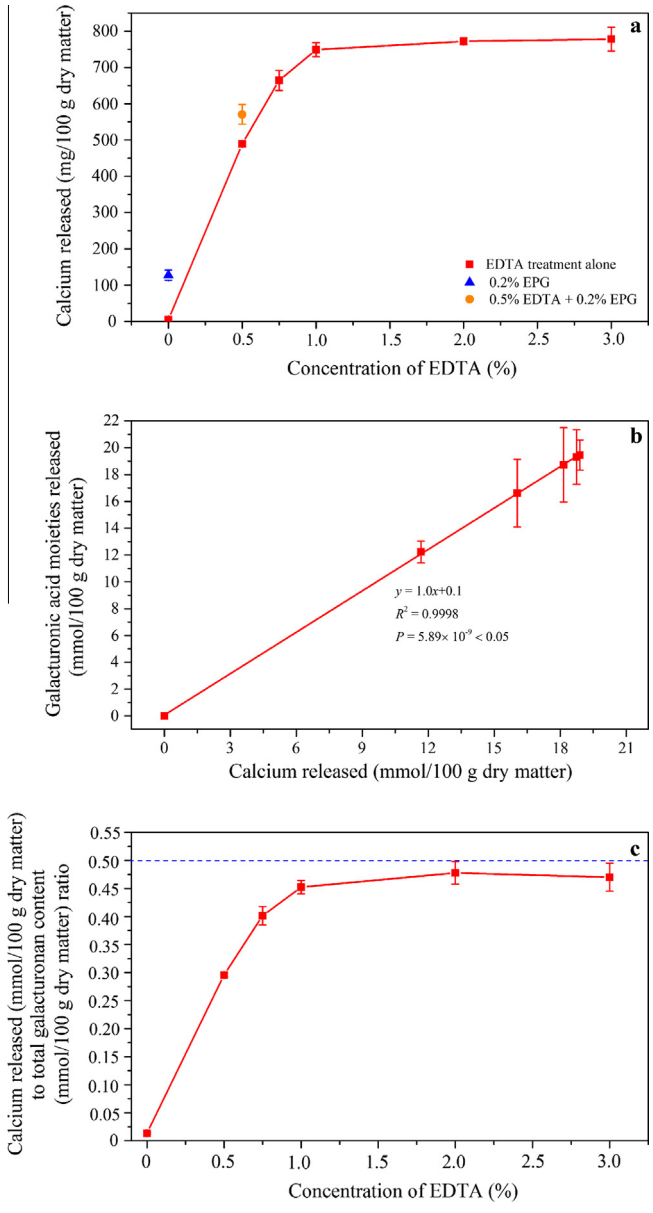

Fig. 1. Calcium released into treatment solutions vs. concentration of EDTA (a); correlation between galacturonic acid released and calcium released from hemp fibres (b), and variation of the ratio of calcium released and total galacturonan content of untreated fibres (c) during EDTA treatment. (For interpretation of the references to color in this figure legend, the reader is referred to the web version of this article.)

acetylated HG is the main component of the pectin in hemp bast fibres.

As shown in Fig. 1, the amount of calcium released during the control treatment (i.e. 0% EDTA) can largely be ignored compared to the experimental groups. In the following study, EDTA and enzymatically treated samples were therefore directly compared with untreated hemp fibres.

Treatment with 10% NaOH was subsequently carried out on the treated hemp fibres using a combination of 0.5% EDTA and 0.2% EPG to remove hemicellulose (e.g. xyloglucan, glucomannan and mannan) from the hemp fibres. After the alkali treatments, most of the monosaccharides which belong to the hemicellulose moiety (e.g. xylose and mannose) were removed (Table 1), resulting in very low contents of xylan (0.2%) and mannan (1.7%).

3.2. Morphology of fibres after pectin and hemicellulose removal

Fig. 2a illustrates a transverse section of a field retted sample with a partially removed epidermis layer and intact bast fibres. Fig. 2b shows a transverse section of untreated hemp with intact bast fibres, including native cellular structures with epidermis and bast fibre layers well organized and packed into a rigid structure. Intact parenchyma cells interspersed between bast fibres can be clearly seen holding the fibres together as in the living plant. By contrast, the epidermis was partly removed (green double-headed arrows in Fig. 2c–g) for EDTA, enzyme and NaOH treated samples. In addition, some parenchyma cells in cross sections of samples treated with a combination of EDTA and EPG were removed (red arrows in Fig. 2f). More parenchyma cells were removed from samples that were further treated with 10% NaOH, which caused the bast fibre region to open considerably (red arrows in Fig. 2g) and resulted in small fibre bundles and large void spaces between fibres/fibre bundles.

Significant physical microstructural changes occurred in the fibre surface during EDTA, enzymatic and alkali treatments. Fig. 3a shows that the surfaces of field retted fibres were covered with a large number of microorganisms and parenchyma cell residues (magenta arrowheads). By contrast, the surfaces of untreated fibres were covered with parenchyma cell residues (magenta arrowheads in Fig. 3b) without void spaces between fibres and/or fibre bundles. The surfaces of samples treated with 1% EDTA showed that areas initially covered with parenchyma cells were partially broken down. As a result, large void spaces between neighbouring fibres and/or fibre bundles (blue arrows in Fig. 3c) were observed, and many parenchyma cell residues still remained on fibre surfaces (magenta arrowheads in Fig. 3c). This gave an appearance of impurities on fibre surfaces. Treatment with 2% EDTA showed similar features as for 1% EDTA treated fibres but resulted in improved fibre separation (blue arrows in Fig. 3d) with more void spaces between fibres.

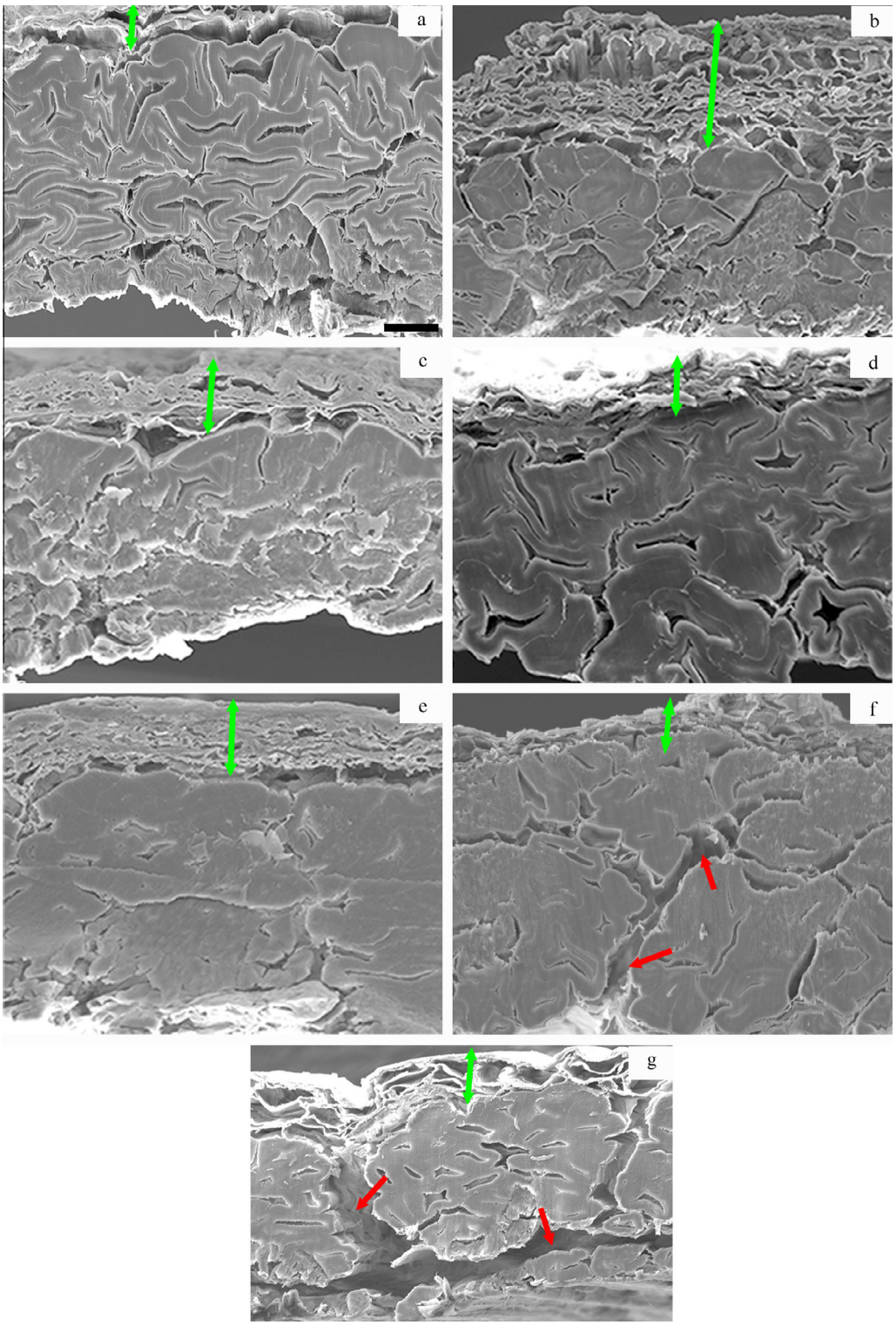

Fig. 2. ESEM micrographs showing cross sections of hemp bast fibre strips: field retted (a), untreated (b), 1% EDTA treated (c), 2% EDTA treated (d), 0.2% EPG treated (e), 0.5% EDTA + 0.2% EPG treated (f), and 0.5% EDTA + 0.2% EPG → 10% NaOH treated (g). Green double-headed arrows show the epidermis layer; red arrows show separated fibres and open spaces between fibres. Scale bar in (a) is 25 μm with the same magnification for the other images. (For interpretation of the references to color in this figure legend, the reader is referred to the web version of this article.)

Hemp fibres treated with EPG only had a smooth surface with fewer impurities compared to EDTA treated samples; parenchyma cell residues were still visible on fibre surfaces (magenta arrowheads in Fig. 3e) and few void spaces between fibres and/or fibre bundles were observed. By contrast, treatment with a combination of 0.5% EDTA and 0.2% EPG produced the best fibre separation (blue arrows in Fig. 3f), and fibre separated from fibre bundles were clearly observed (Fig. 3f). However, the surfaces of the separated fibres were found to be covered with impurities (Fig. 3g). Better fibre separation (Fig. 3h) and much cleaner fibre surfaces (Fig. 3i) were achieved after samples were further treated with 10% NaOH.

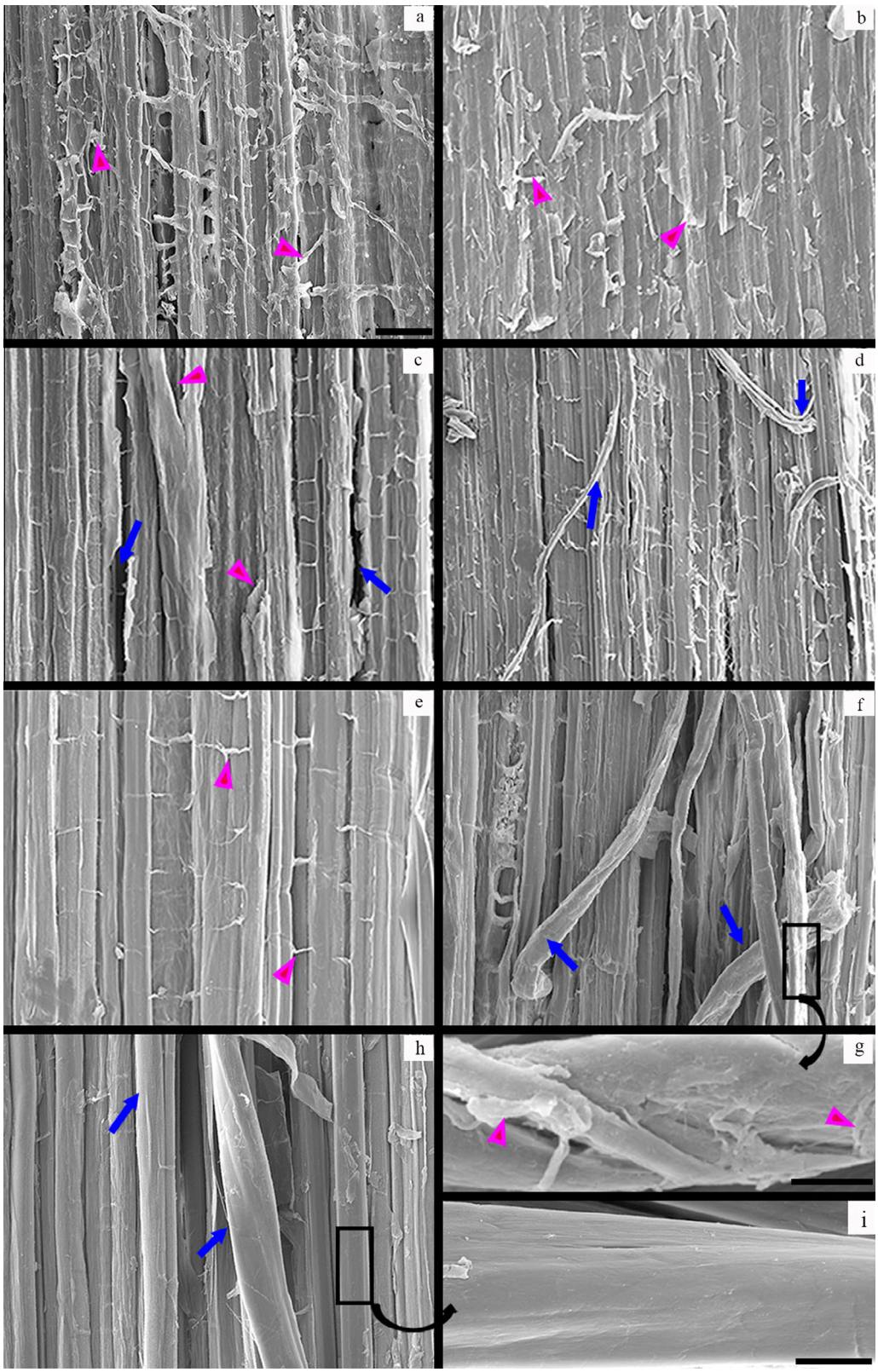

Fig. 3. ESEM micrographs showing surfaces of hemp bast fibre strips: field retted (a), untreated (b), 1% EDTA treated (c), 2% EDTA treated (d), 0.2% EPG treated (e), 0.5% EDTA + 0.2% EPG treated (f)–(g), and 0.5% EDTA + 0.2% EPG → 10% NaOH treated (h)–(i). Magenta arrowheads show parenchyma cell residues on fibre surface; blue arrows show separated fibres and open spaces between fibres. Scale bar in (a) is 50 μm with the same magnification for (b)–(e). Scale bar in (g) and (i) is 10 μm. (For interpretation of the references to color in this figure legend, the reader is referred to the web version of this article.)

The changes in fibre morphology can be explained by the variation in pectin and hemicellulose content of hemp fibres during the EDTA, enzyme and alkali treatments (Table 1). When fibres were treated with EDTA or EPG alone, only a small amount of pectin was removed. By contrast, when hemp fibres were subjected to a mixture of EDTA and enzyme, a significantly greater amount of

pectin was degraded (Table 1) which resulted in weaker bonding between neighbouring cells (i.e. fibre – fibre cell, fibre – parenchyma cell). Consequently, an improvement in fibre separation and fewer parenchyma cell residues were observed (Fig. 3f). After samples were further treated with 10% NaOH, the XG chains and other components of hemicellulose were also removed (Table 1), and thus cleaner fibre surfaces were observed (Fig. 3h and i).

3.3. Tensile behaviour of fibres

As shown in Table 2, stiffness, UTS and failure strain of fibres decreased after EDTA, enzyme and alkali treatments. After EDTA treatments, stiffness and UTS of fibres decreased, respectively, from ~29 GPa and ~770 MPa for the untreated samples, to ~25 GPa and ~580 MPa for 1% EDTA treated fibres and finally to ~15 GPa and ~340 MPa for 3% EDTA treated fibres. After enzyme treatment, the stiffness and UTS of fibres decreased, respectively, from ~24 GPa and ~680 MPa for 0.5% EDTA treated fibres, and from ~17 GPa and ~640 MPa for samples treated with 0.2% EPG alone, to ~15 GPa and ~560 MPa for samples treated with 0.5% EDTA combined with 0.2% EPG. The stiffness and UTS of field retted samples were determined as ~28 GPa and ~683 MPa.

The changes in tensile properties of hemp fibres caused by EDTA and enzyme treatments can be explained by the removal of pectins from hemp fibres (Table 1). Hemp bast fibres can be seen as a natural composite of cellulose microfibrils and matrices of non-cellulosic components, whose mechanical properties are governed not only by the cellulose microfibrils, but also by the coherence between the cellulose microfibrils and the matrices. As pectins are gradually removed from hemp fibres with increasing concentration of EDTA or the addition of EPG, the bonding (or interface) between cellulose microfibrils and the non-cellulosic matrices becomes weaker and thus the mechanical properties decrease.

The weakened interface between cellulose microfibrils and matrices of the non-cellulosic matrices may also be confirmed by changes in the tensile behaviour of resultant fibres. The tensile behaviour of the resultant samples varied greatly after the different fibre treatments. As shown in Fig. 4a, three types of tensile behaviour were observed. The first behaviour (type I) is linear elastic, where the stress-strain curve is a straight line. The second behaviour (type II) includes some plastic flow as indicated by a slightly bent progress curve. The two types of tensile curves have been reported in previous studies on untreated hemp fibres [7].

Type III behaviour, characterized by a non-linear region in the earlier stage of loading, has also been observed for both hemp [32] and flax fibres [33]. The non-linear region during the beginning of deformation was ascribed to the sliding of microfibrils together with their progressive alignment along the fibre towards the direction of external load [34]. More samples tended to demonstrate type III behaviour with increase in concentration of EDTA and with presence of EPG during treatment with 0.5% EDTA. This was indicated by the increase in percentage of tested fibres following a type III behaviour from 0% for untreated samples to approx. 20% for 0.5% EDTA treated samples, to 44% for 1.0% EDTA treated samples, and finally almost to 60% for both 2 and 3% EDTA treated fibres (see Fig. 4b). The shifting of tensile behaviour of treated fibres from type I and II to type III confirms the above explanations that decreased bonding between cellulose microfibrils and non-cellulosic components causes a decrease in fibre mechanical properties (Table 2).

After the fibres were treated with 10% NaOH following treatment with 0.5% EDTA and 0.2% EPG, there was no apparent change in stiffness of fibres but the UTS of fibres decreased from 556 MPa to 432 MPa. The tensile behaviour of alkali treated fibres also demonstrated type I, II and III behaviours with about 25% tested fibres following type I, 45% of tested fibres following type II, and the rest following type III behaviour (Fig. 4b). The decrease in the UTS of fibres can be explained by the removal of XG chains, which are considered as a strengthening component of fibre cell walls [5].

Table 2
Mechanical properties of hemp fibres treated with different concentrations of EDTA. Values are means (standard deviation) for 20 replicates. Values in the column that do not share a letter are significantly different at the 5% level.

Fibre sample	Mechanical properties		
	Stiffness (GPa)	UTS (MPa)	Failure strain (%)
Field retted	27.5^{ab} (4.6)	683^{ab} (107)	4.5^{ab} (1.2)
Untreated	28.5^{a} (2.9)	772^{a} (103)	5.1^{a} (0.9)
0.5% EDTA	24.1^{c} (5.4)	675^{abc} (87)	3.1^{cd} (0.7)
0.75% EDTA	22.0^{c} (4.4)	578^{cde} (49)	3.3^{cd} (1.0)
1.0% EDTA	24.5^{bc} (6.4)	584^{cde} (108)	2.8^{d} (1.0)
2.0% EDTA	14.5^{d} (5.3)	493^{e} (81)	3.6^{bcd} (0.5)
3.0% EDTA	15.2^{d} (5.2)	337^{f} (138)	3.3^{cd} (0.7)
0.2% EPG	17.2^{d} (3.8)	643^{bcd} (49)	3.7^{bcd} (0.6)
0.5% EDTA + 0.2% EPG	15.2^{d} (4.0)	556^{de} (138)	4.1^{abc} (1.1)
0.5% EDTA + 0.2% EPG → 10% NaOH	13.8^{d} (2.3)	432^{f} (86)	4.1^{abc} (1.0)

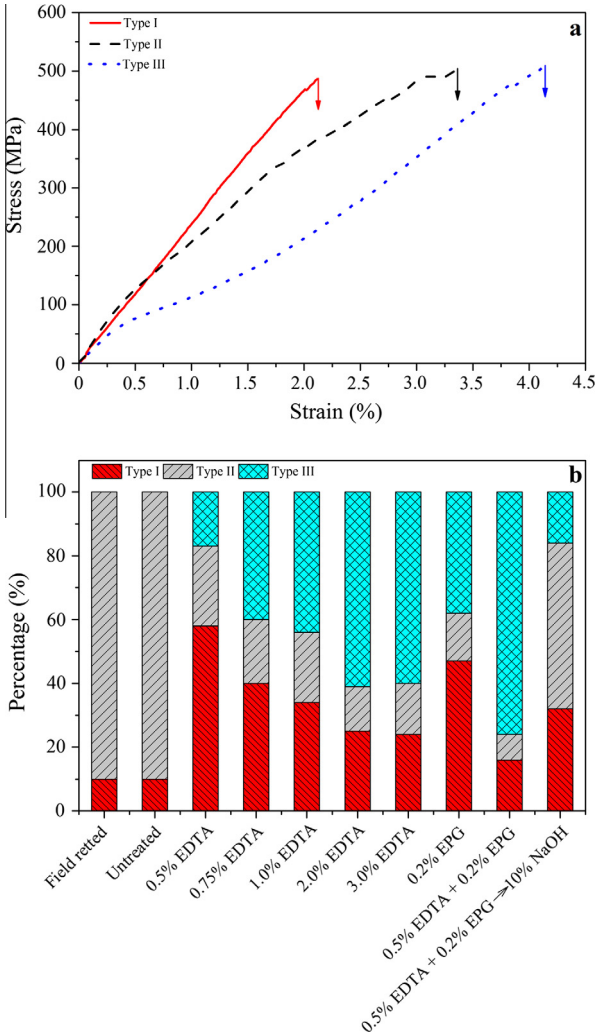

Fig. 4. Typical stress-strain curves of hemp fibres (a) after different treatments, and percentage of each type stress-strain curves for differently treated fibres (b). (For interpretation of the references to color in this figure legend, the reader is referred to the web version of this article.)

3.4. Composite porosity

Plant fibre composites contain a relatively large amount of porosity because plant fibres have voids in fibre, epidermal and parenchyma cells. The presence of voids, especially in epidermis and parenchyma cells, is likely to cause insufficient coherence between fibres and matrices in composites. The insufficient coherence produces un-impregnated fibres. This is assumed to lead to stress concentrations and influence the mechanical performance of the composites [1,24]. The fibre correlated porosity factor (α_{pf}) of composites manufactured using the differently treated hemp fibres was determined based on the experimental values of V_p and V_f using Eq. (1) (Fig. 5). As shown, composites with field retted and untreated fibres had the highest porosity factor of about 0.16. By contrast, composites with EDTA and enzyme treated hemp fibres had much lower porosity factors. Porosity factors decreased from 0.14 for composites with 1% EDTA treated fibres to 0.12 with 3% EDTA treated fibres and enzyme treated fibres, then to 0.09 with fibres treated with 0.5% EDTA and 0.2% EPG together, and finally to 0.04 with fibres treated with 0.5% EDTA and 0.2% EPG followed by 10% NaOH. By comparison, the porosity factor for composites with hydrothermally pretreated and enzymatically treated fibres has been reported as 0.08 [24].

Fig. 6 shows voids presented at cross sections of composite specimens with differently treated fibres. As shown, voids of composites are mainly located at epoxy/epidermis, epidermis/fibre, fibre/fibre, and fibre/epoxy interfaces and inside fibre cell walls (as lumen). Composites with field retted fibres exhibited a large quantity of voids located at epidermis/epoxy, epidermis/epidermis, epidermis/fibre, fibre/fibre interfaces and inside fibres (Fig. 6a). Similar results were observed for composites with untreated fibres (Fig. 6b). Composites with 0.5% EDTA treated fibres (Fig. 6c), 3% EDTA treated fibres (Fig. 6 d) and 0.2% EPG treated fibres (Fig. 6e) showed less voids due to removal of epidermis by fibre treatments. A few voids were observed for composites with 0.5% EDTA + 0.2% EPG (Fig. 6f) due to the complete removal of epidermis. The least amount of voids was observed for composites with 0.5% EDTA + 0.2% EPG → 10% NaOH treated fibres (Fig. 6g–h) due to better separation of fibres, as indicated by small fibre bundles observed in Fig. 6h, and complete removal of epidermis. The observations were collaborated with the results shown in Fig. 3 and 5.

Changes in the fibre correlated porosity factor of composites with differently treated fibres can be explained by changes in fibre microstructure and chemical composition of fibres during fibre processing. When the hemp fibre strips were subjected to EDTA and/or EPG, pectin in the epidermis and in the parenchyma cells and the middle lamella regions between fibre cells, was partly removed by removal of calcium and/or hydrolysed by enzyme-catalysed reactions (Table 1). The removal of pectin is likely to weaken the bonding between epidermis and cortex, between fibres and parenchyma cells, and between fibres, and thus lead to partial removal of epidermal and parenchyma cells from the hemp fibre strips. Such removal of epidermal and parenchyma cells would result in splitting of fibre bundles into smaller bundles (Figs. 2 and 3). The changes to fibre microstructure may collectively contribute to the decrease of α_{pf} after fibre treatment. Furthermore, with the exception of field retted samples, the fibre correlated porosity factors of composites with differently treated fibres were found to be correlated with pectin and hemicellulose content of the fibres (Fig. 7a).

3.5. Tensile properties of hemp fibre/epoxy composites

In Fig. 8, the starting points of model lines at $W_f = 0$ show the measured neat epoxy stiffness (E_m) and failure strength (σ_m^*), respectively, at the average failure strain of the composites. Overall, the model lines are in agreement with the experimental data. When the slopes (k) of the model lines are compared, it is evident that the model lines of composites with field retted fibres have the lowest slope of 48.6 GPa for stiffness (Fig. 8a) and 444 MPa for UTS (Fig. 8b). Composites with untreated fibres have a slope of 62.3 GPa for stiffness and 536 MPa for UTS. By contrast, for composite stiffness and strength, the slopes of the model lines tend to increase for composites made with EDTA and enzyme treated fibres. When the model lines of EDTA and enzyme treated samples are compared, the model lines of composites containing fibres treated with 0.5% EDTA combined with 0.2% EPG have the highest slope of 67.8 GPa for composite stiffness and 598 MPa for composite UTS (Fig. 8).

In addition, for composites with fibres treated with 0.5% EDTA combined with 0.2% EPG followed by 10% NaOH, the failure strain decreased to 0.8% (Table 3 and Fig. 8c) from 1% with untreated,

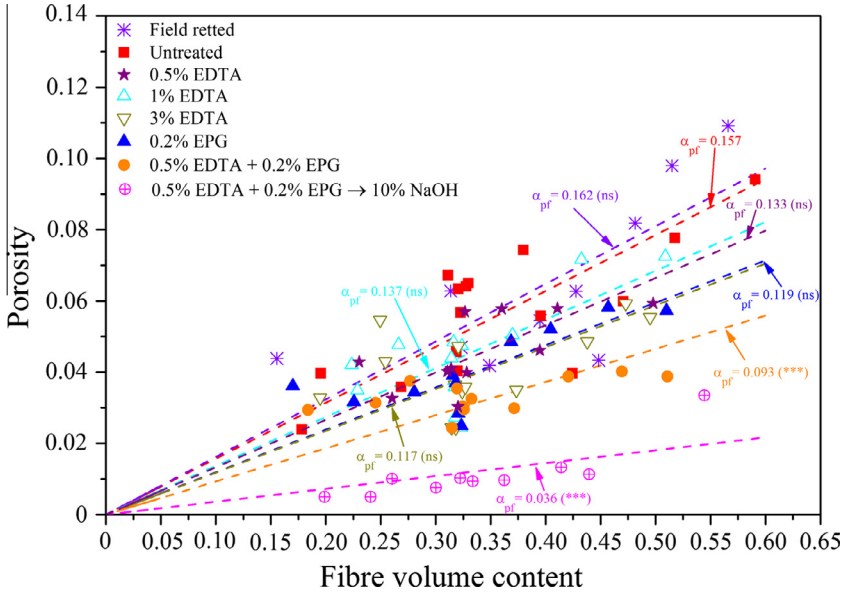

Fig. 5. Porosity of composites reinforced with untreated and treated fibres versus fibre volume contents (V_f). (For interpretation of the references to color in this figure legend, the reader is referred to the web version of this article.)

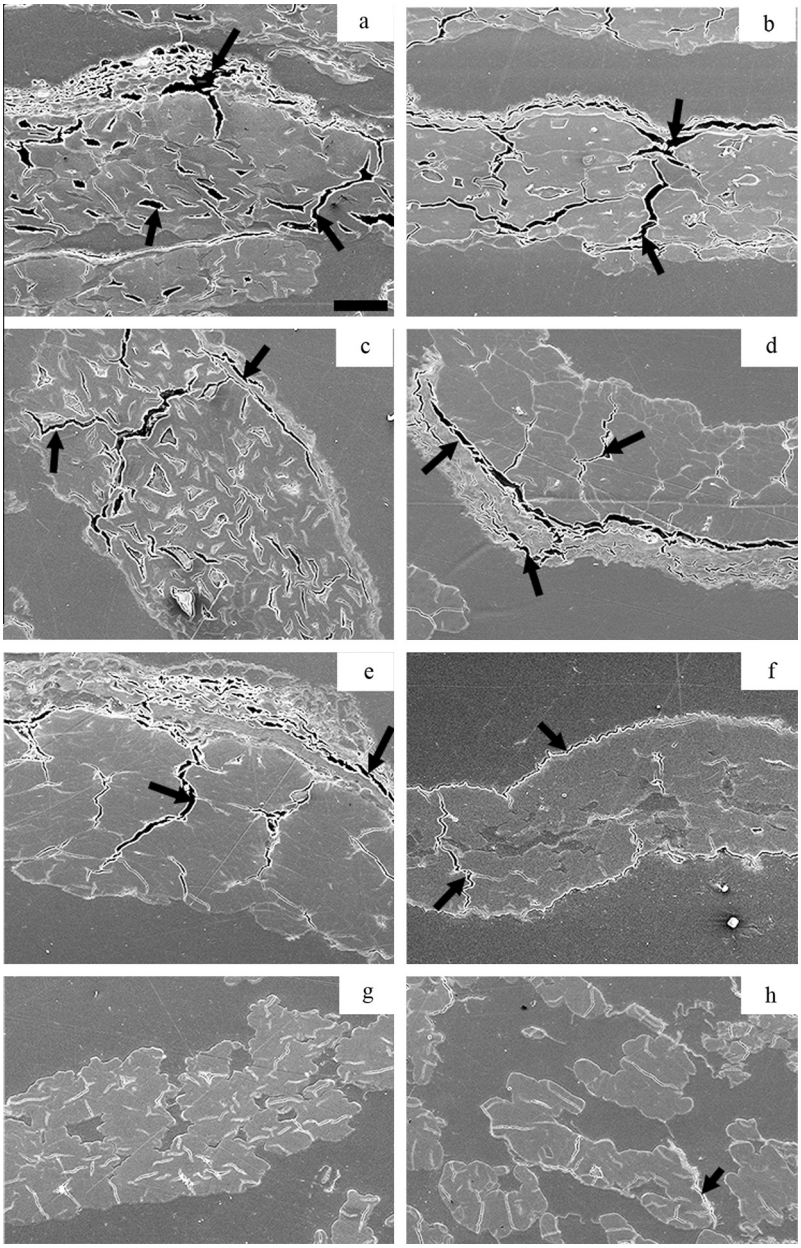

Fig. 6. ESEM micrographs of polished hemp fibre/epoxy composites with field retted (a), untreated (b), 0.5% EDTA treated (c), 3% EDTA treated (d), 0.2% EPG treated (e), 0.5% EDTA + 0.2% EPG treated (f) and 0.5% EDTA + 0.2% EPG → 10% NaOH treated (g–h) fibres. Arrows show examples of porosities at epoxy/epidermis, epidermis/epidermis, epidermis/fibre, fibre/fibre and fibre/epoxy interfaces. Scale bar in (a) is 50 μm with the same magnification for (b)–(h).

EDTA and enzyme treated fibres, and the stiffness of the composites increased considerably from 62.3 GPa (untreated fibres) to 80.9 GPa (Fig. 8a). However, the strength of the composites dramatically decreased compared with composites with fibres treated with 0.5% EDTA combined with 0.2% EPG as indicated by the decrease in the slope from 598 MPa for composites with fibres treated with 0.5% EDTA combined with 0.2% EPG to 506 MPa for composites with such treated fibres (Fig. 8b). A 14% increase in composite stiffness was achieved compared to composites with hydrothermally pretreated and enzymatically treated fibres [24].

The failure strain of the composites with field retted, untreated and 1% EDTA treated fibres was found to decrease with increase in fibre volume content (Fig. 8c), while for composites with a high concentration EDTA (i.e. 3% EDTA), enzyme, and alkali treated fibres, the failure strain was independent of fibre volume content (Fig. 8c). The mechanical properties of composites with differently treated fibres at $V_f = 0.50$ were calculated using the slopes shown in Fig. 8. As shown in Table 3, composites with field retted fibres had both lowest stiffness (27 GPa) and strength (248 MPa). By contrast, composites with fibres treated with 0.5% EDTA and 0.2% EPG together had the highest strength of 327 MPa, which is an increase of 31% compared with composites with field retted samples. Composites with fibres treated with 0.5% EDTA combined with 0.2% EPG followed by 10% NaOH had the highest stiffness (~43 GPa), which is an increase of 60% compared with the composites with field retted samples.

Effective fibre stiffness and strength were established based on the slopes of the model lines shown in Fig. 8 using Eqs. (2) and (3). As shown in Table 3, field retted fibres had the lowest effective fibre stiffness of ~51 GPa with an effective fibre strength of 470 MPa. By contrast, fibres treated with 0.5% EDTA combined with 0.2% EPG had the highest effective fibre strength of 626 MPa, which

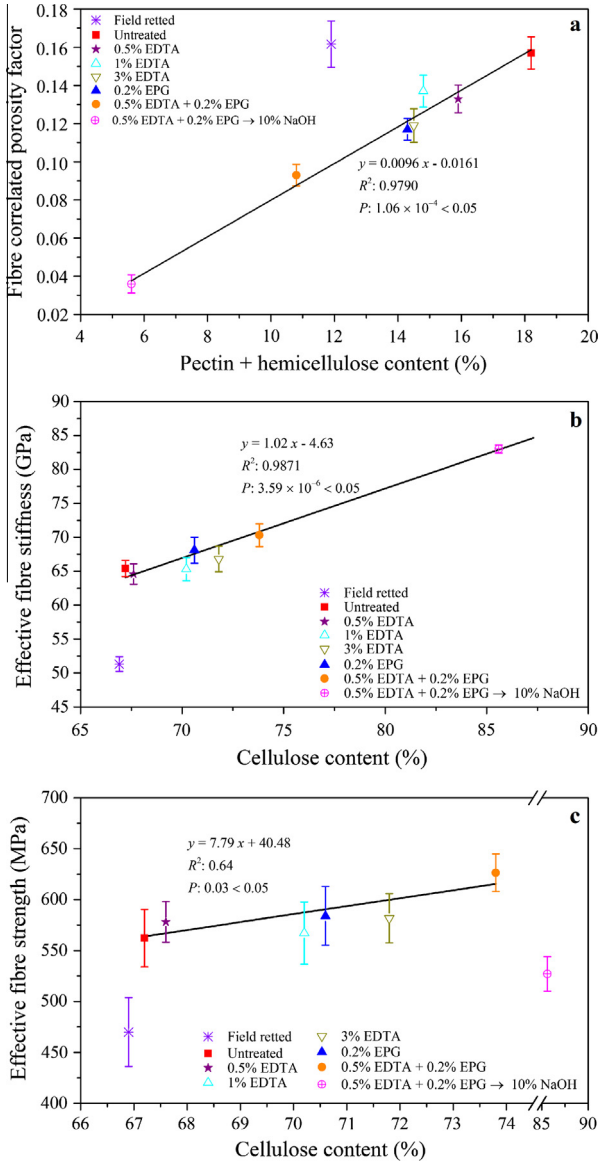

Fig. 7. Fibre correlated porosity factor (α_{pf}) vs. pectin + hemicellulose content (a), effective fibre stiffness vs. fibre cellulose content (b), and effective fibre strength vs. fibre cellulose content (c). (For interpretation of the references to color in this figure legend, the reader is referred to the web version of this article.)

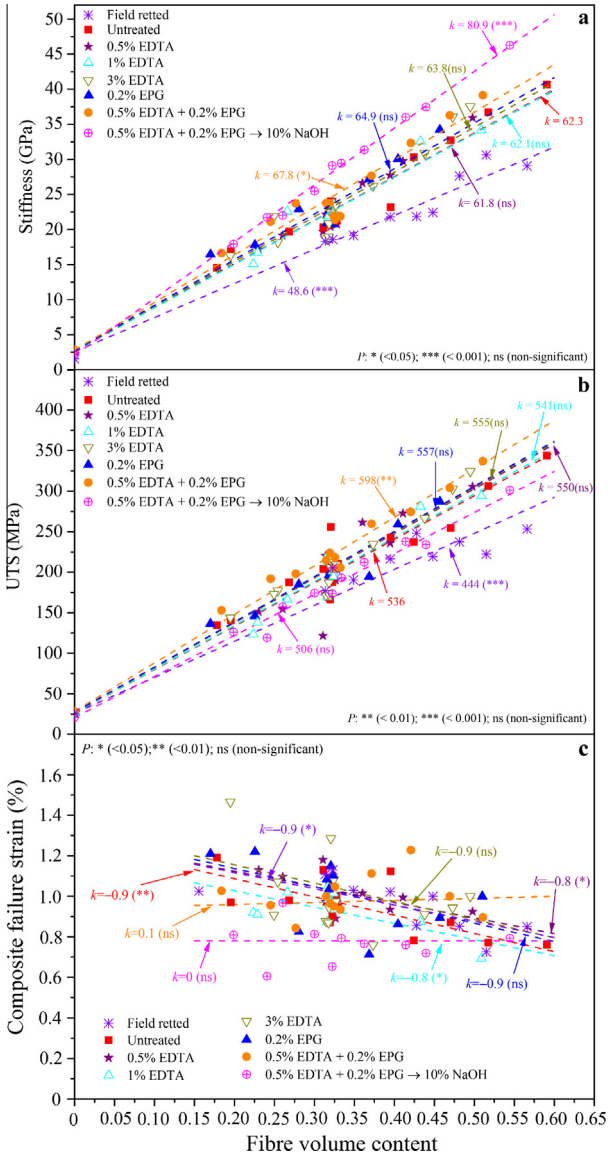

Fig. 8. Stiffness (a), UTS (b) and failure strain (c) of composites reinforced with untreated and treated fibres versus fibre volume contents (V_f). (In (a) and (b), the *P* value indicates the significant level for the slope of model lines between differently treated fibres vs. untreated fibres. In (c), the *P* value indicates the significant level for the slope of model lines vs. 0). (For interpretation of the references to color in this figure legend, the reader is referred to the web version of this article.)

is an increase of 11% compared with untreated fibres. Hemp fibres treated with 0.5% EDTA and 0.2% EPG together followed by 10% NaOH had the highest effective fibre stiffness of 83 GPa, which is an increase of 28% compared with untreated fibres.

The changes in the effective fibre strength and stiffness may be explained by the changes in fibre chemical composition (Table 1) and composite porosity (Fig. 5). During fibre processing with EDTA, enzyme and alkali, the fibres were polished and highly cellulose-rich fibres were obtained which had improved effective fibre stiffness and strength. There is clear evidence that effective fibre stiffness and effective fibre strength correlate with the cellulose content of fibres. As shown in Fig. 7b and c, field retted and alkali treated fibres were out of the line. It was most likely due to damage to the field retted samples caused by the activity of cellulases secreted by microorganisms during field retting, and disrupted cellulose-hemicellulose interlocked network occurred to alkali treated samples during NaOH treatment. In addition, after fibre processing, fibres were better infiltrated within the epoxy matrix and composite porosity was reduced (Fig. 6). The decrease in porosity lowered the influence of stress concentrations. As a result, the effective fibre stiffness and strength were improved (Fig. 9).

3.6. Comparison of structure properties of hemp fibres and hemp fibre/epoxy composites

As discussed above, the mechanical properties of hemp fibre/epoxy composites varied with fibre treatments. Pectin removal by EDTA and EPG increased composite stiffness and UTS due to the decreased composite porosity contents. Hemicellulose removal by NaOH increased composite stiffness due to the decreased composite porosity contents, but decreased composite UTS due to the disrupted cellulose-hemicellulose interlocked network with the removal of hemicellulose during alkali treatment.

Properties of composites depend not only on the fibre themselves but also on the degree to which an applied load is transmitted to the fibres by the matrix phase under stress [35]. Hemp fibres

Table 3
Mechanical properties of fibre/epoxy composites and established effective fibre mechanical properties. Values are shown as mean (standard error).

Fibre sample	Composite mechanical properties[1]			Effective fibre stiffness[2] (GPa)	Effective fibre strength[2] (MPa)
	Stiffness (GPa)	UTS (MPa)	Failure strain (%)		
Field retted	26.9 (0.6)	248 (17)	1.0 (0.1)	51.2 (1.1)	470 (34)
Untreated	33.8 (0.6)	294 (14)	1.0 (0.1)	64.9 (1.2)	562 (28)
0.5% EDTA	33.7 (0.8)	303 (20)	1.0 (0.1)	64.6 (1.5)	578 (20)
1.0% EDTA	33.7 (0.9)	297 (16)	1.0 (0.1)	64.7 (1.7)	567 (31)
3.0% EDTA	34.6 (1.0)	304 (12)	1.0 (0.1)	66.5 (1.9)	582 (24)
0.2% EPG	35.2 (1.0)	306 (15)	1.0 (0.2)	67.6 (1.9)	584 (29)
0.5% EDTA + 0.2% EPG	36.7 (0.9)	327 (9)	1.1 (0.1)	70.6 (1.7)	626 (18)
0.5% EDTA + 0.2% EPG → 10% NaOH	42.5 (0.3)	274 (9)	0.8 (0.1)	83.0 (0.6)	527 (17)

[1] Composite stiffness and UTS were determined at $V_f = 0.5$ based on the results shown in Fig. 8a and b, and composites failure strain was shown as the average value of composite failure strain with different fibre content shown in c.
[2] Effective fibre stiffness and strength were established based on the results shown in Fig. 8.

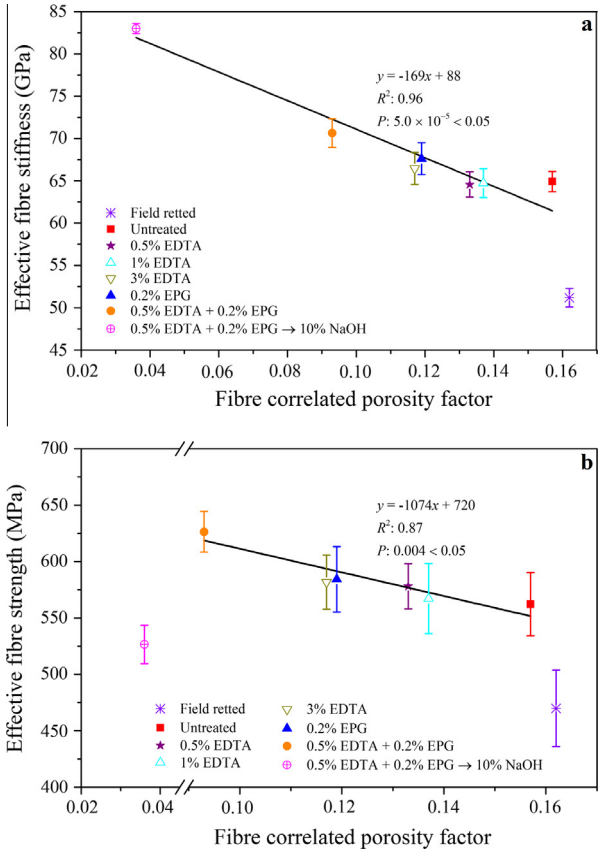

Fig. 9. Effective fibre stiffness (a) and effective fibre strength (b) versus fibre correlated porosity factor (α_{pf}). (For interpretation of the references to color in this figure legend, the reader is referred to the web version of this article.)

can be regarded as the individual fibre reinforced composites with matrix polymers of non-cellulosic components including pectin, hemicellulose and lignin. Hence, changes in hemp fibre properties with fibre treatments can be analogized to the changes in hemp fibre/epoxy composites as discussed above. EDTA and EPG removed pectin from hemp fibres, especially the middle lamella between fibres, resulting in weakened interface between fibres and matrix polymers. The mechanical properties of hemp fibres were thereby reduced (Table 2). Similarly, NaOH treatment removed parenchyma cells between fibres and degraded hemicellulose in hemp fibres resulted in loosened fibre structure (Fig. 2) and improved fibre surface cleanliness (Fig. 3). Those changes in fibre structure resulted in cellulosic fibre/non-cellulosic polymers composites with higher porosity contents and weakened interfaces between fibre and matrix polymers. In addition, the removal of hemicellulose can reduce fibre properties due to the disrupted cellulose-hemicellulose interlocked network. Therefore, fibre stiffness and strength decreased dramatically after NaOH treatment (Table 2).

Comparison of structure properties of hemp fibres and hemp fibre/epoxy composites demonstrated that changes in fibre properties and the interfaces between fibre and matrix polymers could explain the changes in fibre and fibre/epoxy composite properties. In addition, the comparison provided knowledge on how to optimize the properties of fibre/epoxy composites through fibre treatments.

4. Conclusion

The impacts of pectin and hemicellulose removal from hemp fibres on morphology and mechanical properties of hemp fibres, and on the mechanical properties of fibre/epoxy composites were studied. Pectin and hemicellulose were removed from fibres by EDTA and enzyme treatments, and 10% NaOH treatment, respectively. The removal of pectin removed epidermal and parenchyma cells, produced more void spaces between fibres and resulted in improved fibre impregnation with epoxy matrix. These changes contributed to improved mechanical properties of composites. A combination of 0.5% EDTA and 0.2% EPG resulted in greatest removal of pectin (up to 80%), best fibre separation and greatest improvement in mechanical properties of fibre/epoxy composites with a stiffness of ~37 GPa and strength of ~327 MPa at $V_f = 0.50$. Removal of hemicellulose further improved fibre separation and cleanliness of fibre surfaces. As a result, the composites made with fibres treated with 0.5% EDTA combined with 0.2% EPG followed by 10% NaOH had the lowest porosity factor of 0.04. Removal of hemicellulose increased the stiffness of composites, but decreased composite strength.

Acknowledgements

The authors are grateful to the Danish Council for Independent Research supporting the CelFiMat project (No. 0602-02409B: "High quality cellulosic fibres for strong biocomposite materials"). The financial support of China Scholarship Council, China (CSC, no. 201304910245) for Ming Liu's Ph.D. project is acknowledged. The support for short-term scientific mission from Nordforsk Researcher Network (Norway) to Ming Liu in June 2015 is acknowledged. Bo Madsen from Technical University of Denmark is acknowledged for access to composite production and physical tests. In addition, Jonas Kreutzfeldt Heininge and Sinh Hy Nguyen from Technical University of Denmark are thanked for technical support.

References

[1] Madsen B, Thygesen A, Lilholt H. Plant fibre composites–porosity and stiffness. Compos Sci Technol 2009;69:1057–69.
[2] Santamala H, Livingston R, Sixta H, Hummel M, Skrifvars M, Saarela O. Advantages of regenerated cellulose fibres as compared to flax fibres in the processability and mechanical performance of thermoset composites. Compos Part A Appl Sci Manuf 2016;84:377–85.
[3] Pickering KL, Beckermann GW, Alam SN, Foreman NJ. Optimising industrial hemp fibre for composites. Compos Part A Appl Sci Manuf 2007;38:461–8.
[4] Liu M, Fernando D, Daniel G, Madsen B, Meyer A, Ale M, et al. Effect of harvest time and field retting duration on the chemical composition, morphology and mechanical properties of hemp fibers. Ind Crops Prod 2015;69:29–39.
[5] Blamey FPC. A role for pectin in the control of cell expansion. Soil Sci Plant Nutr 2003;49:775–83.
[6] van der Werf HMG, van der Veen JEH, Bouma ATM, ten Cate M. Quality of hemp (*Cannabis sativa* L.) stems as a raw material for paper. Ind Crops Prod 1994;2:219–27.
[7] Liu M, Fernando D, Meyer AS, Madsen B, Daniel G, Thygesen A. Characterization and biological depectinization of hemp fibers originating from different stem sections. Ind Crops Prod 2015;76:880–91.
[8] Mohnen D. Pectin structure and biosynthesis. Curr Opin Plant Biol 2008;11:266–77.
[9] Vincken J-P, Schols HA, Oomen RJFJ, McCann MC, Ulvskov P, Voragen AGJ, et al. If homogalacturonan were a side chain of rhamnogalacturonan I. Implications for cell wall architecture. Plant Physiol 2003;132:1781–9.
[10] Liners F, Letesson JJ, Didembourg C, Van Cutsem P. Monoclonal antibodies against pectin: recognition of a conformation induced by calcium. Plant Physiol 1989;91:1419–24.
[11] Davis MAF, Gidley MJ, Morris ER, Powell DA, Rees DA. Intermolecular association in pectin solutions. Int J Biol Macromol 1980;2:330–2.
[12] Walkinshaw MD, Arnott S. Conformations and interactions of pectins. II. Models for junction zones in pectinic acid and calcium pectate gels. J Mol Biol 1981;153:1075–85.
[13] Hu W, Ton-That MT, Denault J, Rho D, Yang J, Lau PCK. Comparison between dew-retted and enzyme-retted flax fibers as reinforcing material for composites. Polym Eng Sci 2012;52:165–71.
[14] Benen JAE, Kester HCM, Visser J. Kinetic characterization of *Aspergillus niger* N400 endopolygalacturonases I, II and C. Eur J Biochem 1999;259:577–85.
[15] Adamsen APS, Akin DE, Rigsby LL. Chelating agents and enzyme retting of flax. Text Res J 2002;72:296–302.
[16] Stuart T, Liu Q, Hughes M, McCall RD, Sharma HSS, Norton A. Structural biocomposites from flax – Part I: effect of bio-technical fibre modification on composite properties. Compos Part A Appl Sci Manuf 2006;37:393–404.
[17] Griko YV. Energetics of Ca(2+)-EDTA interactions: calorimetric study. Biophys Chem 1999;79:117–27.
[18] Puls J, Janzon R, Saake B. Comparative removal of hemicelluloses from paper pulps using nitren, cuen, NaOH, and KOH. Lenzinger Berichte 2006;86:63–70.
[19] Michalak M, Thomassen LV, Roytio H, Ouwehand AC, Meyer AS, Mikkelsen JD. Expression and characterization of an endo-1,4-β-galactanase from *Emericella nidulans* in *Pichia pastoris* for enzymatic design of potentially prebiotic oligosaccharides from potato galactans. Enzyme Microb Technol 2012;50:121–9.
[20] Bauer S, Vasu P, Mort AJ, Somerville CR. Cloning, expression, and characterization of an oligoxyloglucan reducing end-specific xyloglucanobiohydrolase from *Aspergillus nidulans*. Carbohydr Res 2005;340:2590–7.
[21] Thomassen LV, Larsen DM, Mikkelsen JD, Meyer AS. Definition and characterization of enzymes for maximal biocatalytic solubilization of prebiotic polysaccharides from potato pulp. Enzyme Microb Technol 2011;49:289–97.
[22] Lever M. Colorimetric and fluorometric carbohydrate determination with p-hydroxybenzoic acid hydrazide. Biochem Med 1973;7:274–81.
[23] Bradford MM. A rapid and sensitive method for the quantitation of microgram quantities of protein utilizing the principle of protein-dye binding. Anal Biochem 1976;72:248–54.
[24] Liu M, Silva DAS, Fernando D, Meyer AS, Madsen B, Daniel G, et al. Controlled retting of hemp fibres: effect of hydrothermal pre-treatment and enzymatic retting on the mechanical properties of unidirectional hemp/epoxy composites. Compos Part A Appl Sci Manuf 2016;88:253–62.
[25] Sluiter A, Hames B, Ruiz R, Scarlata C, Sluiter J, Templeton D, et al. Determination of structural carbohydrates and lignin in biomass. In: NREL Technical Report, NREL/TP-510-42618; 2011.
[26] Arnous A, Meyer AS. Comparison of methods for compositional characterization of grape (*Vitis vinifera* L.) and apple (*Malus domestica*) skins. Food Bioprod Process 2008;86:79–86.
[27] Fernando D, Daniel G. Exploring Scots pine fibre development mechanisms during TMP processing: impact of cell wall ultrastructure (morphological and topochemical) on negative behaviour. Holzforschung 2008;62:597–607.
[28] Cheung HY, Ho MP, Lau KT, Cardona F, Hui D. Natural fibre-reinforced composites for bioengineering and environmental engineering applications. Composites Part B 2009;40:655–63.
[29] Kovács A, Nemcsok DS, Kocsis T. Bonding interactions in EDTA complexes. J Mol Struct THEOCHEM 2010;950:93–7.
[30] Grant GT, Morris ER, Rees DA, Smith PJC, Thom D. Biological interactions between polysaccharides and divalent cations: the egg-box model. FEBS Lett 1973;32:195–8.
[31] Morris ER, Powell DA, Gidley MJ, Rees DA. Conformations and interactions of pectins. I. Polymorphism between gel and solid states of calcium polygalacturonate. J Mol Biol 1982;155:507–16.
[32] Duval A, Bourmaud A, Augier L, Baley C. Influence of the sampling area of the stem on the mechanical properties of hemp fibers. Mater Lett 2011;65:797–800.
[33] Charlet K, Baley C, Morvan C, Jernot JP, Gomina M, Bréard J. Characteristics of Hermès flax fibres as a function of their location in the stem and properties of the derived unidirectional composites. Compos Part A Appl Sci Manuf 2007;38:1912–21.
[34] Baley C. Analysis of the flax fibres tensile behaviour and analysis of the tensile stiffness increase. Compos Part A Appl Sci Manuf 2002;33:939–48.
[35] Callister WD. Materials science and engineering. 3rd ed. New York: John Wiley & Sons, INC.; 1994.

Paper VI

Ming Liu, Andrea Baum, Jügen Odermatt, Jens Berger, Liyun Yu, Birgitte Zeuner, Anders Thygesen, &Anne S. Meyer,

Oxidation of lignin in hemp fibers by laccase: Effects on mechanical properties of hemp fibers and unidirectional fiber/epoxy composites

Composites Part A: Applied Science and Manufacturing, 2016, (submitted)

Oxidation of lignin in hemp fibres by laccase: effects on mechanical properties of hemp fibres and unidirectional fibre/epoxy composites

Ming Liu[a], Andreas Baum[a], Jürgen Odermatt[b], Jens Berger[b], Liyun Yu[c], Birgitte Zeuner[a], Anders Thygesen[a], Jesper Holck[a], Anne S. Meyer[a,*]

[a] *Center for Bioprocess Engineering, Department of Chemical and Biochemical Engineering, Technical University of Denmark, 2800 Kongens Lyngby, Denmark.*

[b] *Chemical Wood Technology, University of Hamburg, Leuschnerstraße 91, D-21031 Hamburg, Germany*

[c] *The Danish Polymer Center, Department of Chemical and Biochemical Engineering, Technical University of Denmark, 2800 Kongens Lyngby, Denmark.*

* Corresponding author

Address as above, Tel.: +45 45252800; E-mail address: am@kt.dtu.dk

Abstract

Laccase activity catalyzes oxidation and polymerization of phenols. The effect of laccase treatment on the mechanical properties of hemp fibres and hemp fibre/epoxy composites was examined. Laccase treatment on top of 0.5% EDTA + 0.2% endo-polygalacturonase (EPG) treatments increased the mechanical properties of hemp fibres and fibre/epoxy composites. Comparing all fibre treatments, composites with 0.5% EDTA + 0.2% EPG + 0.5% laccase treated fibres had the highest stiffness of 42 GPa and the highest ultimate tensile strength (UTS) of 326 MPa at a fibre volume content of 50%. The thermal resistance of hemp fibres increased after laccase treatments, and the maximum degradation temperature increased about 5 °C. Cross-linking of hydroxycinnamates by laccase was not observed. Oxidation of lignin-OH groups by laccase was observed. We suggest that the increased mechanical properties of hemp fibres and fibre reinforced composites were due to laccase catalysed polymerization of lignin moieties in hemp fibres.

Keywords: A. Natural fibres; A. Polymer-matrix composites (PMCs); B: Mechanical properties; D: Thermal analysis.

1 Introduction

Cellulose-rich fibres have many unique advantages, such as environmental sustainability, low cost, low density, high stiffness and high strength to weight ratio [1]. Because of those unique advantages and increasing environmental awareness, research interest has been shifting to use natural fibres as substitute to man-made fibres in fibre reinforced composites in recent years [2,3].

The primary fibres of hemp (*Cannabis sativa*) are one of the most suitable, cellulose rich fibres for manufacturing strong biocomposites. These fibres are located in the outer part of the hemp stem beneath the epidermis [4]. The primary fibres are mainly composed of cellulose, hemicellulose, lignin, and pectin [5,6]. Cellulose consists of a linear chain of β-1,4-linked D-glucose units and is organized into microfibrils interlocked by glycans (e.g. xyloglucan, mannan, galactoglucomannan, and galactomannan) [7,8]. The cellulose microfibrils and the cross-linked glycans are previously considered as the two main components which provide cell wall strength. Furthermore, the interlocked network of microfibrils and glycans is embedded in a matrix of pectic substances, and the network is further reinforced with structural protein and aromatic substances (e.g. lignin and hydrocinnamates) [7,9,10].

Lignin is a heterogeneous aromatic biopolymer that forms a three-dimensional structure with ether and carbon-carbon linkage between different phenylpropanoid units, which have been identified as *p*-coumaryl (H type), coniferyl (G type) and sinapyl alcohols (S type) [11]. In hemp fibres, lignin is the main aromatic substances, which accounts for 2 −5% of dry matter of fibre cell walls [4,12]. Laccase (EC 1.10.3.2) is a copper-containing oxidase capable of reacting with a large variety of aromatic substances. It has been recognized that aromatic substances can be polymerized or cross-linked to form a complex structure by laccase enzymes[13–15]. The polymerization and cross-linking of those aromatic substances were suggested add mechanical strength to the cell walls [16,17].

In this study, laccase was used to treat hemp fibres. It was hypothesized that hemp fibre cell walls can be strengthened by laccase catalyzed cross-linking of feruloylated polysaccharides and by generating covalent bonds during lignin polymerization. As a result, mechanical properties of unidirectional hemp fibre-reinforced composites will be increased.

2 Materials and methods

2.1 Raw material and processing

2.1.1 Plant material and enzyme

Hemp (*Cannabis sativa* L.), variety USO-31, was grown in France (N 48.8526°, E 3.0190°(WGS84)) as described in detail by Liu et al. [4]. Hemp stem pieces with a length of 150 ± 10 mm were randomly collected from the stems. Before treatment, hemp bast fibre strips were manually peeled from the stem pieces, gently rinsed with warm water (40 °C) to remove dirt and then dried at 50 °C for 12 h.

The endo-polygalacturonase (EPG), derived originally from *Emericella nidulans*, was produced by fermentation of a *Pichia pastoris* clone (principally as described previously [18]) transformed with the gene AN4372.2 obtained from the Fungal Genetic Stock Center, Kansas State University, USA [19]. Laccase (EC 1.10.3.2) from *Trametes versicolor* was purchased from Sigma Chemical Co. The activity of endo-polygalacturonase and laccase were 17 U mg^{-1} and 15 U mg^{-1}, respectively, at applied conditions in this study.

The activity of EPG was determined by measuring the amount of liberated reducing ends [20] using 2 g L^{-1} polygalacturonic acid as substrate according to the procedure described previously [21]. One unit of the EPG activity is defined as the amount of enzyme (mg) required to liberate 1 µmol reducing ends per minute under the assay conditions. Laccase activity was measured by monitoring the oxidation of azinobis (3-ethylbenz-thiazoline)-6 sulphonate (ABTS) by the enzyme at 420 nm [22]. One unit of laccase activity is defined as the amount of enzyme (mg) required to oxidize 1 µmol ABTS per minute under the assay conditions.

2.1.2 Enzymatic treatment

Hemp bast fibre strips were first treated with 0.5% (g mL^{-1}) EDTA (EDTA.2Na·2H_2O) and 0.2% (g protein per g dry matter) EPG at 40 °C for 4 h. At the end of each treatment, the wet bast fibre strips were rinsed thoroughly with MilliQ water. After fibres were treated with 0.5% EDTA and 0.2% EPG (0.5% EDTA + 0.2% EPG), fibres were divided into two lots: one lot was treated with 0.5% (g protein/g dry matter) laccase; another was first treated with 10% NaOH (g cm^{-1}) for 4 h at 60°C followed by 0.5% (g protein per g dry matter) laccase treatment at 40 °C for 1.5 h. At the end of each treatment, the wet bast fibre strips were rinsed thoroughly with MilliQ water prior to the next treatment.

Alkali treatment was carried in a water bath with agitation of 100 rpm. Enzymatic treatments were carried out at pH 6.0 using 25 mmol dm^{-3} citrate buffer with a liquid (cm^3) to fibre (g) ration of 40:1. At above conditions, the concentration of EPG and laccase was 34 and 75 U g^{-1} (units per gram fibre).

2.2 Characterization and testing of hemp fibres

2.2.1 Extraction and analysis of wall bound ester linked phenolic compounds

The dried bast fibres were firstly ground with a microfine grinder (IKA, MF 10.1; IKA®-Werke GmbH) through a 0.5-mm screen. Grinded hemp fibres (~ 1.0 g) and the internal standards (0.5 mg of *p*-anisic acid and *trans*-cinnamic acid) were added into each sample. Saponification of grinded samples with 2 M NaOH (25 mL for each sample) was carried out for 18 h under nitrogen and protected from light at 25 °C in a water bath with agitation of 100 rpm. The solution was then acidified to pH < 2 with HCl (37%) and extracted three times with ethyl acetate (25 mL, three times). The phenolic ethyl acetate extracts were evaporated at room temperature under reduced pressure using a vacuum evaporator, and the samples redissolved in 20 mL 50% (v/v) aqueous methanol prior to analysis by HPLC.

Phenols extracted from fibre cell walls were analyzed using reversed phase- high performance liquid chromatography (RP-HPLC) with diode array detection, Chemstation 1100 series, Hewlett-Packard, and an ODS-L Optimal (250 × 4.6 mm, 5 µm) column from Capital HPLC as described by Agger et al. [23]. Phenolic compounds were identified by liquid chromatograph electrospray ionization mass spectrometry (LC-ESI-MS) on an Amazon SL ion trap (Bruker Daltonics, Bremen Germany) coupled to an UltiMate 3000 UHPLC from Dionex (Sunnyvale, CA, USA). The chromatography was performed on the same column and under the identical conditions as RP-HPLC. The electrospray was operated in negative mode with enhanced resolution mode and a scan range from 100-2000 m/z, smart parameter setting of 200 m/z, capillary voltage at 4.5 kV, end plate off-set 0.5 kV, nebulizer pressure at 3.0 bar, dry gas flow at 12.0 L min^{-1}, and dry gas temperature at 280 °C. Collision-induced dissociation (CID) fragmentation was performed using SmartFrag enhanced amplitude ramping from 80 to 120%, fragmentation time 20 ms. The presence of phenolic compounds were confirmed by results of LC-MS/MS^2 based on external standards and previously described fragmentation pattern [24]. In addition, UV spectra of external standards was also used as references for the confirmation of phenolic compounds, and quantification of each compound based on a standard curve of t-ferulic acid using the response factors of Waldron et al [25].

2.2.2 Chemical composition analysis

The dried bast fibres were ground with a microfine grinder (IKA, MF 10.1; IKA®-Werke GmbH) through a 1-mm screen. Ground samples were extracted in a Soxhlet apparatus [4], and then the

extractive-free fibres were hydrolysed using a two-step sulfuric acid process from National Renewable Energy Laboratory (NREL) [26]. After acid hydrolysis, the hydrolysate was collected for monosaccharide analysis, and Klason lignin content (acid-insoluble residues) was gravimetrically determined. The chemical composition of the hydrolysate was analysed by high-performance anion-exchange chromatography with pulsed amperometric detection (HPAEC-PAD) [27].

2.2.3 Diffuse reflectance near infrared spectroscopy (NIR)

Diffuse reflectance NIR spectra were obtained using a monochromator-based XDS instrument connected to a Rapid Content Analyzer (FOSS ANALYTICAL, Denmark) at wavelengths between 400 nm – 2500 nm and a resolution of 2 nm^{-1} as previously described [28]. Approx. 1 g of grinded samples (0.5 mm) was applied for the analysis.

2.2.4 Attenuated total reflectance (ATR) - Fourier transform infrared spectroscopy (FTIR)

ATR-FTIR analysis of differently treated samples was carried out using a Thermo Scientific Nicolet iS50 FT-IR spectrometer. For the analysis, a few milligrams of grinded samples (0.5 mm) were applied to a diamond cell and the transmission spectra between 400 and 4000 cm-1 were measured at room temperature.

2.2.5 Thermogravimetric analysis (TGA)

Dynamic thermogravimetric measurements were performed using a TA instrument Discovery TGA. Temperature programs for dynamic tests were run from room temperature to 600 °C at a heating rate of 10 °C min^{-1}. The tests were carried out under nitrogen atmosphere (25 mL min^{-1}).

2.2.6 Pyrolysis gas chromatography mass spectrometry (Py-GC/MS)

The dried bast fibres were ground with a microfine grinder (IKA, MF 10.1; IKA®-Werke GmbH) through a 0.25-mm screen. Approximately 100 µg of the milled sample was weighted by using a microbalance in pyrolysis cup and introduced into Py-2020iD micro-furnace pyrolyzer (Frontier Laboratories Ltd.) equipped with an autosampler (AS-1020E). The pyrolysis system was interfaced to a GC/MS (6890/5973N Agilent Technologies, USA).

Pyrolysis of samples was carried out at temperature of 500 °C. The pyrolysis interface temperature was kept at 360 °C. The GC inlet and the GC/MS interface were kept at 280 °C. The volatile pyrolysis products were separated on a low polarity VF-5ms (Agilent J&W) fused-silica capillary column (60 m × ID 0.25 mm, 0.25 µm film thickness) with helium as carrier gas (2 mL min^{-1}). For effective separation of

the phenol components, the oven temperature was kept at 45 °C for 4 min and raised to 280 °C at 3 °C min^{-1}, and kept at 280 °C for 20 min. The mass spectrometer was operated in EI mode (70 eV) at a source temperature of 230 °C.

Lignin based volatile components were identified by comparison of their mass spectra to NIST and in-house libraries. From the pyrograms of pure lignins (wheat straw and beech) two representative mass fragments per peak of more than 64 lignin related peaks were selected to establish a SIM (selected ion monitoring) method. 8 replicates were carried out using this SIM method. The different samples were analyzed in random order. For the principal component analysis (PCA) one mass fragment for each pyrolysis product was used. The peak area of each peak was mean normalized. Unscrambler 10.0 was used for PCA to estimate the similarities and dissimilarities in lignin related pyrolysis products from differently treated hemp fibres [29].

2.2.7 Tensile properties of fibres

Bast fibre strips (60 mm long × 1 mm wide) of mass in the range of 5 – 20 mg were used for tensile testing. The preparation of test specimens has previously been described in detail [4]. Tensile testing was performed using an Instron Testing Machine 2710-203 equipped with a 1kN load cell. The gauge length was 10 mm and the displacement rate was 0.5 mm min^{-1} (corresponding to a strain rate of 5% min^{-1}). Tensile testing was performed on 20 specimens for each treatment. The cross-sectional area was determined from measured fibre mass and fibre length, and an assumed fibre density (i.e. 1500 kg dm^{-3} [30]). Stiffness (linear regression in the strain interval 0.05 – 0.25%), ultimate tensile strength (UTS), and failure strain were determined based on the measured stress-strain curves.

2.3 Manufacturing and characterization of composites

2.3.1 Manufacturing of composites

Composites manufacturing including the setup for moulding processing, curing of the epoxy matrix, demoulding, and composite specimens preparations for tensile testing was done as described previously [31]. In brief, the treated hemp bast fibre strips were manually aligned to allow the fibres to be processed into unidirectional composites. Fibre strips were firstly cut to a length of 140 mm, and the fibre strips were then justified to a bunch of fibre strips with masses in the range 0.6 – 2.3 g. The bunch of fibre strips was then put in each mould chamber. Afterwards, a press beam was placed on the top of the fibre strips in each chamber, and two insert beams were used to fix the height of the mould chambers to 2 mm. Epoxy

resin (Araldite® LY 1568) and its amine hardener (Aradur® 3489) were mixed at a 100/28 mass ratio and degassed in a vacuum oven. After demoulding, composite samples with dimensions 140 mm × 10 mm × 2 mm were obtained and then glass fibre/epoxy tabs with lengths of 50 mm were mounted on composite specimens using epoxy glue (DP 460).

2.3.2 Volumetric composition of composites

By varying the amount of fibres (m_f) in the mould chambers, the fibre weight content (w_f) in the composites was varied in the range 0 – 0.70. When the w_f was below 0.30, the composite specimens had irregular surfaces, and their thickness could not be measured accurately. For the cases, composite density (ρ_c) was determined by the buoyancy method (Archimedes principle) using water as the displacement medium. When W_f was above 0.30, the composite specimens had flat surfaces, and ρ_c could be accurately calculated based on the composite dimensions (i.e. length, width and thickness).

The volumetric composition of composite samples was determined as described by Liu et al. [31]. In the composites, the porosity (V_p) was assumed to be a linear function of the fibre volume content (V_f), where the established proportionality constant is equal to the fibre correlated porosity constant α_{pf} as expressed in Eq.1[32]. The matrix correlated porosity factor (α_{pm}) was assumed to be 0.

$$V_p = \alpha_{pf} \times V_f \quad (1)$$

2.3.3 Tensile properties of composites

For tensile testing of the composite specimens, an Instron Testing Machine 5566 with a load cell of 10 kN was used. Strain measurements were conducted using two extensometers and the displacement rate was 1 mm min^{-1} (corresponding to a strain rate of 2.5% min^{-1}). Based on the measured stress-strain curves, composite stiffness (E_c) (linear regression in the strain interval 0.05 – 0.25%) and ultimate tensile strength (UTS) were determined. For each treatment, at least 10 specimens with varied fibre content were tested. The rule of mixtures (ROM) model [32] was used to determine the effective fibre stiffness (E_f) and fibre strength (UTS_{fu}) in the composites by linear regression versus fibre volume content (V_f) using Eqs.2 and 3, respectively. The intercept was set equal to the measured matrix stiffness (E_m) and strength (UTS_m^*) at the average failure strain of the composites.

$$E_c = V_f E_f + V_m E_m = E_m + V_f \left(E_f - E_m(1 + \alpha_{pf})\right) = E_m + kV_f \quad (2)$$

$$UTS_c = V_f UTS_{fu} + V_m UTS_m^* = UTS_m^* + V_f \left(UTS_{fu} - UTS_m^*(1 + \alpha_{pf})\right) = UTS_m^* + kV_f \quad (3)$$

where the subscripts c, f and m indicate composite, fibres, and matrix, respectively. *k* is the slope of the linear regression line, i.e. of E_c vs. V_f and UTS_c vs. V_f. Effective fibre stiffness (E_f) and tensile strength (UTS_{fu}) can thus be calculated from Eqs.2 −3 at $V_f = 1.0$ by using an extrapolation method.

3 Results and discussion

3.1 Mechanical and thermal properties fibres and composites

3.1.1 Tensile properties of fibres

After fibres were treated with 0.5% EDTA and 0.2% EPG, the stiffness, ultimate tensile strength (UTS) and failure strain of fibres decreased, respectively, from 29 GPa, 770 MPa and 5%, to 15 GPa, 560 MPa and 4% (Table 1). The decrease in the mechanical properties was attributed to the decrease in the bonding between fibres and non-cellulosic matrices after pectin removal by EDTA and EPG [33]. After the fibres were further treated with 0.5% laccase, the stiffness and UTS of fibres significantly increased to 31 GPa and 840 MPa, respectively, but the failure strain of fibres decreased to 3%. In previous study, increased mechanical properties of laccase treated plantain fibre bundles after laccase treatment has been observed [34].

After the fibres were treated with 10% NaOH on top of 0.5% EDTA and 0.2% EPG treatment, only slight decrease in UTS were noticed (Table 1). After fibres were further treated with 0.5% laccase, an increase in the stiffness and UTS of fibres, respectively, from 14 GPa and 430 MPa, to 17 GPa and 490 MPa was achieved, but the increases in both stiffness and UTS were not statistically significant (Table 1).

3.1.2 Thermal properties of fibres

Thermogravimetric analysis (TGA) was used to measure the thermal stability and decomposition of untreated and differently treated fibres (Fig. 1). Untreated fibres started to decompose at around 230 °C, while treated fibres were decomposed at a lower rate and started to decompose at around 250 °C. The maximum decomposition temperature was determined and shown in Table 2. The maximum decomposition temperature increased from 345 °C to 346 °C and to 361 °C, respectively, after fibres were treated with 0.5% EDTA + 0.2% EPG and 0.5% EDTA + 0.2% EPG → 10% NaOH. The higher resistance of treated fibres to thermal decomposition is due to the removal of hemicellulose and pectic substances by enzymatic and chemical treatments [35].

Furthermore, an increase in the maximum decomposition temperature after laccase treatments was noticed (Fig. 1 and Table 2). The maximum decomposition temperature increased to 350.2 °C from

345.7 °C after fibres were treated with laccase on top of 0.5% EDTA + 0.2% EPG treatments. In addition, the maximum decomposition temperature increased to 367.9 °C from 360.8 °C after fibres were treated with laccase on top of 0.5% EDTA + 0.2% EPG → 10% NaOH treatments. In previous study, the increased maximum degradation temperature of plantain fibre bundles after laccase treatment has been observed [34]. The increased thermal stability of the laccase treated plantain fibre bundles has been explained by the generation of phenoxyl radicals in the fibre lignin which can induce the further generation of covalent bonds and cross-linking of aromatic substances in the fibre [34].

Natural fibres are primarily composed of three classes of polysaccharides: cellulose, hemicellulose and lignin. Hemicellulose degradation occurs at 200 – 260 °C, which is lower than the degradation temperature for cellulose (240 – 350 °C) and lignin (290 – 390 °C) [34]. Therefore the thermal degradation of natural fibres is usually divided into three stages: (a) moisture loss; (b) degradation of cellulose and hemicellulose; (c) degradation of other non-cellulosic components (i.e. lignin) [36]. The increased thermal stability of hemp fibres treated with laccase was presumably due to the modification of lignin by laccase.

3.1.3 Tensile properties of hemp fibre/epoxy composites

In Fig. 2, the starting points of model lines at W_f =0 show the measured neat epoxy stiffness and failure strength, respectively, at the average failure strain of the composites. In comparison of the slopes (*k*) established by linear regression of E_c and UTS_c versus V_f, of the composites with differently treated fibres, it can be found that the composites containing 0.5% EDTA + 0.2% EPG treated fibres had higher slopes for stiffness (68 GPa) and UTS (598 MPa) than that for composites containing untreated fibres (Fig. 2).

A significant increase in the stiffness of composites with fibres treated with laccase on top of 0.5% EDTA + 0.2% EPG treatments were observed (Fig. 2a), as indicated by the slopes of the lines increasing from 67.8 GPa for composites with 0.5% EDTA + 0.2% EPG treated fibres, to 79.7 GPa for the composites with 0.5% EDTA + 0.2% EPG → 0.5% Laccase treated fibres. No apparent changes in the UTS of composites after fibres were treated laccase were found. By contrast, when fibres were treated with 10% NaOH prior to laccase treatments, no noticeable changes in stiffness (Fig. 2a) and UTS (Fig. 2b) of the composites with the resultant fibres were observed. In comparison of all samples, 0.5% EDTA + 0.2% EPG → 0.5% Laccase treated fibres had the best effective fibre properties with the highest stiffness

of 82 GPa and strength of 630 MPa (Table 3). In addition, composites with such treated fibres had the best mechanical properties with the highest stiffness of 42 GPa and strength of 330 MPa at a fibre volume content of 50% (Table 3), which was 56% and 33% higher, respectively, compared to the mechanical properties of composites with field retted fibres [31].

The fibre correlated porosity factor (α_{pf}) of composites manufactured with the differently treated hemp fibres was determined based on the experimental values of V_p and V_f using Eq. 1 (Fig. 3). As shown, composites with untreated fibres had the highest porosity factor of 0.16. By contrast, composites with 0.5% EDTA + 0.2% EPG treated fibres had much lower porosity factors of 0.09. As hemp fibres were further treated with 10% NaOH, the porosity factor of the composites decreased further to 0.04. The decrease in the porosity of composites after pectin removal by 0.5% EDTA + 0.2% EPG and after hemicellulose removal by 10% NaOH were previously used to explain the changes in the mechanical properties of composites [33].

Laccase treatment did not decrease the porosity of the composites, as indicated by the non-significant changes in porosity factors of the composites after laccase treatments (Fig. 3). Hence, the improvement in the mechanical properties of composites (Fig. 2) was caused by other factors such as the oxidative cross-linking of hydroxycinnamates and enzymatic polymerization of lignin by laccase. In previous study, it has been known that polymerization of lignin during laccase treatment to form complex products and cross-linking of feruloylated polysaccharides can be completed by laccase enzymes[13–15]. The polymerization and cross-linking of those aromatic substances were suggested add mechanical strength to the cell walls [16,17].

3.2 Phenolic acids and lignin changes

3.2.1 Lignin hydroxyl groups changes (NIR)

The effect of laccase treatments on lignin in hemp fibres were assessed by near infrared spectroscopy (NIR). It has been reported that oxidation of lignin-OH group can be carried out with the presence of laccase, and radicals were produced and covalent bonds (radical-radical coupling) can be further generated due to the interactions of those radicals [15,37]. NIR can provide information of organic compounds regarding the first overtone and combined overtone of –OH group (e.g. lignin-OH group). The first overtone of the lignin-OH vibrations occurs at 1400 – 1520 nm, and the first and second overtones of the lignin-OH vibrations are also seen at 1635 – 1825 nm [38]. The NIR spectra from 1100 –

1860 nm of differently treated hemp fibres were selected for principal component analysis (PCA) to reveal the effect of laccase on the lignin-OH in hemp fibres.

The NIR spectra were processed by standard normal variate (SNV) prior to PCA. The score plots from PCA (Fig. 4a) showed that there was a systematic difference among untreated fibres, 0.5% EDTA + 0.2% EPG treated fibres, and 0.5% EDTA + 0.2% EPG → 10% NaOH treated fibres. The first principal component PC1 described 94% of the variance among those samples. The systematic difference was primarily due to the pectin removal from 0.5% EDTA + 0.2% EPG, and hemicellulose removal by 10% NaOH, as indicated by the changes in chemical composition in Table 4.

The third principal component PC3 described 2% of the variance, which could separate the near infrared spectra for samples treated with and without laccase (i.e. 0.5% EDTA + 0.2% EPG vs. 0.5% EDTA + 0.2% EPG → 0.5% Laccase, and 0.5% EDTA + 0.2% EPG → 10% NaOH vs. 0.5% EDTA + 0.2% EPG → 10% NaOH → 0.5% Laccase). Therefore, the 2% of the variance represents the effect of laccase treatments. As shown in the PC3 loadings, the variance was mainly due to the changes occurred in the NIR spectra between 1400 – 1520, in particular at 1432 nm (Fig. 4b), which were assigned for the first overtone of lignin-OH vibrations [38]. The NIR spectra of differently treated fibres were processed by SNV, mean centering, and then displayed in Fig. 5. The changes reflected in the PC3 loadings can be visualized in the NIR spectra. As shown, the peak shifted to 1432 nm from lower wavelength (i.e. 1410 nm and 1421 nm) after fibres were treated with laccase, regardless of the prior treatments. The shifting of the peak in the NIR spectra was probably due to the oxidation of lignin hydroxyl groups by laccase.

3.2.2 Py-GC/MS

A PCA was calculated using lignin related signals (peaks from the pyrogram which will be called variables further on). All samples cluster according to different types of fibre treatments as shown in the PC1-PC2 scores plot (Fig. 6a). Approximately 66% of the validated variations in all the tested samples are described by PC1 (42%) and PC2 (24%). The PC 1 – PC 2 scores plot allows to distinguish between different fibre treatments except between fibre treatment of 0.5% EDTA + 0.2% EPG → 10% NaOH and 0.5% EDTA + 0.2% EPG → 10% NaOH → 0.5% Laccase. The score plot showed a systematic difference between fibres treated with 0.5% EDTA + 0.2% EPG and 0.5% EDTA + 0.2% EPG → 0.5% Laccase. However, no systematic difference was noted between fibres treated with 0.5% EDTA + 0.2% EPG → 10% NaOH and 0.5% EDTA + 0.2% EPG → 10% NaOH → 0.5% Laccase.

The loading plots (Fig. 6b and c) revealed that 0.5% EDTA + 0.2% EPG treated fibres can be differentiated from 0.5% EDTA + 0.2% EPG → 0.5% Laccase treated fibres primarily because of the differences in content of 4-vinylphenol (49/120 FI) and cresol (39/107 FI). Of course also other variables contributed to the clustering but only the most important were mentioned here. Since 4-vinylphenol and cresol belong to the H-moiety in lignin, the results thus indicated there was some changes occurred to lignin, especially the H-lignin moiety during laccase treatment on hemp fibres when they were not pre-treated with 10% NaOH. When fibres were treated with 10% NaOH prior to laccase treatment, no clear changes in lignin were found during laccase treatment. Oxidation and polymerization of cresol and vinylphenol by laccase was observed in previous studies [39–41].

3.2.3 Lignin content changes

As discussed above, the oxidation of lignin by laccase may play a role in increasing the mechanical properties of fibres and fibre/epoxy composites via lignin polymerization. Mechanical properties of fibres and fibre/epoxy composites significantly increased after fibres were treated with laccase on top of 0.5% EDTA and 0.2% EPG treatments. No increase in the mechanical properties of fibres and fibre/epoxy composites was found once 10% NaOH treatment was applied prior to laccase treatments (Fig. 2). The differences in the responses of mechanical properties of fibres and fibre/epoxy composites to the laccase treatments presumably resulted from the alkali treatments, and the effect of alkali treatments on fibres was examined by FTIR (Fig. 7). After alkali treatment, absorbance of the resultant fibres at 1232 – 1270 cm^{-1}, 1632 cm^{-1}, and 1730 cm^{-1} decreased, and the corresponding absorbance peaks disappeared in the FTIR spectra (Fig. 6). In the FTIR spectra, 1232 – 1270 cm^{-1} was assigned for the vibrations of aryl-alkyl ether in lignin, and 1632 cm^{-1} was assigned for benzene stretching ring related with lignin, and 1730 cm^{-1} was also assigned for aromatic signals [42]. The results demonstrated that alkali treatment removed at least some of lignin from hemp fibres. The removal of lignin by alkali treatment was also corroborated by the significant decrease in Klason lignin content from 5% for fibres treated without 10% NaOH to 2.7 – 2.9% for fibres treated with 10% NaOH (Table 4). As a result, less lignin was available for the catalyzed polymerization reactions with laccase. Therefore, no change in the mechanical properties of fibres and fibre/epoxy composites after laccase treatments was noticed when alkali treatment was applied prior to laccase treatments (Fig. 2).

3.2.4 Phenolic acids changes

Hydroxycinnamic acids are a class of aromatic acids, which are present in small quantities in cell walls of hemp fibres [43]. It has been shown that hydroxycinnamic acids (e.g. ferulic acid) actively participate in the cross-linking of arabinoxylans in hemicellulose polymers of plant cell walls, where some arabinose residues are esterified at the O -5 position with a ferulate [14,44]. Other studies demonstrate that hydroxycinnamates serve as linkages between polysaccharides (e.g.arabinoglucuronoxylan) and lignin, and a fraction of the linkages involve a structure of polysaccharide-ester-hydroxycinnmic acid (e.g. ferulic acid)-ether-lignin [45,46].

In hemp fibre cell wall extracts, hydroxycinnamic acids, benzoic acids and their derivatives were identified (Fig. 8), including ferulic acid, coumaric acid, vanillic acid, 4-hydroxybenzaldehyde, and diferulates. The amount of hydroxycinnamic acids in hemp fibre cell walls was lower than 0.1% (by weight), and only infinitesimal amount of ferulic acid was observed (< 0.005%, by weight). However, diferulates in 8, 5′ benzofuran diferulic acid form were observed with the amount of around 0.1% (by weight). As shown in Fig. 8, phenolic acids and their derivatives disappeared after alkali treatments, but no noticeable changes in the content of hydroxycinnamic acids and their derivatives were found before and after laccase treatments.

4 Conclusion

After pectin and hemicellulose were sequentially removed from hemp fibres, the fibres were further treated with laccase to polymerize the phenolic compounds in hemp fibres. The mechanical properties of the laccase treated hemp fibres and the resultant fibre/epoxy composites showed an increase in UTS and stiffness, in particular for the 0.5% EDTA + 0.2% EPG → 0.5% Laccase treated fibres. The thermal resistance of hemp fibres also increased after laccase treatments. There was no indication that hydroxycinnamates were oxidatively cross-linked by laccase treatments, while there was evidence that lignin hydroxyl groups were oxidized by laccase treatments. Once a part of the lignin was removed by alkali treatment, the improvement in mechanical properties of fibres and fibre/epoxy composites by laccase treatments were less profound compared to the case that all the lignin was remained before laccase treatments. Oxidation of lignin forming a much stiffer structure provides a new tool to reshape and strengthen cellulose fibres for the application in high-quality fibre reinforced composites.

5 Acknowledgements

The authors are grateful to the Danish Council for Independent Research supporting the CelFiMat project (No. 0602-02409B: "High quality cellulosic fibres for strong biocomposite materials"). The financial support of China Scholarship Council, China (CSC, no. 201304910245) for Ming Liu's Ph.D. project is acknowledged. Bo Madsen from Technical University of Denmark is acknowledged for access to composite production and physical tests. In addition, Jonas Kreutzfeldt Heininge from Technical University of Denmark is thanked for technical support.

6 References

[1] Shah DU, Schubel PJ, Clifford MJ. Can flax replace E-glass in structural composites? A small wind turbine blade case study. Compos Part B Eng 2013;52:172–81.

[2] Summerscales J, Dissanayake NPJ, Virk AS, Hall W. A review of bast fibres and their composites. Part 1 – Fibres as reinforcements. Compos Part A Appl Sci Manuf 2010;41:1329–35.

[3] Stuart T, Liu Q, Hughes M, McCall RD, Sharma HSS, Norton A. Structural biocomposites from flax - Part I: Effect of bio-technical fibre modification on composite properties. Compos Part A Appl Sci Manuf 2006;37:393–404.

[4] Liu M, Fernando D, Daniel G, Madsen B, Meyer A, Ale M, et al. Effect of harvest time and field retting duration on the chemical composition, morphology and mechanical properties of hemp fibres. Ind Crops Prod 2015;69:29–39.

[5] Liu M, Fernando D, Meyer AS, Madsen B, Daniel G, Thygesen A. Characterization and biological depectinization of hemp fibres originating from different stem sections. Ind Crops Prod 2015;76:880–91.

[6] Thygesen A, Liu M, A. M, Daniel G. Hemp fibres: Enzymatic effect of microbial processing on fibre bundle structure. Risoe Int Symp Mater Sci Proc 2013;34:373–80.

[7] Carpita NC, Gibeaut DM. Structural models of primary cell walls in flowering plants: consistency of molecular structure with the physical properties of the walls during growth. Plant J 1993;3:1–30.

[8] Peña MJ, Vergara CE, Carpita NC. The structures and architectures of plant cell walls define dietary fibre composition and the textures of foods. In: McCleary B V., Prosky L, editors. Adv. Diet. fibre Technol., Blackwell Science; 2008, p. 42–60.

[9] Chesson A, Gordon AH, Lomax JA. Substituent groups linked by alkali-labile bonds to arabinose and xylose residues of legume, grass and cereal straw cell walls and their fate during digestion by rumen microorganisms. J Sci Food Agric 1983;34:1330–40.

[10] Markwalder HU, Neukom H. Diferulic acid as a possible crosslink in hemicelluloses from wheat germ. Phytochemistry 1976;15:836–7.

[11] Lange H, Decina S, Crestini C. Oxidative upgrade of lignin - Recent routes reviewed. Eur Polym J 2013;49:1151–73.

[12] Rrez Ä, Odri ISMR, Guez Ä. Chemical characterization of lignin and lipid fractions in industrial hemp bast fibres used for manufacturing high-quality paper pulps. Agric Food Chem 2006;54:2138–44.

[13] Zaidel DNA, Arnous A, Holck J, Meyer AS. Kinetics of enzyme-catalyzed cross-linking of feruloylated arabinan from sugar beet. J Agric Food Chem 2011;59:11598–607.

[14] Grabber JH, Hatfield RD, Ralph J, Zoń J, Amrhein N. Ferulate cross-linking in cell walls isolated from maize cell suspensions. Phytochemistry 1995;40:1077–82.

[15] Ikeda R, Uyama H, Kobayashi S. Novel synthetic pathway to a poly (phenylene oxide). laccase-catalyzed oxidative polymerization of syringic acid. Macromolecules 1996:3053–4.

[16] Ralph J. Hydroxycinnamates in lignification. Phytochem Rev 2010;9:65–83.

[17] Lupoi JS, Singh S, Parthasarathi R, Simmons BA, Henry RJ. Recent innovations in analytical methods for the qualitative and quantitative assessment of lignin. Renew Sustain Energy Rev 2015;49:871–906.

[18] Michalak M, Thomassen L V., Roytio H, Ouwehand AC, Meyer AS, Mikkelsen JD. Expression and characterization of an endo-1,4-β-galactanase from *Emericella nidulans* in *Pichia pastoris* for enzymatic design of potentially prebiotic oligosaccharides from potato galactans. Enzyme Microb Technol 2012;50:121–9.

[19] Bauer S, Vasu P, Mort AJ, Somerville CR. Cloning, expression, and characterization of an oligoxyloglucan reducing end-specific xyloglucanobiohydrolase from *Aspergillus nidulans*. Carbohydr Res 2005;340:2590–7.

[20] Lever M. Colorimetric and fluorometric carbohydrate determination with p-hydroxybenzoic acid hydrazide. Biochem Med 1973;7:274–81.

[21] Thomassen L V., Larsen DM, Mikkelsen JD, Meyer AS. Definition and characterization of enzymes for maximal biocatalytic solubilization of prebiotic polysaccharides from potato pulp. Enzyme Microb Technol 2011;49:289–97.

[22] Li A, Zhu Y, Xu L, Zhu W, Tian X. Comparative study on the determination of assay for laccase of *Trametes* sp. African J Biochem Res 2008;2:181–3.

[23] Agger J, Viksø-Nielsen A, Meyer AS. Enzymatic xylose release from pretreated corn bran arabinoxylan: Differential effects of deacetylation and deferuloylation on insoluble and soluble substrate fractions. J Agric Food Chem 2010;58:6141–8.

[24] Hao M, Beta T. Qualitative and quantitative analysis of the major phenolic compounds as antioxidants in barley and flaxseed hulls using HPLC/MS/MS. J Sci Food Agric 2012;92:2062–8.

[25] Waldron KW, Parr AJ, Ng A, Ralph J. Cell wall esterified phenolic dimers: Identification and quantification by reverse phase high performance liquid chromatography and diode array detection. Phytochem Anal 1996;7:305–12.

[26] Sluiter A, Hames B, Ruiz R, Scarlata C, Sluiter J, Templeton D, et al. Determination of structural carbohydrates and lignin in biomass. 2008.

[27] Arnous A, Meyer AS. Comparison of methods for compositional characterization of grape (*Vitis vinifera* L.) and apple (*Malus domestica*) skins. Food Bioprod Process 2008;86:79–86.

[28] Baum A, Agger J, Meyer AS, Egebo M, Mikkelsen JD. Rapid near infrared spectroscopy for prediction of enzymatic hydrolysis of corn bran after various pretreatments. N Biotechnol 2012;29:293–301.

[29] Alves A, Gierlinger N, Schwanninger M, Rodrigues J. Analytical pyrolysis as a direct method to determine the lignin content in wood. Part 3. Evaluation of species-specific and tissue-specific differences in softwood lignin composition using principal component analysis. J Anal Appl Pyrolysis 2009;85:30–7.

[30] Cheung H, Ho M, Lau K, Cardona F, Hui D. Natural fibre-reinforced composites for bioengineering and environmental engineering applications. Compos Part B Eng 2009;40:655–63.

[31] Liu M, Silva DAS, Fernando D, Meyer AS, Madsen B, Daniel G, et al. Controlled retting of hemp fibres: effect of hydrothermal pre-treatment and enzymatic retting on the mechanical properties of unidirectional hemp/epoxy composites. Compos Part A Appl Sci Manuf 2016;88:253–62.

[32] Madsen B, Thygesen A, Lilholt H. Plant fibre composites – porosity and stiffness. Compos Sci Technol 2009;69:1057–69.

[33] Liu M, Meyer AS, Fernando D, Silva DAS, Geoffrey D, Thygesen A. Effect of pectin and hemicellulose removal from hemp fibres on the mechanical properties of unidirectional hemp/epoxy composites. Compos Part A Appl Sci Manuf n.d.:Unpublished.

[34] Álvarez C, Rojano B, Almaza O, Rojas OJ, Gañán P. Self-bonding boards from plantain fibre bundles after enzymatic treatment: adhesion improvement of lignocellulosic products by enzymatic pre-treatment. J Polym Environ 2011;19:182–8.

[35] Hossain MK, Karim MR, Chowdhury MR, Imam MA, Hosur M, Jeelani S, et al. Comparative mechanical and thermal study of chemically treated and untreated single sugarcane fibre bundle. Ind Crops Prod 2014;58:78–90.

[36] Hossain MK, Dewan MW, Hosur M, Jeelani S. Effect of surface treatment and nanoclay on thermal and mechanical performances of jute fabric/biopol "green" composites. J Reinf Plast Compos 2011;30:1841–56.

[37] Mattinen ML, Suortti T, Gosselink R, Argyropoulos DS, Evtuguin D, Suurnäkki A, et al. Polymerization of different lignins by laccase. BioResources 2008;3:549–65.

[38] Huang A, Li G, Fu F, Fei B. Use of visible and near infrared spectroscopy to predict klason lignin content of bamboo, Chinese fir, paulownia, and poplar. J Wood Chem Technol 2008;28:194–206.

[39] Prasetyo EN, Semlitsch S, Nyanhongo GS, Lemmouchi Y, Guebitz GM. Laccase oxidation and removal of toxicants released during combustion processes. Chemosphere 2016;144:652–60.

[40] Gavezzotti P, Navarra C, Caufin S, Danieli B, Magrone P, Monti D, et al. Synthesis of enantiomerically enriched dimers of vinylphenols by tandem action of laccases and lipases. Adv Synth Catal 2011;353:2421–30.

[41] Ko CH, Chen SS. Enhanced removal of three phenols by laccase polymerization with MF/UF membranes. Bioresour Technol 2008;99:2293–8.

[42] Morán JI, Alvarez VA, Cyras VP, Vázquez A. Extraction of cellulose and preparation of nanocellulose from sisal fibres. Cellulose 2008;15:149–59.

[43] Crônier D, Monties B, Chabbert B, Cronier, D ; Monties, B; Chabbert B. Structure and chemical composition of bast fibres isolated from developing hemp stem. J Agric Food Chem 2005;53:8279–89.

[44] Mueller-Harvey I, Hartley RD, Harris PJ, Curzon EH. Linkage of p-coumaroyl and feruloyl groups to cell-wall polysaccharides of barley straw. Carbohydr Res 1986;148:71–85.

[45] Iiyama K, Lam TBT, Stone BA. Phenolic acid bridges between polysaccharides and lignin in wheat internodes. Phytochemistry 1990;29:733–7.

[46] Lapierre C, Pollet B, Ralet MC, Saulnier L. The phenolic fraction of maize bran: Evidence for lignin-heteroxylan association. Phytochemistry 2001;57:765–72.

Figure captions

Fig. 1. Thermogravimetric analysis for derivatives of weight (%) vs. temperature of untreated and differently treated fibres.

Fig. 2. Stiffness (a) and UTS (b) of composites reinforced with untreated and treated fibres vs. fibre volume contents (V_f).

Fig. 3. Porosity of composites reinforced with untreated and differently treated fibres versus fibre volume contents (V_f).

Fig. 4. (a) Score plot of PCA of near infrared spectra of untreated and differently treated hemp fibres. The data are acquired in 11 replicates for each sample and processed by Standard Normal Variate (SNV); (b) PC3 loadings of PCA.

Fig. 5. Near infrared spectra after processed by SNV and mean centering.

Fig. 6. (a) Score plot of PCA of Py-GC/MS data with lignin signals of untreated and differently treated hemp fibres; (b) PC1 loadings of PCA; (c) PC2 loadings of PCA.

Fig. 7. FTIR spectra measured from untreated and differently treated fibres.

Fig. 8. Phenols extracted from untreated and differently treated hemp fibres.

Tables

Table 1. Mechanical properties of differently treated hemp fibres. Values are means (standard deviation) for 20 replicates. Values in the column that do not share a letter are significantly different at the 5% level.

Fibre sample	Mechanical properties		
	Stiffness (GPa)	UTS (MPa)	Failure strain (%)
Untreated	28.5 (2.9)[a]	772 (103)[a]	5.1 (0.9)[a]
0.5% EDTA + 0.2% EPG	15.2 (4.0)[b]	556 (138)[b]	4.1 (1.1)[b]
0.5% EDTA + 0.2% EPG → 0.5% Laccase	31.2 (4.4)[a]	842 (150)[a]	3.1 (1.1)[c]
0.5% EDTA + 0.2% EPG → 10% NaOH	13.8 (2.3)[b]	432 (86)[c]	4.1 (1.0)[b]
0.5% EDTA + 0.2% EPG → 10% NaOH → 0.5% Laccase	16.8 (3.3)[b]	492 (89)[bc]	4.1 (1.0)[b]

520 **Table 2.** The maximum degradation temperature (°C) and the maximum degradation rate (%/°C) as

521 measured by dynamic thermogravimetric analysis

Fibre sample	Maximum degradation temperature (°C)	Maximum degradation rate (%/°C)
Untreated	344.5	1.00
0.5% EDTA + 0.2% EPG	345.7	1.14
0.5% EDTA + 0.2% EPG → 0.5% Laccase	350.2	1.18
0.5% EDTA + 0.2% EPG → 10% NaOH	360.8	1.32
0.5% EDTA + 0.2% EPG → 10% NaOH → 0.5% Laccase	367.9	1.44

522

523 **Table 3.** Mechanical properties of fibre/epoxy composites at fibre volume content of 0.5 (V_f=0.5) and

524 established effective fibre mechanical properties. Values are shown as mean (standard error).

Fibre sample	Composite mechanical properties[1]		Effective fibre properties[2]	
	Stiffness (GPa)	UTS (MPa)	Stiffness (GPa)	UTS (MPa)
Untreated	33.8 (0.6)	294 (14)	64.9 (1.2)	562 (28)
0.5% EDTA + 0.2% EPG	36.7 (0.9)	327 (9)	70.6 (1.7)	626 (18)
0.5% EDTA + 0.2% EPG → 0.5% Laccase	41.9(0.8)	326(8)	81.6(1.5)	631(20)
0.5% EDTA + 0.2% EPG → 10% NaOH	42.5 (0.3)	274 (9)	83.0 (0.6)	527 (17)
0.5% EDTA + 0.2% EPG → 10% NaOH → 0.5% Laccase	41.9(0.7)	281(10)	81.8(1.0)	542(21)

525

526 [1]Composite stiffness and UTS were determined at V_f =0.5 based on the results shown in Fig. 1a and Fig.

527 1b.

528 [2] Effective fibre stiffness and strength were established based on the results shown in Fig. 1 using Eqs.
529 2−3 at V_f=1.0.

530 **Table 4.** Chemical composition of hemp fibres treated with different concentrations of EDTA. Values are
531 means (standard deviation) for 3 replicates. Values in each column that do not share a letter are
532 significantly different at the 5% level.

Fibre sample	Amount (%)					
	Ara	Glu	Xyl	Man	GalA	Lignin
Untreated	1.2 (0.1)^{a}	67.2 (2.6)^{c}	1.3 (0.2)^{a}	4.6(0.2)^{a}	8.3(0.4)^{a}	5.3(0.2)^{a}
0.5% EDTA + 0.2% EPG	0.8 (0.1)^{b}	73.8(3.0)^{bc}	1.0 (0.1)^{b}	4.6(0.4)^{a}	2.1(0.4)^{bc}	5.1(0.3)^{a}
0.5% EDTA + 0.2% EPG → 0.5% Laccase	0.7 (0)^{b}	75.3(2.5)^{b}	1.3(0.1)^{ab}	4.8(0.2)^{a}	2.5(0.1)^{b}	4.9(0.4)^{a}
0.5% EDTA + 0.2% EPG → 10% NaOH	0.5 (0.1)^{c}	85.6 (0.6)^{a}	0.2 (0)^{c}	1.7(0.1)^{b}	1.5(0.1)^{c}	2.9(0.3)^{b}
0.5% EDTA + 0.2% EPG → 10% NaOH → 0.5% Laccase	0.5 (0.1)^{c}	84.2(1.6)^{a}	0.4(0.2)^{c}	2.0(0.1)^{b}	1.6(0.2)^{c}	2.7(0.4)^{b}

533

534 [1]Ara-arabinan, Glu-glucan, Xyl-xylan, Man-mannan, GalA-galacturonan, Lignin- Klason lignin.

535

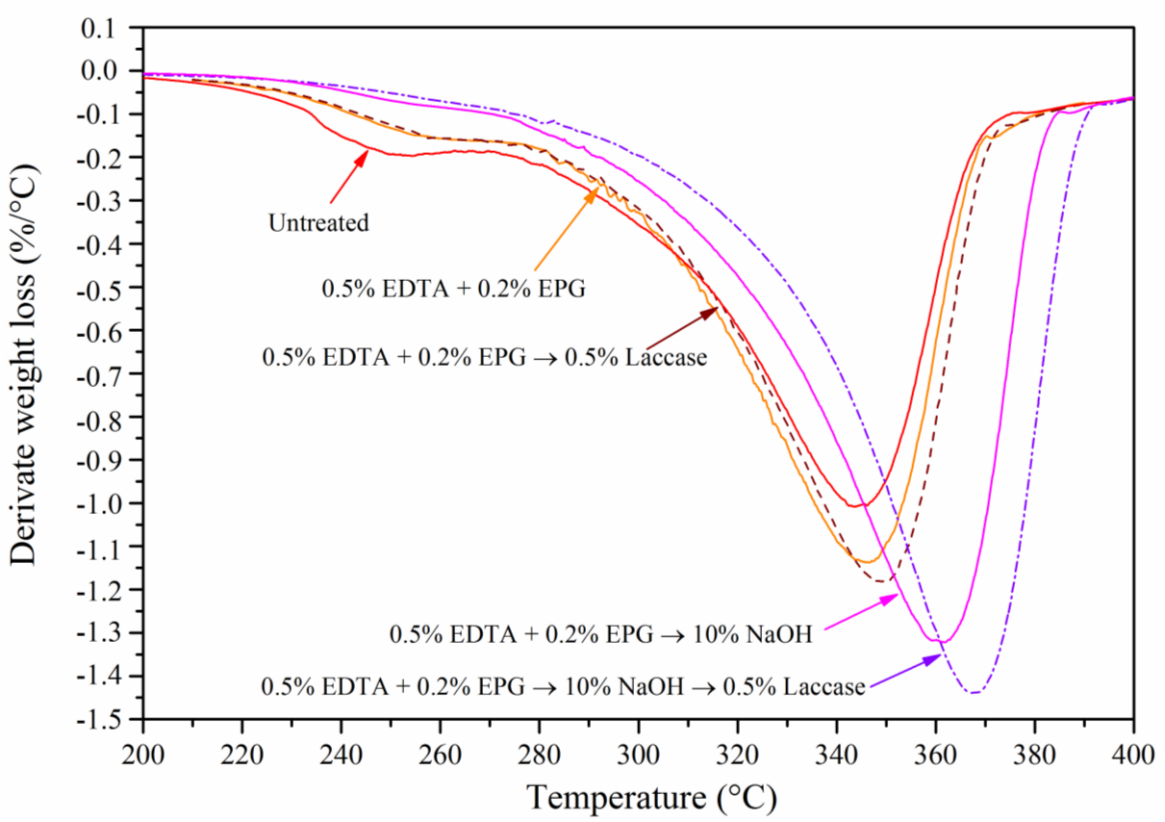
Derivate weight loss (%/°C)
Temperature (°C)
Untreated
0.5% EDTA + 0.2% EPG
0.5% EDTA + 0.2% EPG → 0.5% Laccase
0.5% EDTA + 0.2% EPG → 10% NaOH
0.5% EDTA + 0.2% EPG → 10% NaOH → 0.5% Laccase

536

537 **Fig. 1.**

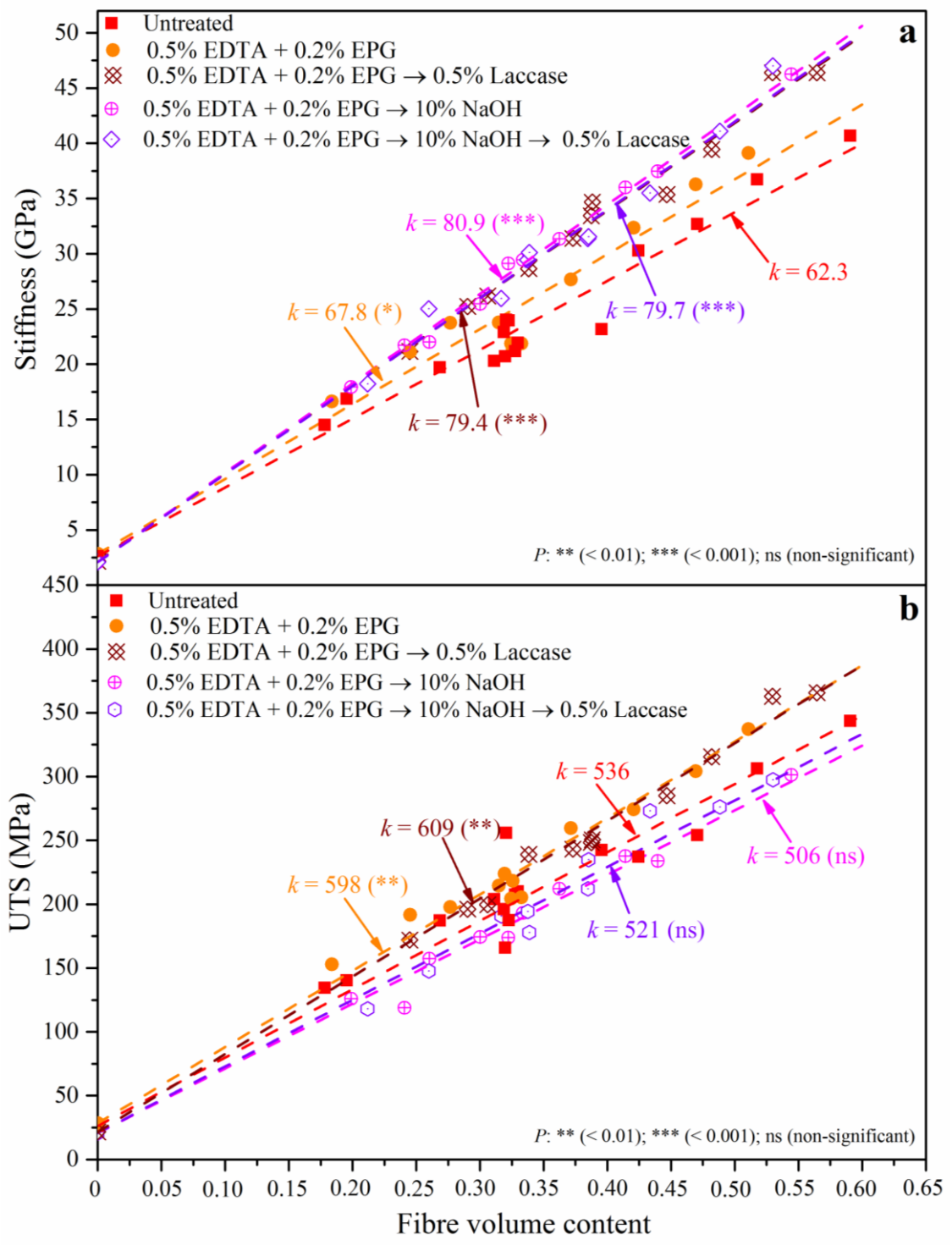
a
Untreated
0.5% EDTA + 0.2% EPG
0.5% EDTA + 0.2% EPG → 0.5% Laccase
0.5% EDTA + 0.2% EPG → 10% NaOH
0.5% EDTA + 0.2% EPG → 10% NaOH → 0.5% Laccase
Stiffness (GPa)
k = 80.9 (***)
k = 62.3
k = 67.8 (*)
k = 79.7 (***)
k = 79.4 (***)
P: ** (< 0.01); *** (< 0.001); ns (non-significant)
b
Untreated
0.5% EDTA + 0.2% EPG
0.5% EDTA + 0.2% EPG → 0.5% Laccase
0.5% EDTA + 0.2% EPG → 10% NaOH
0.5% EDTA + 0.2% EPG → 10% NaOH → 0.5% Laccase
UTS (MPa)
k = 536
k = 609 (**)
k = 506 (ns)
k = 598 (**)
k = 521 (ns)
P: ** (< 0.01); *** (< 0.001); ns (non-significant)
Fibre volume content

538

539 **Fig. 2.**

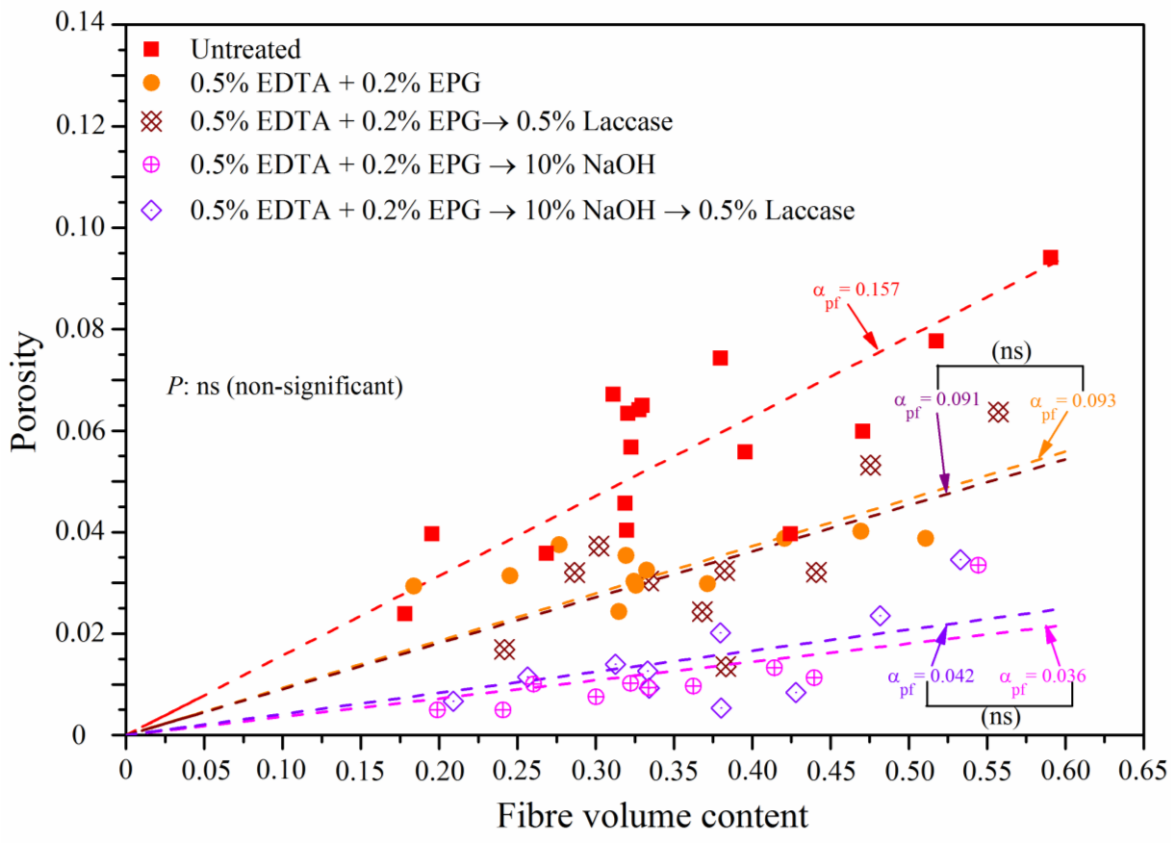
Untreated
0.5% EDTA + 0.2% EPG
0.5% EDTA + 0.2% EPG→ 0.5% Laccase
0.5% EDTA + 0.2% EPG → 10% NaOH
0.5% EDTA + 0.2% EPG → 10% NaOH → 0.5% Laccase
P: ns (non-significant)
α pf = 0.157
(ns)
α pf = 0.091
α pf = 0.093
α pf = 0.042
α pf = 0.036
(ns)
Porosity
Fibre volume content
0.14
0.12
0.10
0.08
0.06
0.04
0.02
0
0.05
0.15
0.20
0.25
0.30
0.35
0.40
0.45
0.50
0.55
0.60
0.65

540

541 **Fig. 3.**

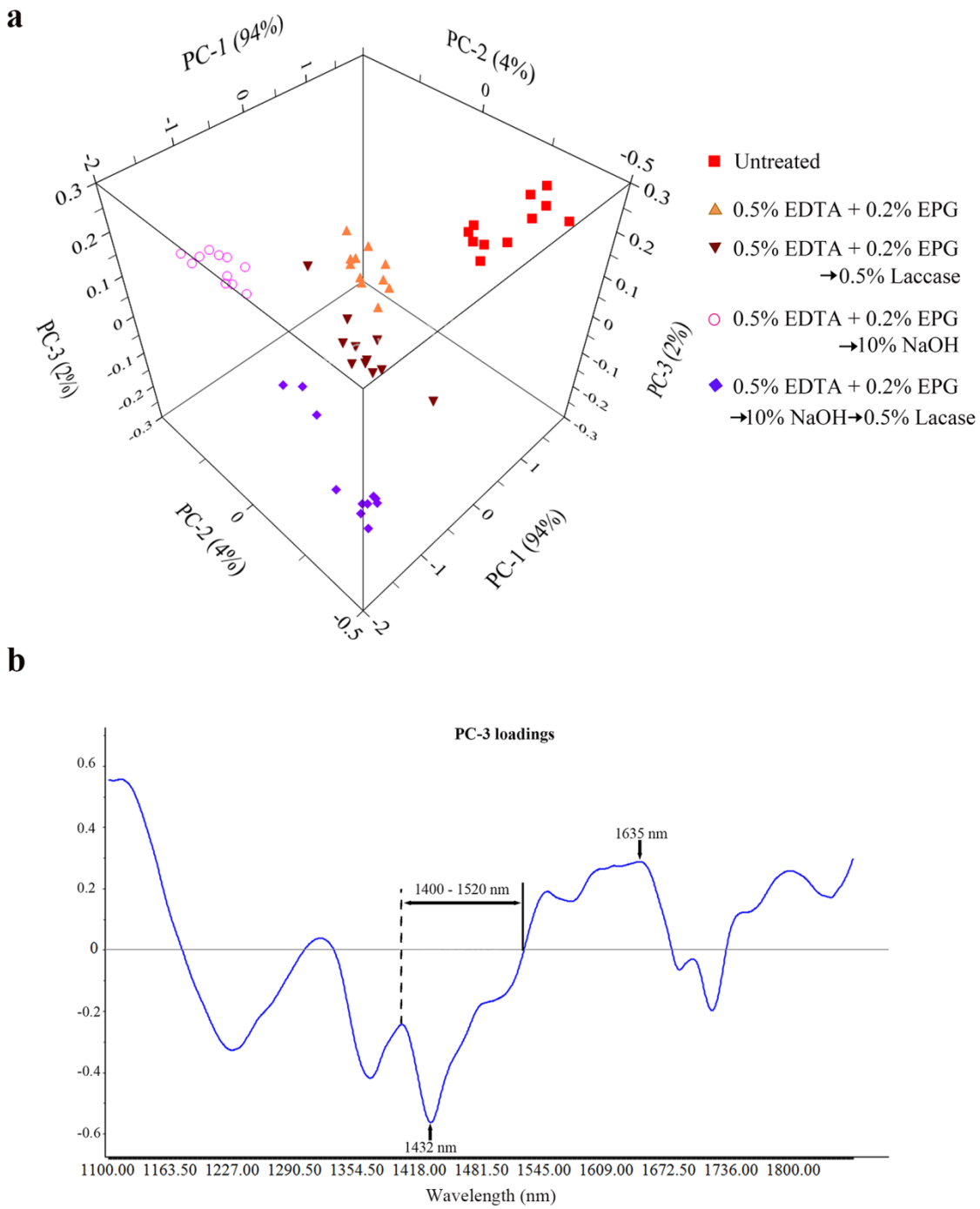
a
PC-1 (94%)
PC-2 (4%)
PC-3 (2%)
Untreated
0.5% EDTA + 0.2% EPG
0.5% EDTA + 0.2% EPG →0.5% Laccase
0.5% EDTA + 0.2% EPG →10% NaOH
0.5% EDTA + 0.2% EPG →10% NaOH→0.5% Lacase
b
PC-3 loadings
1635 nm
1400 - 1520 nm
1432 nm
1100.00 1163.50 1227.00 1290.50 1354.50 1418.00 1481.50 1545.00 1609.00 1672.50 1736.00 1800.00
Wavelength (nm)

542

543 **Fig. 4.**

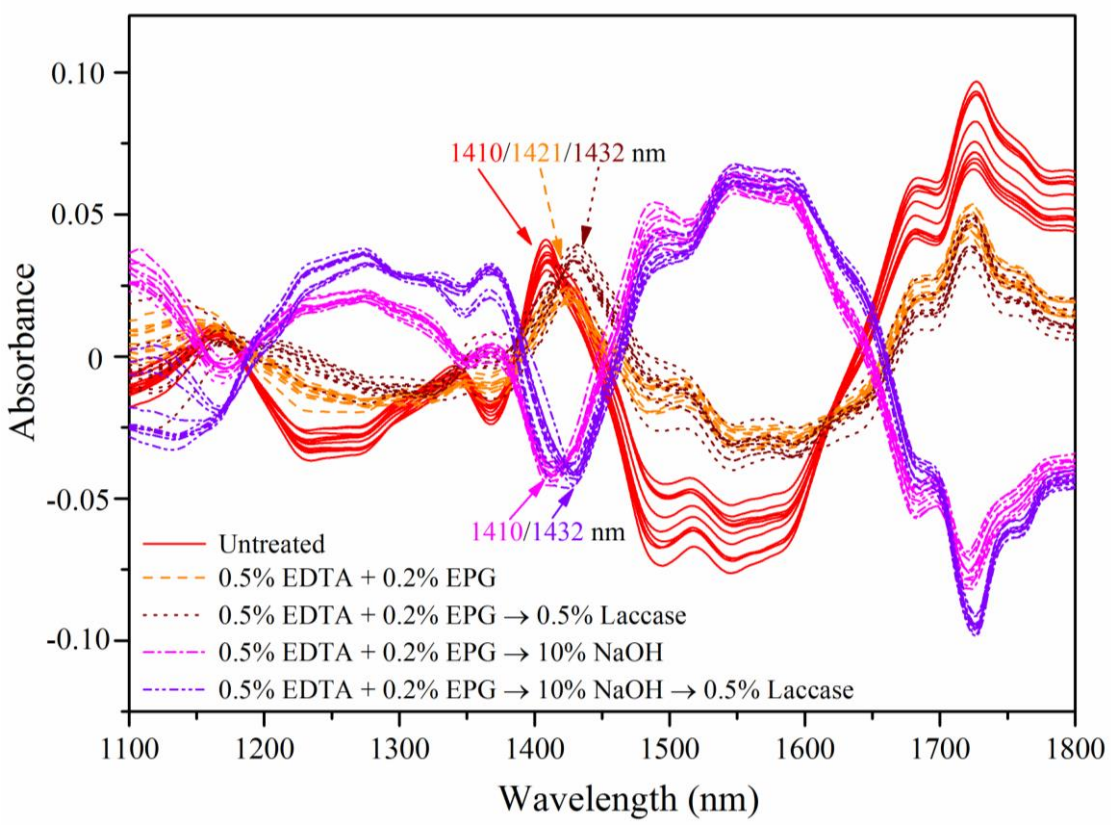

544

545 **Fig. 5.**

546

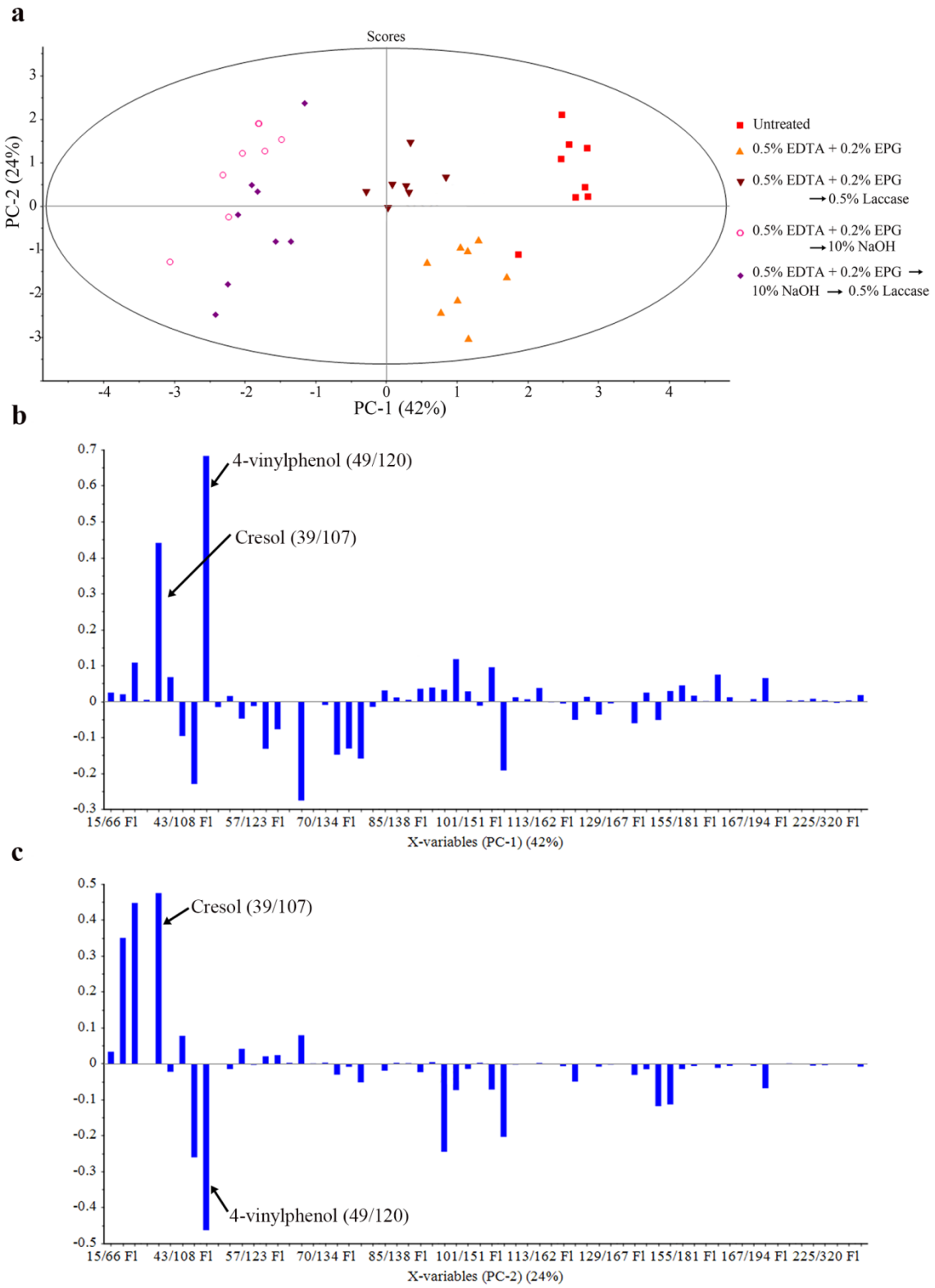
a
Scores
PC-2 (24%)
PC-1 (42%)
Untreated
0.5% EDTA + 0.2% EPG
0.5% EDTA + 0.2% EPG →0.5% Laccase
0.5% EDTA + 0.2% EPG →10% NaOH
0.5% EDTA + 0.2% EPG → 10% NaOH → 0.5% Laccase
b
4-vinylphenol (49/120)
Cresol (39/107)
15/66 Fl 43/108 Fl 57/123 Fl 70/134 Fl 85/138 Fl 101/151 Fl 113/162 Fl 129/167 Fl 155/181 Fl 167/194 Fl 225/320 Fl
X-variables (PC-1) (42%)
c
Cresol (39/107)
4-vinylphenol (49/120)
15/66 Fl 43/108 Fl 57/123 Fl 70/134 Fl 85/138 Fl 101/151 Fl 113/162 Fl 129/167 Fl 155/181 Fl 167/194 Fl 225/320 Fl
X-variables (PC-2) (24%)

Fig. 6.

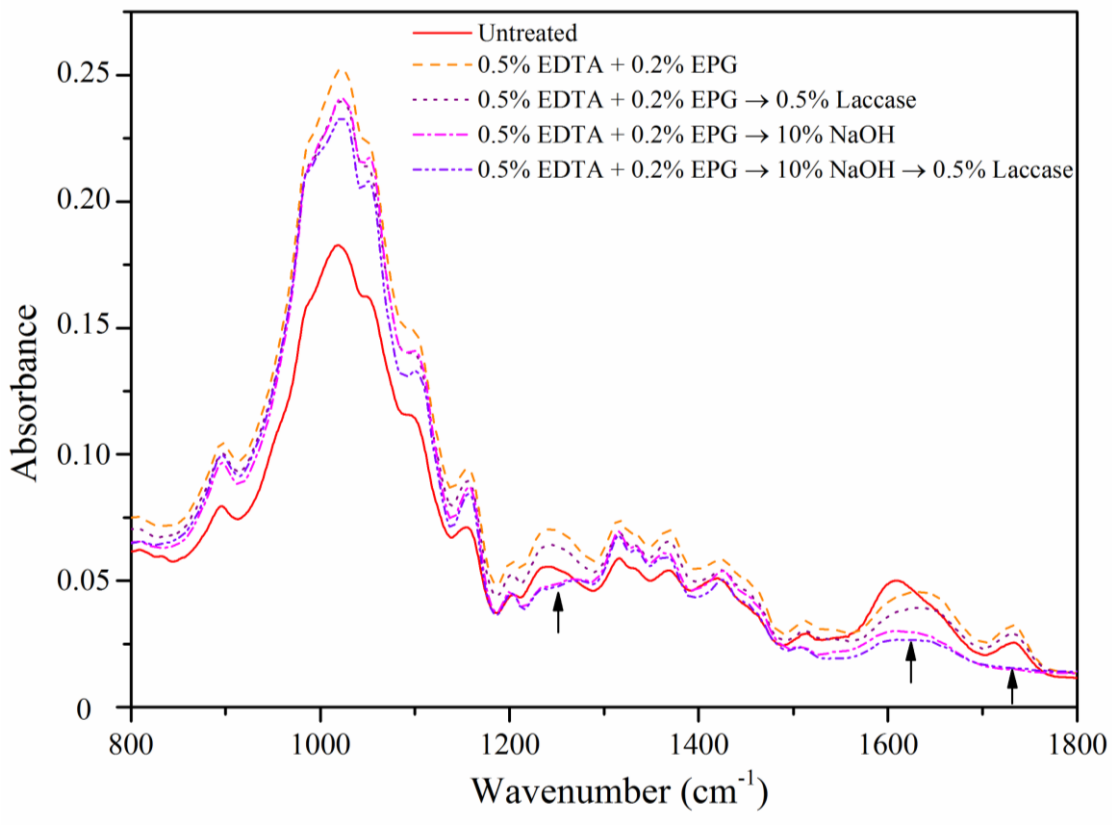

550

551 **Fig. 7.**

552

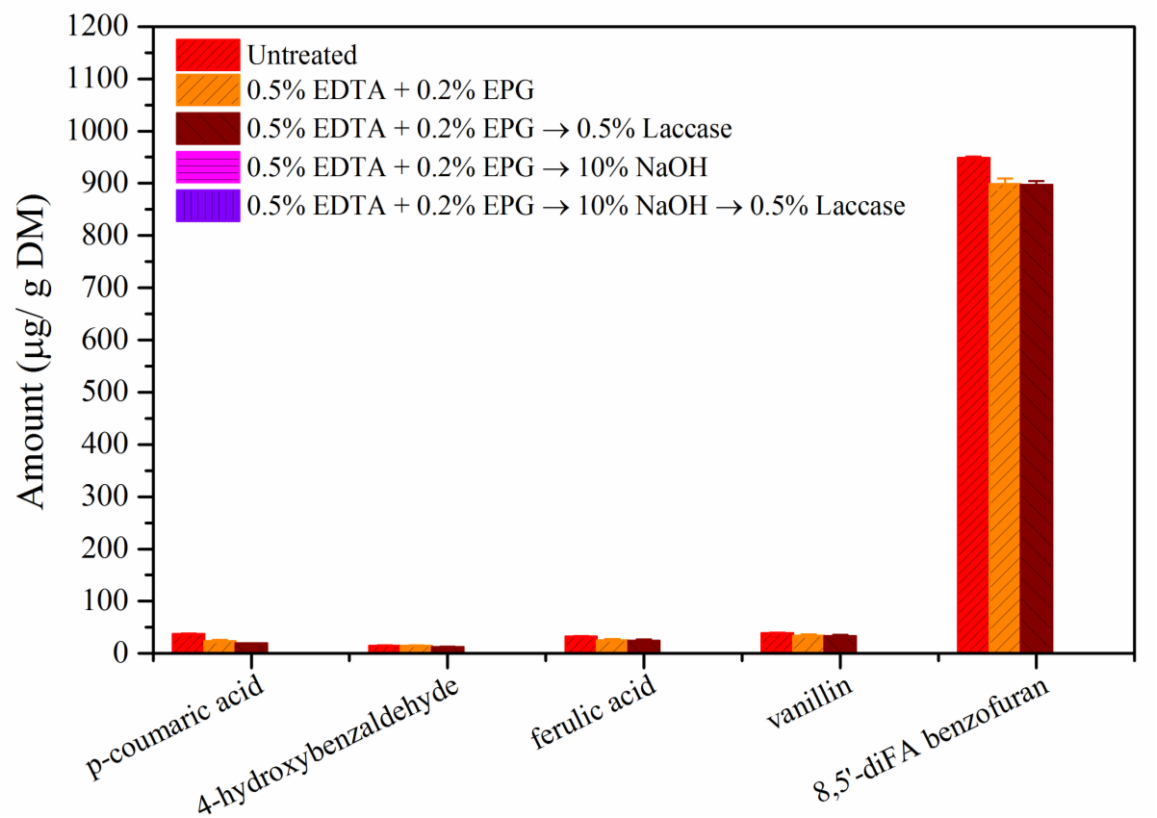
Amount (µg/ g DM)
1200
1100
1000
900
800
700
600
500
400
300
200
100
0
Untreated
0.5% EDTA + 0.2% EPG
0.5% EDTA + 0.2% EPG → 0.5% Laccase
0.5% EDTA + 0.2% EPG → 10% NaOH
0.5% EDTA + 0.2% EPG → 10% NaOH → 0.5% Laccase
p-coumaric acid
4-hydroxybenzaldehyde
ferulic acid
vanillin
8,5'-diFA benzofuran

553

554 **Fig. 8.**

Paper VII

Ming Liu, Anders Thygesen, Anne S. Meyer, & Bo Madsen

Modelling of volumetric composition and mechanical properties of unidirectional hemp/epoxy composites – Effect of enzymatic fiber treatment

IOP Conference Series: Materials Science and Engineering, 2016, 139, 12-31

IOP Conf. Series: Materials Science and Engineering **139** (2016) 012031 doi:10.1088/1757-899X/139/1/012031

Modelling of volumetric composition and mechanical properties of unidirectional hemp/epoxy composites - Effect of enzymatic fibre treatment

M Liu[1], A Thygesen[1], AS Meyer[1], B Madsen[2]

[1]Center for Bioprocess Engineering, Department of Chemical and Biochemical Engineering, Technical University of Denmark, 2800 Kongens Lyngby, Denmark.
[2]Section of Composites and Materials Mechanics, Department of Wind Energy, Technical University of Denmark, Frederiksborgvej 399, 4000 Roskilde, Denmark.

E-mail: miliu@kt.dtu.dk

Abstract. The objective of the present study is to assess the effect of enzymatic fibre treatments on the fibre performance in unidirectional hemp/epoxy composites by modelling the volumetric composition and mechanical properties of the composites. It is shown that the applied models can well predict the changes in volumetric composition and mechanical properties of the composites when differently treated hemp fibres are used. The decrease in the fibre correlated porosity factor with the enzymatic fibre treatments shows that the removal of pectin by pectinolytic enzymes results in a better fibre impregnation by the epoxy matrix, and the mechanical properties of the composites are thereby increased. The effective fibre stiffness and strength established from the modelling show that the enzymatic removal of pectin also leads to increased mechanical properties of the fibres. Among the investigated samples, the composites with hydrothermally pre-treated and enzymatically treated fibres have the lowest porosity factor of 0.08 and the highest mechanical properties. In these composites, the effective fibre stiffness and strength are determined to be 83 GPa and 667 MPa, respectively, when the porosity efficiency exponent is set equal to 2. Altogether, it is demonstrated that the applied models provide a concept to be used for the evaluation of performance of treated fibres in composites.

1. Introduction

As a result of increasing environmental awareness, research interest has been shifting to use natural fibres as substitute to man-made fibres in fibre reinforced composites due to their unique advantages, such as environmental sustainability, low cost, low density, together with their high stiffness and strength to weight ratio [1,2]. However, their potential use as reinforcement could be considerably reduced by some of their disadvantages including moderate strength of fibres, less controlled processing methods, and seasonal variation in quality [3–5].

In principle, the aim of fibre processing is to obtain more separated and cellulose rich fibres by removing non-cellulosic components, in order to optimize the strength and form of the fibres before being used as reinforcement in composites. Traditional cellulose fibre processing methods for hemp and flax fibres, which have mainly been targeted for yarn production, include field retting and water retting. These retting methods remove non-cellulosic components via spontaneously flourishing microbial activity, and they have been reported to have negative impacts on both fibre properties and the environment [5,6]. As an alternative method, treatment of fibres with pectinolytic enzymes could

be a more efficient and controlled method, in addition to overcoming the limitations of the traditional fibre processing methods [7–9].

Porosity is a parameter that is used to assess the quality of composites. Porosity in natural fibre composites is not only created due to insufficient impregnation of the fibres by the matrix, but also due to the air filled cavities inside the fibres, the so-called lumen. Porosity has a direct influence on the volumetric composition (i.e. the volume contents of fibres and matrix) and the mechanical properties of composites [9–11]. A study of the relations between fibre processing routes, and the volumetric composition and mechanical properties of composites is central to the goal of assessing the effect of various fibre treatments.

In the present study, enzymatic treatments with and without hydrothermal pre-treatment were carried out on hemp bast fibres. For comparison, traditional field retting of fibres was also carried out [5]. It is expected that porosity is highest in the composites with the untreated fibres due to the presence of the epidermis layer and parenchyma cells, which consist of a large amount of voids [9,12]. In contrast, it is expected that the enzymatic treatments will produce fibres where the epidermis layer and part of parenchyma cells are removed, in addition to splitting larger fibre bundles into smaller ones [7,9,13]. Those changes are expected to decrease the porosity in the composites, and the mechanical properties will thereby be increased.

The objective of the present study is to use previously developed models for composite volumetric composition and mechanical properties for a quantitative analysis of the effect of enzymatically based fibre processing methods. This approach is shown to provide valuable understanding of the effect of the fibre treatments on the properties of the composites.

2. Model

In the present study, experimental data is modelled by previously reported models [11,14]. Experimental data for composite volumetric composition, density and mechanical properties (i.e. stiffness and strength) were obtained for composites with a fibre weight content (W_f) below the transition value ($W_{f\,trans}$). For the modelling of composites with W_f above $W_{f\,trans}$ only model lines will be shown. A summary of the applied model parameters is shown in Table 1. The parameters, fibre density (ρ_f), matrix density (ρ_m), matrix correlated porosity factor (α_{pm}), maximum obtainable fibre volume content ($V_{f\,max}$), and porosity efficiency exponent for composite stiffness (n_E) and strength (n_σ) are assumed to be constant and independent of the applied fibre treatments. The parameters, transition fibre weight content ($W_{f\,trans}$) and fibre correlated porosity factor (α_{pf}) are assumed to be dependent on the fibre treatment.

Table 1. Summary of model parameters applied in the present study.

Parameter	Meaning	Value	Way of determining the value
ρ_f	fibre density	1.50 g/cm^3	assumed
ρ_m	matrix density	1.14 g/cm^3	measured
α_{pm}	matrix correlated porosity factor	0	assumed
$V_{f\,max}$	maximum obtainable fibre volume content	0.65	assumed
n_E	porosity efficiency exponent for composite stiffness	0 or 2	assumed
n_σ	porosity efficiency exponent for composite strength	0 or 2	assumed
$W_{f\,trans}$	transition fibre weight content	see Table 2	determined from Eq.1
α_{pf}	fibre correlated porosity factor	see Table 2	determined from Eq.2

2.1. Volumetric composition

In the selected model [11], the volumetric composition in composites is correlated to the fibre weight content (W_f) in two regions: region A, where W_f is below a transition value ($W_{f\ trans}$), and region B, where W_f is above a transition value ($W_{f\ trans}$), respectively. The transition value ($W_{f\ trans}$) separating region A and B is calculated by Eq.1.

$$W_{f\ trans} = \frac{V_{f\ max}\rho_f(1+\alpha_{pm})}{V_{f\ max}(1+\alpha_{pm}) - V_{f\ max}\rho_m(1+\alpha_{pf})+\rho_m} \quad (1)$$

In this study, it is assumed that there is no matrix correlated porosity in the composites, and therefore α_{pm} is set to 0. The fibre correlated porosity factor (α_{pf}) is determined by using Eq.2, where the porosity (V_p) is assumed to be a linear function of the fibre volume content (V_f) [11].

$$V_p = \alpha_{pf} \times V_f \quad (2)$$

The volumetric composition in the composites in region A and region B are shown in Eqs.3 – 8.

Region A ($W_f \leq W_{f\ trans}$)

$$V_f = \frac{W_f\rho_m}{W_f\rho_m(1+\alpha_{pf})+(1-W_f)\rho_f(1+\alpha_{pm})} \quad (3)$$

$$V_m = \frac{(1-W_f)\rho_f}{W_f\rho_m(1+\alpha_{pf})+(1-W_f)\rho_f(1+\alpha_{pm})} \quad (4)$$

$$V_p = 1 - V_f - V_m = \frac{W_f\rho_m\alpha_{pf} + (1-W_f)\rho_f\alpha_{pm}}{W_f\rho_m(1+\alpha_{pf})+(1-W_f)\rho_f(1+\alpha_{pm})} \quad (5)$$

Region B ($W_f \geq W_{f\ trans}$)

$$V_f = V_{f\ max} \quad (6)$$

$$V_m = V_{f\ max}\frac{(1-W_f)\rho_f}{W_f\rho_m} \quad (7)$$

$$V_p = 1 - V_f - V_m = 1 - V_{f\ max}\left(1 + \frac{(1-W_f)\rho_f}{W_f\rho_m}\right) \quad (8)$$

2.2. Composite density

Equations for composite density, Eqs.10 – 11, can be derived from Eq. 9 by using the expression for volumetric composition in composites.

$$\rho_c = \frac{m_c}{V_c} = \frac{m_f/W_f}{m_f/(\rho_f V_f)} = \frac{\rho_f V_f}{W_f} \quad (9)$$

Region A ($W_f \leq W_{f\ trans}$)

$$\rho_c = \frac{\rho_m\rho_f}{W_f\rho_m(1+\alpha_{pf})+(1-W_f)\rho_f(1+\alpha_{pm})} \quad (10)$$

Region B ($W_f \geq W_{f\ trans}$)

$$\rho_c = \frac{V_{f\ max}}{W_f}\rho_f \quad (11)$$

In the modelling of composite density, the fibre weight content (W_f) is set as the independent variable, and composite density (ρ_c) is set as the dependent variable. The values of the other parameters are given in Tables 1 and 2. The experimental data of ρ_c vs. W_f is compared with the model predictions (Eqs. 10 − 11).

2.3. Mechanical properties

A large number of modified rule of mixtures models for stiffness of composites have been proposed in the literature [14,15]. In one of these models, by including the effect of porosity [14], stiffness (E_c) and strength (σ_{cu}) of composites with a unidirectional fibre orientation and with continuous fibres can be expressed by Eq.12 and Eq.13, respectively.

$$E_c = \left(V_f E_f + V_m E_m\right)\left(1 - V_p\right)^{n_E} \tag{12}$$

$$\sigma_{cu} = \left(V_f \sigma_{fu} + V_m \sigma_m^*\right)\left(1 - V_p\right)^{n_\sigma} \tag{13}$$

where E is the stiffness, V is the volume content, the subscripts c, m, f and p are composite, matrix, fibres and porosity, respectively. σ_{cu} is the composite strength, σ_{fu} is the fibre strength, and σ_m^* is the stress in the matrix at the failure strain of the composite, and n_E and n_σ are the porosity efficiency exponents (PEE) for stiffness and strength, respectively. When PEE = 0, it is assumed that the porosity in the composites has no effect on the mechanical properties of the composites beyond lowering the load bearing volume. When PEE > 0, it is assumed that the porosity in the composites has an effect on the mechanical properties of composites by introducing stress concentrations [14]. Values of PEE equal to 0 and 2 are used in the present study to show these two cases.

By using the models for the composite volumetric composition, equations for the correlation between composite stiffness (E_c) and strength (σ_{cu}) and the fibre weight fraction (W_f) can be established.

Region A ($W_f \leq W_{f\,trans}$)

$$E_c = \frac{\left(W_f\rho_m E_f + \left(1-W_f\right)\rho_f E_m\right)\left(W_f\rho_m + \left(1-W_f\right)\rho_f\right)^{n_E}}{\left(W_f\rho_m\left(1+\alpha_{pf}\right) + \left(1-W_f\right)\rho_f\left(1+\alpha_{pm}\right)\right)^{n_E+1}} \tag{14}$$

$$\sigma_{cu} = \frac{\left(W_f\rho_m\sigma_{fu} + \left(1-W_f\right)\rho_f\sigma_m^*\right)\left(W_f\rho_m + \left(1-W_f\right)\rho_f\right)^{n_\sigma}}{\left(W_f\rho_m\left(1+\alpha_{pf}\right) + \left(1-W_f\right)\rho_f\left(1+\alpha_{pm}\right)\right)^{n_\sigma+1}} \tag{15}$$

Region B ($W_f \geq W_{f\,trans}$)

$$E_c = \frac{\left(W_f\rho_m V_{f\,max} E_f + \left(1-W_f\right)\rho_f V_{f\,max} E_m\right)\left(W_f\rho_m V_{f\,max} + \left(1-W_f\right)\rho_f V_{f\,max}\right)^{n_E}}{\left(W_f\rho_m\right)^{n_E+1}} \tag{16}$$

$$\sigma_{cu} = \frac{\left(W_f\rho_m V_{f\,max}\sigma_{fu} + \left(1-W_f\right)\rho_f V_{f\,max}\sigma_m^*\right)\left(W_f\rho_m V_{f\,max} + \left(1-W_f\right)\rho_f V_{f\,max}\right)^{n_\sigma}}{\left(W_f\rho_m\right)^{n_\sigma+1}} \tag{17}$$

In the modelling of composite mechanical properties, the fibre weight content (W_f) is set as the independent variable, and composite stiffness (E_c) and strength (σ_{cu}) are set as the dependent variables. The effective fibre stiffness (E_f) and effective fibre strength (σ_{fu}) are set as derived parameters. The values of the remaining parameters are given in Tables 1 and 2. The models are fitted to the experimental data of E_c vs. W_f and σ_{cu} vs. W_f by using non-linear regression. The goodness of fitting is evaluated by adjusted R-squared values, which has been adjusted for the number of predictors in the model from R-squared values.

3. Materials and methods

3.1. Plant material

Hemp (*Cannabis sativa* L.), variety USO-31, was sown in France (N 48.8526°, E 3.0190°(WGS84)) as described in detail in Liu et al. [5]. The whole hemp stem under the inflorescence base was used as the starting material in the present study. Hemp stem pieces with a length of approx. 15 cm were randomly collected from the stems. The hemp stems were hydrothermally pre-treated at 121 °C for 30 min in an autoclave. Hemp fibre strips were manually peeled off from the pre-treated stems, and then they were enzymatically treated by using pectinases as described in detail by Liu et al. [9]. After enzymatic treatment, the fibre strips were dried at 50 °C for 12 h. For comparison, field retting of the hemp stems was carried out for 20 days after harvest [4].

3.2. Manufacturing of composites

The treated bast fibre strips were manually untangled and aligned to allow the fibres to be processed into unidirectional composites. Bundles of fibre strips were firstly cut to a length of 140 mm, and the fibre strips were then justified to a bunch of fibre strips with masses in the range 0.6 – 2.3 g. Bunches of fibre strips were then put in the mould chambers. Afterwards, a press beam was placed on the top of the fibre strips in each chamber, and two insert beams were used to fix the height of the mould chambers to 2 mm. An epoxy resin (Araldite® LY 1568) and its amine hardener (Aradur® 3489) were mixed at a 100/28 mass ratio, and degassed in a vacuum oven. The setup for the vacuum infusion and moulding process is described in detail in the study by Liu et al. [9]. After curing for 12 h at 80 °C, the composite tensile specimens with dimensions of 140 × 10 × 2 mm were demoulded. Tabs with lengths of 50 mm were mounted on the composite specimens using epoxy resin (DP 460).

3.3. Volumetric composition

Composites with fibre weight contents (W_f) in the range 0 – 0.70 were obtained by varying the amount of fibres (m_f) in the mould chambers during manufacturing of composites. The fibre volume content (V_f) was determined by Eq.18.

$$V_f = \frac{m_f/\rho_f}{m_c/\rho_c} = \frac{m_f}{m_c} \times \frac{\rho_c}{\rho_f} \tag{18}$$

where m_c, ρ_f and ρ_c are composite mass, fibre density and composite density, respectively. When W_f was below 0.30, the composite specimens made by using the above mentioned moulding process were found to have irregular surfaces, and their thickness could not be measured accurately. For those cases, ρ_c was determined by the buoyancy method (Archimedes principle) using water as the displacement medium. When W_f was above 0.30, the composites specimens had flat surfaces, and their density (ρ_c) could be accurately calculated based on their dimensions (length, width and thickness).

The matrix volume content (V_m) was determined using Eq.19.

$$V_m = \frac{m_m/\rho_m}{m_c/\rho_c} = \frac{m_m}{m_c} \times \frac{\rho_c}{\rho_m} \tag{19}$$

where m_m is matrix mass. The porosity (V_p) was then determined using Eq.20.

$$V_p = 1 - V_f - V_m \tag{20}$$

3.4. Tensile properties of composites

For tensile testing of the composite specimens, an Instron Testing Machine 5566 with a load cell of 10 kN was used. Two extensometers were used for strain measurements, and a displacement rate of 1 mm/min (corresponding to a strain rate of 2.5 %/min) was used. Based on the measured stress-strain curves, stiffness (linear regression in the strain interval 0.05 – 0.25%), strength and failure strain was

determined. For each type of composite with the differently treated hemp fibres, at least 10 specimens with varied fibre content were tested.

4. Results and discussion

4.1. Composite volumetric composition

The fibre correlated porosity factor (α_{pf}) of the composites manufactured with the differently treated fibres is determined in Figure1a based on the experimental values of V_p and V_f using Eq.2. The values of α_{pf} for the different fibre treatments are shown in Table 2. As shown, composites with field retted and untreated fibres have the highest porosity factor of about 0.16. In contrast, composites with the enzymatically treated fibres have a much lower porosity factor of 0.12, followed by the lowest porosity factor of 0.08 for composites with the hydrothermally pre-treated and enzymatically treated fibres.

The variation of the composite porosity factor with the different fibre treatments can be explained by the changes of the fibre microstructure. When the hemp fibre strips are subjected to pectinases, pectin in the epidermis, in the parenchyma cells, and in the middle lamella regions between fibre cells are partly hydrolysed by enzyme catalysed reactions. This degradation of pectin loosen the bonding between epidermis and cortex, between fibres and parenchyma cells, and between fibres, and consequently, the epidermis and parenchyma cells are partly removed from the hemp fibre strips. With the partly removal of epidermis and parenchyma cells, which consist of a large amount of voids, the fibre bundles are split into smaller fibre bundles [9]. All these changes to the fibre microstructure collectively contribute to the decrease of α_{pf} after the enzymatic treatment.

The transition fibre weight content ($W_{f\ trans}$) for each type of fibre treatment was calculated by using Eq.1 with the obtained fibre correlated porosity factors. The values of $W_{f\ trans}$ are shown in Table 2. It is found that the transition value decreases from 0.77 for composites with field retted and untreated fibres, to 0.75 for composites with enzymatically treated fibres, and finally to 0.74 for composites with hydrothermally pre-treated and enzymatically treated fibres. According to Eq.1, it is evident that the decrease of $W_{f\ trans}$ with fibre processing is directly governed by the decrease of the fibre correlated porosity factor.

Experimental data on the volumetric composition in the composites with the differently treated fibres, and the corresponding model lines are shown in Figure 1b. Besides the difference in the values of $W_{f\ trans}$, it is shown that composites with hydrothermally pre-treated and enzymatically treated fibres have higher fibre volume content (V_f) and matrix volume content (V_m), and lower porosity than the composites with field retted and untreated fibres at any given fibre weight content below $W_{f\ trans}$. According to Eqs.3 – 5, the difference in α_{pf} explains the difference in volumetric composition between the composites. Altogether, the results in Figure 1b reveal that the full volumetric composition in composites with a given type of fibre treatment can be predicted by using the model, and by using a given fibre weight content that is used for the manufacturing of the composites as input.

Table 2. Fibre correlated porosity factor (α_{pf}) and transition fibre weight content ($W_{f\ trans}$) of composites with differently treated hemp fibres.

Fibre sample	Fibre correlated porosity factor (α_{pf})	Transition fibre weight content ($W_{f\ trans}$)
Field retted	0.162	0.772
Untreated	0.157	0.770
Enzymatically treated	0.119	0.753
Hydrothermally pre-treated + enzymatically treated	0.084	0.738

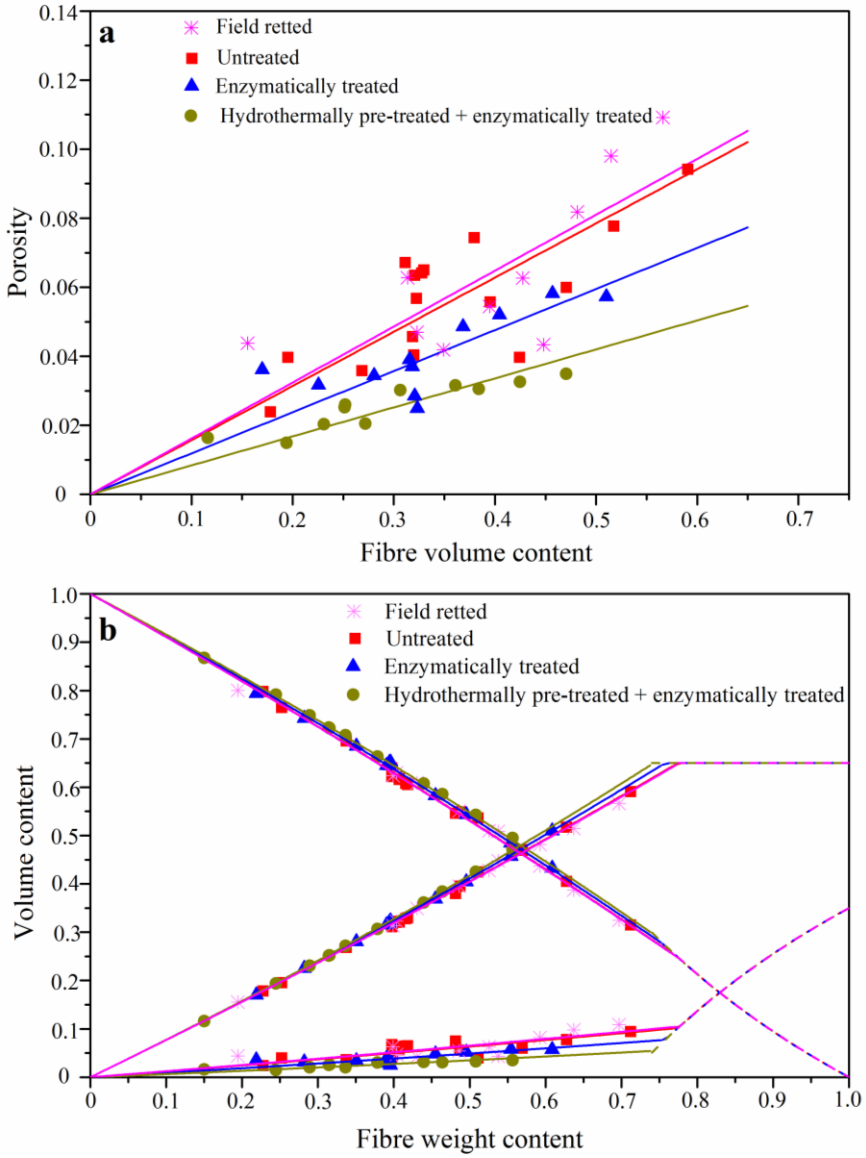

Figure 1. Composite porosity vs. fibre volume content (a), and composite volumetric composition (V_f, V_m and V_p) vs. fibre weight content (b).

4.2. Composite density

Figure 2 shows that the composites with the untreated and field retted fibres have the lowest density, which is a result of the highest porosity content and lowest fibre volume content in these composites (see Figure 1). In contrast, the composites with the enzymatically treated fibres, particularly the hydrothermally pre-treated and enzymatically treated fibres, exhibit clearly higher density due to their lower porosity contents and higher fibre volume contents. The model predictions of composite density in Figure 2 show that the predicted composite density is in good agreement with the experimental data. Therefore, the density of composites with a given type of fibre treatment can also be well predicted as a function of the fibre weight content.

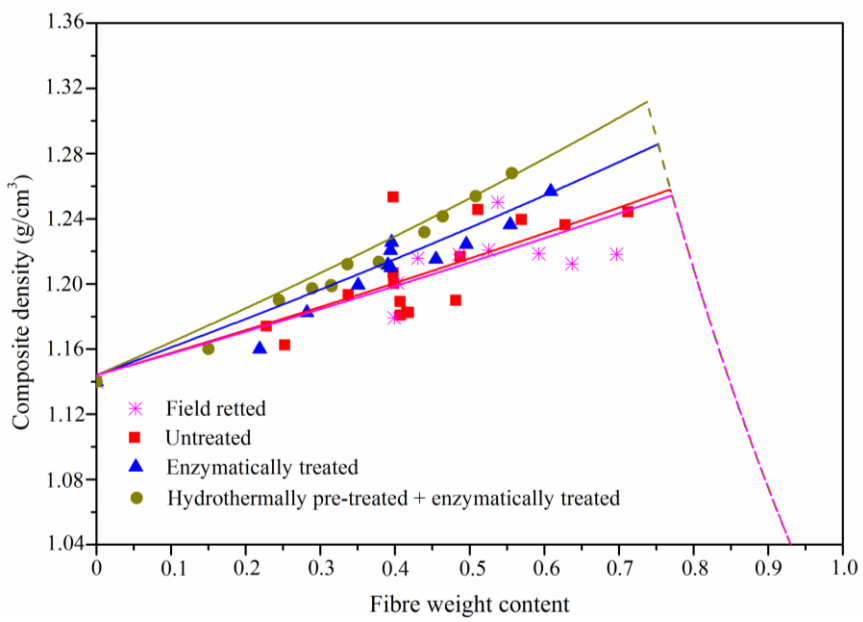

Figure 2. Composite density vs. fibre weight content.

4.3. Composite mechanical properties

In Figures 3 and 4, showing composite stiffness and strength as a function of the fibre weight content, the starting points of the model lines at $W_f = 0$ are equal to the measured epoxy matrix stiffness (E_m) of 2.7 GPa, and the epoxy matrix stress of 27 MPa at the average composite failure strain of 1.0%. Generally, the model lines are in good agreement with the experimental data.

The model lines in Figures 3 and 4 are established by setting the porosity efficiency exponent (n) equal to 0 and 2. For n = 0, it is assumed that all the porosity is located inside the fibres, in the so-called lumen, and this is assumed to have no effect on the mechanical properties of the composites. For n = 2, it is assumed that all the porosity is located outside the fibres, e.g. at the fibre/matrix interface or in the fibre bundles to produce un-impregnated fibres. This is assumed to lead to stress concentrations, which is modelled by setting n equal to 2 [14,15]. When n = 0, as shown in Figures 3a and 4a, composite stiffness and strength are increased non-linearly with W_f with a upward curvature until $W_{f\,trans}$, and thereafter, stiffness and strength are only slightly reduced. When n = 2, as shown in Figures 3b and 4b, composite stiffness and strength are increased non-linearly with W_f with a downward curvature until $W_{f\,trans}$, and thereafter, stiffness and strength are reduced radically. The downward curvature of the model lines is most obvious for the composites with the highest porosity content, such as the composites with the field retted and untreated fibres.

When comparing the model lines in Figures 3 and 4 for composites with the differently treated fibres, it is evident that the composites with hydrothermally pre-treated and enzymatically treated fibres have the highest stiffness and strength, followed by the composites with enzymatically treated and untreated fibres, while the composites with field retted fibres have the lowest stiffness and strength.

The fitted values of the effective fibre stiffness (E_f) and fibre strength (σ_{fu}) established by the model lines in Figures 3 and 4 are shown in Table 3. Field retted samples are found to have the lowest effective fibre stiffness of 52 and 61 GPa, and the lowest effective fibre strength of 474 and 558 MPa, when the porosity efficiency exponent is set equal to 0 and 2, respectively. There is a tendency that the effective fibre stiffness and strength increase from untreated fibres, to enzymatically treated fibres, and finally to hydrothermally pre-treated and enzymatically treated fibres, irrespective of the porosity efficiency exponent values. The hydrothermally pre-treated and enzymatically treated fibres have the

highest effective stiffness of 74 GPa and 83 GPa, and the highest effective strength of 625 MPa and 667 MPa, when porosity efficiency exponent is set equal to 0 and 2, respectively.

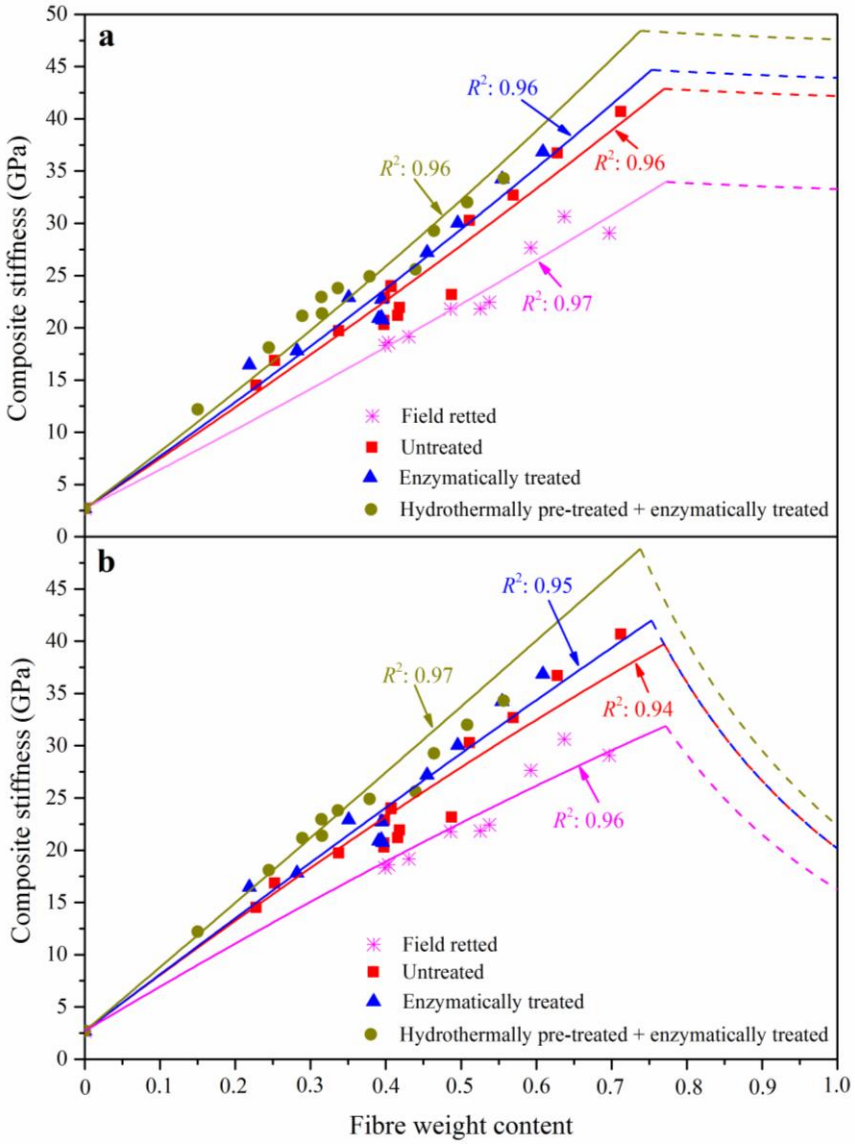

Figure 3. Composite stiffness vs. fibre weight content. Model lines are made using a porosity efficiency exponent of (a) 0 and (b) 2. Values of adjusted R-squared of fitting are shown next to the model lines.

Table 3. Established values of effective fibre stiffness (E_f) and fibre strength (σ_{fu}) in composites with differently treated hemp fibres. The porosity efficiency exponents (n_E and n_σ) are set to be either 0 or 2.

Fibre sample	E_f (GPa)		σ_{fu} (MPa)	
	n_E=0	n_E=2	n_σ=0	n_σ=2
Field retted	52	61	474	558
Untreated	65	75	569	655
Enzymatically treated	68	75	587	644
Hydrothermally pre-treated + enzymatically treated	74	83	625	667

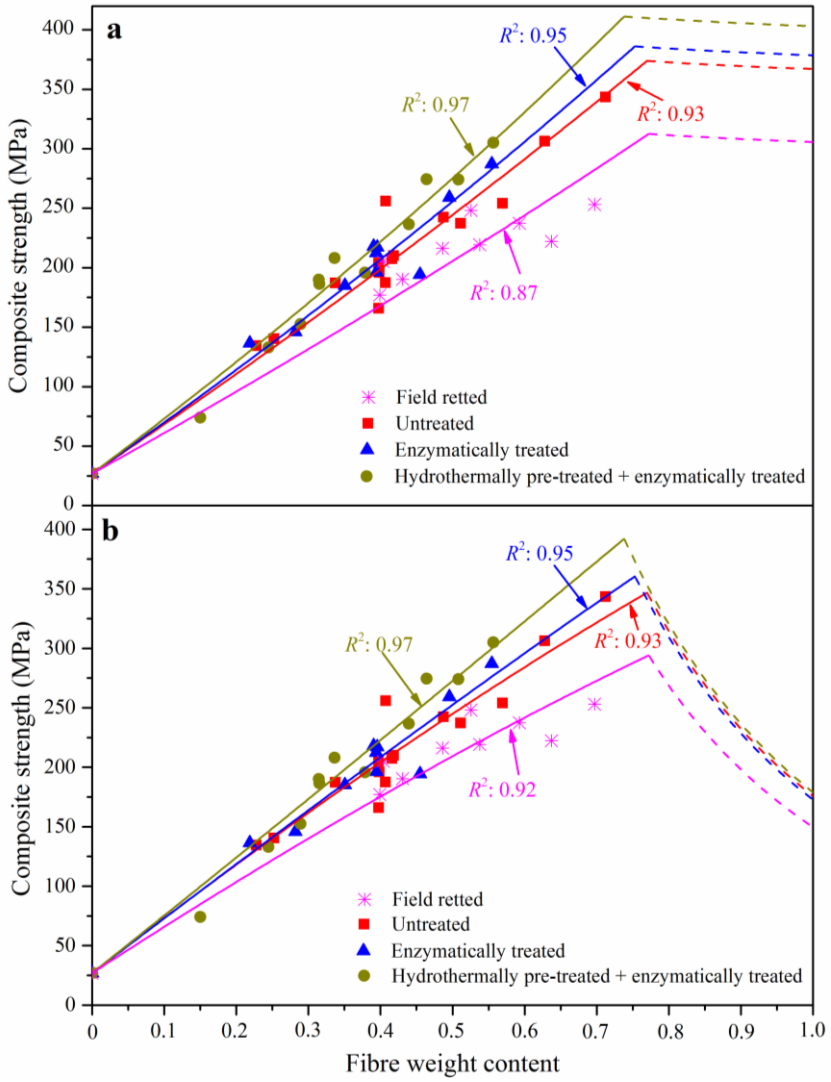

Figure 4. Composite strength vs. fibre weight content. Model lines are made using a porosity efficiency exponent of (a) 0 and (b) 2. Values of adjusted R-squared of fitting are shown next to the model lines.

5. Conclusions

Models for the volumetric composition, density and mechanical properties (i.e. stiffness and strength) of composites with differently treated hemp fibres were applied for evaluating the effect of enzymatic fibre treatments on fibre performance in composites. It is shown that the applied models are in good agreement with the experimental data. The established effective fibre stiffness and strength are used to quantify the effect of the enzymatic fibre treatments on the performance of the fibres in the composites. Altogether, the applied models are shown to be useful tools for the prediction of properties of composites with differently treated hemp fibres.

Acknowledgements

The authors are grateful to the Danish Council for Independent Research supporting the CelFiMat project (No. 0602-02409B: "High quality cellulosic fibres for strong biocomposite materials"). The financial support of China Scholarship Council (CSC, no. 201304910245) for Ming Liu's Ph.D. project is acknowledged. Jonas Kreutzfeldt Heininge and Jan Sjølin from Technical University of Denmark are acknowledged for technical support.

References

[1] Faruk O, Bledzki A K, Fink H P and Sain M 2012 *Prog. Polym. Sci.* **37** 1552
[2] Joshi S V, Drzal L T, Mohanty A K and Arora S 2004 *Compos. Part A Appl. Sci. Manuf.* **35** 371
[3] Arshad M, Kaur M and Ullah A 2016 *ACS Sustain. Chem. Eng.* **4** 1785
[4] Liu M, Fernando D, Meyer A S, Madsen B, Daniel G and Thygesen A 2015 *Ind. Crops Prod.* **76** 880
[5] Liu M, Fernando D, Daniel G, Madsen B, Meyer A S, Ale M and Thygesen A 2015 *Ind. Crops Prod.* **69** 29
[6] Di Candilo M, Bonatti P M, Guidetti C, Focher B, Grippo C, Tamburini E and Mastromei G 2010 *J. Appl. Microbiol.* **108** 194
[7] Li Y and Pickering K L 2008 *Compos. Sci. Technol.* **68** 3293
[8] Dreyer J, Müssig J, Koschke N, Ibenthal W D and Harig H 2002 *J. Ind. Hemp* **7** 43
[9] Liu M, Silva D A S, Fernando D, Meyer A S, Madsen B, Daniel G and Thygesen A 2016 *Compos. Part A Appl. Sci. Manuf.* doi: http://dx.doi.org/10.1016/ j.compositesa.2016.06.003
[10] Shibata S, Bozlur R M, Fukumoto I and Kanda Y 2010 BioResources **5** 2097
[11] Madsen B, Thygesen A and Lilholt H 2007 *Compos. Sci. Technol.* **67** 1584
[12] Shang L, Jiang Z, Liu X, Tian G, Ma J, Yang S 2016 *Bioresources* **11** 2071
[13] Akin D E, Gamble G R, Morrison W H, Rigsby L L, Dodd R B 1996 *J. Sci. Food Agric.* **72** 155
[14] Madsen B, Thygesen A and Lilholt H 2009 *Compos. Sci. Technol.* **69** 1057
[15] Madsen B and Lilholt H 2003 *Compos. Sci. Technol.* **63** 1265